2014

Holocene Paleoenvironmental Reconstruction From Mexico's Pacific Coast-A Paleotempestological Investigation

Thomas Bianchette

Louisiana State University and Agricultural and Mechanical College

HOLOCENE PALEOENVIRONMENTAL RECONSTRUCTION FROM MEXICO'S PACIFIC COAST – A PALEOTEMPESTOLOGICAL INVESTIGATION

A Dissertation

Submitted to the Graduate Faculty of the
Louisiana State University and
Agricultural and Mechanical College
in partial fulfillment of the
requirements for the degree of
Doctor of Philosophy

in

The Department of Oceanography and Coastal Sciences

by
Thomas Bianchette
B.S., Western Michigan University, 2005
M.S., Louisiana State University, 2007
May 2014

ACKNOWLEDGEMENTS

For the completion of this work I owe many people a great deal of thanks. I want to thank Dr. Kam-biu Liu, my major advisor. I have been a part of his laboratory since my arrival as a spry, young, and naïve student in 2005. He spent a countless number of hours grooming me into a coastal scientist, while always keeping his office door open in case I had questions or problems. Throughout the years his passion and enthusiasm for earth science and solving complex problems has been highly contagious, and I greatly respect the fact that during all of my struggles and pitfalls, he never, ever gave up on me. I think I will remember him most for that reason. I also give many thanks to my committee members: Drs. Samuel Bentley, Jaye Cable, Nina Lam, Robert Rohli, as well as the Dean's Representative, Dr. Andy Nyman. Other LSU faculty members mentored me through collaboration inside and outside of the classroom, most notably Drs. Michael Leitner and Lei Wang.

For his aid in fieldwork, I want to express my appreciation to Dr. Terrence McCloskey. His fieldwork expertise was invaluable, and this project would have never gotten off of the ground without him. Mr. Ulises Cruz Valera met me in Acapulco, and was quite the trooper in reference to his hard work and efforts with sediment coring and communicating with locals, as well as driving in some heavy urban traffic! A special thank you goes to Drs. Blanca Figueroa Rangel and Miguel Olvera Vargas for meeting me in Jalisco and helping me with the overall travel logistics. Drs. Jose Luis Antinao, Luis Farfan, Graciela Raga, and Jorge Sanchez-Sesma were also integral in their logistical support for the research trips.

This project could never take place without gracious funding from a few agencies. I received generous grants from the National Science Foundation (Doctoral Dissertation Research Improvement grant), Geological Society of America (Graduate Student Research grant), and

Association of American Geographers (Dissertation Research grant). I would also like to thank the Inter-American Institute for Global Change Research (IAI) for additional funding.

I would like to thank my parents, John and Susanne, and my lil' sister Emily for their unwavering support throughout this process, and for constantly telling me "it will all be worth it in the long run." Indeed, they were right. A special thanks goes out to my brother Giovanni, as his time spent with me watching sports and discussing topics not pertaining to scientific research or anything academic served as a major stress reliever. Last, but certainly not least, I would like to thank my beautiful wife, Erin. She was often home alone and bored while I spent many nights in the lab or office working. She tolerated my grumpiness on many occasions, while always picking me up when I 'had enough.' She was certainly my inspiration in completing this seemingly never-ending task.

TABLE OF CONTENTS

ABSTRACT

This dissertation examines the paleoenvironments of four lagoons from Mexico's Pacific coast, with the aim of retrieving sediment deposition from storm surge events to determine long-term tropical cyclone (TC) records. Lagoons Agua Dulce, Boquita, Mitla, and Nuxco are located along a 700 km stretch in states Jalisco and Guerrero. Roughly 70 meters of sediment were collected and subjected to multiple proxies, including loss-on ignition, a microfossil survey, and geochemical analysis.

Nuxco's dynamism is caused by intense and prolonged rainfall (largely from TCs), responsible for increasing water level, opening the tidal inlet, and draining the site (termed "blowouts"). High amounts of shell hash entering Nuxco's nearshore from ~1280-~530 yrs BP suggests turbulent conditions, likely from recurrent blowouts caused by a wet climate and frequent TCs. A decrease in nearshore hash from ~530 yrs BP to present suggests a more stable environment from a drier climate and less TCs.

Mitla and Boquita's backbarrier environments were formed ~5200 yrs BP during a period of stabilizing sea level. The longest core extracted from Mitla reveals peat alternating with lagoonal clay layers, indicating limnic environments (inferred 4430-4220 yrs BP, 4080, 3950, 3680-3480, 3170-3080, 2990-2870, 1570-present) triggered by increases in precipitation. Limnic phases show good temporal correlation to wet periods determined from coastal and upland paleorecords, and long term El Niño records, a main cause of wet conditions, along with frequent and wetter eastern north Pacific TCs. Mitla's cores lack overwash evidence from TCs and tsunamis, posing questions regarding the documented attribution of clastic deposition to extreme events here. Similar to Mitla, Boquita's sediments indicate changes in water level. Namely, a desiccated blue clay section adjacent to gray clay with low water and organic

contents, and high Cl concentration, suggests low water level and dry conditions from ~3150-1030 yrs BP. While Laguna Agua Dulce is the only site susceptible to overwash, individual events cannot be deciphered due to its sandy sediments and typical resuspension from strong currents.

Findings from this dissertation shed light on the insensitivity of these lagoons to overwash processes from extreme events, while improving regional paleoclimatological and paleoenvironmental records and understanding.

CHAPTER 1. INTRODUCTION

1.1 The problem

A tropical cyclone (TC) is a powerful meteorological phenomenon common in tropical and subtropical areas worldwide. These events are capable of wreaking havoc on a landscape, through a combination of lingering and torrential rainfall, fierce winds, tornadic activity, and uncontainable storm surge. Artists and poets including Percy Bysshe Shelly, Emily Dickinson, and William Shakespeare have long marveled at these forces through paintings of vibrant shades and flowery language and metaphor regarding their strength and majesty, while photographers often capture snapshots of impressive cloud formations (see Emanuel, 2005a for examples). Residents of hurricane-prone areas, however, generally view these storms as forces creating substantial destruction, whether economic, infrastructural, cultural, psychological, ecological, or geophysical. TCs are capable of inflicting mass mortality, as documented from the 1900 Galveston hurricane killing at least 8000 people (Blake et al., 2007). Their subsequent damage is often expensive as recently observed by Hurricane Katrina, the costliest hurricane in U.S. recorded history, amounting to $81 billion in loss (Blake et al., 2007). TC activity and damage are consistently exacerbated by increasing populations in United States coastal areas (Pielke et al., 2008). For developing nations, TC damage is often magnified due to poor emergency preparation and infrastructure. A glaring example is Hurricane Mitch, which devastated El Salvador, Honduras, and Nicaragua in 1998, killing approximately 10,000 people and causing $5-7 billion U.S. in damage (Pielke et al., 2003).

TCs develop in warm, low-latitude waters around the globe, from the Caribbean Sea and Atlantic Ocean, to the Indian Ocean and western Pacific. Many tropical and subtropical areas are affected, most notably countries such as India and China with dense coastal populations. Yet

it is cumbersome to properly assess coastal risk due to the short record for TC data. For the Atlantic basin and Gulf of Mexico (GOM), historical documentation begins in 1851. Scientists have studied activity trends at varying timescales, namely seasonal (Elsner et al., 2000; Saunders and Lea, 2005), to annual (Landsea et al., 1996; Elsner et al., 1999; Emanuel, 2005b) and decadal (Gray et al., 1997; Goldenberg et al., 2001; Mann and Emanuel, 2006), to understand better where storms will make landfall, the frequency of occurrence, and what controls their intensity. While temporal analyses have been documented for other basins (Pielke et al., 2003; Chan, 2004), these studies are hampered by a relatively short historical dataset, such as for the western North Pacific (~1884), Indian Ocean (~1842), and Caribbean Sea (~1851) (National Oceanic and Atmospheric Administration, 2011), despite efforts to extend historical datasets through written documentation from newspaper accounts, ship logbooks, diaries, etc. (Mock, 2008; Grossman and Zaiki, 2009). On an annual timescale, global inter-basin correlations in TC activity have been established (Lander and Guard, 1998). While annual global TC frequencies are fairly constant, significant inter-basin variability is common (Henderson-Sellers et al., 1998). Establishing long term inter-basin correlations is therefore vital to understand global TC behavior. On multi-centennial to -millennial timescales, are the ocean basins experiencing an active or quiescent period in TC activity? And what are the climatological mechanisms for these shifts? What can we expect in certain coastal regions for the next hundred years in terms of activity? What can we expect for the next few thousand years and beyond?

1.2 Paleotempestology

Paleotempestology is the study of past TC activity mainly through geological or biological proxies (Liu, 2007). Scientists have discovered activity regimes at many Atlantic and Gulf sites, with recent studies stretching to other TC prone regions (chapter 2). Despite recent

discoveries and developments in paleotempestology (chapter 2), an investigation concerning eastern North Pacific TCs and western Mexico had never been performed.

1.3 Setting the stage

The eastern North Pacific (ENP) basin is globally the most active region for cyclogenesis, per unit time and area (Molinari et al., 2000). Tropical activity in the ENP basin surpasses the Atlantic basin, with 15 named systems annually as opposed to 11 named systems (National Hurricane Center, 2011). Fortunately, ENP landfalling TCs are generally less intense than those in the Gulf of Mexico or Caribbean Sea (Jauregui, 2003). Regardless, devastating Pacific coast TCs are an integral part of Mexico's past and present. Pauline (1997) hit the coastal state of Oaxaca as a weak Category 2 hurricane, subsequently stalling over land as a Category 1 storm near Acapulco, killing hundreds and leaving in its wake millions of U.S. dollars of damage. In addition to frequent mudslides (Spang et al., 2003), many cases of cholera and dengue fever arose due to days of stagnant water (Luhnow, 1997; Preston, 1997). With Mexico's Pacific coastal population increasing (Aguilar, 1999; Consejo Nacional de Poblacion, 2006), long-term risk assessment becomes increasingly important. The historical TC record only stretches back to 1949, while some argue that it begins in 1963 with the implementation of satellite imagery (Jauregui, 2003). While decadal shifts in hurricane activity have been established (Jauregui, 2003), centennial and millennial scale risk is unknown, yet essential to develop proper TC risk evaluation.

A paleotempestological investigation for western Mexico comes equipped with difficulties and uncertainties. Challenges arise from western Mexico's physical geography as coastal areas are unstable from tectonism and affected by increased sediment supply, leading to wide beach ridge systems. Tsunami can lead to complications in the sedimentary record, since

these deposits (Dawson and Shi, 2000; Fujiwara et al., 2000; Chague-Goff et al., 2002) can resemble TC storm surge signatures (Liu and Fearn, 1993; Kortekaas, 2002; Kortekaas and Dawson, 2007). TC trajectories contrast from a characteristic landfalling event for the GOM. With the Sierra Madre mountains acting as a "barrier," TCs frequently parallel the west coast whether onshore or offshore (Sanson, 2004) and often fail to make a 'direct' landfall. While paralleling TCs are capable of catastrophic damage, they can be inconsistent in triggering a storm surge capable of overtopping these coastal beach barriers, due to variables including the distance of the tropical system to land. This inconsistency may diminish the effectiveness of using overwash sand as a consistent proxy. A paralleling offshore hurricane, John (2006 - Figure 1.1) created a ten-foot storm surge in Acapulco (Pasch, 2006) as it trekked WNW through the Pacific Ocean. Meanwhile, Pauline (Figure 1.1) created a significant storm surge as an offshore paralleling hurricane in Oaxaca (Goman et al., 2005), yet significant storm surge was never reported in the Acapulco area (Lawrence, 1997) where the bulk of the damage resulted from heavy precipitation causing flooding and mudslides.

1.4 Objectives

A paleoenvironmental reconstruction from two areas of Mexico's Pacific coast, a southern location (Guerrero) and a more northerly setting (Jalisco) (Figure 1.2), require a host of sedimentological, geochemical, and biological proxies to help identify TC history. Sedimentological proxies (e.g., loss-on ignition, grain-size analysis) are useful in detecting long-term paleoenvironmental changes and extreme event deposition. The internal structure (e.g., fining or coarsening upward) of marine or terrestrial deposits can also be determined. Geochemical methods (X-ray fluorescence) can reveal sediment provenance, whether marine or terrigenous. Fossil pollen can determine ecological changes, possibly triggered by extreme

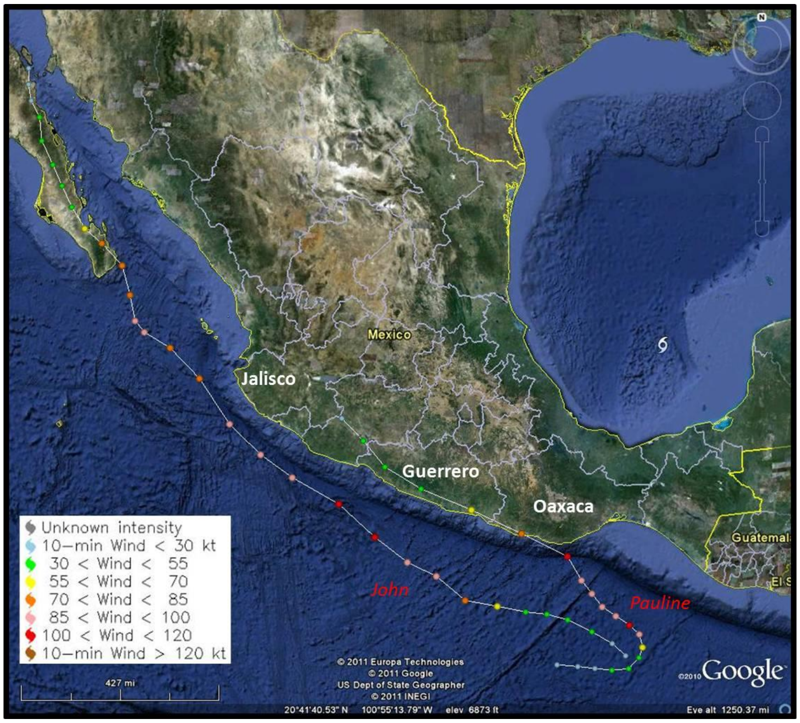

Figure 1.1 – Hurricane tracks for John (2006) and Pauline (1997). Track data can be obtained from the National Oceanic and Atmospheric Administration (2011).

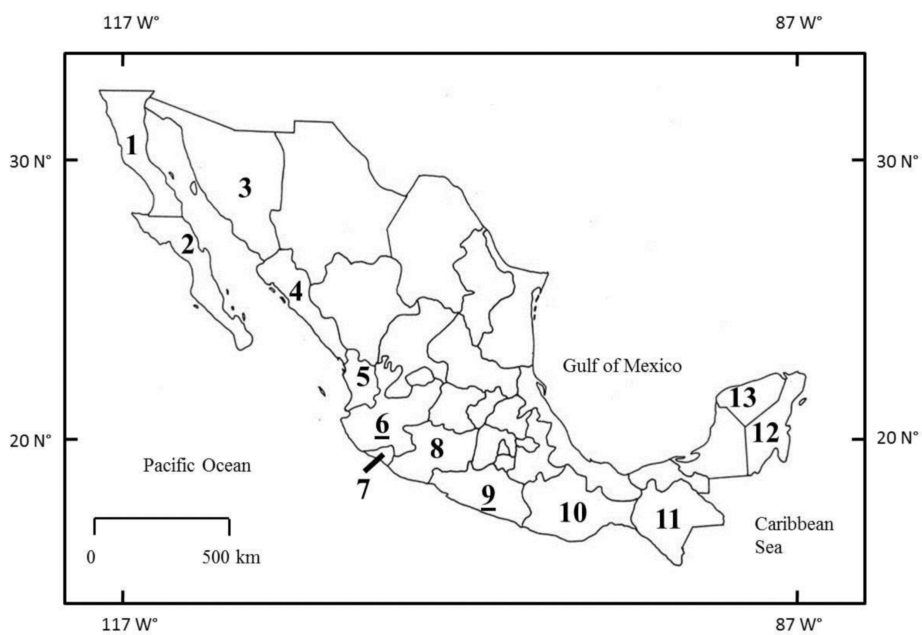

Figure 1.2 – Mexican states mentioned in this dissertation. 1 - Baja California Norte. 2- Baja California Sur. 3- Sonora. 4- Sinaloa. 5- Nayarit. 6 - Jalisco. 7- Colima. 8 - Michoacan. 9 - Guerrero. 10 - Oaxaca. 11 - Chiapas. 12 - Quintana Roo. 13 - Yucatan. Research in this dissertation is focused in Jalisco (6) and Guerrero (9), both underlined.

events, climate change, or tectonic activity. Fungal spores provide records of erosional processes and human activity (McAndrews and Turton, 2010; Gelorini et al., 2011; van Geel et al., 2011). Microscopic charcoal concentrations indicate evidence of local or regional fires (Tinner et al., 1998). Elevated charcoal has been discovered adjacent to overwash sand layers in coastal lake sediments from the Gulf Coast, indicating a relationship between hurricane landfalls and post-disturbance burning (Liu et al., 2008).

The main objective of this dissertation is the establishment of paleo-cyclone records for coastal states Jalisco and Guerrero. Western Mexico's geomorphic setting and frequent geophysical destruction from TCs suggest that evidence will be identifiable in sediments as overwash sand layers and/or slopewash deposition, triggered by prolonged and intense TC rainfall (e.g., Kennedy et al., 2006). If deposition from individual TC events can be discovered, the time periods and main climatological drivers of active periods must be determined.

It is possible that deposition from individual TCs will be absent in these coastal sites. If this occurs, it is still likely to determine paleoenvironmental conditions that are indicative of heightened TC activity. For instance, it is suggested that wet climate periods are synonymous with an active TC period, since TC precipitation accounts for a significant portion of annual rainfall throughout western Mexico's arid to semi-arid coasts (chapter 2). Wet periods can be detected through a variety of means, including an increase in mesic-type pollen or alterations in water level at the sites.

1.5 Expected significance

This study aims to be the first paleotempestological study analyzing ENP TCs, as well as the first such analysis in western Mexico. Data retrieved here are vital to help analyze global inter-basin correlations at longer timescales and to comprehend TC activity fluctuations on

various temporal scales. The historical period here is brief, deeming it crucial to develop a reliable TC history through geological and biological proxies, a need further intensified by increasing Pacific coastal populations. Palynological studies in western Mexico are rare, deeming any paleoenvironmental information useful for paleoclimatology, disturbance ecology, and/or coastal geomorphology. If this methodology proves successful in detecting TC activity periods, paleotempestological studies could transition to inland sites and detecting evidence independent of coastal overwash processes. A TC record can improve forecasting of future activity periods, vital in strengthening risk and mitigation policies. Risk assessment remains crucial for government officials, insurance agencies, earth scientists, and local residents.

1.6 References

Aguilar, G. 1999. Human settlements and climate change in Mexico - A scenario of regional vulnerability. Pages 171-194 *in* C. Gay, editor. El cambio climatico en Mexico. INE/PUMA.

Blake, E. S., E. N. Rappaport, and C. W. Landsea. 2007. The deadliest, costliest, and most intense United States tropical cyclones from 1851 to 2006 (and other frequently requested hurricane facts). National Weather Service.

Chague-Goff, C., S. Dawson, J. R. Goff, J. Zachariasen, K. R. Berryman, D. L. Garnett, H. M. Waldron, and D. C. Mildenhall. 2002. A tsunami (ca. 6300 years BP) and other Holocene environmental changes, northern Hawke's Bay, New Zealand. Sedimentary Geology **150**:89-102.

Chan, J. C. L. 2004. Variations in tropical cyclone activity over the western North Pacific: From interdecadal to intraseasonal. Pages 269-296 *in* R. J. Murnane and K. B. Liu, editors. Hurricanes and Typhoons: Past, Present, and Future. Columbia University Press, New York.

Consejo Nacional de Poblacion. 2006. Poblacion y principales caracteristicas por entidad federativa.

Dawson, A. G. and S. Z. Shi. 2000. Tsunami deposits. Pure and Applied Geophysics **157**:875-897.

Elsner, J. B., A. B. Kara, and M. A. Owens. 1999. Fluctuations in North Atlantic hurricane frequency. Journal of Climate **12**:427-437.

Elsner, J. B., K. B. Liu, and B. Kocher. 2000. Spatial variations in major US hurricane activity: statistics and a physical mechanism. Journal of Climate **13**:2293-2305.

Emanuel, K. 2005a. Divine Wind: The History and science of hurricanes. Oxford University Press, USA.

Emanuel, K. 2005b. Increasing destructiveness of tropical cyclones over the past 30 years. Nature **436**:686-688.

Fujiwara, O., F. Masuda, T. Sakai, T. Irizuki, and K. Fuse. 2000. Tsunami deposits in Holocene bay mud in southern Kanto region, Pacific coast of central Japan. Sedimentary Geology **135**:219-230.

Gelorini, V., A. Verbeken, B. van Geel, C. Cocquyt, and D. Verschuren. 2011. Modern non-pollen palynomorphs from East African lake sediments. Review of Palaeobotany and Palynology **164**:143-173.

Goldenberg, S. B., C. W. Landsea, A. M. Mestas-Nunez, and W. M. Gray. 2001. The recent increase in Atlantic hurricane activity: Causes and implications. Science **293**:474-479.

Goman, M., A. Joyce, and R. Mueller. 2005. Stratigraphic evidence for anthropogenically induced coastal environmental change from Oaxaca, Mexico. Quaternary Research **63**:250-260.

Gray, W. M., J. D. Sheaffer, and C. W. Landsea. 1997. Climate trends associated with multi-decadal variability of Atlantic hurricane activity. Pages 15-53 *in* H. F. Diaz and R. S. Pulwarty, editors. Hurricanes: Climate and Socioeconomic Impacts. Springer-Verlag, New York.

Grossman, M. and M. Zaiki. 2009. Reconstructing typhoons in Japan in the 1880s from documentary records. Weather **64**:315-322.

Henderson-Sellers, A., H. Zhang, G. Berz, K. Emanuel, W. Gray, C. Landsea, G. Holland, J. Lighthill, S. L. Shieh, P. Webster, and K. McGuffie. 1998. Tropical cyclones and global climate change: A post-IPCC assessment. Bulletin of the American Meteorological Society **79**:19-38.

Jauregui, E. 2003. Climatology of landfalling hurricanes and tropical storms in Mexico. Atmosfera **16**:193-204.

Kennedy, L. M., S. P. Horn, and K. H. Orvis. 2006. A 4000-year record of fire and forest history from Valle de Bao, Cordillera Central, Dominican Republic. Palaeogeography Palaeoclimatology Palaeoecology **231**:279-290.

Kortekaas, S. 2002. Tsunamis, storms, and earthquakes: distinguishing coastal flooding events. Coventry University, UK.

Kortekaas, S. and A. G. Dawson. 2007. Distinguishing tsunami and storm deposits: An example from Martinhal, SW Portugal. Sedimentary Geology **200**:208-221.

Lander, M. A. and C. P. Guard. 1998. A look at global tropical cyclone activity during 1995: contrasting high Atlantic activity with low activity in other basins. Monthly Weather Review **126**:1163-1173.

Landsea, C. W., N. Nicholls, W. M. Gray, and L. A. Avila. 1996. Downward trends in the frequency of intense Atlantic hurricanes during the past five decades. Geophysical Research Letters **23**:1697-1700.

Lawrence, M. B. 1997. Hurricane Pauline - Preliminary Report. National Hurricane Center. Retrieved 06-30-2011. http://www.nhc.noaa.gov/1997pauline.html.

Liu, K. B. 2007. Paleotempestology. Pages 1978-1986 *in* S. Elias, editor. Encyclopedia of Quaternary Science. Elsevier, Amsterdam.

Liu, K. B. and M. L. Fearn. 1993. Lake-sediment record of late Holocene hurricane activities from coastal Alabama. Geology **21**:793-796.

Liu, K. B., H. Lu, and C. Shen. 2008. A 1200-year proxy record of hurricanes and fires from the Gulf of Mexico coast: Testing the hypothesis of hurricane-fire interactions. Quaternary Research **69**:29-41.

Luhnow, D. 1997. Cholera breaks out in Acapulco. Reuters Foundation, editor. My Relief Web.

Mann, M. E. and K. Emanuel. 2006. Atlantic hurricane trends linked to climate change. EOS, Transactions, American Geophysical Union **87**:233-244.

McAndrews, J. H. and C. L. Turton. 2010. Fungal spores record Iroquoian and Canadian agriculture in 2nd millennium A.D. sediment of Crawford Lake, Ontario, Canada. Vegetation History and Archaeobotany **19**:495-501.

Mock, C. J. 2008. Tropical cyclone variations in Louisiana, USA, since the late eighteenth century. Geochemistry, Geophysics, and Geosystems **9**(Q05V02).

Molinari, J., D. Vollaro, S. Skubis, and M. Dickinson. 2000. Origins and mechanisms of eastern Pacific tropical cyclogenesis: A case study. Monthly Weather Review **128**:125-139.

National Hurricane Center. 2011. Tropical cyclone climatology. Retrieved 06-29-2011. http://www.nhc.noaa.gov/pastprofile.shtml.

National Oceanic and Atmospheric Administration. 2011. Historical hurricane tracks. Retrieved 06-29-2011. http://www.csc.noaa.gov/hurricanes/#.

Pasch, R. J. 2006. Tropical cyclone report - Hurricane John. National Hurricane Center.

Pielke, R. A., J. Gratz, C. W. Landsea, D. Collins, M. A. Saunders, and R. Musulin. 2008. Normalized Hurricane Damage in the United States: 1900-2005. Natural Hazards Review **9**:29-42.

Pielke, R. A., J. Rubiera, C. Landsea, M. L. Fernandez, and R. Klein. 2003. Hurricane variability in Latin America and the Caribbean: Normalized damage and loss potentials. Natural Hazards Review **4**:101-114.

Preston, J. 1997. Acapulco tourist areas are open after storm. New York Times.

Sanson, L. Z. 2004. The mechanical influence of continental topography on the trajectories of tropical cyclones near the west coast of Mexico. Atmosfera **17**:151-170.

Saunders, M. A. and A. S. Lea. 2005. Seasonal prediction of hurricane activity reaching the coast of the United States. Nature **434**:1005-1008.

Spang, R. M., S. H. Castaneda, and E. M. Gomez. 2003. Hurricane Pauline - its impact on Acapulco and subsequent debris flow prevention measures. *in* Proc. 3rd Int. Conf. Debris Hazards Mitigation, Davos, Switzerland.

Tinner, W., M. Conedera, B. Ammann, H. W. Gaggeler, S. Gedye, R. Jones, and B. Sagesser. 1998. Pollen and charcoal in lake sediments compared with historically documented forest fires in southern Switzerland since AD 1920. The Holocene **8**:31-42.

van Geel, B., V. Gelorini, A. Lyaruu, A. Aptroot, S. Rucina, R. Marchant, J. S. S. Damste, and D. Verschuren. 2011. Diversity and ecology of tropical African fungal spores from a 25,000-year palaeoenvironmental record in southeastern Kenya. Review of Palaeobotany and Palynology **164**:174-190.

CHAPTER 2. GENERAL BACKGROUND AND LITERATURE REVIEW

2.1 Paleotempestology

Early studies analyzing geomorphological change from tropical cyclones focus on coral deposition (Baines and McLean, 1976) or overwash sand lobe formation (Ball et al., 1967; Perkins and Enos, 1968; Morton, 1978; Ritchie and Penland, 1988) via storm surge. The pioneer paleotempestological work (Liu and Fearn, 1993) sought to discover a sedimentary imprint from Hurricane Frederic overwashing the coastal beach in Gulf Shores, Alabama. Information recovered from Alabama's Lake Shelby helped spur paleotempestological design and innovation after the following were discovered:

- Background information regarding the study site, including geological stability, tidal activity, beach height, and human disturbance is requisite to perform a sedimentary paleotempestological study. They determined that lacustrine sand layers were likely from hurricanes, not other mechanisms including aeolian transport, tsunami runup, winter storms, sea level rise, and tectonics.
- Frederic, a category 3 hurricane at landfall, failed to produce an overwash deposit in the center of Lake Shelby despite depositing a sand layer near its southern shore in two different sediment cores. Therefore, sand layers toward the lake center qualitatively indicate catastrophic hurricanes of category 4 or 5 intensity.
- They concluded that the Frederic sedimentary imprint is therefore a useful modern analog.
- An interval of increased sand layer frequency (3200-1000 ^{14}C years) is probably an active hurricane period. This activity period is bracketed by periods of hurricane inactivity from ~5000-3200 ^{14}C years and 1000-0 present.

Liu and Fearn (2000) then expanded Gulf Coast paleotempestological research, working at Western Lake in the Florida Panhandle. Here an active period was discovered from 3400-1000 ^{14}C yr BP, with inactive periods from 5000-3400 and 1000-present ^{14}C yr BP. They used Hurricane Opal, a category 3 storm, as a modern analog, suggesting that sand layers landward of the Opal overwash were attributed to catastrophic category 4 and 5 hurricanes. The increase in sand layer frequency was determined to be due to spatial shifts in the Bermuda High pressure system. With this pressure system in the western Atlantic Ocean, hurricanes steer toward the Atlantic coast. As this system migrates southwestward toward the Caribbean, tropical activity steers into the Gulf Coast (Figure 2.1).

Paleotempestology swiftly gained momentum with many landmark studies conducted throughout the United States. Paramount works took place in Rhode Island (Donnelly et al., 2001a), New Jersey (Donnelly et al., 2001b; 2004), and South Carolina (Collins et al., 1999; Hippensteel and Martin, 1999; Scott et al., 2003). Short-lived radioisotopic techniques such as ^{210}Pb (Collins et al., 1999; Scott et al., 2003) and ^{137}Cs (Donnelly et al., 2004) were used to date clastic layers during the historical record. Novel storm detection methods were developed, including X-radiography for clastic layer identification (Collins et al., 1999; Scott et al., 2003) and foraminifera to detect saltwater intrusion (Collins et al., 1999; Hippensteel and Martin, 1999). Aerial photography to track temporal geomorphological change (Donnelly et al., 2001b, 2004) helped decipher alterations in site sensitivity.

Paleotempestology continued to evolve spatially and methodologically. Studies diffused into the Caribbean to Puerto Rico (Donnelly, 2005; Donnelly and Woodruff, 2007; Woodruff et al., 2008a, b), The Bahamas (Knowles, 2008), and the Dominican Republic (Kar, 2010), with research also spreading into the Central American countries Belize (Frappier et al., 2007;

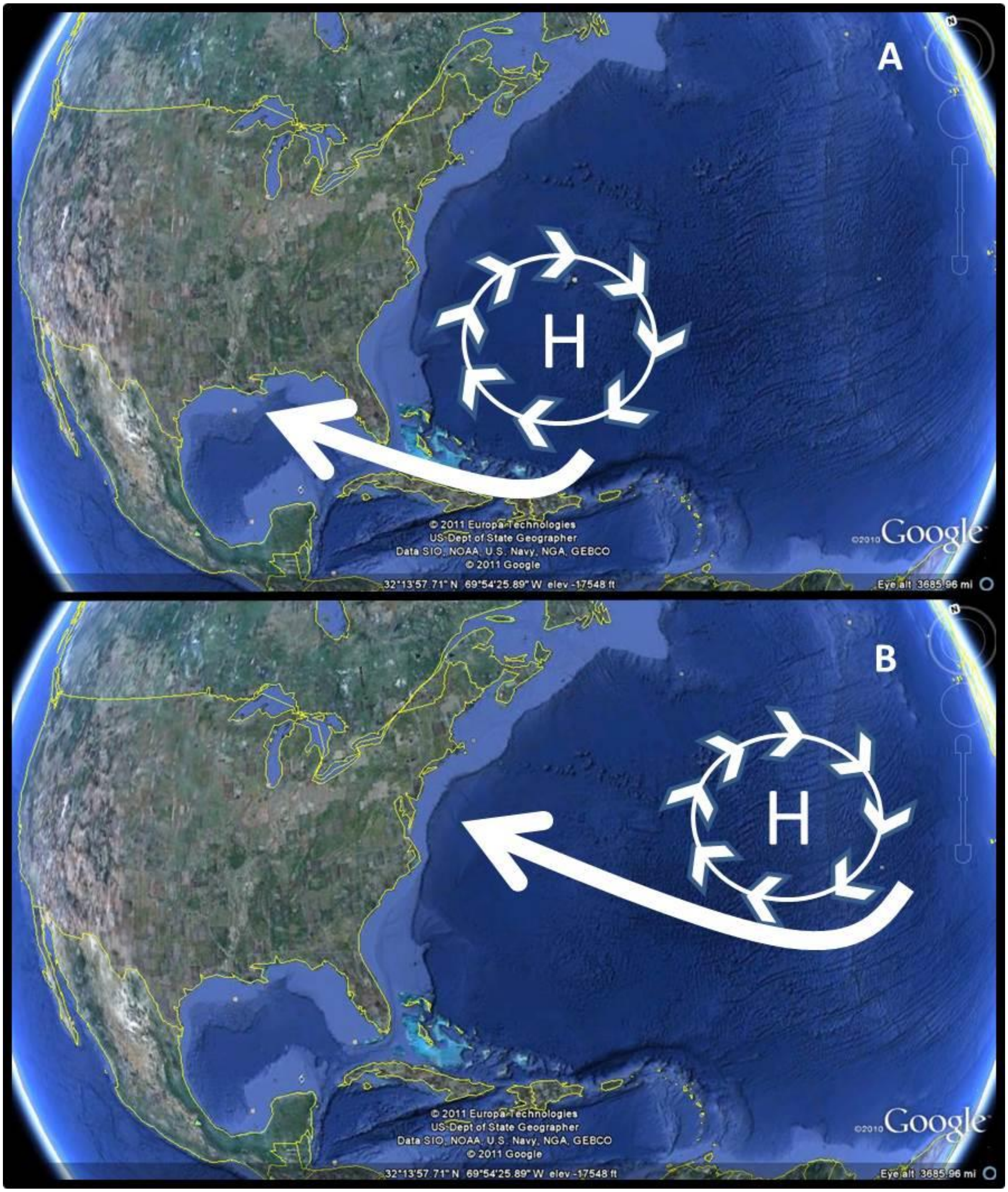

Figure 2.1 – Bermuda High pressure system movement leads to active periods for the Gulf (A) and Atlantic (B) coasts, depending on position. The base maps were downloaded from Google Earth.

McCloskey and Keller, 2009; McCloskey and Liu, 2013a, 2013b), Honduras (Knowles, 2004; Cochran et al., 2009), and Nicaragua (McCloskey, 2009; McCloskey and Liu, 2012). Across the globe, pioneer studies occurred in Japan (Woodruff et al., 2009), Australia (Nott, 2003; Nott et al., 2011), China (Liu et al., 2001; Louie and Liu, 2003; Fan and Liu, 2008), Israel (Kolodny et al., 2009), and France (Dezileau et al., 2011).

Recent paleotempestological research has been aided by innovative methodologies. Lu and Liu (2005) analyzed phytolith signatures to help detect overwash signals. The association between microscopic charcoal and overwash sand led to the hurricane-fire hypothesis (Liu et al., 2008). Additional proxies include dinoflagellates (Liu et al., 2008), diatoms (Hathorn, 2008), grain size (Reese et al., 2008, Woodruff et al., 2008b), geochemistry (Lambert et al., 2008; Dezileau et al., 2011), and isotopic analysis of calcium carbonate stalagmites (Frappier et al., 2007; Nott, 2009), tree ring cellulose (Mora et al., 2007) and coral reef skeletons (Kilbourne et al., 2011). Mathematical models helped in analyzing hurricane-induced deposits in sediments with contrasting sedimentation rates (Woodruff et al., 2008a) and by determining coastal lake overwash sensitivities (Elsner et al., 2008).

The plethora of recent methodological innovations and intellectual discoveries in paleotempestology will likely lead to many controversies and "hot topics," including:

- THE PAST - Bermuda High hypothesis or basin wide activity regimes? Many studies (Liu and Fearn, 2000; Scott et al., 2003; Elsner, 2006; McCloskey, 2009; Wallace and Anderson, 2010) suggest that activity regimes affecting the U.S. Gulf and Atlantic coasts are due to Bermuda High pressure system movement, creating an inverse relationship between U.S. Gulf and Atlantic coast active periods. Others argue that activity is based on a basin wide model covering the entire Atlantic basin including the Gulf of Mexico,

with examples from New York (Scileppi and Donnelly, 2007) and the Caribbean (Donnelly and Woodruff, 2007; Woodruff et al., 2008b) indicating similar active periods. Increased spatial distribution of future study sites might help shed light on this controversy, especially in areas 'between' the Atlantic and Gulf coast activity hot spots (e.g., eastern Florida, Georgia, etc.) and geographical outliers (e.g., Maine, Newfoundland, eastern Mexican states of Tamaulipas, Quintana Roo, Yucatan).

- THE PRESENT – Improve geographical coverage, modern analog studies. Scientists can learn more about activity regimes by globally expanding paleotempestological areas of research. Inter-basin studies can help compare activity regimes between different ocean basins (Lander and Guard, 1998; Elsner and Kara, 1999; Woodruff et al., 2009). Future works must analyze the characteristics of modern storm deposits (e.g., Reese et al., 2008; Crosby and Reese, 2009; Williams, 2010) to better understand how variables including storm intensity and track, geomorphology, sediment supply, and erosion affect the spatial distribution and physical structure of overwash signatures.
- THE FUTURE – Hurricane trends in a warming world? With recent media attention regarding the geophysical effects of global warming, how can scientists correlate paleo-TC findings to expected trends in a warming world? Would global warming lead to an increase in the frequency or intensity of future storms? Would future TC activity exhibit significant spatial differences? Bender et al. (2010) suggest that intense storms will be more common due to global warming, despite a decrease in overall storm frequency. Others state the importance in understanding future trends of ENSO (Donnelly and Woodruff, 2007; Mann et al., 2009) and the West African Monsoon (Donnelly and Woodruff, 2007). Future collaboration between paleotempestologists and

paleoclimatologists would help pinpoint climatological conditions during historically active periods to improve TC forecasting.

2.2 Tsunamis

A tsunami is a series of ocean waves created by an earthquake (National Oceanic and Atmospheric Administration, 2011a; Open University, 1989; Smith, 2006). These phenomena occur mostly in the Pacific Ocean associated with the "Ring of Fire," an area of active seismic flux due to tectonic collisions from the Pacific, Nazca, North American, South American, and Australian plates (Smith, 2006). Tsunamis are rare but can also occur in the Atlantic Ocean and Mediterranean Sea (UNESCO, 2005).

Tsunami waves differ from meteorologically-generated waves. In the open sea tsunami waves are generally less steep (Dawson and Shi, 2000) and longer (Smith, 2006) than cyclone-generated surge. Tsunami waves are highly dynamic and can exhibit both landward and backwash motions over land (Goff et al., 2004), often leading to mass deposition of sediment (Dawson and Shi, 2000). Deposition is dependent on certain factors, including the amount of material, ocean bathymetry, and topography (Kortekaas and Dawson, 2007) with low-lying areas generally possessing the thickest clastic layers (Peters et al., 2007). Sediment sources are usually a coastal beach, beach ridge, or gravel area (e.g., Goff et al., 2000, 2004; Switzer et al., 2005; Kortekaas and Dawson, 2007; Nanayama et al., 2007) though certain areas possess an offshore sand source (Dawson, 2007).

A thorough description of tsunami deposits identifies certain definable traits (Kortekaas and Dawson, 2007, and references therein).

- Landward and seaward layering (e.g., Massari and D'Alessandro, 2000; Bussert and Aberhan, 2004; Scasso et al., 2005). These bi-directional layers can be visualized by

either shells or low-angle layering (Dominey-Howes et al., 2006). Analysis can be troublesome since after initial sediment deposition, seaward flow can erode tsunami layers and/or deposit fresh sediment (Dawson and Shi, 2000). In northern Japan, Nanayama et al. (2000) describe landward flow containing nearshore components including both marine and coastal beach sand, and seashells, while seaward deposits possess inland materials including plant pieces, soil, and stream gravel.

- Landward fining (e.g., Minoura et al., 1996; Sawai, 2002). In New Zealand Goff et al. (2004) discovers a mean grain size of a tsunami deposit near 1 φ (phi-scale) 175 m inland from mean high water, opposed to –2 φ for locations 50 m inland.
- Upward fining (e.g., Dawson and Smith, 2000; Chagué-Goff et al., 2002; Fujiwara et al., 2000; Goff et al., 2004). This can occur due to the lessened shear velocities over time along with slowly declining erosion from weakening waves, while the sedimentation process often commences with fine silt deposition (Dawson and Shi, 2000). In Papua New Guinea, McSaveney et al. (2000) discovers three sand sheets estimated to be from the 1998, 1934/1935, and 1907 tsunamis, all with coarse- or medium-grained sand fining upwards.
- Basal discontinuity and erosion (e.g., Goff et al., 2000, 2004). Basal erosion of the sand sheet is common, despite some scientists discovering only layers with distinct basal boundaries (e.g., Dominey-Howes et al., 2006; Peters et al., 2007). In Japan, Fujiwara et al. (2000) discovers sand sheets containing a basal unit that is eroded with contacts including rocks and shell fragments, with certain layers overlying an oyster and coral bed.

- Additional characteristics. Other characteristics are documented regarding tsunami deposition. The sediment frequently thins with increasing distance inland from the sediment source (e.g., Massari and D'Allessandro, 2000; Nanayama et al., 2000; Chagué-Goff et al., 2002; Peters et al., 2007). The high energy waves can move boulders long distances (e.g., Bussert and Aberhan, 2004), cause sediment reworking (Peters et al., 2007), and produce rip-up clasts (Morton et al., 2007). The latter are mud or silt embedded in the sand sheet derived from underlying sediments (e.g., Fujiwara et al., 2000; Goff et al., 2001; Scasso et al., 2005).

Similarities and differences between tsunami and cyclone deposits are summarized by Kortekaas (2002) as cited in Kortekaas and Dawson (2007). Similarities persist as tsunami and storm deposits generally thin and become finer with greater distance inland. They both generally contain microfossils, plant pieces, and whole shells or shell hash, while possessing erosional bases. Differences can arise from sedimentological contrasts, since TC deposits form from unidirectional storm surge rather than from bi-directional flow for tsunamis. Sand grains are generally better sorted in TC layers (e.g., Goff et al., 2004), and rip-up clasts are rare in TC deposits (Morton et al., 2007). TC deposits generally adhere to topography by dropping sediment in elevational lows and crevasses, uncommon in tsunami deposits (Morton et al., 2007). These characteristics are common in paleotempestological literature as TC-induced deposits generally thin landward from the sediment source (e.g., Liu and Fearn, 1993, 2000; Donnelly et al., 2004), are comprised of well-sorted sand (e.g., Donnelly et al., 2004), and contain sharp contacts with surrounding sediment (e.g., Liu and Fearn, 1993; Donnelly et al., 2004; Donnelly, 2005).

TCs are generally far more frequent than tsunamis. This is exemplified in the sedimentary record, as paleotempestological studies generally indicate shorter TC return periods (Liu and Fearn, 2000; Donnelly et al., 2004) than tsunami return periods from paleotsunami literature (Goff et al., 2000; Cochran et al., 2005; Nanayama et al., 2007). Longer return periods in paleotsunami studies can be exacerbated from sediment erosion, leading to lack of preservation (Tappin, 2007).

Jalisco possesses a fairly inactive tsunami history, while containing a decent spatial coverage with observations spanning most of its coast (National Geophysical Data Center, 2011). Only four tsunamis have been documented, occurring in 1975, 1976, and 1995 (2). The most significant tsunami was derived from the infamous Jalisco-Colima 1995 earthquake, magnitude 8.0. The observed tsunami impacts mainly occurred in southern Jalisco, with runup ranging from 3.2 – 5.1 m (Figure 2.2, Table 2.1), without any observed maximum water heights farther north. The remaining tsunamis were observed in Puerto Vallarta with low maximum water heights (<0.25 m).

Guerrero possesses a richer historical tsunami record than Jalisco. From 1732-2011, the Guerrero coast contains records of 42 tsunamis (National Geophysical Data Center, 2011). Most tsunami runup was observed in Acapulco, with others to the east (San Marcos) and west (Ixtapa, Zihuatanejo). Locations with significant runup (≥ 2m) are shown in Figure 2.3, with details of the tsunamis listed in Table 2.2.

2.3 Physical environment of Mexico

Mexico mostly consists of hilly to mountainous terrain. The Mexican Plateau (average elevation 1500 m a.s.l.) stretches from the Texas/central Mexico border to near Mexico City. It is sandwiched between the Sierra Madre Occidental range to the west, and the Sierra Madre

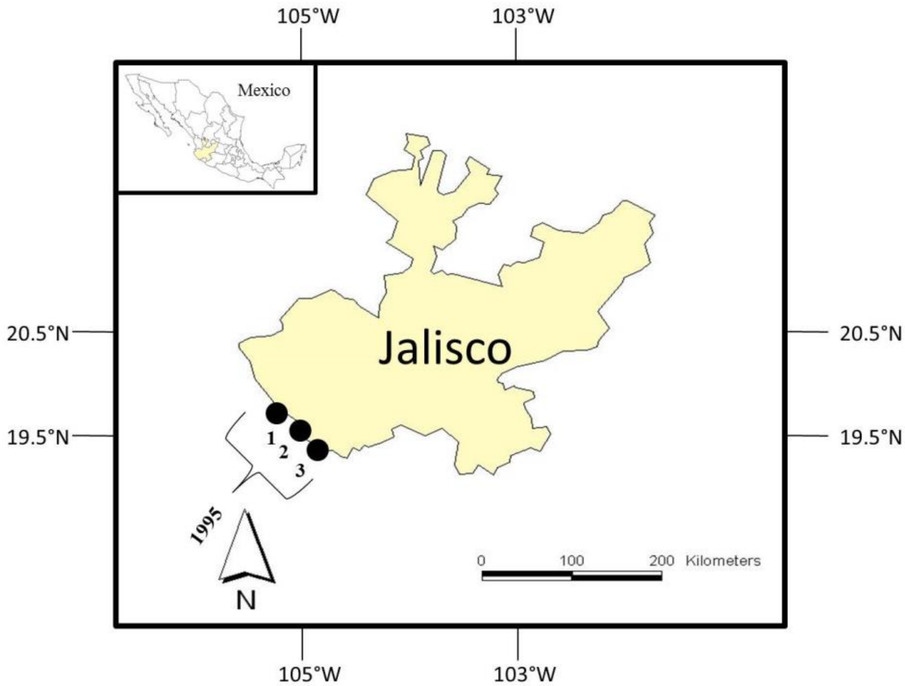

Figure 2.2 – Map of Jalisco depicting areas with documented runup from historical tsunamis. An earthquake in 1995 triggered a tsunami, with runup documented in: 1-San Mateo, Chamela. 2 – El Tecuan. 3-La Manzanila, Cuastecomate, Boca de Iguanas, Melaque. Data are from the National Geophysical Data Center (2011).

Table 2.1 – All historical tsunamis documented on the Jalisco coast (National Geophysical Data Center, 2011).

Year	**Earthquake magnitude**	**Observed**	**Lat/Long**	**Distance from epicenter (km)**	**Max water height (m)**	**Max inundation distance (m)**
1995	8	San Mateo	19.567/-105.08	108	4.9	NA
1995	8	Chamela	19.533/-105.08	106	3.2	NA
1995	8	El Tecuan	19.366/-104.91	82	3.8	NA
1995	8	La Manzanilla	19.267/-104.78	65	4	NA
1995	8	Cuastecomate	19.217/-104.72	57	4.4	NA
1995	8	Boca de Iguanas	19.2/-104.72	56	5.1	NA
1995	8	Melaque	19.21/-104.72	57	4.5	NA

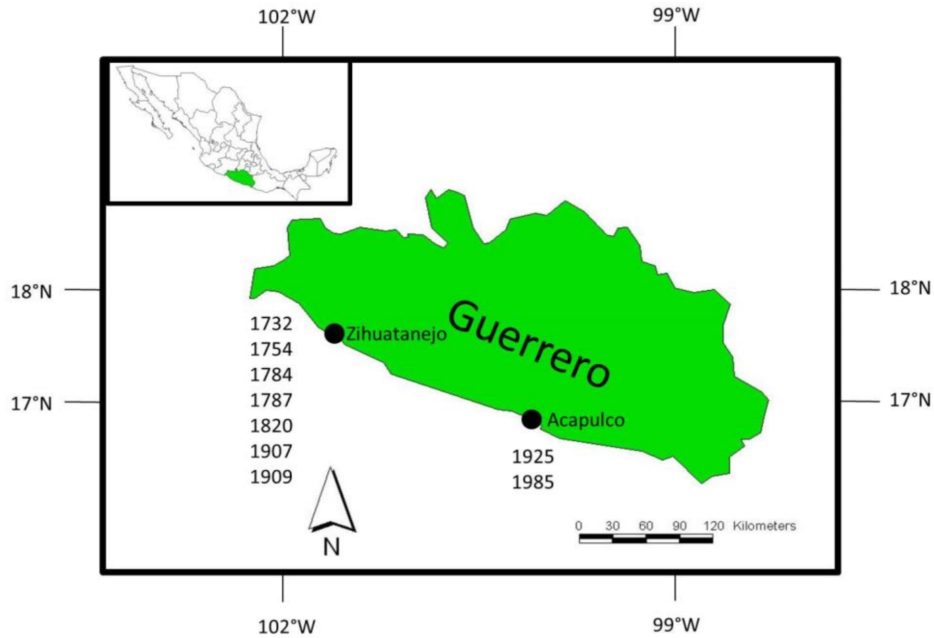

Figure 2.3 – Map of Guerrero depicting sites and years of significant tsunami runup (>2m) during the historical period. Data are from the National Geophysical Data Center (2011).

Table 2.2 – Historical tsunamis with runup >2m for the Guerrero coast (National Geophysical Data Center, 2011).

Year	Earthquake mag.	Observed	Lat/Long	Distance from epicenter (km)	Max water height (m)	Max inundation distance (m)
1732	NA	Acapulco	16.833, -99.917	4	3	NA
1754	NA	Acapulco	16.833, -99.917	76	4	NA
1784	NA	Acapulco	16.833, -99.917	8	3.65	NA
1787	8.3	Acapulco	16.833, -99.917	155	4	NA
1820	7.6	Acapulco	16.833, -99.917	53	4	NA
1907	8.1	Acapulco	16.833, -99.917	21	2	150
1909	7.4	Acapulco	16.833, -99.917	13	9	NA
1925	7	Zihuatanejo	17.667, -101.64	574	11	NA
1985	8	Zihuatanejo	17.667, -101.64	111	3	NA

Oriental range to the east. South of the Sierra Madre Occidental lies the Sierra Madre del Sur range (Figure 2.4).

Much of Mexico is a region of active tectonism. Mexico lies on the western edge of the North American plate on the Oaxaca Block (Dengo, 1985). The oceanic Cocos Plate borders to the west. These two plates collide to form the Middle American Trench Subduction Zone, an area of frequent earthquakes and tsunamis affecting the west coast (Figure 2.5). Geomorphological evidence suggests long-term uplift throughout much of western Mexico. Evidence from Jalisco includes wave-cut notches and marine terraces, some as high as 4.4 m above sea level (a.s.l.) (Ramirez-Herrera and Urrutia-Fucugauchi, 1999).   Ramirez-Herrera et al. (2004) calculated a ~3 mm/yr uplift for coastal Jalisco over the last 1300 years. It is unclear

Figure 2.4 - Physical features of Mexico and surrounding area.

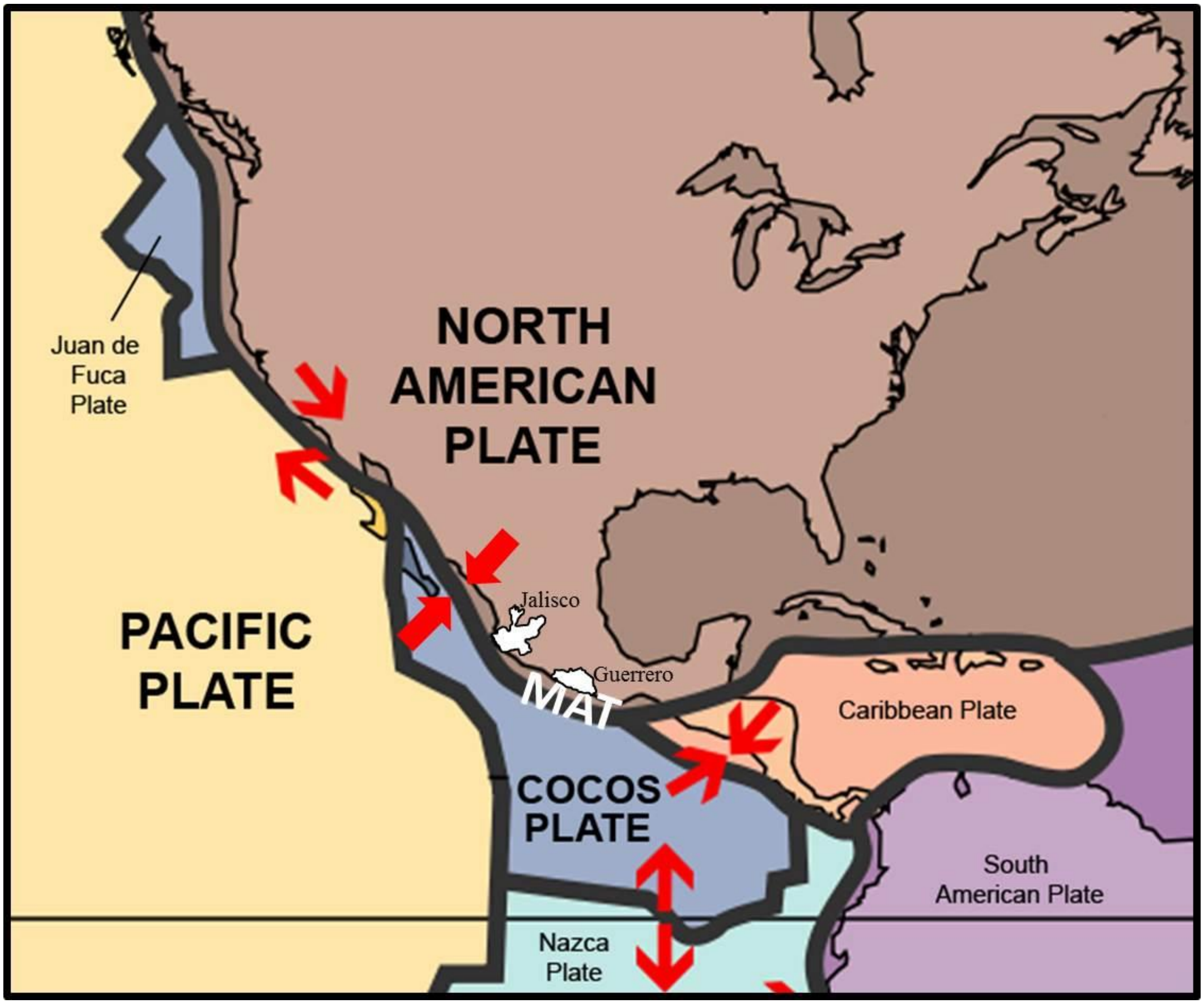

Figure 2.5 – Regional tectonic plates. Direction of plate movement is indicated by red arrows. States Jalisco and Guerrero are outlined. Modified from USGS (http://pubs.usgs.gov/gip/dynamic/slabs.html).

whether uplift is caused by swift events (earthquakes on active plate boundary), longer-term change (alteration through plate subduction), or a combination. While offshore earthquakes often cause Jalisco to subside, plate elasticity causes the land to rebound and slowly uplift (Ramirez-Herrera et al., 2004). Similar to Jalisco, evidence of uplift in Guerrero is exhibited by elevated wave-cut grooves and marine surfaces, some 10-20 m a.s.l. Yet adjacent to the study sites (Chapters 4-6), evidence of uplift does not exist (Ramirez-Herrera and Urrutia-Fucugauchi, 1999).

Western Mexico's coastal geomorphology is shaped largely by its sea level history. Sea level was up to 8 m higher than present during a Pleistocene highstand, responsible for depositing beach ridge remnants inland along the coast (Curray et al., 1969; Lankford, 1977; Voorheis, 2004). A sea level lowstand occurred around 18,000 years BP, a period in which the continental shelf was dominated by terrestrial processes (Lankford, 1977). The most proximate Holocene sea level curve comes from the coastal state of Nayarit (Figure 2.6) (Curray et al., 1969). Rapid sea level rise beginning 18,000 years BP transported offshore sand toward the land and caused the continental shelves to regress. This elevated rate of transgression slightly decreased around 7,000 years BP. Marine waters soon approached the coast, flooding depressions along the continental shelf margins. The rate of transgression began to slow significantly approximately 5000 years BP, which was responsible for the deposition of offshore sands and the beginning stages of coastal beach ridge development. Sea level soon stabilized, as levels have been near present for the last ~3500 years. Stable seas have significantly accelerated beach ridge progradation from both marine and terrestrial processes (Curray et al., 1969; Ramirez-Herrera and Urrutia-Fucugauchi, 1999). Landward of the beach ridge system lie many coastal lagoons, most of them formed as filled-in depressions closed off from the ocean during beach ridge formation (Lankford, 1977). Other characteristics of Pacific coastal lagoons show that they generally possess one narrow channel to the ocean, leading to restricted marine influence (Table 2.4). Largely controlled by local hydrology and rivers, lagoons are usually not connected to the ocean during the dry season, but often open in the wet season from increased riverine input (Kjerve, 1986).

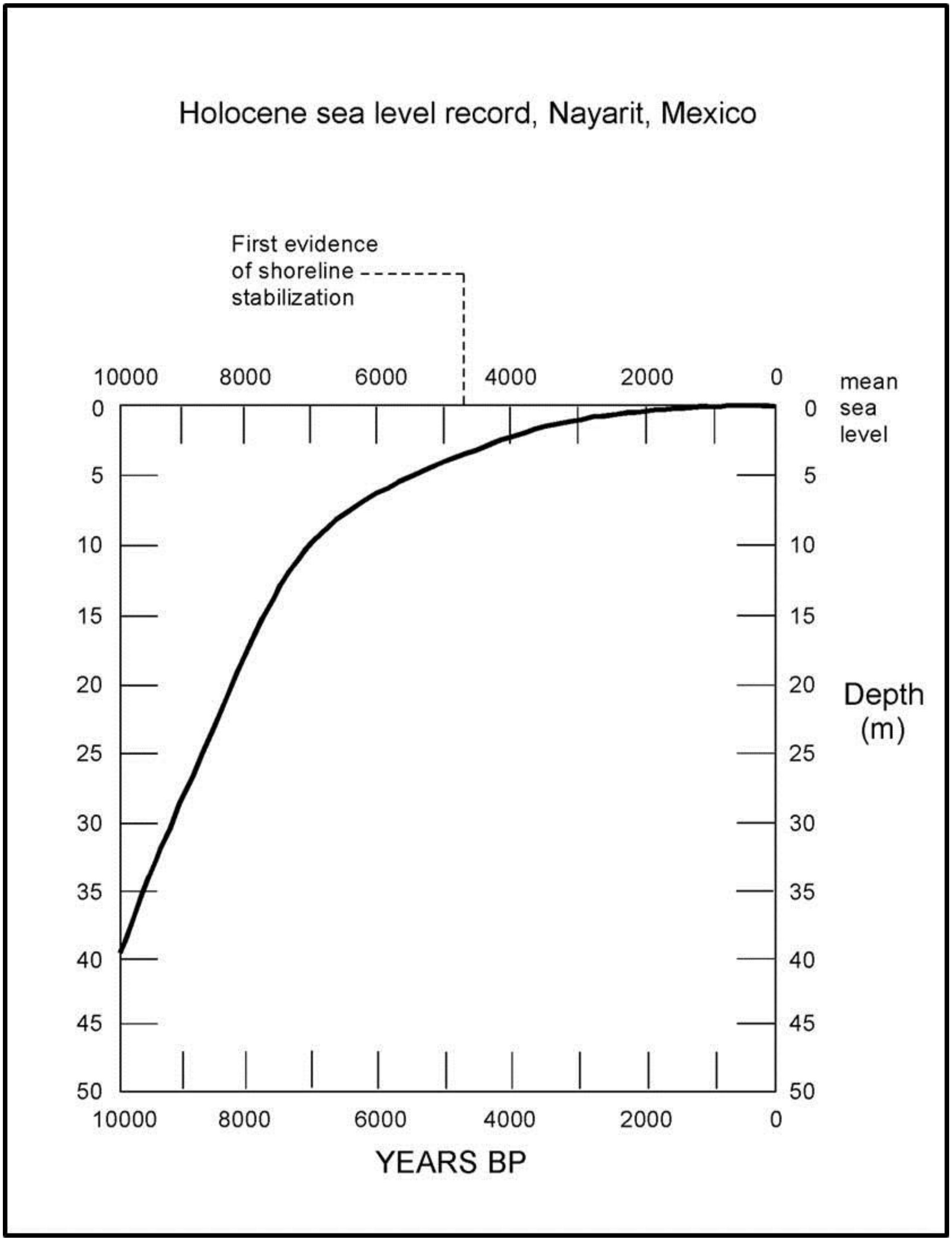

Figure 2.6 - A Holocene sea level record from a 200 km long coastal section of Nayarit (Figure 1.2), Mexico (modified from Curray et al., 1969). Shorelines first began to stabilize around 4750 years BP. This record provides the best regional sea level estimate throughout western Mexico.

Table 2.4 – Characteristics of Pacific coastal lagoons and surroundings (Lankford, 1977).

Characteristics of Pacific coastal lagoons and adjacent areas
Localized runoff
Lagoon energy low, except near channels and during a storm
Tides, storm surges, streams, etc. can change bathymetry
Wide sand barriers
Narrow continental shelf
High wave energy

2.3.1 Climate

Under the Köppen climate classification system, the area of western Mexico between 10-20°N is categorized as *Aw*, indicating a tropical wet/dry climate with all twelve monthly mean temperatures over 64.4°F (18°C) (Blouet, 2002). As a region, Mexico is dominated by a contrasting set of atmospheric controls in the summer months when compared to the winter months (Figure 2.7). Throughout the summer, the subtropical high pressure belt in the northern hemisphere pushes farther north, as precipitation is fueled by a high-pressure system over the Gulf of Mexico, causing moist easterly trade flow. This easterly flow is strengthened by the northward migration of the Inter-Tropical Convergence Zone (ITCZ), leading to increased rainfall throughout much of Mexico (Blouet, 2002). Orographic enhancement in the high elevation of the Mexican Plateau and surrounding mountain ranges enables eastern Mexico to receive more precipitation than the western coast, which sits on the leeward slopes. Meanwhile, easterly flow originating in the eastern tropical Pacific affects western Mexico (Mosiño-Aleman

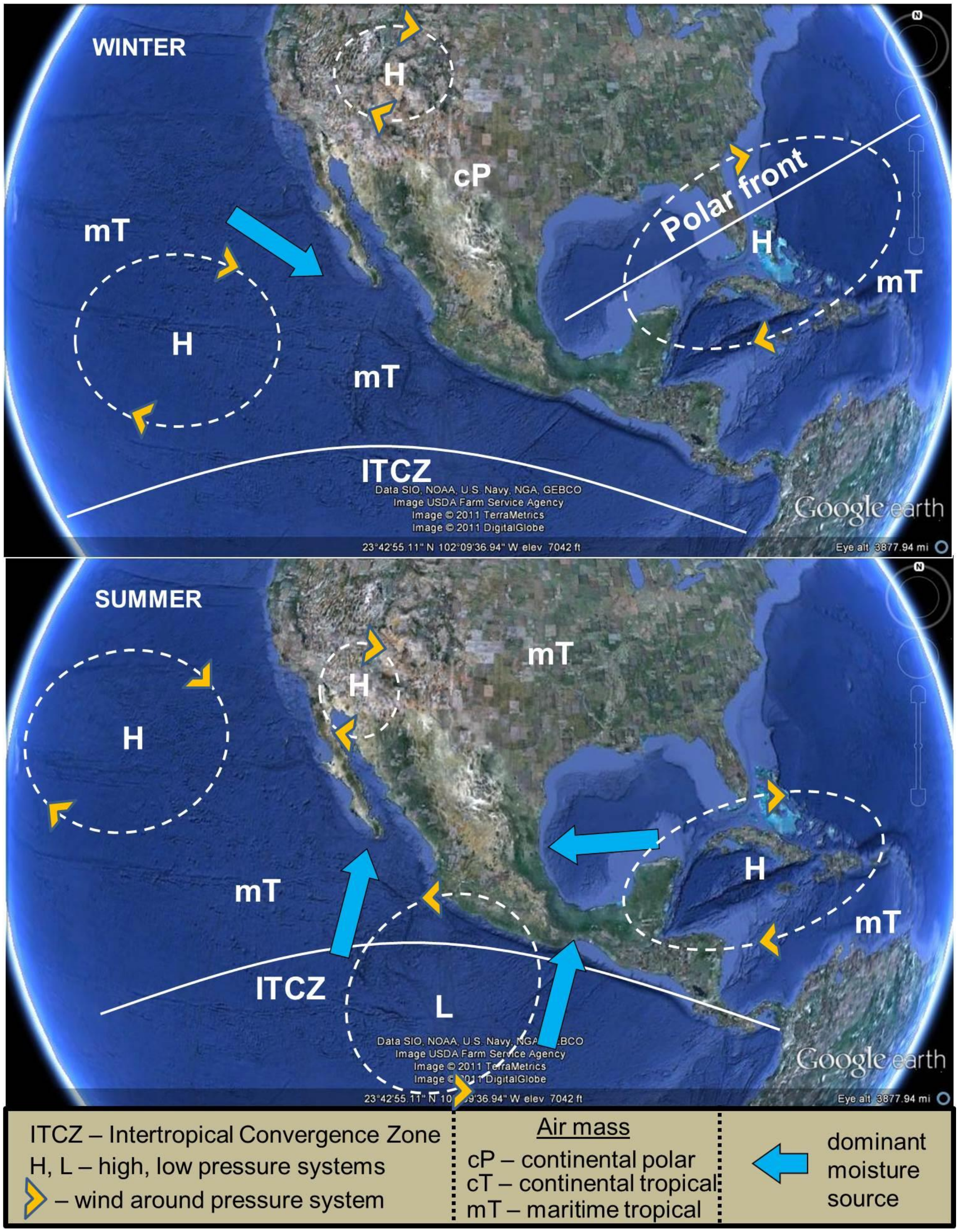

Figure 2.7 - Major circulation and climatological patterns during the winter and summer months. Developed from information in Mosiño-Aleman and Garcia (1974), Metcalfe et al. (2000), and Blouet (2002).

and Garcia, 1974; Metcalfe et al., 2000). During an El Niño period, precipitation along the Pacific coast is increased from a combination of the northward migration of the mid-tropospheric subtropical ridge and increased tropical cyclone frequency (Metcalfe et al., 2000).

Rainfall totals are generally lower nearer the Pacific coast compared to the inland hills and mountains. During the winter months, a shift in mid-tropospheric winds (Douglas et al., 1993) leads to dry westerly flow dominating much of the region as the subtropical high pressure system is positioned northwest of Mexico (Mosiño-Aleman and Garcia, 1974; Blouet, 2002) and the ITCZ lingers to a more southerly position (Rees, 2002). The polar front creeps down from the north toward Mexico, increasing rainfall and snowfall totals around the Sierra Madre Occidental range. Frigid winds and strong storms (*nortes*) are common, with temperatures often dipping below freezing in tropical latitudes (Blouet, 2002).

2.3.2 Vegetation

Mexico's altitudinal zonation leads to a wide variety of flora (Figure 2.8). For western Mexico the elevation gradient is steep toward the Sierra Madre Occidental with precipitation increasing with elevation. Pine-oak forest dominates throughout high elevation areas. Between the pine-oak forest belt and the coast, tropical deciduous forest dominates, home to such genus as *Bursera* and *Lonchocarpus*. At or near the coast lie shrubland (e.g., *Acacia*, *Prosopis*, *Mimosa*) and grassland (Poaceae, Cyperaceae, and Asteraceae) communities (CANABIO, 2008). Low-lying vegetation also consists of mangroves, saltscrubs, and brushwood. This description is echoed in the landmark vegetation classification by Leopold (1950), terming this low-lying, scrub vegetation along the Jalisco, Colima, Michoacan, and NW Guerrero coasts as "thorn forest."

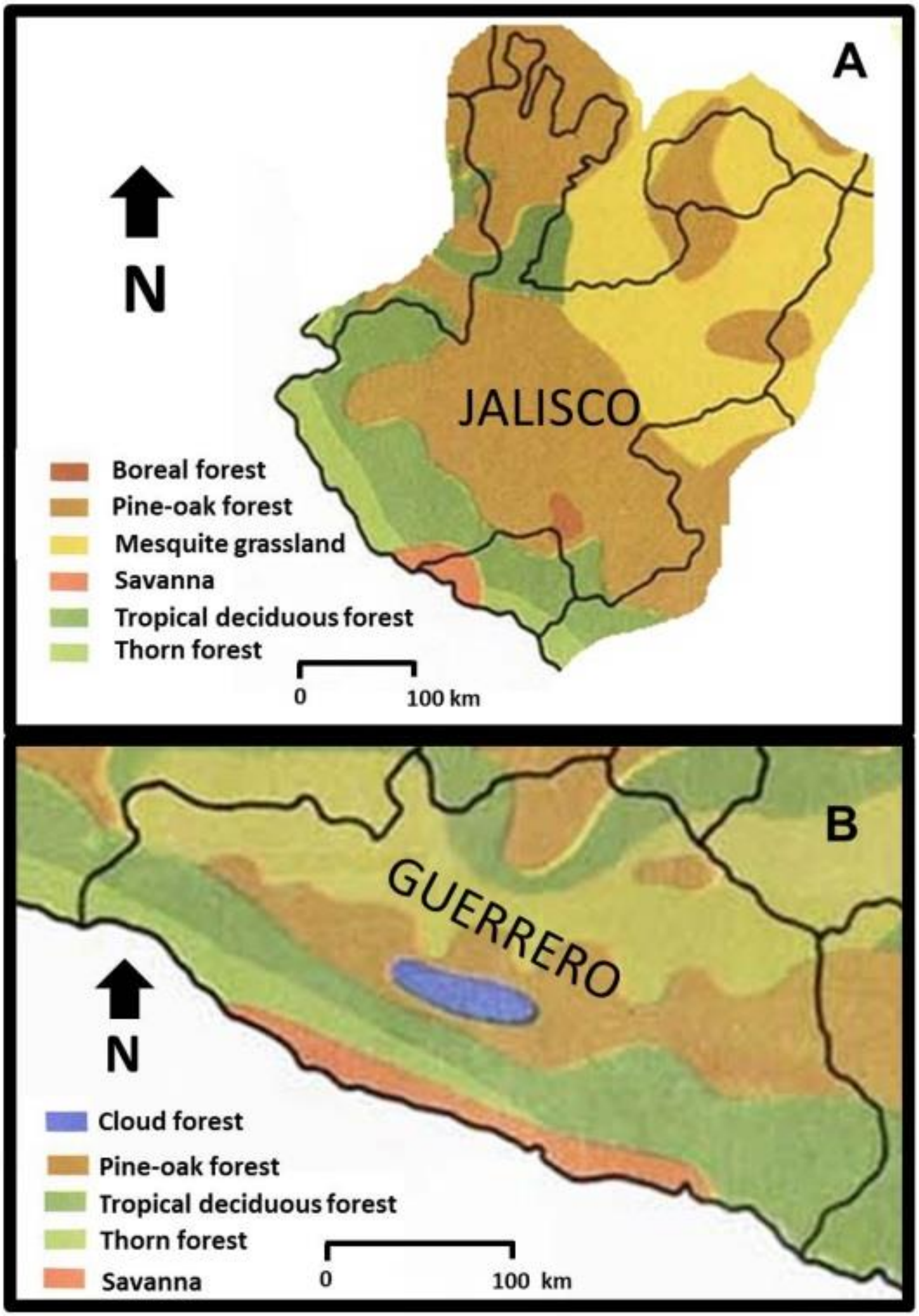

Figure 2.8 - Vegetation map for Jalisco (A) and Guerrero (B). Adapted from Leopold (1959) and modified from the University of Texas (1975).

2.4 ENP hurricane climatology

The historical record for ENP hurricanes begins in 1949, yet data from the satellite era (1963-current) yield more accurate and reliable results (Jauregui, 2003). The ENP basin, per unit area and time, is the most active basin globally (Molinari et al., 2000), averaging 15 named systems annually (National Hurricane Center, 2011). Hurricane season exists from May to November with most activity occurring in September and October (Jauregui, 2003).

ENP TCs originate south of mainland Mexico. Around 72% of cyclogenesis points lie between 90°-110°W (Figure 2.9) (Farfan, 2009). During El Niño, cyclogenesis points are slightly westward compared to La Niña, with tracks more likely to possess a westward trajectory away from land (Irwin and Davis, 1999; Chu, 2004; Camargo et al., 2008), perhaps leading to a longer lifetime (Kimberlain, 1999). General TC track patterns are depicted in Figure 2.9.

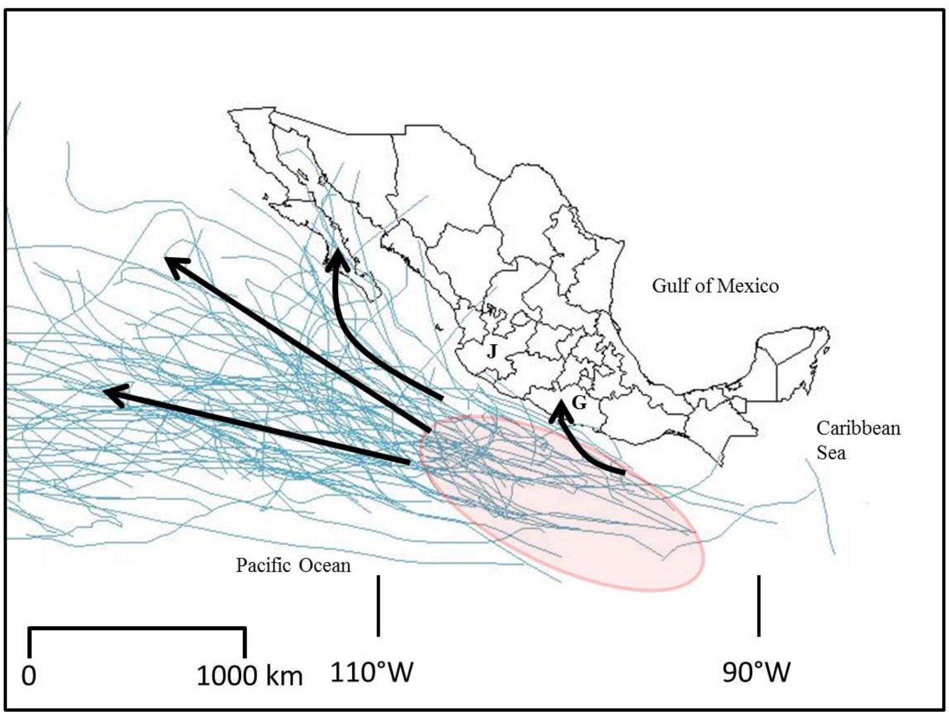

Figure 2.9 – Recent (2001-2008) TC tracks (blue) with area of high cyclogenesis circled (red), between 90° and 110° W. Black arrows depict main qualitative directions of TC movement. The locations of Jalisco (J) and Guerrero (G) are pinpointed. Hurricane track data are from the National Oceanic and Atmospheric Administration (2011b).

Approximately 50% of all TCs travel west or west-northwest, eventually dissipating in the central Pacific Ocean (Romero-Vadillo et al., 2007). The remaining ~50% of TCs traverse in a more northerly direction, pummeling the coast with heavy wind and rainfall. The high elevations of the Sierra Madre mountains often act as a 'buffer,' preventing consistent direct landfalls (Sanson, 2004). When TCs directly hit mainland states (Jalisco, down to Oaxaca) it is usually caused by upper westerlies hovering near the surface of the Mexican plateau (Mosiño-Aleman and Garcia, 1974).

Jauregui (2003) tabulated western Mexico TC landfalls per state (Figure 2.10). Despite their long coastlines, TCs rarely hit Chiapas (5 TC strikes), as typically they travel northward or away from the coast. TC landfall frequency increases northwest in Oaxaca (13 landfalls) and Guerrero (13) while increasing further in more northwesterly states Michoacán (18) and Jalisco (20), both with relatively small coastlines. Baja California Sur (49 landfalls) and Sinaloa (26) exhibit the highest activity due to the typical curving tracks hitting these areas. Remaining states are either too distant (Baja California Norte-4) or sheltered (Sonora-1, Nayarit-2) to be frequently hit by TCs.

ENP TC rainfall is noteworthy, with erosion, slopewash, and mudslides common in western Mexico. Some areas have 50% of seasonal rainfall attributed to TCs (Fig 2.11). Larson et al. (2005) suggest that El Niño periods are responsible for increased TC rainfall to northwestern Mexico, yet farther south the effects could be minimal. Rodgers et al. (2000) agree, noting that TCs dump more precipitation during El Niño due to influence of the monsoon trough and warmer SSTs. However, they suggest that the most significant effects might occur in the open ocean, with possibly a lesser impact along western Mexico.

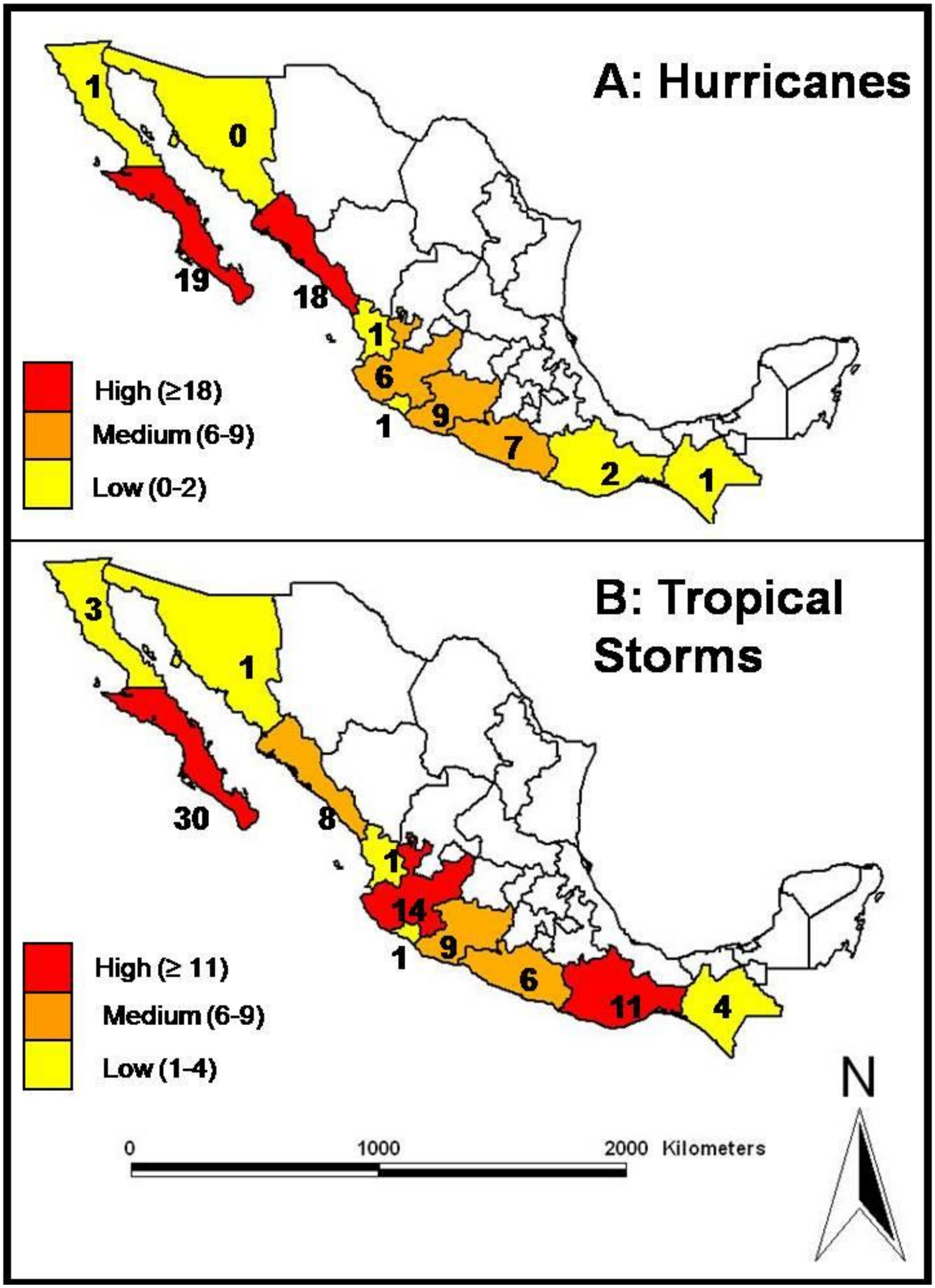

Figure 2.10 – Hurricane (A) and Tropical Storm (B) landfalls for western Mexico from 1951 to 2000. Data from Jauregui (2003).

Figure 2.11 – Percentage of warm season rainfall (May to November) attributed to tropical cyclones, passing within 550 km of the weather stations. Elevated TC rainfall percentages occur in regions with high TC activity and low annual rainfall totals, such as Baja California Sur, Guerrero, and Jalisco. Data are from Englehart and Douglas (2001).

Climatological controls regarding ENP TC intensity and frequency operate on monthly (Madden Julian Oscillation [MJO], 30-60 day cycle) and interannual (ENSO, 2-7 year cycle) timescales. TCs are generally stronger during the MJO western phase, when westerly 850-mb equatorial zonal wind anomalies lead to decreased vertical wind shear and high relative vorticity (Maloney and Hartmann, 2000). ENSO effects on intensity have been more controversial, as some (Whitney and Hobgood, 1997) claim that ENSO is not a major factor in relative or maximum intensities while most (Landsea and Gray, 1989; Gray and Sheaffer, 1991; Rodgers et al., 2000) suggest that more intense ENP hurricanes occur during El Niño, mainly from warm surface waters (Romero-Vadillo et al., 2007). Similar to intensity, TCs are more frequent during a westerly MJO than an easterly phase (Maloney and Hartmann, 2000). Some conclude (Whitney and Hobgood, 1997) that ENSO does not affect TC frequency, yet most (Landsea and Gray, 1989; Goldenberg and Shapiro, 1996; Rodgers et al., 2000; Chu, 2004) conclude that

during El Niño TCs are more frequent, as 116 El Niño TCs and only 90 La Niña TCs occurred from 1987-1998 (Rodgers et al., 2000). Whitney and Hobgood (1997) document a small decrease in TC frequency during westerly phase of the Quasi-biennial Oscillation (QBO).

Globally, TCs exhibit temporal variability, whether seasonal (Elsner et al., 2000) or decadal (Elsner et al., 1999; Goldenberg et al., 2001), with paleotempestologists expanding these to centennial (Donnelly and Woodruff, 2007) even millennial timescales (Liu and Fearn, 2000). For ENP TCs both short- and long-term variations have been documented. Using Bayesian change point analysis, Zhao and Chu (2006) discovered an active period from 1982-1998, which is between two inactive periods, from 1972-1981 and 1999-2003. Goman et al. (2005) discovered an active period from 3500-2300 cal yr BP from sediments in coastal Oaxaca, attributed to an increase in El Niño frequency.

2.5 Geophysical and ecological damage from ENP hurricanes

ENP TC effects on Mexico's coastal geomorphology are not well-documented. TC-induced overwash fans have been discovered, most notably in Oaxaca from Hurricane Pauline and its 9 m storm surge (Goman et al., 2005).

ENP TCs disturb western Mexico tropical dry forests. Type and severity of damage depends upon storm intensity and duration, soil type, topography, and vegetation susceptibility. Wind damage often leads to defoliation (Tanner et al., 1991; Sanchez and Islebe, 1999), and snapped branches (Dittus, 1985). In severe cases large trees can be uprooted (Pascarella et al., 2004) and understory brush can be toppled (Dittus, 1985; Sanchez and Islebe, 1999). Heliophytic (light-loving) species emerge in forest gaps as evidenced from Hurricane Gilbert damage in Quintana Roo (Sanchez and Islebe, 1999). Due to the aridity of Mexico's Pacific coast, TCs result in a substantial amount of a region's annual rainfall (Figure 2.11), while

responsible for most intense rainfalls (Bullock, 1986). TC rain can saturate and weaken topsoil, increasing vegetation susceptibility to damage (Clark and Ward, 2000). The general aridity suggests that the hurricane-fire interaction (Myers and van Lear, 1998; Liu et al., 2008) could exist in western Mexico as forest fires can occur after hurricanes, documented after Hurricane Gilbert in the Yucatan peninsula (Trejo, 2008).

Mangrove swamps are common on the Pacific coast of Mexico. They mainly consist of red mangrove (*Rhizophora mangle*), which is able to handle extreme environments including tidal influence and salinity uptake. Damage surveys in mangrove swamps (McCoy et al., 1996; Kovacs et al., 2004) suggest that *Rhizophora mangle* is least affected from hurricane damage compared to black (*Avicennia germinans*) and white mangrove (*Laguncularia racemosa*).

2.6 Paleoclimate and paleoenvironment

Paleoclimatological and paleoenvironmental research has been conducted throughout much of Mexico. The regional foci have been the Sierra Madre highlands, Yucatan peninsula, and northern desert regions, while Pacific coastal studies are rare (Figure 2.12). Two reviews provide thorough information regarding Mexico's paleoclimatological history. Brown's (1985) synopsis covers early works divided into marine, lacustrine, and archaeological studies. Marine studies (Table 2.5) include research from the Gulf of California (Byrne, 1982; Heusser, 1982), Middle American Trench just offshore of Oaxaca (Habib et al., 1970), and Laguna Tetitlan from coastal Guerrero (Gonzalez-Quintero, 1980), with results from the Gulf of California covering the longest time period. Studies from the Gulf of California and the Middle American Trench contain certain parallels, namely a relatively warm and wet period from ~6,000-3,000 yr BP. While both areas were dry from ~9,000 to ~6,000 years BP, the temperature was warmer in the Gulf of California than the Middle American Trench. The Late Holocene climate record from

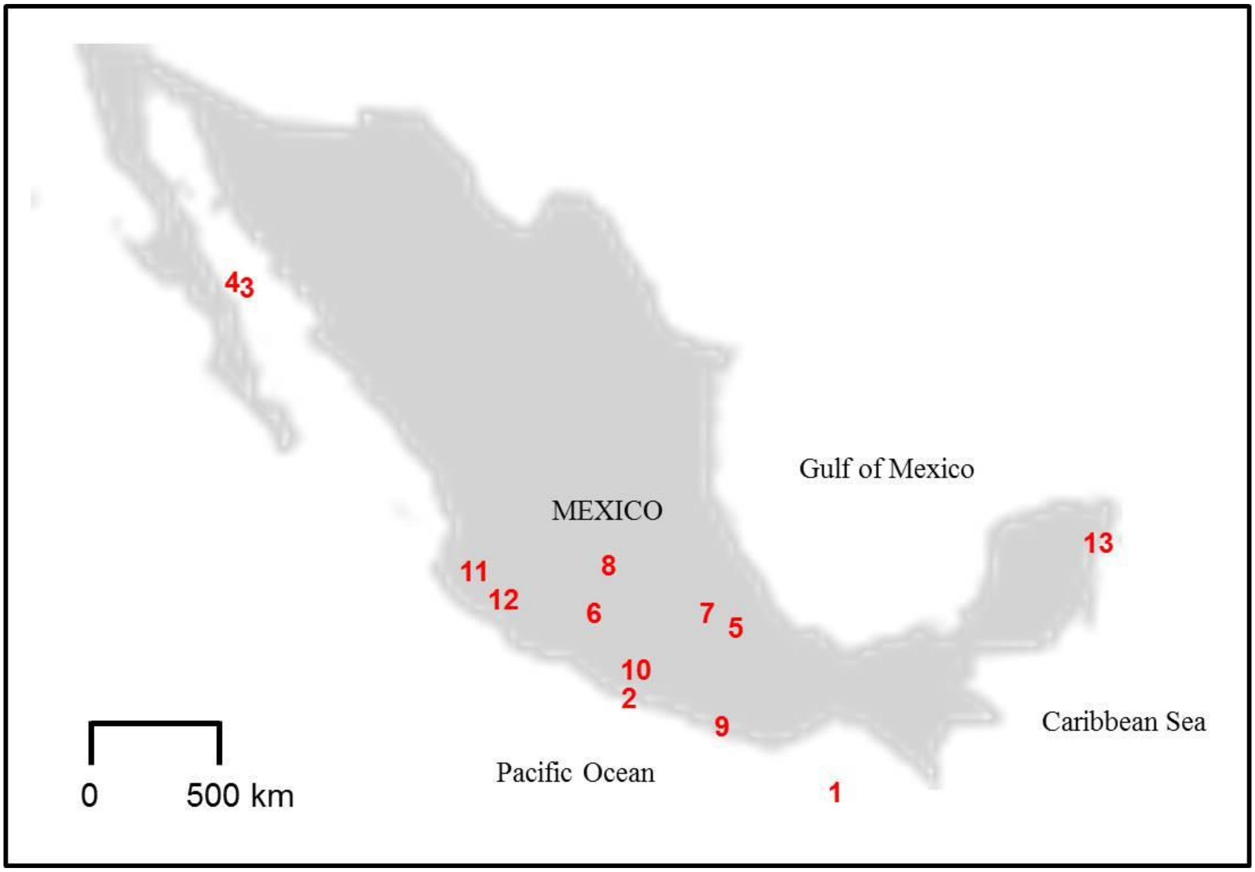

Figure 2.12 – Notable paleoclimatological/paleoenvironmental study sites. 1 – Middle American Trench (Habib et al., 1970). 2 – Laguna Tetitlan (Gonzalez-Quintero, 1980), Laguna Mitla (Ramirez-Herrera et al., 2009). 3 – Guaymas Basin (Heusser, 1982). 4 – Gulf of California (Byrne, 1982). 5 – Tlaqua Crater (Ohngemach, 1977). 6 – Lake Patzcuaro (Watts and Bradbury, 1982). 7 – Texcoco, Mexico City Basin (Gonzalez-Quintero and Fuentes-Mata, 1980). 8 – Multiple sites throughout Central Mexico (Brown, 1984). 9 – Laguna Pastoria (Goman et al., 2005, 2010). 10 – Lakes Tixtla, Huitziltepic (Berrio et al., 2006). 11 – Laguna de Juancatlan (Metcalfe et al., 2010). 12 – Sierra de Manantlan Biosphere Reserve (Figueroa-Rangel et al., 2008, 2010). 13 – Quintana Roo (Islebe and Sanchez, 2002).

Laguna Tetitlan is gauged by pollen percentages of tropical (*Rhizophora*, Palmae) versus temperate elements (*Pinus*, *Quercus*).

Long-term records from lacustrine settings (Table 2.6) were mainly recovered in the Sierra Madre region. Throughout the late Holocene, human disturbance was significant as expressed by influx of Cheno-Am and Graminae pollen during the Mesoamerican civilization and subsequent land degradation. Despite agreement throughout the lacustrine records,

Table 2.5 - Summary of paleoclimate conditions from three ‘marine’ (two oceanic, one lagoonal) environments. Information compiled by Brown (1985).

Marine cores (Brown, 1985)	Time (cal yr BP)	Conditions
Middle American Trench (Habib et al., 1970)		
	0-1000	Dry
	1000-1750	Wet
	1750-3000	Very dry
	3000-5000/6000	Very warm, very wet
	5000/6000-8000/9000	Cool and dry/moist
Laguna Tetitlan, Guerrero (Gonzalez-Quintero, 1980)		
	0-1000	Warm, wet
	1000-1800	Temperate
	1800-2500	Hot, dry
	>2500	Very hot, wet
Gulf of California (Byrne, 1982; Heusser, 1982)		
	0-3000	Decreasing summer rain
	3000-5500/6500	Substantial winter rain
	~6500-9500/10000	Warm, dry
	>9500/10000	Cool, dry

discrepancies occurred during the early transition from cold/dry to warm/wet. This shift occurred in the Mexico City Basin around 12,000 yr BP, yet in other areas such as Lake Patzcuaro in the Michoacan uplands around ~9500 yr BP. Another discrepancy occurred around ~5,000-3,000 yr BP, when much of central Mexico was dry yet eastern Mexico was rather moist around the Puebla-Tlaxcala Basin (Ohngemach, 1977).

Metcalfe et al. (2000) compiled additional data from central and northern Mexico, along with the Yucatan peninsula to detect temporal and geographic trends in moisture. The

Table 2.6 - Summary of paleoclimate conditions from lacustrine settings in the highland region. Information compiled by Brown (1985).

Lacustrine (Brown, 1985)			
Time (cal yr BP)	Conditions	Notes and examples (study sites)	Examples
Late Holocene	Human disturbance	La Malinche Volcano, Tlaxcala	Ohngemach, 1977
3000/3500 - 4500/5000	Mostly dry, but wetter toward the east	Lake Patzcuaro, Michoacan La Malinche Volcano, Tlaxcala	Ohngemach, 1977; Watts and Bradbury, 1982
4500/5000 - 6500	Dry	Lake Texcoco, Mexico City Basin	Gonzalez-Quintero and Fuentes-Mata, 1980
6500 - 9500	Generally warm, wet	Climatic fluctuations in Mexico City Basin, dry in Hoya de San Nicolas	Gonzalez-Quintero and Fuentes-Mata, 1980; Watts and Bradbury, 1982; Brown, 1984
12000	Shift from cold/dry to warm/wet	Lake Texcoco, Mexico City Basin	Gonzalez-Quintero and Fuentes-Mata, 1980
		Occurs some areas ~9500 yrs BP (Patzcuaro, La Malinche)	Ohngemach, 1977; Watts and Bradbury, 1982

information is simplified (Figure 2.13) to indicate broad trends. At times northern Mexico and the Yucatan peninsula exhibit similar moisture trends, while other times their signals are contrasting. Central Mexico is the most variable region, as trends can shift in the Basin of Mexico while not occurring in nearby regions (also indicated in Brown, 1985). Evidence of a dry period discovered from the Yucatan peninsula from 1500-900 yr BP is suggested as a major contributor toward the collapse of the Mayan civilization (Leydan et al., 1996; Metcalfe et al., 2000). Metcalfe et al. (2000) admit that many variables could cause climatic shifts in the

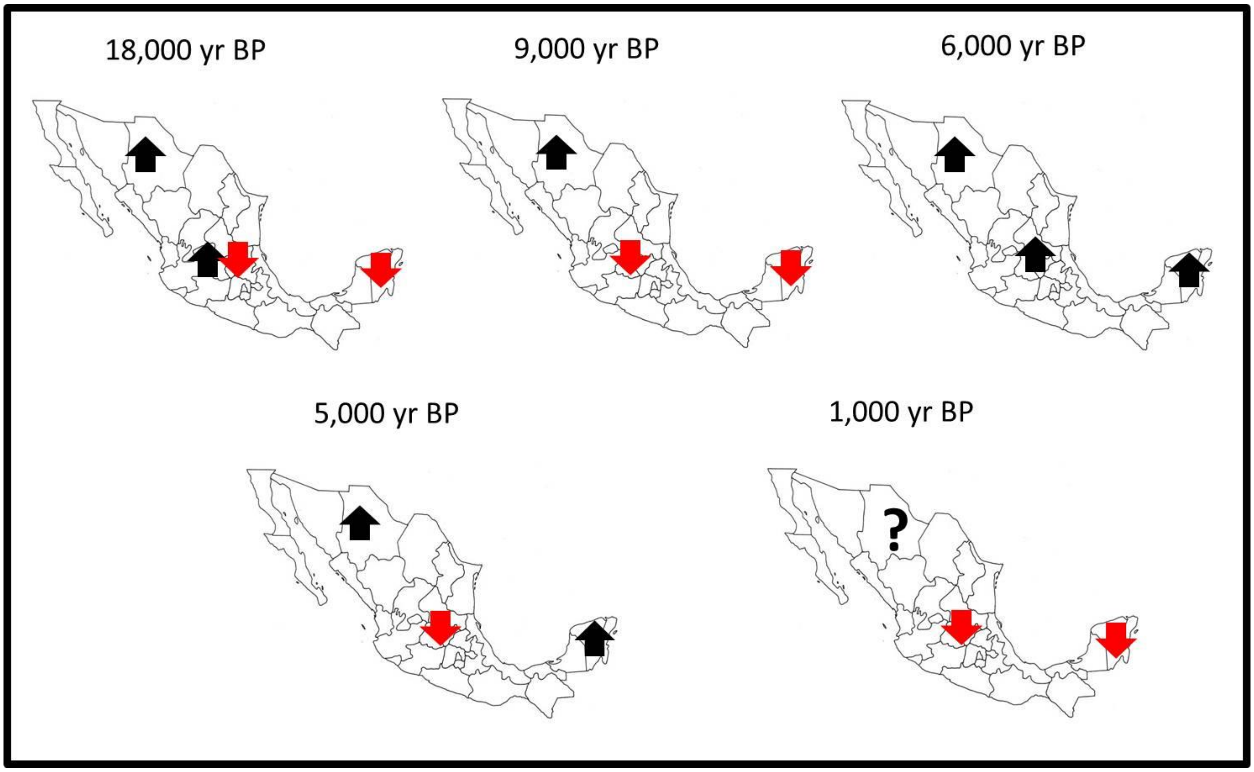

Figure 2.13 – Spatial distribution of moisture increases (black arrow) or decreases (red arrow) compared with current period. Up and down arrows pinpointed on the Sierra Madre highlands at 18,000 yr BP indicate a mixed climatic signal. Information is from Metcalfe et al. (2000).

paleorecord. One example is sea surface temperature and its effect on the spatial locations of upper air ridge locations, notably the Bermuda High. At 12,000 yr BP the Bermuda High pressure system migrated west and strengthened during a period with a 6 C° cooler Gulf of Mexico, leading to increased aridity along eastern and central Mexico while the southwest USA was rather moist (Kutzbach and Guetter, 1986). Section 2.3 summarizes major atmospheric patterns that could explain climatic shifts.

2.6.1 Guerrero, regional focus

Guerrero, like the rest of coastal western Mexico, contains rather limited paleoclimatological and paleoenvironmental information. Paleoenvironmental studies have been conducted east in Oaxaca, with human disturbance, agricultural expansion, coastal barrier formation, and ENSO activity being the main foci (Goman et al., 2005, 2010). The pioneer

palynological record from Guerrero comes from the aforementioned study from Laguna Tetitlan (Gonzalez-Quintero, 1980). A palynological investigation from Laguna Mitla conducted by Kennett et al. (2004) cited by Ramirez-Herrera et al. (2009) detected land-level changes and evidence of marine influence. A summary of environmental and climatic change from a recent analysis in the Guerrero highlands is given by Berrio et al. (2006) (see Table 2.7).

2.6.2 Jalisco, regional focus

While paleoenvironmental literature is poor for the Jalisco coast, upland areas have been analyzed more thoroughly. Climate (ITCZ migration, ENSO variability, solar forcing) and anthropogenic influence are the main forcing mechanisms regarding upland cloud forest (e.g., *Pinus*) expansion (Figueroa-Rangel et al., 2008, 2010). In a study at Laguna de Juanacatlan in upland Jalisco, Metcalfe et al. (2010) interpreted peaks in titanium (Ti) as an influx of runoff/precipitation, climatically driven by ENSO variability and solar forcing (Table 2.8).

2.6.3 Mangroves

While several palynological studies from mangrove swamps are available from Central America and the Caribbean (Peros et al., 2007; Wooller et al., 2007; Urrego et al., 2009; Gonzalez et al., 2010), they are rather rare in western Mexico. Similar to work from Gonzalez-Quintero (1980), a study from the Yucatan Peninsula (Islebe and Sanchez, 2002) interpreted an increase in *Rhizophora* as an increase in humidity, while a surplus of *Conocarpus* signified drier conditions. Dry periods existed between 1000-0 and 1500-1200 ^{14}C yr BP, while humid periods occurred around 1200-1000, 1500, and 2500 ^{14}C yr BP. Notably, the recent 1000-0 ^{14}C yr dry period for the Yucatan is a humid period for Laguna Tetitlan, while the 2500-1800 yr dry period for Laguna Tetitlan is humid in the Yucatan. The discrepancy between the Yucatan and Tetitlan records suggests a possible anti-phase pattern between eastern and western Mexico.

Table 2.7 – Paleoclimatic conditions over the last 2700 years for the Guerrero highlands. Data from Berrio et al. (2006).

Time (cal yr BP)	Condition	Notes
0-225	Still dry	Increase in dry deciduous taxa, decrease in mesophyllus taxa
225-750	Drier	Increase in dry deciduous taxa, decrease in mesophyllus taxa
750-1070	Still humid	Abundance of mesophyllus taxa, still rather low in deciduous taxa
1070-1550	Further increase in humidity	Maximum expansion of mesophyllus taxa
1550-1950	Increase in humidity	Increase in mesophyllus taxa, decrease in deciduous taxa
1950-2450	Fairly transitional	Mix of dry, moist taxa
2450-2700	Dry	Dry, deciduous taxa

Table 2.8 – Paleoclimatic conditions for Laguna Juanacatlan. Data from Metcalfe et al. (2010).

Time (yr AD)	Climate
Mid 1900s-current	Variable
Early 1800s to mid 1900s	Wet
Late 1700s to early 1800s	Dry
1700s	Wet
1600s	Transition
1400-1600	Dry (Little Ice Age)
1200-1350	Wet (Medieval Period)
300-900	Dry

2.7 References

Baines, G. B. K. and R. F. McLean. 1976. Sequential studies of hurricane deposit evolution at Funafuti Atoll. Marine Geology **21**:M1-M8.

Ball, M. M., E. A. Shinn, and K. W. Stockman. 1967. The geologic effects of Hurricane Donna in south Florida. The Journal of Geology **75**:583-597.

Bender, M. A., T. R. Knutson, R. E. Tuleya, J. J. Sirutis, G. A. Vecchi, S. T. Garner, and I. M. Held. 2010. Modeled impact of anthropogenic warming on the frequency of intense Atlantic hurricanes. Science **327**:454-458.

Berrio, J. C., H. Hooghiemstra, B. van Geel, and B. Ludlow-Wiechers. 2006. Environmental history of the dry forest biome of Guerrero, Mexico, and human impact during the last c. 2700 years. Holocene **16**:63-80.

Blouet, B. W. 2002. The Environment. Pages 13-50 *in* B. W. Blouet and O. M. Blouet, editors. Latin America and the Caribbean: A systematic and regional survey. John Wiley and Sons, New York.

Brown, R. B. 1984. The paleoecology of the northern frontier of Mesoamerica. Unpublished. University of Arizona, Tucson.

Brown, R. B. 1985. A summary of late-Quaternary pollen records from Mexico west of the Isthmus of Tehuantepec. Pages 71-94 *in* V. M. Bryant and R. G. Holloway, editors. Pollen records of late-Quaternary North American sediments. AASP Foundation.

Bullock, S. H. 1986. Climate of Chamela, Jalisco, and trends in the south coastal region of Mexico. Archives for Meteorology Geophysics and Bioclimatology Series B-Theoretical and Applied Climatology **36**:297-316.

Bussert, R. and M. Aberhan. 2004. Storms and tsunamis: evidence of event sedimentation in the Late Jurassic Tendaguru Beds of southeastern Tanzania. Journal of African Earth Sciences **39**:549-555.

Byrne, R. 1982. Preliminary pollen analysis of deep sea drilling project leg 64, hole 480, cores 1-11. US Government Printing Office, Washington, D.C.

Camargo, S. J., A. W. Robertson, A. G. Barnston, and M. Ghil. 2008. Clustering of eastern North Pacific tropical cyclone tracks: ENSO and MJO effects. Geochemistry Geophysics Geosystems **9**. DOI 10.1029/2007GC001861.

CANABIO. 2008. Main Vegetation Types: Michoacan Case. Retrieved December 13, 2011, from http://www.conabio.gob.mx/conocimiento/cambios_veg/doctos_ing/tipos.html.

Chagué-Goff, C., S. Dawson, J. R. Goff, J. Zachariasen, K. R. Berryman, D. L. Garnett, H. M. Waldron, and D. C. Mildenhall. 2002. A tsunami (ca. 6300 years BP) and other Holocene environmental changes, northern Hawke's Bay, New Zealand. Sedimentary Geology **150**:89-102.

Chu, P. S. 2004. ENSO and Tropical Cyclone Activity. Pages 297-332 *in* R. J. Murnane and K. B. Liu, editors. Hurricanes and Typhoons: Past, Present, and Future. Columbia University Press, New York.

Clark, W. H. and D. M. Ward. 2000. Hurricane impacts in the central desert of Baja California Norte, Mexico. Haseltonia **7**:81-85.

Cochran, D. M., C. A. Reese, and K. B. Liu. 2009. Tropical Storm Gamma and the Mosquitia of eastern Honduras: a little-known story from the 2005 hurricane season. Area **41**:425-434.

Cochran, U. A., K. R. Berryman, D. C. Mildenhall, B. W. Hayward, K. Southall, and C. J. Hollis. 2005. Towards a record of Holocene tsunami and storms for northern Hawke's Bay, New Zealand. New Zealand Journal of Geology and Geophysics **48**:507-515.

Collins, E. S., D. B. Scott, and P. T. Gayes. 1999. Hurricane records on the South Carolina coast: Can they be detected in the sediment record? Quaternary International **56**:15-26.

Crosby, M. K. and C. A. Reese. 2009. Geologic evidence of Hurricane Rita recovered from Texas Point, TX. Southeastern Geographer **49**:41-48.

Curray, F., J. Emmel, and P. J. Crampton. 1969. Holocene history of a strand plain lagoonal coast, Nayarit, Mexico. Pages 63-100 *in* A. Ayala-Castanares, editor. Coastal Lagoons: A Symposium. Universidad Nacional Autonoma de Mexico. Mexico City.

Dawson, A. G. and S. Z. Shi. 2000. Tsunami deposits. Pure and Applied Geophysics **157**:875-897.

Dawson, S. 2007. Diatom biostratigraphy of tsunami deposits: Examples from the 1998 Papua New Guinea tsunami. Sedimentary Geology **200**:328-335.

Dawson, S. and D. E. Smith. 2000. The sedimentology of Middle Holocene tsunami facies in northern Sutherland, Scotland, UK. Marine Geology **170**:69-79.

Dengo, G. 1985. Mid America: Tectonic setting for the Pacific margin from southern Mexico to northwestern Colombia. Pages 123-180 *in* A. E. M. Nairn, F. G. Stehli, and S. Uyeda, editors. The Ocean Basins and Margins. Plenum Press, New York.

Dezileau, L., P. Sabatier, P. Blanchemanche, B. Joly, D. Swingedouw, C. Cassou, J. Castaings, P. Martinez, and U. Von Grafenstein. 2011. Intense storm activity during the Little Ice Age on the French Mediterranean coast. Palaeogeography Palaeoclimatology Palaeoecology **299**:289-297.

Dittus, W. P. J. 1985. The influence of cyclones on the dry evergreen forest of Sri-Lanka. Biotropica **17**:1-14.

Dominey-Howes, D. T. M., G. S. Humphreys, and P. P. Hesse. 2006. Tsunami and palaeotsunami depositional signatures and their potential value in understanding the late-Holocene tsunami record. Holocene **16**:1095-1107.

Donnelly, J. P. 2005. Evidence of past intense tropical cyclones from backbarrier salt pond sediments: A case study from Isla de Culebrita, Puerto Rico, USA. Journal of Coastal Research **SI42**:201-210.

Donnelly, J. P., S. S. Bryant, J. Butler, J. Dowling, L. Fan, N. Hausmann, P. Newby, B. Shuman, J. Stern, K. Westover, and T. Webb. 2001a. 700 yr sedimentary record of intense hurricane landfalls in southern New England. Geological Society of America Bulletin **113**:714-727.

Donnelly, J. P., J. Butler, S. Roll, M. Wengren, and T. Webb. 2004. A backbarrier overwash record of intense storms from Brigantine, New Jersey. Marine Geology **210**:107-121.

Donnelly, J. P., S. Roll, M. Wengren, J. Butler, R. Lederer, and T. Webb. 2001b. Sedimentary evidence of intense hurricane strikes from New Jersey. Geology **29**:615-618.

Donnelly, J. P. and J. D. Woodruff. 2007. Intense hurricane activity over the past 5,000 years controlled by El Niño and the West African monsoon. Nature **447**:465-468.

Douglas, M. W., R. A. Maddox, K. Howard, and S. Reyes. 1993. The Mexican Monsoon. Journal of Climate **6**:1665-1677.

Elsner, J. B. 2006. Evidence in support of the climate change - Atlantic hurricane hypothesis. Geophysical Research Letters **33**:10.1029/2006GL026869.

Elsner, J. B. and A. B. Kara. 1999. Hurricanes of the North Atlantic: Climate and Society. Oxford University Press, New York.

Elsner, J. B., A. B. Kara, and M. A. Owens. 1999. Fluctuations in North Atlantic hurricane frequency. Journal of Climate **12**:427-437.

Elsner, J. B., T. H. Jagger, and K. B. Liu. 2008. Comparison of hurricane return levels using historical and geological records. Journal of Applied Meteorology and Climatology **47**:368-374.

Elsner, J. B., K. B. Liu, and B. Kocher. 2000. Spatial variations in major US hurricane activity: Statistics and a physical mechanism. Journal of Climate **13**:2293-2305.

Englehart, P. J. and A. V. Douglas. 2001. The role of eastern North Pacific tropical storms in the rainfall climatology of western Mexico. International Journal of Climatology **21**:1357-1370.

Fan, D. and K. B. Liu. 2008. Perspectives on the linkage between typhoon activity and global warming from recent research advances in paleotempestology. Chinese Science Bulletin **53**:2907-2922.

Farfan, L. M. 2009. Eastern Pacific hurricanes and their impact over western Mexico. Lecture, Louisiana State University, Department of Oceanography and Coastal Sciences. Baton Rouge, Louisiana.

Figueroa-Rangel, B. L., K. J. Willis, and M. Olvera-Vargas. 2008. 4200 years of pine-dominated upland forest dynamics in west-central Mexico: Human or natural legacy? Ecology **89**:1893-1907.

Figueroa-Rangel, B. L., K. J. Willis, and M. Olvera-Vargas. 2010. Cloud forest dynamics in the Mexican neotropics during the last 1300 years. Global Change Biology **16**:1689-1704.

Frappier, A. B., D. Sahagian, S. J. Carpenter, L. A. Gonzalez, and B. R. Frappier. 2007. Stalagmite stable isotope record of recent tropical cyclone events. Geology **35**:111-114.

Fujiwara, O., F. Masuda, T. Sakai, T. Irizuki, and K. Fuse. 2000. Tsunami deposits in Holocene bay mud in southern Kanto region, Pacific coast of central Japan. Sedimentary Geology **135**:219-230.

Goff, J., C. Chagué-Goff, and S. Nichol. 2001. Palaeotsunami deposits: a New Zealand perspective. Sedimentary Geology **143**:1-6.

Goff, J., B. G. McFadgen, and C. Chagué-Goff. 2004. Sedimentary differences between the 2002 Easter storm and the 15th-century Okoropunga tsunami, southeastern North Island, New Zealand. Marine Geology **204**:235-250.

Goff, J. R., H. L. Rouse, S. L. Jones, B. W. Hayward, U. Cochran, W. McLea, W. W. Dickinson, and M. S. Morley. 2000. Evidence for an earthquake and tsunami about 3100-3400 yr ago, and other catastrophic saltwater inundations recorded in a coastal lagoon, New Zealand. Marine Geology **170**:231-249.

Goldenberg, S. B. and L. J. Shapiro. 1996. Physical mechanisms for the association of El Niño and west African rainfall with Atlantic major hurricane activity. Journal of Climate **9**:1169-1187.

Goldenberg, S. B., C. W. Landsea, A. M. Mestas-Nunez, and W. M. ñ. 2001. The recent increase in Atlantic hurricane activity: Causes and implications. Science **293**:474-479.

Goman, M., A. Joyce, and R. Mueller. 2005. Stratigraphic evidence for anthropogenically induced coastal environmental change from Oaxaca, Mexico. Quaternary Research **63**:250-260.

Goman, M., A. Joyce, R. Mueller, and L. Paschyn. 2010. Multiproxy paleoecological reconstruction of prehistoric land-use history in the western region of the lower Rio Verde Valley, Oaxaca, Mexico. Holocene **20**:761-772.

Gonzalez, C., L. E. Urrego, J. I. Martinez, J. Polania, and Y. Yokoyama. 2010. Mangrove dynamics in the southwestern Caribbean since the 'Little Ice Age': A history of human and natural disturbances. Holocene **20**:849-861.

Gonzalez-Quintero, L. 1980. Paleoecologia de un sector costero de Guerrero, Mexico (3000 anos). Memorias **86**:133-157.

Gonzalez-Quintero, L. and M. Fuentes-Mata. 1980. El Holoceno de la porcon central de la Cuenca del Valle de Mexico. Pages 133-158 Memorias III Coloquio sobre Paleobotanica y Palinologia (Coordinacion, Fernando Sanchez). Instituto Nacional de Antropologia e Historia, Mexico.

Gray, W. M. and J. D. Sheaffer. 1991. El Niño and QBO influences on tropical cyclone activity. Pages 257-284 *in* M. H. Glantz, R. W. Katz, and N. Nicholls, editors. Teleconnections linking worldwide climate anomalies. Cambridge University Press, New York.

Habib, D., D. Thurber, D. Ross, and J. Donahue. 1970. Holocene palynology of the Middle American Trench near Tehuantepec, Mexico. Memoirs of the Geological Society of America **126**:233-261.

Hathorn, J. H. 2008. Paleoecology and paleotempestology of the Pascagoula Marsh, Mississippi. M.S. Thesis. Louisiana State University, Baton Rouge.

Heusser, L. E. 1982. Pollen analysis of laminated and homogenous sediment from the Guaymas Basin, Gulf of California. US Government Printing Office, Washington, D.C.

Hippensteel, S. P. and R. E. Martin. 1999. Foraminifera as an indicator of overwash deposits, Barrier Island sediment supply, and Barrier Island evolution: Folly Island, South Carolina. Palaeogeography Palaeoclimatology Palaeoecology **149**:115-125.

Irwin, R. P. and R. E. Davis. 1999. The relationship between the Southern Oscillation Index and tropical cyclone tracks in the eastern north Pacific. Geophysical Research Letters **26**:2251-2254.

Islebe, G. and O. Sanchez. 2002. History of Late Holocene vegetation at Quintana Roo, Caribbean coast of Mexico. Plant Ecology **160**:187-192.

Jauregui, E. 2003. Climatology of landfalling hurricanes and tropical storms in Mexico. Atmosfera **16**:193-204.

Kar, D. 2010. Integration of paleotempestology with coastal risk and vulnerability assessment: Case studies from the Dominican Republic and Nicaragua. PhD Dissertation. Louisiana State University, Baton Rouge.

Kennett, D. J., B. Voorheis, J. Iriarte, J. G. Jones, D. Piperno, M. T. Ramirez-Herrera, and T. A. Wake. 2004. Avances en el proyecto Arcaico-Formativo: Costa de Guerrero. Instituto Nacional de Antroplogia e Historia.

Kilbourne, K. H., R. P. Moyer, T. M. Quinn, and R. G. Grottoli. 2011. Testing coral-based tropical cyclone reconstructions: An example from Puerto Rico. Palaeogeography Palaeoclimatology Palaeoecology **307**:90-97.

Kimberlain, T. B. 1999. The effects of ENSO on North Pacific and North Atlantic tropical cyclone activity. Pages 472-473 *in* The 23rd Conference on Hurricanes and Tropical Meteorology. American Meteorological Society, Boston.

Kjerve, B. 1986. Comparative oceanography of coastal lagoons. Pages 63-81 *in* D. A. Wolfe, editor. Estuarine Variability. Academic Press, Orlando.

Knowles, J. T. 2004. Coastal lake-sediment records of prehistoric hurricane strikes in Honduras and Turks and Caicos Islands of the Caribbean Islands of the Caribbean Basin. M. S. Thesis. Louisiana State University, Baton Rouge.

Knowles, J. T. 2008. A 5000-year history of Caribbean environmental change and hurricane activity reconstructed from coastal lake sediments of the West Indies. PhD Dissertation. Louisiana State University, Baton Rouge.

Kolodny, Y., R. Calvo, and D. Rosenfeld. 2009. "Too low" δ18O of paleo-meteoric, low latitude, water; do paleo-tropical cyclones explain it? Palaeogeography Palaeoclimatology Palaeoecology **280**:387-395.

Kortekaas, S. 2002. Tsunamis, storms, and earthquakes: distinguishing coastal flooding events. Coventry University, United Kingdom.

Kortekaas, S. and A. G. Dawson. 2007. Distinguishing tsunami and storm deposits: An example from martinhal, SW Portugal. Sedimentary Geology **200**:208-221.

Kovacs, J. M., J. Malczewski, and F. Flores-Verdugo. 2004. Examining local ecological knowledge of hurricane impacts in a mangrove forest using an analytical hierarchy process (AHP) approach. Journal of Coastal Research **20**:792-800.

Kutzbach, J. E. and P. J. Guetter. 1986. The influence of changing orbital parameters and surface boundary conditions on climate simulations for the past 18000 years. Journal of Atmospheric Science **33**:1726-1759.

Lambert, W. J., P. Aharon, and A. B. Rodriguez. 2008. Catastrophic hurricane history revealed by organic geochemical proxies in coastal lake sediments: a case study of Lake Shelby, Alabama (USA). Journal of Paleolimnology **39**:117-131.

Lander, M. A. and C. P. Guard. 1998. A look at global tropical cyclone activity during 1995: Contrasting high Atlantic activity with low activity in other basins. Monthly Weather Review **126**:1163-1173.

Landsea, C. W. and W. M. Gray. 1989. Eastern North Pacific tropical cyclone climatology - low frequency variations. Report of WG 6.2 (Northeast Pacific Ocean) of IWTC-II, WMO, WMO/TD no. 319. Geneva.

Lankford, R. R. 1977. Coastal lagoons of Mexico: their origin and classification. Pages 182-215 *in* M. Wiley, editor. Estuarine Processes. Academic Press Inc.

Larson, J., Y. P. Zhou, and R. W. Higgins. 2005. Characteristics of landfalling tropical cyclones in the United States and Mexico: Climatology and interannual variability. Journal of Climate **18**:1247-1262.

Leopold, A. S. 1950. Vegetation zones of Mexico. Ecology **31**:507-518.

Leopold, A. S. 1959. Wildlife of Mexico. University of California Press.

Leydan, B. W., M. Brenner, T. Whitmore, J. H. Curtis, D. Piperno and B. H. Dahlin. A record of long and short-term climatic variation from northwest Yucatan: Cenote San Jose Chulcaca. Pages 30-50 *in* S. L. Fedick, editor. The Managed Mosaic: Ancient Maya Agriculture and Resource Use. University of Utah Press.

Liu, K. B. and M. L. Fearn. 1993. Lake-sediment record of late Holocene hurricane activities from coastal Alabama. Geology **21**:793-796.

Liu, K. B. and M. L. Fearn. 2000. Reconstruction of prehistoric landfall frequencies of catastrophic hurricanes in northwestern Florida from lake sediment records. Quaternary Research **54**:238-245.

Liu, K. B., H. Lu, and C. Shen. 2008. A 1200-year proxy record of hurricanes and fires from the Gulf of Mexico coast: Testing the hypothesis of hurricane-fire interactions. Quaternary Research **69**:29-41.

Liu, K. B., C. M. Shen, and K. S. Louie. 2001. A 1,000-year history of typhoon landfalls in Guangdong, southern China, reconstructed from Chinese historical documentary records. Annals of the Association of American Geographers **91**:453-464.

Louie, K. S. and K. B. Liu. 2003. Earliest historical records of typhoons in China. Journal of Historical Geography **29**:299-316.

Lu, H. Y. and K. B. Liu. 2005. Phytolith assemblages as indicators of coastal environmental changes and hurricane overwash deposition. Holocene **15**:965-972.

Maloney, E. D. and D. L. Hartmann. 2000. Modulation of eastern North Pacific hurricanes by the Madden-Julian oscillation. Journal of Climate **13**:1451-1460.

Mann, M. E., J. D. Woodruff, J. P. Donnelly, and Z. Zhang. 2009. Atlantic hurricanes and climate over the past 1,500 years. Nature **460**:880-U115.

Massari, F. and A. D'Alessandro. 2000. Tsunami-related scour-and-drape undulations in Middle Pliocene restricted-bay carbonate deposits (Salento, south Italy). Sedimentary Geology **135**:265-281.

McCloskey, T. A. 2009. Proxy records of paleohurricanes for the western and southern Caribbean. PhD Dissertation. Louisiana State University, Baton Rouge.

McCloskey, T. A. and G. Keller. 2009. 5000 year sedimentary record of hurricane strikes on the central coast of Belize. Quaternary International **195**:53-68.

McCloskey, T. A. and K. B. Liu. 2012. A sedimentary-based history of hurricane strikes on the southern Caribbean coast of Nicaragua. Quaternary Research **78:**454-464.

McCloskey, T. A. and K. B. Liu. 2013a. A 7000 year record of paleohurricane activity from a coastal wetland in Belize. Holocene **23**:278-291.

McCloskey, T. A. and K. B. Liu. 2013b. Sedimentary history of mangrove cays in Turneffe Islands, Belize: evidence for sudden environmental reversals. Journal of Coastal Research **29**: 971-983.

McCoy, E. D., H. R. Mushinsky, D. Johnson, and W. E. Meshaka. 1996. Mangrove damage caused by hurricane Andrew on the southwestern coast of Florida. Bulletin of Marine Science **59**:1-8.

McSaveney, M. J., J. R. Goff, D. J. Darby, P. Goldsmith, A. Barnett, S. Elliott, and M. Nongkas. 2000. The 17 July 1998 tsunami, Papua New Guinea: evidence and initial interpretation. Marine Geology **170**:81-92.

Metcalfe, S. E., S. L. O'Hara, M. Caballero, and S. J. Davies. 2000. Records of Late Pleistocene-Holocene climatic change in Mexico - a review. Quaternary Science Reviews **19**:699-721.

Metcalfe, S. E., M. D. Jones, S. J. Davies, A. Noren, and A. MacKenzie. 2010. Climate variability over the last two millennia in the North American Monsoon region, recorded in laminated lake sediments from Laguna de Juanacatlan, Mexico. Holocene **20**:1195-1206.

Minoura, K., V. G. Gusiakov, A. Kurbatov, S. Takeuti, J. I. Svendsen, S. Bondevik, and T. Oda. 1996. Tsunami sedimentation associated with the 1923 Kamchatka earthquake. Sedimentary Geology **106**:145-154.

Molinari, J., D. Vollaro, S. Skubis, and M. Dickinson. 2000. Origins and mechanisms of eastern Pacific tropical cyclogenesis: A case study. Monthly Weather Review **128**:125-139.

Mora, C. I., D. L. Miller, and H. D. Grissino-Mayer. 2007. Oxygen isotope proxies in tree-ring cellulose:Tropical cyclones, drought, and climate oscillations. Pages 63-75 *in* T. E. Dawson and R. T. W. Siegwolf, editors. Stable Isotopes as Indicators of Ecological Change. Elsevier, San Diego.

Morton, R. A. 1978. Large-scale rhomboid bed forms and sedimentary structures associated with hurricane washover. Sedimentology **25**:183-204.

Morton, R. A., G. Gelfenbaum, and B. E. Jaffe. 2007. Physical criteria for distinguishing sandy tsunami and storm deposits using modem examples. Sedimentary Geology **200**:184-207.

Mosiño-Aleman, P. A. M. and E. Garcia. 1974. The climate of Mexico. Pages 345-391 *in* H. E. Landsberg, editor. Climates of North America. Elsevier.

Myers, R. K. and D. H. van Lear. 1998. Hurricane-fire interactions in coastal forests of the south: a review and hypothesis. Forest Ecology and Management **103**:265-276.

Nanayama, F., R. Furukawa, K. Shigeno, A. Makino, Y. Soeda, and Y. Igarashi. 2007. Nine unusually large tsunami deposits from the past 4000 years at Kiritappu marsh along the southern Kuril Trench. Sedimentary Geology **200**:275-294.

Nanayama, F., K. Shigeno, K. Satake, K. Shimokawa, S. Koitabashi, S. Miyasaka, and M. Ishii. 2000. Sedimentary differences between the 1993 Hokkaido-nansei-oki tsunami and the 1959 Miyakojima typhoon at Taisei, southwestern Hokkaido, northern Japan. Sedimentary Geology **135**:255-264.

National Geophysical Data Center. 2011. NOAA/WDC Tsunami Runup Database. Retrieved 8-24-2011, from http://www.ngdc.noaa.gov/nndc/struts/form?t=101650&s=167&d=166.

National Hurricane Center. 2011. Tropical cyclone climatology. Retrieved 10-20-2011, from http://www.nhc.noaa.gov/climo/.

National Oceanic and Atmospheric Administration. 2011a. Tsunami vocabulary and terminology. Retrieved 08-02-2011, from http://www.tsunami.noaa.gov/terminology.html.

National Oceanic and Atmospheric Administration. 2011b. Historical hurricane tracks. Retrieved 06-29-2011, from http://www.csc.noaa.gov/hurricanes/.

Nott, J. F. 2003. Intensity of prehistoric tropical cyclones. Journal of Geophysical Research-Atmospheres **108**: DOI:10.1029/2002JD002726.

Nott, J. F. 2009. Long-term natural variability of tropical cyclones in Australia. Pages 35-59 *in* J. B. Elsner and T. H. Jagger, editors. Hurricanes and Climate Change. Springer, New York.

Nott, J. F. 2011. A 6000 year tropical cyclone record from Western Australia. Quaternary Science Reviews **30**: 713-722

Ohngemach, D. 1977. Pollen sequence of the Tlaqua crater (La Malinche Volcano, Tlaxcala, Mexico). Boletin de la Sociedad Botanica de Mexico **36**:33-44.

Open University. 1989. Waves, tides, and shallow-water processes. Pergamon, Oxford.

Pascarella, J. B., T. M. Aide, and J. K. Zimmerman. 2004. Short-term response of secondary forests to hurricane disturbance in Puerto Rico, USA. Forest Ecology and Management **199**:379-393.

Perkins, R. D. and P. Enos. 1968. Hurricane Betsy in the Florida-Bahama area - Geologic effects and comparison with Hurricane Donna. Journal of Geology **76**:710-717.

Peros, M. C., E. G. Reinhardt, and A. M. Davis. 2007. A 6000-year record of ecological and hydrological changes from Laguna de la Leche, north coastal Cuba. Quaternary Research **67**:69-82.

Peters, R., B. Jaffe, and G. Gelfenbaum. 2007. Distribution and sedimentary characteristics of tsunami deposits along the Cascadia margin of western North America. Sedimentary Geology **200**:372-386.

Ramirez-Herrera, M. T., A. B. Cundy, V. Kostoglodov, and M. Ortiz. 2009. Late Holocene tectonic land-level changes and tsunamis at Mitla lagoon, Guerrero, Mexico. Geofisica Internacional **48**:195-209.

Ramirez-Herrera, M. T., V. Kostoglodov, and J. Urrutia-Fucugauchi. 2004. Holocene-emerged notches and tectonic uplift along the Jalisco coast, Southwest Mexico. Geomorphology **58**:291-304.

Ramirez-Herrera, M. T. and J. Urrutia-Fucugauchi. 1999. Morphotectonic zones along the coast of the Pacific continental margin, southern Mexico. Geomorphology **28**:237-250.

Rees, P. 2002. Mexico. Pages 235-267 *in* Latin America and the Caribbean: A Systematic and Regional Survey. John Wiley and Sons, New York.

Reese, C. A., T. P. Strange, W. D. Lynch, and K. B. Liu. 2008. Geologic Evidence of Hurricane Katrina Recovered from the Pearl River Marsh, MS/LA. Journal of Coastal Research **24**:1601-1607.

Ritchie, W. and S. Penland. 1988. Rapid dune changes associated with overwash processes on the deltaic coast of south Louisiana. Marine Geology **81**:97-122.

Rodgers, E. B., R. F. Adler, and H. F. Pierce. 2000. Contribution of tropical cyclones to the North Pacific climatological rainfall as observed from satellites. Journal of Applied Meteorology **39**:1658-1678.

Romero-Vadillo, E., O. Zaytsev, and R. Morales-Perez. 2007. Tropical cyclone statistics in the northeastern Pacific. Atmosfera **20**:197-213.

Sanchez, O. S. and G. A. Islebe. 1999. Hurricane Gilbert and structural changes in a tropical forest in south-eastern Mexico. Global Ecology and Biogeography **8**:29-38.

Sanson, L. Z. 2004. The mechanical influence of continental topography on the trajectories of tropical cyclones near the west coast of Mexico. Atmosfera **17**:151-170.

Sawai, Y. 2002. Evidence for 17th-century tsunamis generated on the Kuril-Kamchatka subduction zone, Lake Tokotan, Hokkaido, Japan. Journal of Asian Earth Sciences **20**:903-911.

Scasso, R. A., A. Concheyro, W. Kiessling, M. Aberhan, L. Hecht, F. A. Medina, and R. Tagle. 2005. A tsunami deposit at the Cretaceous/Paleogene boundary in the Neuquen Basin of Argentina. Cretaceous Research **26**:283-297.

Scileppi, E. and J. P. Donnelly. 2007. Sedimentary evidence of hurricane strikes in western Long Island, New York. Geochemistry Geophysics Geosystems **8**. DOI 10.1029/2006GC001463.

Scott, D. B., E. S. Collins, P. T. Gayes, and E. Wright. 2003. Records of prehistoric hurricanes on the South Carolina coast based on micropaleontological and sedimentological evidence, with comparison to other Atlantic Coast records. Geological Society of America Bulletin **115**:1027-1039.

Smith, C. B. 2006. Extreme waves. Joseph Henry, Washington D.C.

Switzer, A. D., K. Pucillo, R. A. Haredy, B. G. Jones, and E. A. Bryant. 2005. Sea level, storm, or tsunami: Enigmatic sand sheet deposits in a sheltered coastal embayment from southeastern New South Wales, Australia. Journal of Coastal Research **21**:655-663.

Tanner, E. V. J., V. Kapos, and J. R. Healey. 1991. Hurricane effects on forest ecosystems in The Caribbean. Biotropica **23**:513-521.

Tappin, D. R. 2007. Sedimentary features of tsunami deposits - Their origin, recognition and discrimination: An introduction. Sedimentary Geology **200**:151-154.

Trejo, D. A. R. 2008. Fire regimes, fire ecology, and fire management in Mexico. Ambio **37**:548-556.

UNESCO. 2005. Tsunamis on the move; Where and how frequently are tsunamis generated? http://ioc3.unesco.org/itic/contents.php?id=163.

University of Texas. 1975. Vegetation Map of Mexico.

Urrego, L. E., G. Bernal, and J. Polania. 2009. Comparison of pollen distribution patterns in surface sediments of a Colombian Caribbean mangrove with geomorphology and vegetation. Review of Palaeobotany and Palynology **156**:358-375.

Voorheis, B. 2004. Coastal collectors in the Holocene: The Chantuto People of Southwest Mexico. University Press of Florida.

Wallace, D. J. and J. B. Anderson. 2010. Evidence of similar probability of intense hurricane strikes for the Gulf of Mexico over the late Holocene. Geology **38**:511-514.

Watts, W. A. and J. P. Bradbury. 1982. Paleoecological studies at Lake Patzcuaro on the west-central Mexican Plateau and at Chalco in the Basin of Mexico. Quaternary Research **17**:56-70.

Whitney, L. D. and J. S. Hobgood. 1997. The relationship between sea surface temperatures and maximum intensities of tropical cyclones in the eastern North Pacific Ocean. Journal of Climate **10**:2921-2930.

Williams, H. F. L. 2010. Storm surge deposition by Hurricane Ike on the McFaddin National Wildlife Refuge, Texas: Implications for paleotempestology studies. Journal of Foraminiferal Research **40**:210-219.

Woodruff, J. D., J. P. Donnelly, K. Emanuel, and P. Lane. 2008a. Assessing sedimentary records of paleohurricane activity using modeled hurricane climatology. Geochemistry Geophysics Geosystems **9**.

Woodruff, J. D., J. P. Donnelly, D. Mohrig, and W. R. Geyer. 2008b. Reconstructing relative flooding intensities responsible for hurricane-induced deposits from Laguna Playa Grande, Vieques, Puerto Rico. Geology **36**:391-394.

Woodruff, J. D., J. P. Donnelly, and A. Okusu. 2009. Exploring typhoon variability over the mid-to-late Holocene: evidence of extreme coastal flooding from Kamikoshiki, Japan. Quaternary Science Reviews **28**:1774-1785.

Wooller, M. J., R. Morgan, S. Fowell, H. Behling, and M. Fogel. 2007. A multiproxy peat record of Holocene mangrove palaeoecology from Twin Cays, Belize. Holocene **17**:1129-1139.

Zhao, X. and P. S. Chu. 2006. Bayesian multiple changepoint analysis of hurricane activity in the Eastern North Pacific: A Markov chain Monte Carlo approach. Journal of Climate **19**:564-578.

CHAPTER 3. PALEOENVIRONMENTAL RECONSTRUCTIONS FROM LAGOONS BOQUITA AND AGUA DULCE, JALISCO, MEXICO'S PACIFIC COAST

3.1 Introduction

Approximately 8,475 km of wetlands line Mexico's Pacific coast, covering 892,800 hectares (Contreras-Espinosa and Warner, 2004) and including over 79 large water bodies. Local oceanographic, geologic, and climatologic controls aided in creating a wide array of coastal inlets, bays, sounds, estuaries, lagoons, and lakes (Lankford, 1977). These regions are generally unprobed and lacking paleoenvironmental investigation. Jalisco state is no exception, containing 342 km of coastal wetland covering 3200 ha (Contreras-Espinosa and Warner, 2004) and featuring many large water bodies. Paleoenvironmental reconstructions have been focused on the interior highlands (Figueroa-Rangel et al., 2008, 2010) with coastal work limited to only analysis of surface sediment samples (Landa-Jaime, 2003).

Paleoenvironmental reconstructions on Mexico's Pacific coast have the capability of shedding light among many scientific disciplines. Since this region contains substantial economic value (Lankford, 1977), reconstructions also potentially contain immense societal benefit. Due to the regional development and rapid growth of the tourism industry, risk assessment of natural processes including sea level rise, coastal erosion, and climate change could provide benefit to scientists, policy makers, and residents. Notably, instrumental tropical cyclone (TC) records only start in 1949 (Jauregui, 2003), rendering event frequency and long-term activity regimes poorly understood. The Eastern North Pacific (ENP) is the world's most active basin for tropical cyclogenesis, per unit time and area (Molinari et al., 2000). Jalisco is frequently hit by TCs, many of which are of catastrophic intensity and capable of substantial damage. One example is the infamous 1959 unnamed hurricane making landfall at category 5 intensity (on the Saffir-Simpson scale) near Jalisco's southern edge with top wind speeds

approaching 160 mph (260 kph). The fierce winds coupled with torrential rainfall and mudslides caused substantial damage, including over 1000 deaths and the loss of five merchant ships (Crooks, 1960). Regional geomorphological damage from strong TCs can include storm surge inundation and coastal erosion (Lankford, 1977).

Sediments extracted from coastal lakes, lagoons, swamps, and marshes can be ideal archives for paleo-TC reconstruction through a host of geological and biological proxies (Liu, 2007). Scientists are unsure, however, of the suitability of Jalisco's coast for the capture and preservation of TC-derived geophysical evidence, namely overwash sand layers via storm surge inundation. Despite this uncertainty, coastal Jalisco is deemed ideal for paleotempestological analyses due to its susceptibility to TC damage and the unlikelihood of tsunami, which are potentially confusing to storm surge signatures. Challenges and uncertainties exist when conducting paleotempestological reconstructions on Mexico's Pacific coast. Impressive beach ridges dot Jalisco's coast, perhaps prohibiting storm surge inundation and coastal sediment transport. Other complicating factors include tectonic activity and limited regional paleoenvironmental literature. In conjunction with the implementation of overwash sand as a TC proxy, it is possible that intense TC precipitation can produce a reliable slopewash signal, ranging from thin clastic bands to thick graded beds (Page et al., 1994) and potentially containing plant macrofossils (Noren et al., 2002). Slopewash discovered in lake sediment from inland Jalisco is attributed to both TCs (Byrne et al., 1996) and non-TC precipitation events (Metcalfe et al., 2010). Hilly topography near Jalisco's coast suggests that this is a fitting region to test the reliability and utility of slopewash deposits as a TC proxy in coastal sediments. If deposition is absent from individual events, it is suggested that alternative evidence can help

determine periods of high activity. TCs are a significant regional climate driver responsible for high totals of annual rainfall throughout coastal Jalisco (Englehart and Douglas, 2001).

In this chapter I present paleoenvironmental reconstructions from Boquita and Agua Dulce, two water bodies with contrasting formations and characteristics to understand coastal dynamics and regional suitability toward paleotempestological analysis. The objectives of this research are twofold: (a) to reconstruct the paleoenvironment of these dynamic and multifaceted coasts; (b) to determine the time period(s) when TCs were likely more active, with evidence either from storm surge/slopewash deposition, or alternative means (e.g., detection of wet periods).

3.2 Physical environment and study sites

Jalisco state (20.5667º N, 103.6764º W) is located in central-western Mexico (Figure 3.1), bordered by Colima to the SE and Nayarit to the north. The Sierra Madre del Sur Mountains run parallel along Mexico's west coast, containing ranges surpassing 2000 m a.s.l in Jalisco's interior. Ephemeral rivers and streams sourced in these uplands flow toward the coast, emptying into the Pacific Ocean or coastal water bodies. Coastal climate is semi-arid and monsoonal with a rainy season occurring from June-October and annual precipitation increasing inland. Jalisco's coast receives about 700 mm of precipitation annually, with approximately 30% of precipitation from TCs during the warm season, stemming from May to November (Englehart and Douglas, 2001). Local tectonism stems from the collision of the oceanic Cocos plate subducting under the North American plate at the Middle America Trench, located 70 km from the study sites (Lankford, 1977). Jalisco's coast is dotted with rocky cliffs and marine terraces, indicative of paleo-uplift (Ramirez-Herrera and Urrutia-Fucuguchi, 1999). Separating

the Middle America Trench and the coast is a steep continental slope and a narrow shelf. Tidal range is low, at approximately 0.5 m (Ramirez-Herrera and Urrutia-Fucuguchi, 1999).

Boquita (LBO) is a small (750 m by 250 m) irregularly-shaped ‘lagunilla’ (20.1939° N, 105.5418° W) (Figure 3.1). Water depth is ~ 50 cm with slightly more depth toward the landward edges. LBO fills with water from precipitation and land runoff (e.g., Moore and Slinn, 1984). An ephemeral stream located one km to the south overflows its bank during the rainy season, forcing additional water into LBO. When filled to capacity, a narrow tidal opening along LBO’s southern edge aids in drainage. Limited rainfall and river discharge during the dry season decreases water depth. Topography 1 km inland surpasses 70 m, and 10 km inland of LBO it exceeds 200 m.

Separating LBO from the Pacific Ocean is an 80 m wide beach rising over 3 m a.s.l, and a 170 m wide relic beach ridge system, approximately 5-6 m a.m.s.l. LBO is landward of the beach ridges and has a surface elevation of ~3 m a.m.s.l. Mangroves line LBO’s seaward edge. LBO’s characteristics resemble “barred inner shelf” lagoons, the most common classification along Mexico’s Pacific coast with at least 27 others formed during stable mid-Holocene seas (Lankford, 1977).

Located 15 km south of LBO, Agua Dulce (LAD) (20.0451° N, 105.5150° W) is a long lagoon, 6 km by 2.25 km (Figure 3.1). A canal connects LAD to Estero El Ermitaño, receiving flow from the Rio Maria Garcia, located 4 km south of the lagoon. LAD’s water surface is near sea level. Water depth is ~1-2 m at the coring locations along LAD’s western edge, and >3 m toward the center. Average salinity is ~27 psu (Landa-Jaime, 2003). Landward elevation 1 km inland surpasses 20 m, and 10 km inland it exceeds 200 m. LAD is classified as one of the

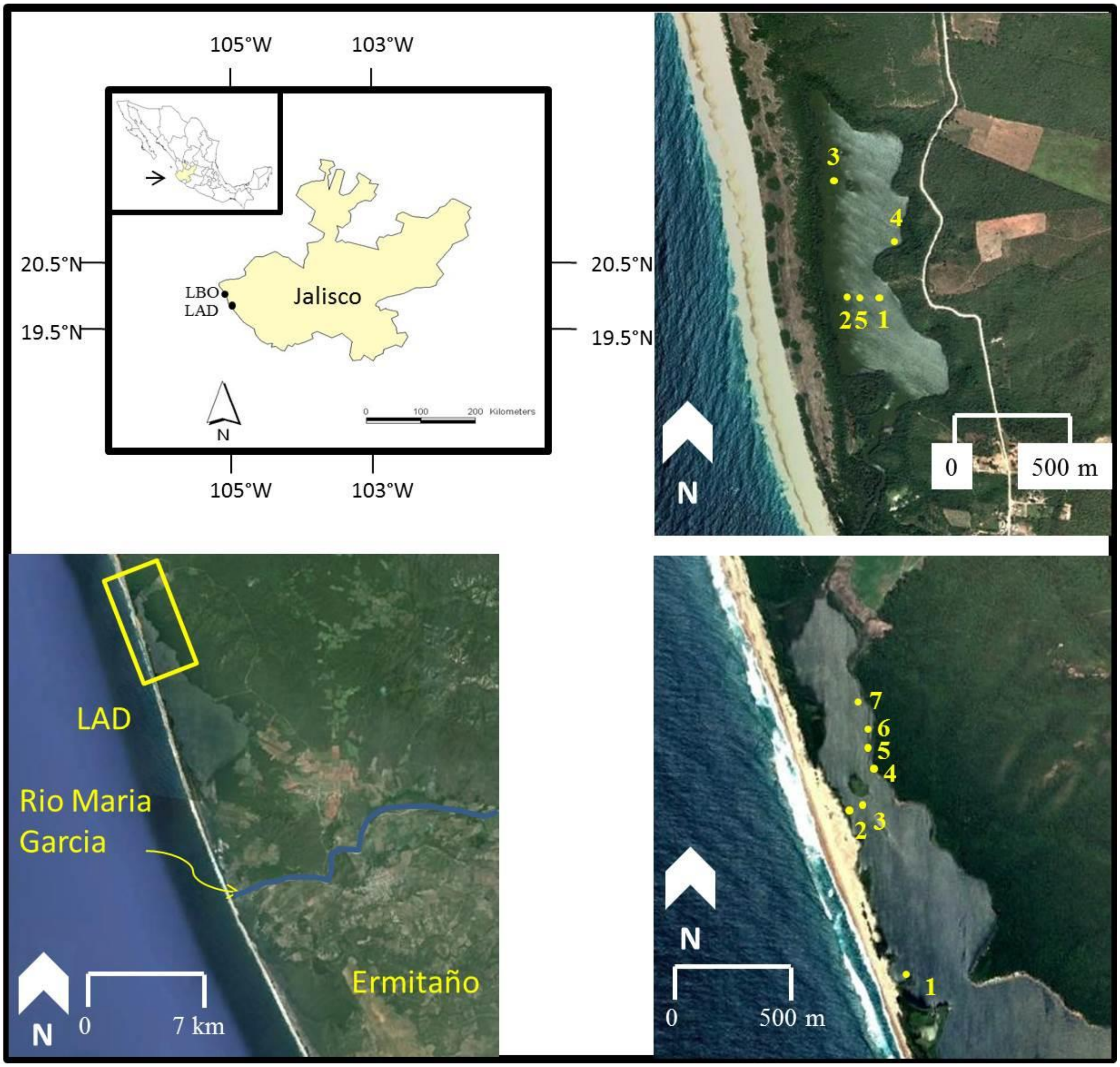

Figure 3.1 – Map of Jalisco, with subset of Mexico (top left). Laguna Boquita (LBO) and Laguna Agua Dulce (LAD) locations are labeled. Aerial image of Laguna Boquita (top right) indicating coring locations (1-5). Aerial image of Laguna Agua Dulce (bottom left) displaying the nearby Rio Maria Garcia and Estero El Ermitaño. Core locations (1-7) from LAD's western side are shown separately (bottom right).

four "differential erosion" lagoons along Mexico's Pacific coast, characterized as a "barred drowned valley" erosional depression formed during low sea level and filled during Holocene transgression (Lankford, 1977). Its coastal sand barrier formed by stabilizing seas and littoral drift. Dune height is impressive as some rise over 10-12 m a.m.s.l., a common occurrence along

this coast (Phleger and Ewing, 1962). Beach height is low along LAD's western section as fishermen seasonally dig trenches to allow saltwater intrusion, improving harvests.

3.3 Historical extreme events and geophysical effects

ENP cyclogenesis occurs west of Guatemala mostly between 110ºW and 90ºW, with tracks moving in a WNW to NW direction. Twenty-five hurricanes passed within 200 km of LBO and LAD from 1949-2010 (Figure 3.2). Hurricane Kenna (2002), a category 4 storm as it approached the coast, caused a 5-m storm surge that breached LAD's NW section. In addition, Hurricane Rick (2009), a category 5 storm paralleling Jalisco ~500 km away only weeks before our fieldwork, created impressive overwash lobes near LAD (Figure 3.3). Longshore drift closed both breaches within six weeks, according to local residents. Locals assert that TCs often resuspend LAD sediment, turning water into a shiny, "coffee" color. Likewise, intense TC

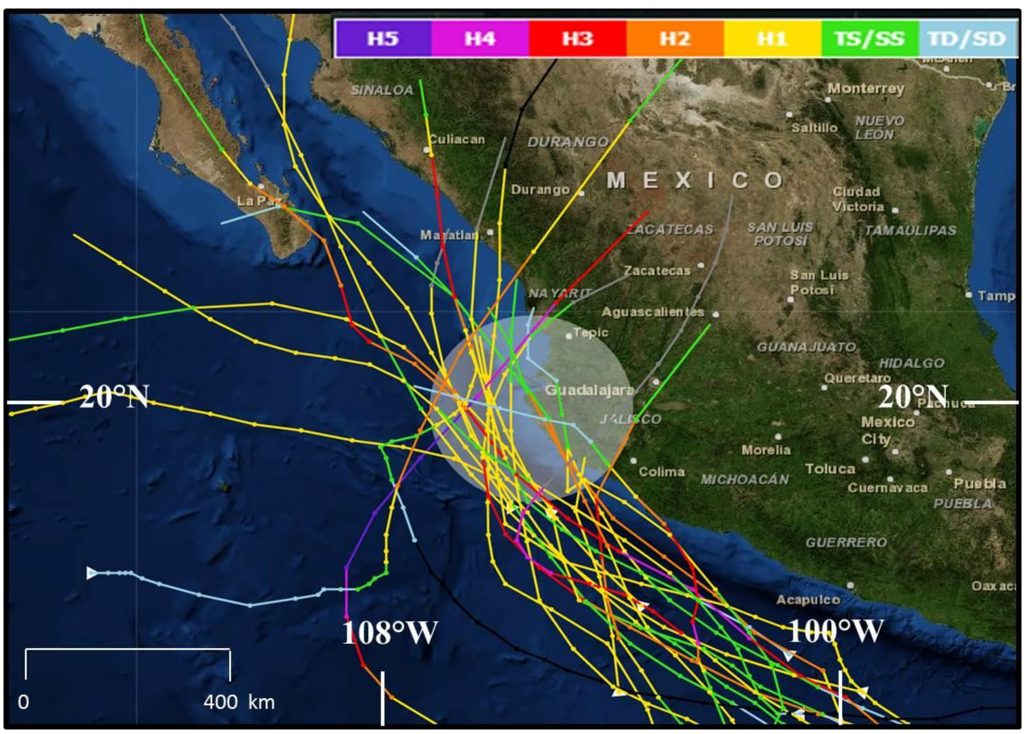

Figure 3.2 – Twenty-five hurricanes traveling within 200 km (white circle) of LBO and LAD from 1949-2010 (National Oceanic and Atmospheric Administration, 2011). TCs generally move in a WNW direction paralleling the coast.

Figure 3.3 –Hurricane Rick (2009) track path (National Oceanic and Atmospheric Administration, 2011) passing through region weeks prior to fieldwork (top). Sand lobe from Hurricane Rick's storm surge (bottom) deposited by overwash processes near LAD.

precipitation events wash inorganic sediments into the lagoon, causing surface waters to turn reddish. TC-induced geophysical impact was not eyewitnessed at LBO.

Jalisco does not possess a rich tsunami history. Only four tsunamis have been recorded since the early 1700s (National Geophysical Data Center, 2011). The most significant impact resulted from the 8.0 magnitude Jalisco-Colima earthquake of 1995, causing a tsunami with a 5.1 m maximum water height in southern Jalisco. Tsunami-induced geophysical impacts are undocumented near both study sites.

3.4 Methodology

Fieldwork was conducted during the dry season in late October/early November of 2009. Sediments were extracted from LBO's central and northern sections to avoid potential disturbance from excessive stream runoff from the south. LAD's western side was probed due to its apparent overwash sensitivity, suspected by the proximate overwash fans. Twelve cores totaling ~ 17 m were retrieved with a Russian peat borer (RPB), yielding ~50 cm segments, and a modified Livingstone corer capturing sediments in cylindrical clear polycarbonate tubes. A 5-cm overlap was measured for each core segment to account for coretop disturbance. RPB cores were transferred to pre-cut PVC pipe and covered with plastic wrap and duct tape to prevent moisture loss. Surface samples were collected from the lagoon surfaces and adjacent environments to determine modern conditions. Sample locations were determined by a Garmin ETRAX global positioning system. Sediment was transported to the Global Change and Coastal Paleoecology Laboratory at Louisiana State University and stored in a 4ºC refrigerated room.

Cores were inspected soon after arrival to ensure moisture containment and color preservation. Sediment was described lithologically, noting shells, plant fibers, and color changes with a Munsell soil color chart. Cores were subjected to high-resolution loss-on ignition

(LOI) analysis (Dean, 1974) at 1-cm sampling intervals to determine water, organic, and carbonate contents. Plant or wood pieces were rinsed with deionized water and sent to the National Ocean Sciences Accelerator Mass Spectrometry Facility (NOSAMS) at the Woods Hole Oceanographic Institution (WHOI) for radiocarbon dating. The Calib 6.0 program and the INTCAL09 curve (Stuiver et al., 2005) converted output to calendar years. Sedimentation rates were determined by linear interpolation between radiocarbon samples, and extrapolation to the core base and top. Chemical elemental concentrations were determined with a Delta Innov-X handheld X-ray fluorescence (XRF) unit with 2-cm resolution, scanning the sediment for 90 seconds per sample. The tantalum X-ray tube used 15 and 40 kilovolt excitation to detect heavy and light elements. Plastic film covered the sediment surface to prevent disturbance and moisture loss.

3.5 Results

3.5.1 Laguna Boquita

Sediment cores are comprised mostly of peat (relatively high water and organic contents) and clays (low water and organic contents). Clay sections are generally brown (higher water and organic contents) or gray (slightly drier, lower water and organic contents). Some clay sections were a faint blue color, noted immediately after extraction in the field, only to fade during cold storage. Some peat sections are embedded with sand (low water and organic contents).

3.5.1.1 Seaward sediments

3.5.1.1.1 Core 1. Extracted near LBO’s center in ~50 cm of water, core 1 (294 cm) is deemed most representative of the paleoenvironment, therefore chosen for geochemical analysis. Core 1 is divided into four stratigraphic zones based on lithology, LOI, and XRF results (Figure 3.4)

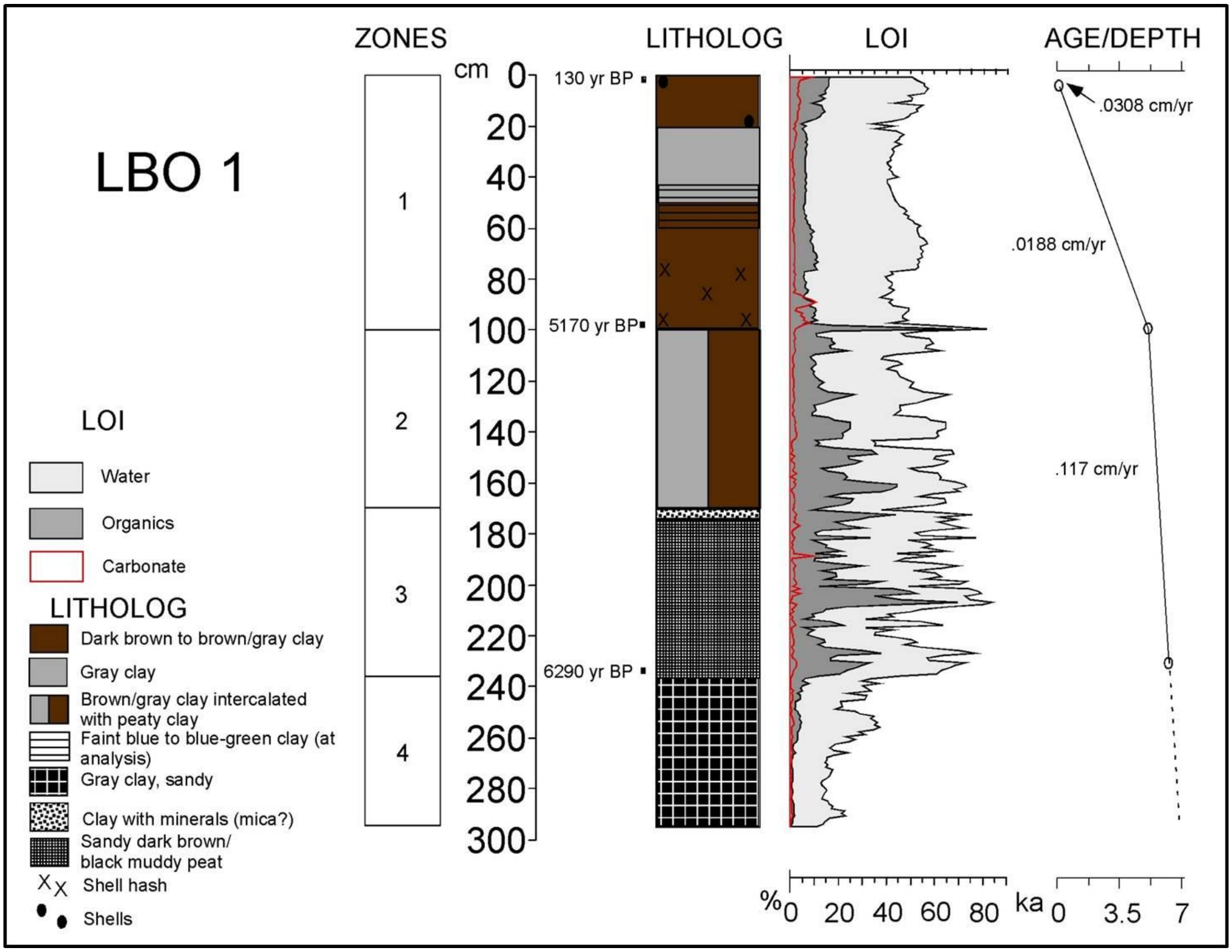

Figure 3.4 - LBO core 1 zone delineation, lithology, LOI results, and calibrated radiocarbon dates (calendar years). Sedimentation is assumed to begin at modern. Sedimentation rate is assumed equal between each radiocarbon sample. Dotted line represents estimated age throughout the remainder of core 1 using 0.117 cm/yr rate.

Zone 4 (294-240 cm) consists of structureless sandy gray clay (Munsell 7.5YR 3/1, 5/1) low in water (~10-30%), organics (1-5%), and carbonate (~1%) (Figure 3.4). Most chemical elements are present in high concentrations, including S, Fe, Ti, K, Rb, and Zr (Figure 3.5).

Zone 3 (240-170 cm) contains dark muddy peat (7.5YR 2.5/1, 3/1) with intermittently-deposited sand. Non-sandy sections have elevated water (80%), organic (50%), and carbonate (5%) contents, while sandy facies exhibit lower water (40%), organic (10%), and carbonate (2%) percentages. S concentrations are steady, while most remaining elements including Fe, Ti, K, Co, Rb, Zn, and Zr occur in low concentrations.

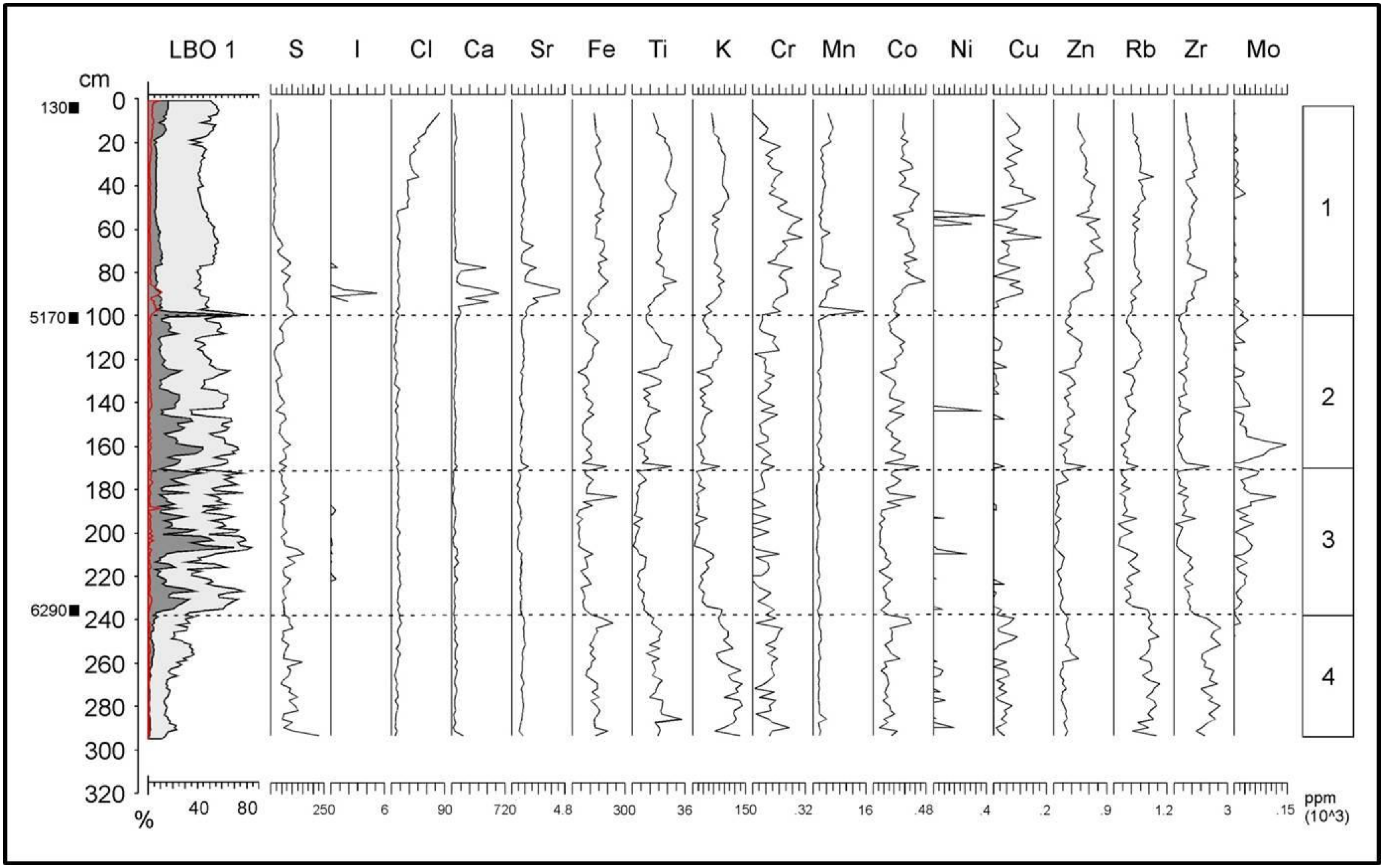

Figure 3.5 – Core 1 XRF results (ppm) aligned with LOI curve. Inter-zone variability is high throughout core 1.

Zone 2 (170-100 cm) consists of dark brown/gray clay intercalated with peaty clay (7.5YR 3/1, 4/1). Water, organic, and carbonate contents fluctuate similar to zone 3. A mineral-rich (mica?) layer is present at 170-168 cm. S remains steady, and relative increases are exhibited for most elements, namely Fe, Ti, K, Co, Zn, Rb, and Zr.

Zone 1 (100-0 cm) consists of dark brown to gray clay (7.5YR 5/1) with shell hash at 99-76 cm and small white shells (likely of terrestrial origin) throughout the top 21 cm. Clay from 61-45 cm was faint blue at extraction, while completely fading with time likely from oxidation (e.g., Moll, 2001). The texture of the faint blue clastic section is slightly dry. Water (35-55%), organics (5-15%), and carbonate (1-8%) contents are fairly constant. One exception is a carbonate spike at 99-76 cm. High S, I, Ca, and Sr concentrations occur at the zone bottom. Remaining elements including Fe, Ti, K, Cr, Co, Cu, Zn, Rb, and Zr are elevated throughout zone 1. Samples were sent for radiocarbon dating from 4 cm (125±45 ^{14}C yr BP, 130 cal yr BP), 99 cm (4500±30 ^{14}C yr BP, 5170 cal yr BP), and 230 cm (5480±35 ^{14}C yr BP, 6290 cal yr BP).

Sedimentation rate is determined for core 1, containing the most radiocarbon dates and best dating coverage, demarcating most significant stratigraphic changes. Sedimentation rate throughout zones 2-4 is relatively high (0.117 cm/yr), but decreases upcore in zone 1 (0.0308 and 0.0188 cm/yr).

3.5.1.1.2 Core 5. Core 5 (184 cm - Figure 3.6) is extracted near core 1 but closer to the beach. Zone 2 (184-86 cm) is dark brown clay (7.5 YR 3/1) with three thin sand layers. Small white shells are scattered at 116-102 cm and 184-138 cm. Structureless gray-blue clay (GLEY2 4/10B) exists at extraction from 101-86 cm, turning grayer during cold storage. Zone 1 (86-0 cm) is brown/gray (7.5YR 3/1, 4/1) to gray clay (7.5 YR 5/2). Crumbly yellow clay (2.5Y 7/4) at 86-79 cm contains a decrease in water with increases in organics and carbonate contents

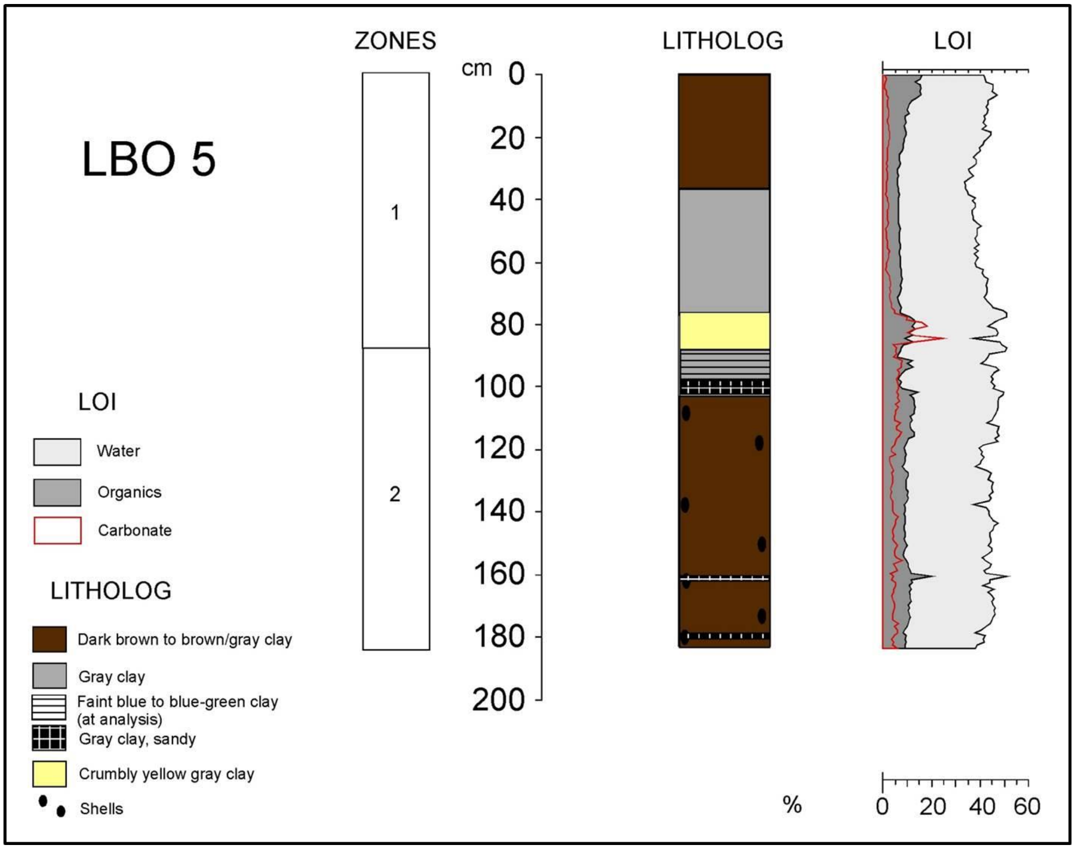

Figure 3.6 – Core 5 zone delineation, lithology, LOI results, and calibrated radiocarbon dates (calendar years). LOI contents are generally consistent throughout core 5, with a carbonate spike at 86-79 cm a notable exception.

compared to adjacent sections. Notwithstanding this yellow section, core 5 is fairly homogeneous in water (33-50%) and organics (6-20%). Carbonate is slightly higher in zone 2 (~5-7%) than zone 1 (~1-2%).

3.5.1.1.3 Core 3. Core 3 (212 cm - Figure 3.7) is extracted toward the northern, seaward edge. Zone 3 (212-205 cm) contains muddy peat with intermittently deposited sand. Zone 2 (205-127 cm) consists of brown/gray clay intercalated with peaty clay (7.5YR 3/1, 4/1, 5/1) with fluctuating water, organic, and carbonate content. Zone 1 (127-0 cm) is a rotating series of dark brown-gray (7.5 YR 3/1, 4/2) and gray clay (7.5 YR 6/2) with shell hash at 82-78 cm and 120-97 cm, and sand at 122-120 cm. Slightly dry blue-green (GLEY2 6/10B) clay at 67-49 cm turned

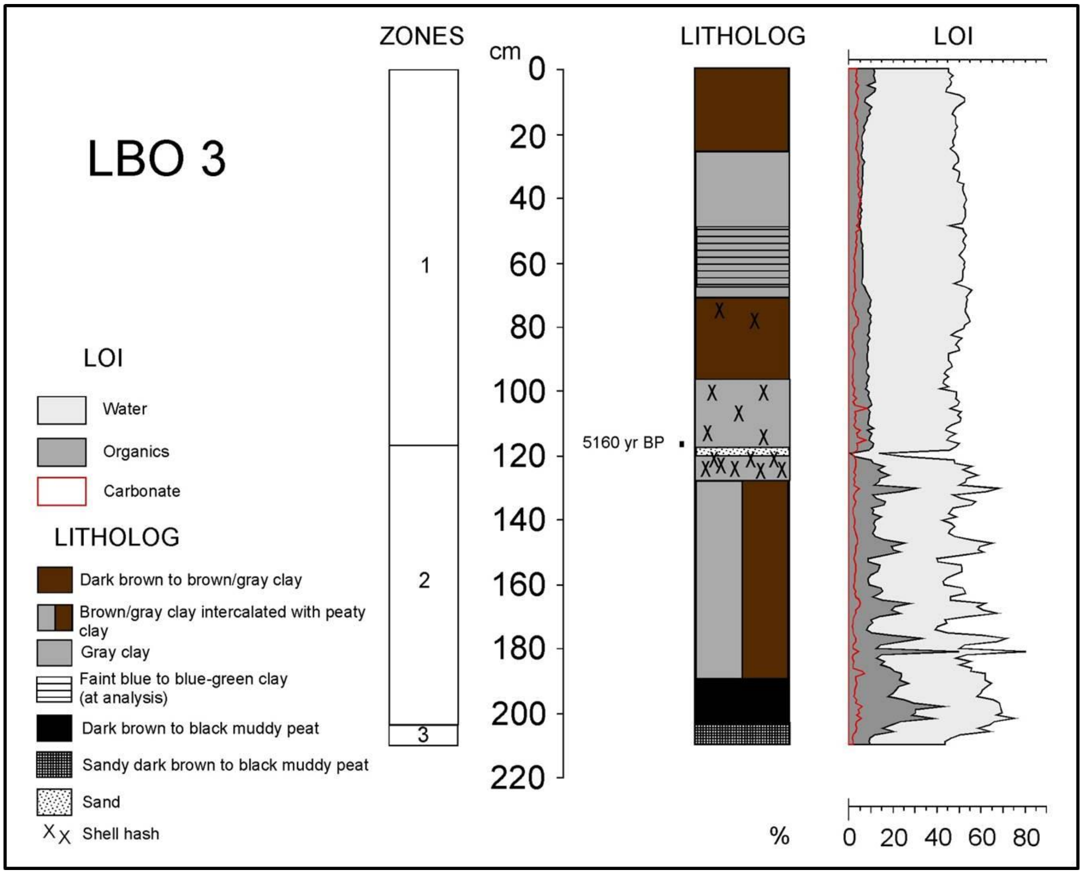

Figure 3.7 - Core 3 zone delineation, lithology, LOI results, and calibrated radiocarbon dates (calendar years). Zone 2 clayey peat contains significant LOI variation whereas zone 1 brown/gray clay is homogeneous.

gray during cold storage. Zone 1 is rather homogeneous in water (41-56%), organics (5-12%), and carbonate (1-8%) contents. One sample at 118 cm is radiocarbon dated to 4500±40 ^{14}C yr BP (5160 cal yr BP).

3.5.1.1.4 Core 2. Core 2 (Figure 3.8) is only 95 cm long due to resistance from stiff sediments at the bottom. Dark brown clay (7.5YR 4/1) comprises the core bottom from 95-83 cm. From 83-65 cm lies a crumbly blue-green clay unit (GLEY 1 6/5GY) turning yellow/gray over time. Gray clay (2.5YR 6/2, 7.5YR 6/1) occurs at 68-16 cm, turning darker brown for the top 16 cm. Water, organic, and carbonate contents are consistent throughout core 2.

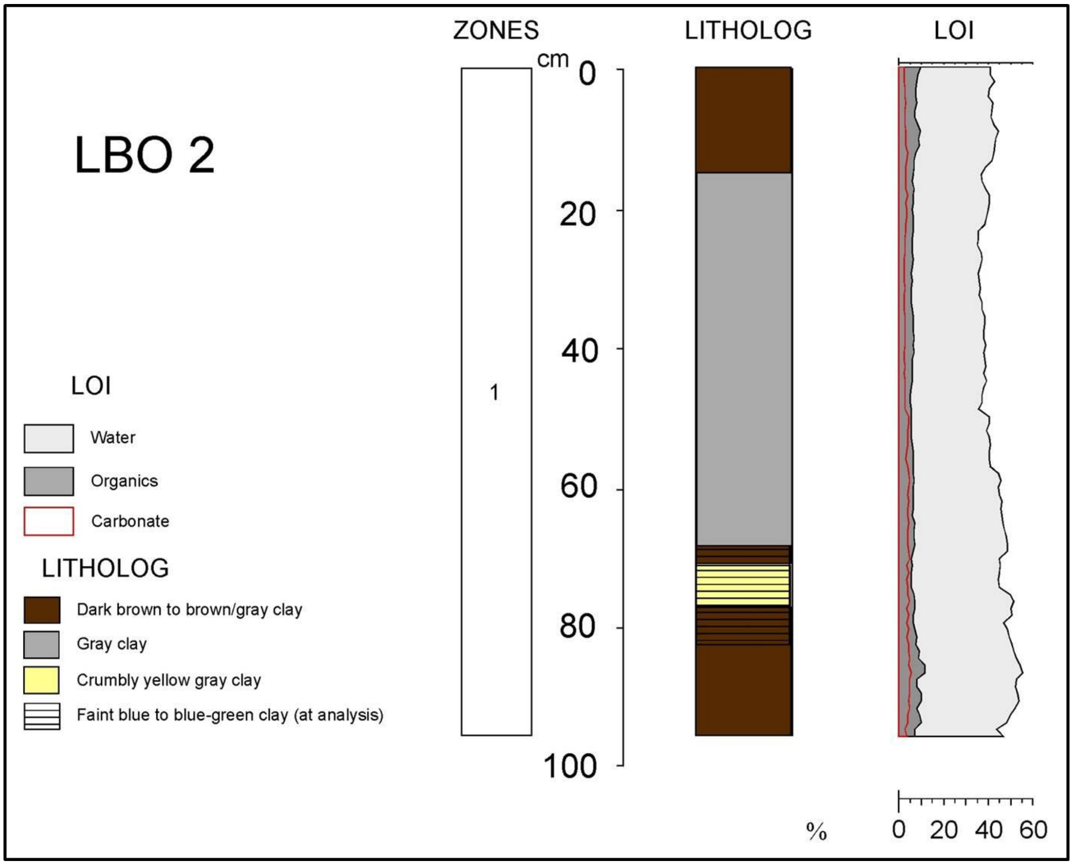

Figure 3.8 – Core 2 zone delineation, litholog, and LOI results. The most notable stratigraphic change remains the crumbly yellow clay unit at 76-70 cm and the gray clay unit at 68-16 cm.

3.5.1.2 Landward sediments

3.5.1.2.1 Core 4. Core 4 (306 cm – Figure 3.9) is extracted from LBO's northeast edge. Zone 2 (306-182 cm) is peat (7.5YR 2.5/1) high in water and organics (~70%) with gray clay at 266-264 and 278-274 cm. Zone 1 (182-0 cm) contains a transitional layer featuring dark gray clay intercalated with black clayey/muddy peat (7.5YR 2.5/1, 3/1) at the zone bottom (182-171 cm). The zone top is brown/gray clay (7.5 YR 3/2, 4/1) with crumbly blue-green clay (GLEY1 3/5G) at 76-70 cm turning yellow gray. Small shells (47-23 cm) and scattered shell hash (171-127 cm) are present. Zone 1 contains rather homogeneous water, organic, and carbonate contents. Radiocarbon dates were obtained from 166 cm (3700±35 ^{14}C yr BP, 4040 cal yr BP) and 304 cm (4700±30 ^{14}C yr BP, 5400 cal yr BP) (Table 3.1).

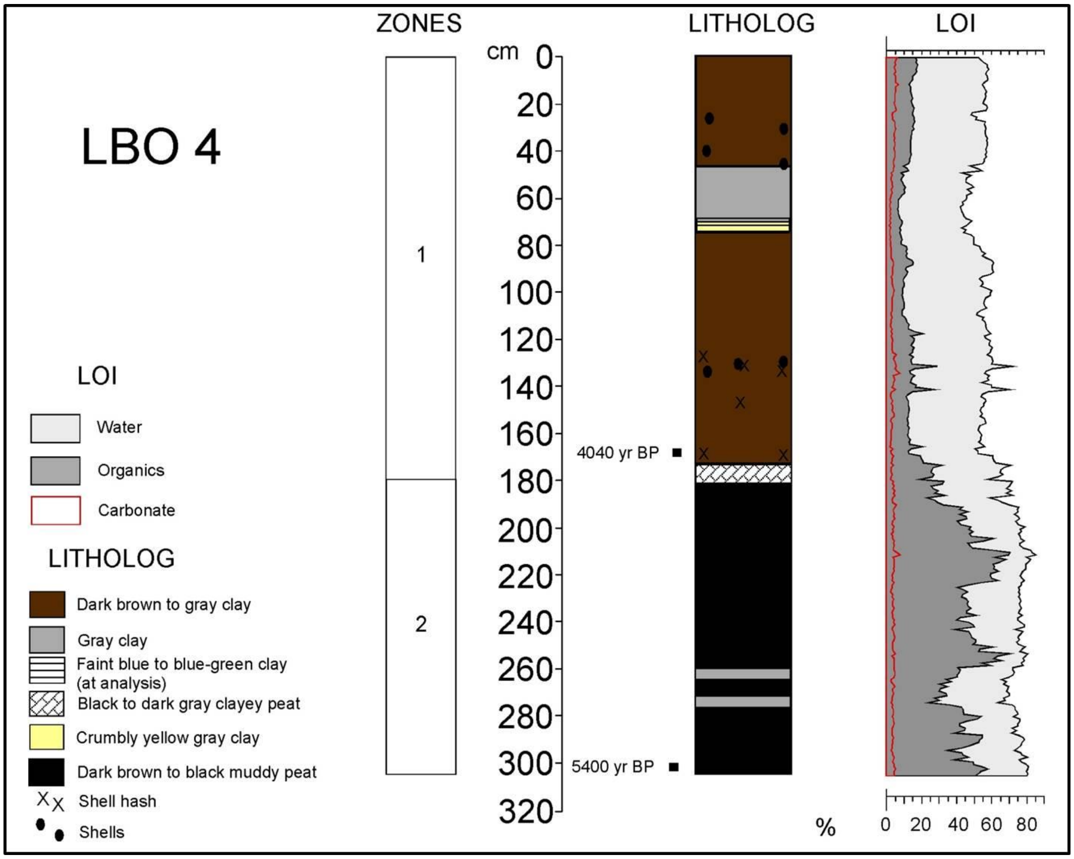

Figure 3.9 – Core 4 zone delineation, lithology, LOI results, and calibrated radiocarbon dates (calendar years). Zone 2 peat is high in water and organic content. Zone 1 clay is relatively low in water, organics, and carbonate.

3.5.2 Laguna Agua Dulce

LAD sediments are composed of sand, clay, and clayey silt, resembling the clastic components of documented surface samples (Landa-Jaime, 2003). Strong winds during fieldwork coupled with impenetrable sandy sediments led to unsuccessful extraction near LAD's center. Seaward cores (1-3) along LAD's western edge contain medium to coarse-grained sand lacking definitive stratigraphic change. Core 2 lithology and LOI contents are representative of seaward sediments. The bottom of core 2 (92-78 cm) is dominated by tan (7.5 YR 4/1) clayey sand. Coarse, multi-colored sand and gravel with scattered shell hash dominates from 78-24 cm.

Table 3.1 – Radiocarbon dating results and supplemental information for LBO cores 1, 3, and 4.

Core/sample ID	Depth (cm)	Lab #	Material	Radiocarbon age BP	Cal BP (2δ)	Relative area under prob distribution	Med. Prob
LBO 1A 4	4	OS-91849	Plant/Wood	125±45	-3-0	0.01	
					8-151	0.59	130
					171-280	0.4	
LBO 1 99	99	OS-83890	Plant/Wood	4500±30	5046-5296	1	5167
LBO 1 230	230	OS-83952	Plant/Wood	5480±35	6205-6321	0.961	6285
					6339-6341	0.001	
					6370-6393	0.038	
LBO 3C 26	118	OS-91547	Plant/Wood	4500±40	4980-5000	0.024	
					5038-5305	0.976	5163
LBO 4D 33	166	OS-91710	Plant/Wood	3700±35	3927-3948	0.04	
					3962-4104	0.841	4038
					4107-4149	0.119	
LBO 4G 48	304	OS-91717	Plant/Wood	4700±30	5321-5420	0.599	5400
					5438-5481	0.226	
					5531-5578	0.175	

The top 24 cm is tan, sandy clay (7.5 YR 3/1). Water (5-30%), organics (1-2%), and carbonate (1%) are low and consistent throughout (Figure 3.10). Landward cores (4-7) possess heterogeneous sands (mostly medium to coarse-grained) toward the bottom and clayey sand nearer the top. Core 6 is representative of seaward sediments, containing brown/gray (7.5 YR, 4/1) sand with minimal shell hash from 83-36 cm, low in water (10-20%), organics (1-3%), and carbonate (<1%). Medium to coarse sand for the top 36 cm contains two tan (7.5 YR 4/3) clayey sections with shell hash at 11-0 and 36-19 cm, with increases in water (50-60%), organics (7-10%), and carbonate (~1%). Lack of stratigraphy and datable material throughout LAD sediments prevented the construction of a reliable chronology.

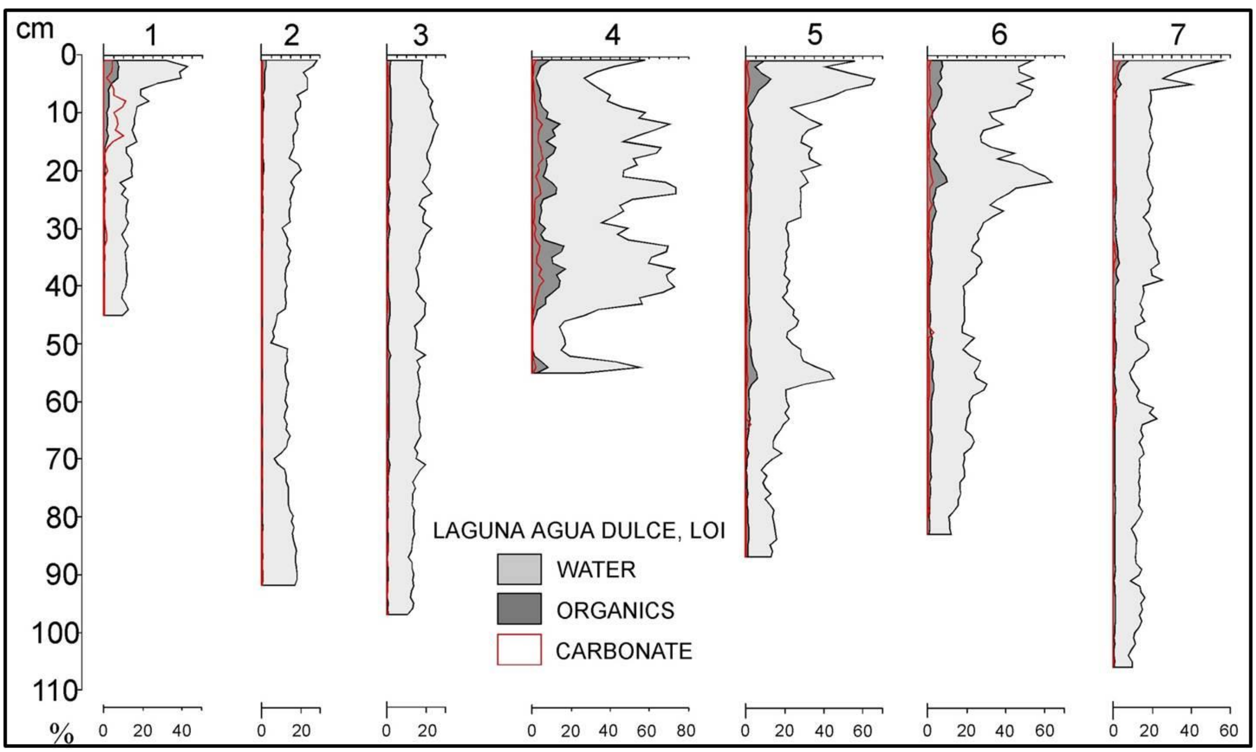

Figure 3.10 – LOI results for Laguna Agua Dulce cores. Low LOI values throughout most core sections indicate medium to coarse sand.

3.6 Discussion

3.6.1 Stratigraphic comparison of Laguna Boquita cores

Lithologic differences exist among seaward cores 1, 2, 3, and 5, and in comparison to the landward core 4 (Figure 3.11). Basal sandy clay exists solely in core 1 (zone 4, ~ 6800-6290 yrs BP). Zones 3 and 2 (6290 – ~5160 yr BP) consist of clastics intercalated with peaty mud in cores 1 and 3. Zone 3 is more apt for sand deposition than zone 2, which is dominated by peaty clay. One notable exception is a sand layer at the top of zone 2 in core 3, exhibited by a sudden drop in LOI contents. Nearby core 5 contains clay intercalated with peat throughout zone 2, with three thin sand layers including one near the zone top similar to core 3. Core 4 peat contains the highest water and organic contents among LBO sediments. Unlike other cores, clastic deposition in this peat section is limited to two thin clay layers.

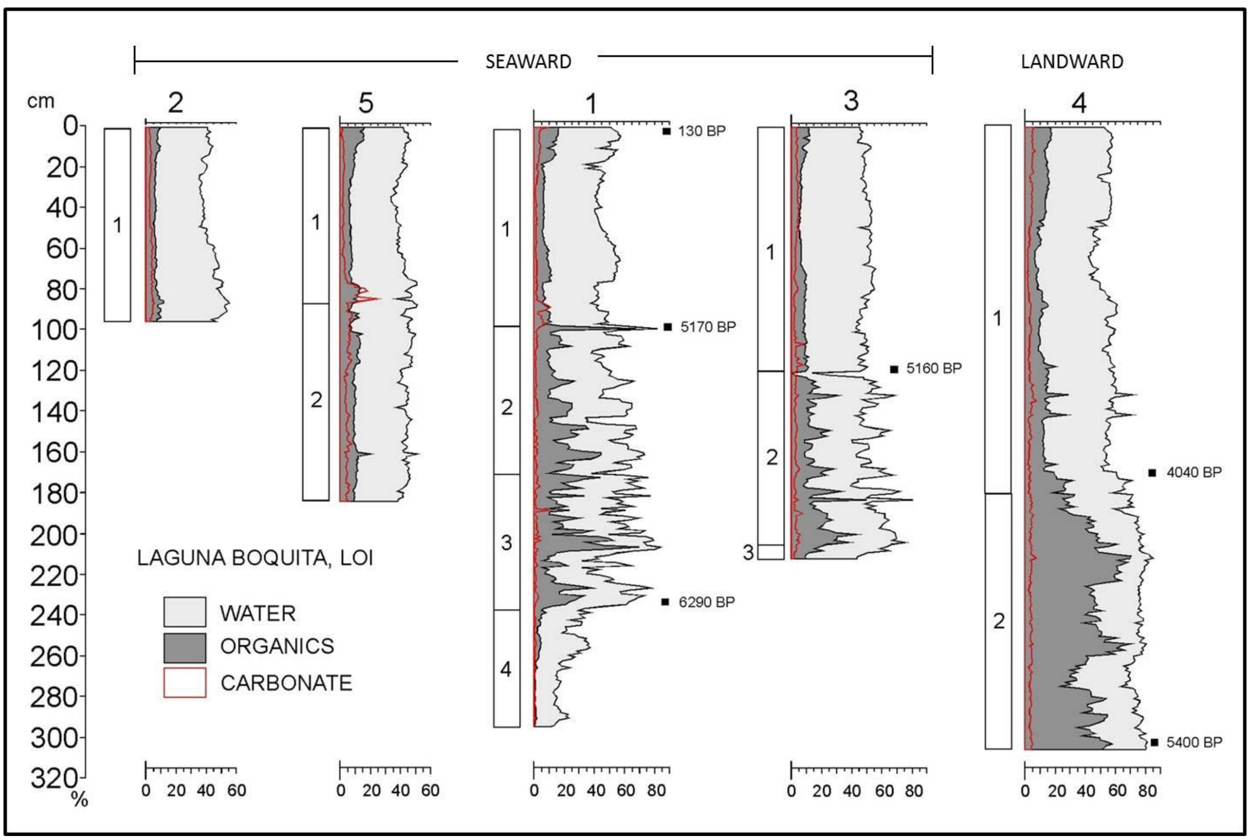

Figure 3.11 – LBO LOI results. Seaward cores 2, 5, 1, and 3 are grouped, with landward core 4 at the right. Inter-zone stratigraphic similarities are common among different cores.

A two-pronged carbonate spike at the bottom of zone 1 (~5160 yr BP – current) exists in seaward cores 1, 3, and 5, while absent in the landward core 4 and the short core 2. Carbonate-rich facies are characterized by yellow clay in core 5, while cores 1 and 3 lack discernible stratigraphic markings. Remaining zone 1 sediments are dominated by brown to gray clay. Cores 1, 2, 3, and 4 contained bluish clastic sections during extraction, which were severely desiccated in cores 2 and 4.

3.6.2 Environmental reconstruction of Laguna Boquita

The most relevant Holocene sea level reconstruction for the region comes from the neighboring state of Nayarit (Curray et al., 1969), providing the most practical estimate for the sites. Accordingly, sea level may have been 8 m below present 6800 years ago, the inferred age of the bottom of core 1. Regional sea level rise was relatively fast at this time, possibly rising ~2 m from 6800 years BP to 6000 years BP. Rapid sea level rise was capable of transporting deep sea and terrigenous shelf sediments landward toward the coast (Curray et al., 1969). Regional sea level began to stabilize around 5000 years BP at an estimated 4 m below present levels. This drop in the rate of sea level rise aided sediment deposition and the creation of Jalisco's coastal beach ridges, sparking the formation of backbarrier lakes and lagoons. Stabilization continued throughout the Late Holocene, with levels near present throughout the last 3000 years. This regression has been responsible for the vertical accretion and progradation of these beach ridges.

As LBO sediments contain definitive paleoenvironmental change spanning 6800 years, it is deemed more suitable for reconstruction than LAD. Peat sediments are indicative of a marsh or swamp environment proximate to sea level, containing minimal water level. Clastic sections generally indicate flooding stemming from either terrestrial or marine processes. Inorganic sediments entering via runoff or fluvial discharge are generally indicated by elevated

concentrations of terrigenous elements. Surface samples extracted adjacent to both LBO and LAD contain high concentrations of many lithogenic elements (e.g., Fe, Ti, Zr, Cr, Co, Zn). While lithogenic elemental concentrations may be elevated in marine sediments, certain elements are indicative of marine inundation and/or increased salinity. These elements are usually present in higher concentrations in seawater than freshwater, and include Cl, I, Sr, Ca, and S (Wakefield and Elderfield, 1985; Chen et al., 1997; Ramirez-Herrera et al., 2007; Woodruff et al., 2009; Nichol et al., 2007; Schofield et al., 2010).

3.6.3 Paleoenvironmental history of Laguna Boquita

3.6.3.1 Zone 4 – ~6800-~6290 yr BP

Basal sandy clay in core 1 represents a terrestrial environment (Figure 3.12). During this time period the site was probably only slightly above sea level. High S concentration suggests occasional marine inundation during storms or high tides. El Niño phases, for example, can cause sea surface temperature increases and sea level rise for the ENP, totaling up to 30 cm (e.g., Gonzalez et al., 1996).

3.6.3.2 Zones 3, 2 – ~6290-~5170 yr BP

Peat deposition beginning ~6290 yr BP in core 1 suggests that relative sea level has increased, aiding in wetland development. Beach ridge formation began during this period, as high energy conditions are suggested by offshore sand and finer-grained inorganic deposition into cores 1 and 3 coupled with intermittent I, Cd, K, Fe, and Ti spikes. Beach ridge development similarly occurred during this timeframe at Laguna Mitla in Guerrero state (Ramirez-Herrera et al., 2009; Chapters 5, 6). Elevated S concentration similar to zone 4 indicates relatively high salinity from marine influence.

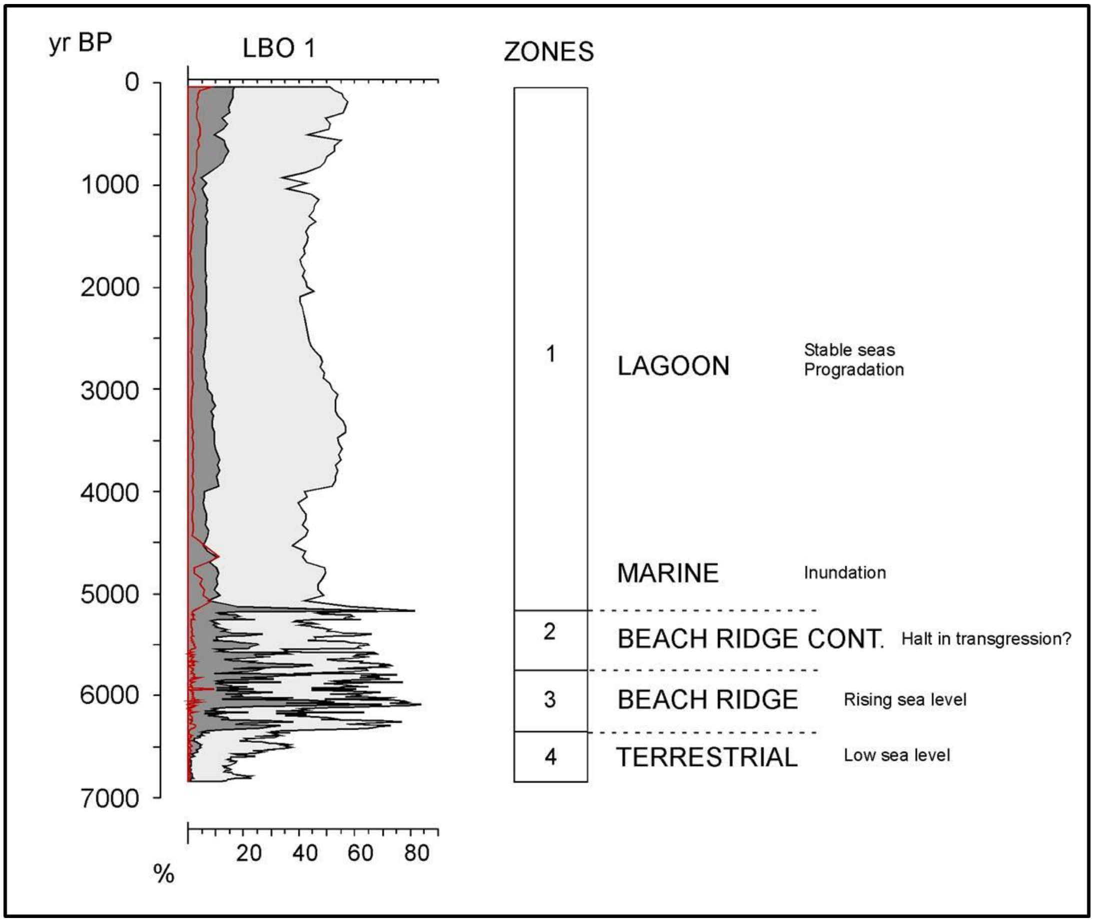

Figure 3.12 – LBO 1 paleoenvironmental change, per zone.

Brown and gray clay intercalating with peat throughout zone 2 in cores 1 and 3 indicates sustained oceanic influence. A halt in relative sea level rise inhibited larger-grain clastic transport into the nearshore in LBO, allowing the site to emerge at a faster rate than sea level. Another possible cause is a large offshore earthquake, capable of uplifting this coastal section (Ramirez-Herrera et al., 2004). Steady S concentration in core 1 and relatively high carbonate content in core 5 indicates continued marine influence. A sea level resurgence occurs at the top of zone 2 in cores 3 and 5, depositing offshore sand into the site. Clay with small shells in core 5 indicates topographical variation throughout the site, as this section is dominated by both terrestrial and marine-sourced clastics unlike adjacent areas dominated solely by marine-generated processes. The landward sections of LBO are stable and minimally disturbed, as

indicated by core 4 possessing the "purest" peat with highest water and organic contents, and limited clastic intrusion.

3.6.3.3 Zone 1 – ~5170 yr BP – present

Marine intrusion at the zone bottom is suggested from elevated marine elemental concentrations, high carbonate content, and the presence of shell hash in the seaward cores (Figures 3.4-3.7, 3.11). Similar evidence at ~5200 yr BP has been documented from Pacific coast states Nayarit (Curray et al., 1969; Sirkin, 1985) and Guerrero (Chapter 5), as well as Guatemala (Neff et al., 2006), attributed to marine transgression. Inundation signals the beginning of sea level stabilization and regression, forming LBO's backbarrier environment.

Remaining zone 1 sediment consists of brown, gray and blue clays, some sections crumbly and desiccated. Coastal progradation decreased sensitivity to marine intrusion, indicated by miniscule carbonate content for all cores and low marine element concentrations for core 1. Low sedimentation rates suggest a lack of direct fluvial input throughout zone 1. Human migration began in the region about 3400 years ago, documented from the Sierra de Manantlan Biosphere Reserve located in Jalisco's uplands (Figueroa-Rangel et al., 2008). Land disturbance from land use practices increased soil erosion, likely contributing to higher lithogenic concentrations closer to the top of core 1.

3.6.3.4 Tectonic uplift

LBO's sediment stratigraphy suggests that this region has been sensitive to uplift throughout the mid- and late-Holocene. Uplift has been triggered by both earthquakes near the coast and strain deformation during interseismic periods (Ramirez-Herrera et al., 2004), and is a main contributor of the relatively low water depth throughout zone 1. Core 1 sedimentation totaled 230 cm throughout the last ~6290 years, a time when the LBO site was even with sea

level and an estimated ~6-7 m below current sea level. Since LBO's surface is presently ~3 m above sea level, this peat section at ~230 cm uplifted ~670-770 cm. Taking sedimentation rate into account, this indicates roughly 430-530 cm of emergence and an uplift rate of 0.68-0.84 mm/yr. This is lower than the 3 mm/yr rate over the last 1300 years estimated by Ramirez-Herrera et al. (2004) for southern Jalisco. Discrepancy between these two estimates can stem from contrasting timeframes or geographical settings, along with inaccuracies in the sea level estimate. Similarly, poor dating control from the southern Jalisco site (Ramirez-Herrera et al., 2004) might have hampered their ability to arrive at a more accurate estimate. As large offshore earthquakes are capable of inducing subsidence (Ramirez-Herrera et al., 2004), it is troublesome to determine the contributions of individual earthquakes to land elevation changes. Seismological intricacies and tectonic histories of this area are intriguing and require additional work.

3.6.4 Sedimentary evidence of tropical cyclones at Agua Dulce and Boquita

3.6.4.1 Evidence of individual events

A combination of low water depth, truncated beach height from human modification, and nearby overwash deposition from Hurricanes Rick and Kenna suggest heightened sensitivity to storm surge deposition along LAD's northwestern edge. A submerged shoal located 70 m from the shoreline and near core 4 probably represents a relict overwash feature, likely from an intense TC or multiple events during an active period. Minor overwash fans could be reworked from barrier breaching, coastal modification, and high energy currents, which are capable of resuspending bottom sediments. The absence of sand lobes along the eastern side of the lagoon suggests that this area does not receive inundation from storm surge.

LBO is deemed fitting for overwash detection during its stable backbarrier phase (zone 1). LOI and XRF results coupled with physical inspection reveal an absence of sand layers or other evidence of overwash deposition (e.g., marine shells, shell hash). While geochemical analysis is a reliable tool toward extreme event detection when clastic deposition is lacking (e.g., Minoura and Nakaya, 1991), intermittent spikes in marine indicators are absent. The lack of breaching and overwash events may be attributed to the vast beach ridge system, forming an effective barrier to storm surge inundation. Storm surge height is stymied by the narrow (70 km wide) continental shelf and steep (-4000 m deep along edge) continental slope.

Macrofossil-laden debris layers suggestive of TC-induced slopewash events (e.g., Kennedy et al., 2006) are absent throughout LBO's backbarrier phase. Such high energy slopewash deposition is likely site-specific, dependent upon factors including adjacent geomorphology, soil type, and magnitude of land degradation. Additional cores extracted along the Pacific coast and inland Mexico could shed light on ideal settings and environmental conditions to receive high energy slopewash deposition. Lithogenic clays are often used as an alternative slopewash proxy, embedded throughout dark lacustrine sediments in nearby upland lakes (e.g., Byrne et al., 1996; Metcalfe et al., 2010). Since Jalisco's coastal lagoons and estuaries are affected by runoff and/or riverine sedimentation, it may not be easy to detect and separate TC-induced events from other types of deposits in massive clay sediments.

3.6.4.2 Climate change

The most distinct stratigraphic units throughout zone 1 are found at the bases of the water and organic-depleted gray clay facies, as these sections were generally bluish at extraction with textures ranging from slightly dry and cakey in cores 1 and 3 to completely desiccated in the peripheral cores 2 and 4. While bluish clay facies have been documented in freshwater

environments (e.g., Grove and Warren, 1968), they are mostly associated with estuarine/brackish (Ota et al., 1989; Brunetti et al., 1998) and marine (Ramirez-Herrera et al., 2007) conditions. Their existence can occur in regions with a seasonal precipitation regime and relatively low yearly totals, as flooded depressions with low water depth and elevated salinity can undergo significant chemical alterations over centennial-scale periods (e.g., Davis and Stevenson, 2007). Scholz et al. (2007) discovered water and organic-depleted blue-gray clay units from sediment from lakes Malawi and Bosumtwi in Africa, suggestive of paleo-lowstands. At Boquita, the low carbonate content and lack of sand and marine shells of these facies indicate that they stem from environmental change unrelated to marine deposition. Their stiff texture and cracking suggest complete desiccation of the site from a lack of water level. Similar ‘cracking’ has been interpreted to indicate site desiccation from lack of water from lakes in California (Kirby et al., 2004), Uganda (Russell et al., 2007) and Peru (Abbott et al., 1997). These facies in the Boquita sediments likely formed during a long period of limited water, leading to subaerial weathering and possibly brackish conditions, with an inferred date range of 3150-1700 years BP (Figure 3.13).

The adjacent and more recent dry gray clay units with decreased LOI might indicate an absence of nearby vegetation, or an increase in clastic sediment deposition. Abbott et al. (1997) pinpointed periods of low water levels and dry conditions at Peru’s Lake Titicaca from sedimentary units containing low organic contents, suggesting an increase in clastic content. Notably, elevated Cl concentrations occurred at the base of the dry gray clay unit in core 1. High Cl concentration has been implemented as an indicator of low water level and dry climatic conditions at Hoya San Nicolas Lake, located in central Mexico (Park, 2005). Minimal water

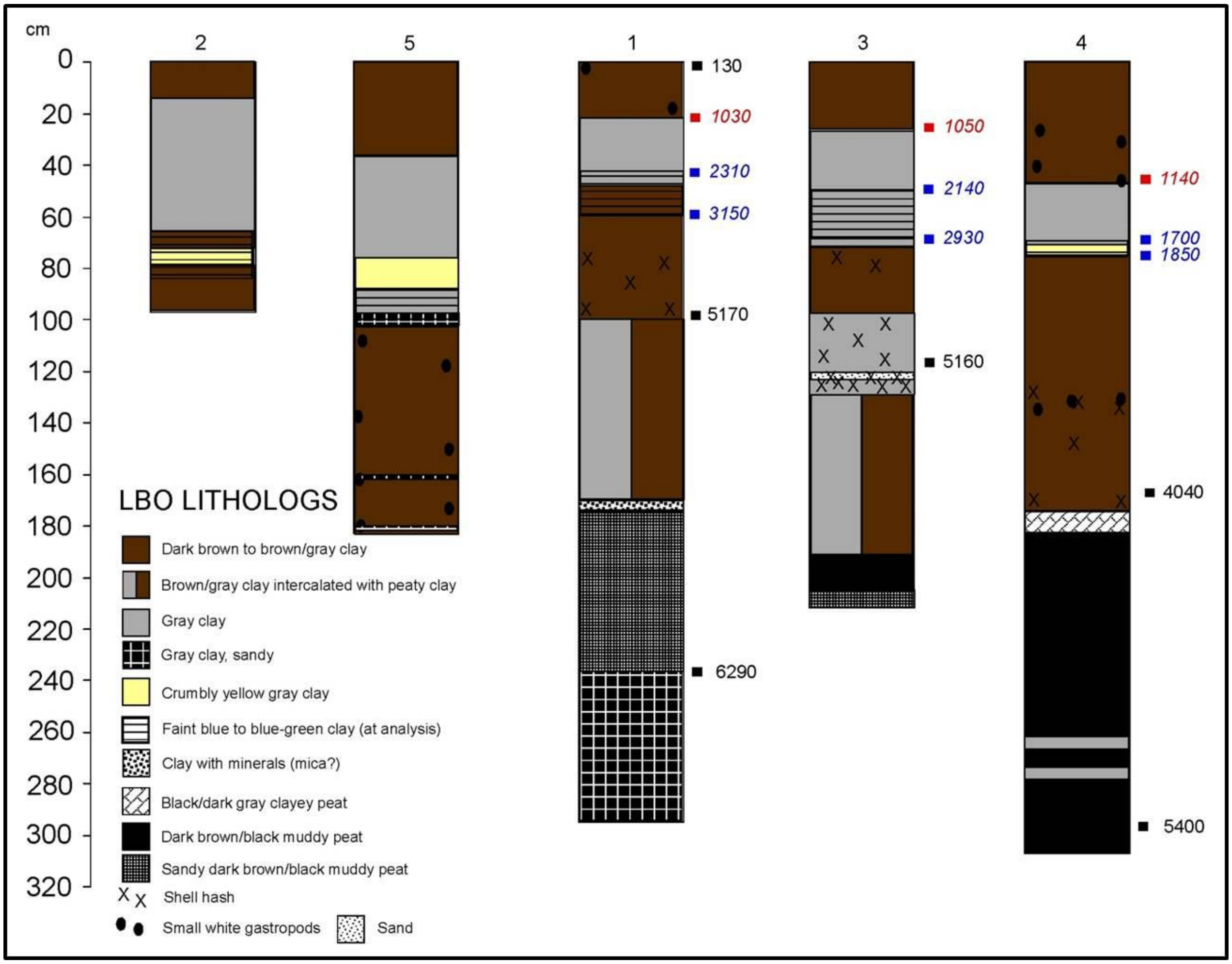

Figure 3.13 – Lithologs for all LBO cores. Seaward cores are grouped toward the left, with the landward core 4 at the far right. All dates (black text, square) are calibrated and rounded. Blue italicized dates for cores 1, 3, and 4 are inferred, bracketing the slightly dry to crumbly blue-gray unit. Red italicized dates for cores 1 and 3 are inferred, bracketing gray clay.

level and dry conditions likely continued throughout the entirety of the gray clay facies, ending ~1140-1030 years BP. Located at the core tops, brown clay containing small snails and increased LOI contents suggest re-establishment of nearby vegetation, finer grain deposition, and higher water level, suggestive of a wetter period. Despite the increase in water level, elevated Cl concentration suggests levels might not have been significant enough to drastically alter salinity. High Cl concentration at the core top might indicate miniscule amounts of salt remaining from freshwater evaporation. Cl concentration might have been further skewed by the presence of the many mud snails of terrestrial origin. Shells are capable of unique geochemical signatures (e.g.,

Kurunczi et al., 2001) with many types containing high Cl content (Armenteros et al., 2012), even species favoring freshwater environments (e.g., Appleton and Newell, 1977).

The dry and cakey to desiccated sections at the base of the gray clay units (~3150-1700 yr BP) are interpreted as the driest lagoonal conditions, while conditions likely remained dry until ~1030 yrs BP. During this period, wet season rainfall was probably below average, while minimal dry month precipitation led to the complete and prolonged desiccation of the site. This arid climate is coincident with a period of decreased TC frequency, significantly reducing rainfall totals for the coast and adjacent uplands as these events are a main contributor to regional precipitation totals (Bullock, 1986). The occurrence of this dry period is also supported by paleoclimatic records from the uplands. Byrne et al. (1996) attributed a dry period documented from Laguna de Juanacatlan from 3000-1000 yrs BP to TC inactivity. The Sierra de Manantlan Biosphere Reserve located in the Jalisco highlands contained palynological evidence of aridity at 2500 yrs BP (Figueroa-Rangel et al., 2008). A decrease in terrestrially-sourced slopewash entering the Gulf of California was also attributed to aridity from 2400-1900 yrs BP (Perez-Cruz, 2013). Alternatively, the recent brown clay facies suggesting wetter conditions during the past millennium suggest an increase in TC frequency. Wetter conditions are similarly documented throughout the uplands during this time (e.g., Metcalfe et al., 2010). Gray clay or organic-rich brown clay occurring in different cores during the early years of the backbarrier environment from ~5170-3170 yrs BP suggests inter-site variations in water level and adjacent vegetation development. Due to this sedimentological inconsistency, a definitive environmental and climatic signal is difficult to deduce. It must be noted that factors including upland river diversion from land degradation or farming (e.g., Gonzalez-Quintero, 1980) might affect the amount of water entering LBO. While sudden tectonic uplift from strong earthquakes is capable

of altering lagoonal water level (Garduno-Monroy et al., 2011), these events would likely cause distinct erosional deposits in the sediments, which are absent throughout LBO.

El Niño-Southern Oscillation (ENSO) is a significant control of precipitation frequency and intensity for the ENP. Warm surface water and decreased vertical shear during El Niño phases are responsible for increases in non-TC precipitation, along with wetter and more frequent ENP TCs (Reyes and Mejia-Trejo, 1991). Throughout recent times, these sites have experienced increased TC frequency during El Niño when compared to La Niña (Figure 3.14).

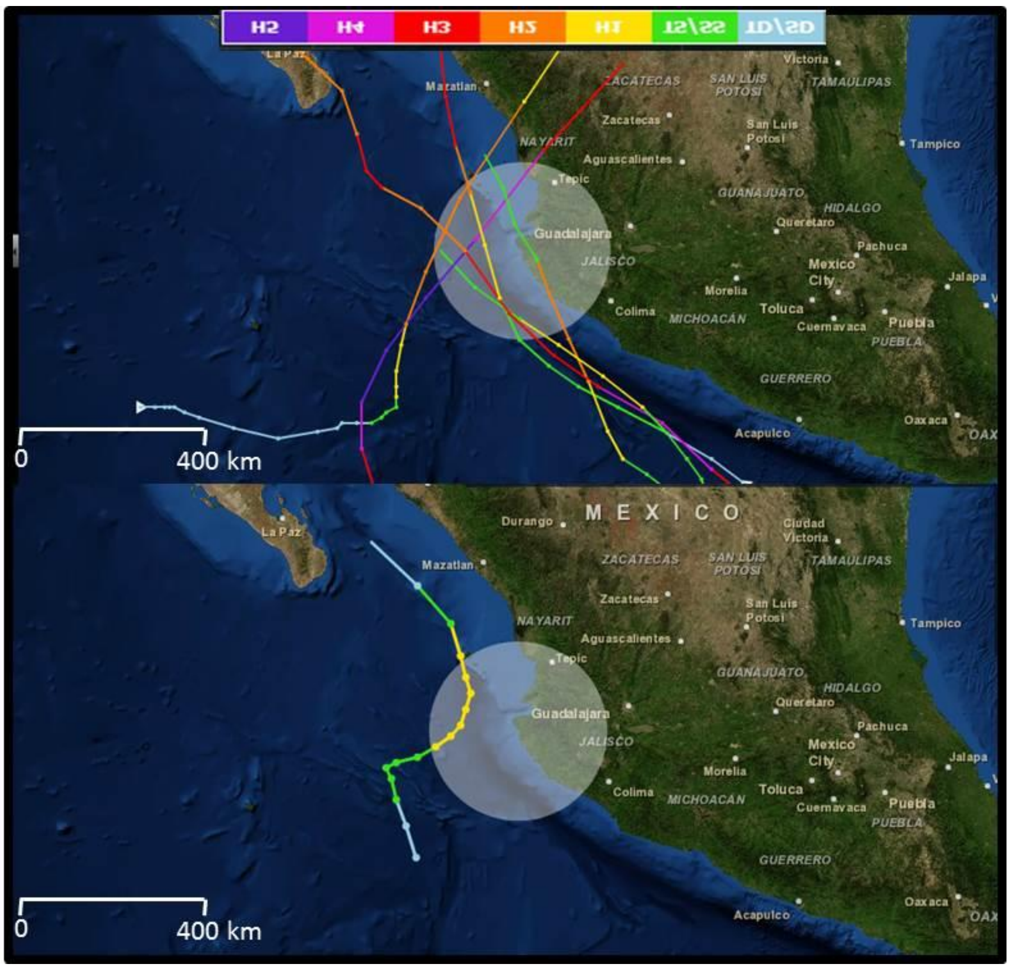

Figure 3.14 - TC tracks 200 km from Boquita during the last ten El Niño (‘09, ‘06, ‘04, ‘02, ‘97, ‘94, ‘91, ‘87, ‘82, ‘77 - top) and La Niña (‘11, ‘10, ‘07, ‘05, ‘00, ‘99, ‘98, ‘95, ‘88, ‘84 – bottom) years, based on ≥0.5 C° anomaly for five consecutive months from the Niño 3.4 region. Six tracks (Andres – 2009, John – 2006, Lane – 2006, Kenna – 2002, Rosa – 1994, Eugene – 1987) have severely impacted coastal Jalisco. Only Hurricane Madeline (1998) impacted this region during these La Niña years. Track data are from the National Oceanic and Atmospheric Administration (2011).

Dry conditions determined for Boquita temporally correlates to a period of decreased ENSO frequency detected from Ecuador's Laguna Pallacacocha, exhibited by a diminution in precipitation-induced slopewash entering the site from roughly 2500-1000 years ago (Moy et al., 2002). A period of low water level from 2870-1570 yrs BP detected from Laguna Mitla in nearby Guerrero state, 700 km southeast of LBO, is similarly attributed to decreased ENSO frequency (Chapter 6). Correlation between the Boquita and Mitla records indicates ENSO's relatively large-scale influence along this coast. An increase in ENSO frequency during recent times (Moy et al., 2002; Koutavas et al., 2006) is documented for Boquita as well as Mitla, due to evidence of wetter conditions. The relationship between ENSO and other climatic phenomena, namely the Inter-Tropical Convergence Zone (ITCZ) is poorly understood for the ENP (Koutavas et al., 2006). It is suggested that a southerly migrating ITCZ throughout the current millennium has contributed to wet periods at Boquita by strengthening El Niño phases due to the weakening easterly flow (Perez-Cruz, 2013). Likewise, a northwardly-migrating ITCZ might trigger drier coastal conditions in this area by cooling ENP water and increasing oceanic upwelling (Koutavas et al., 2006). Additional coastal and upland records are therefore requisite to complement LBO's paleoenvironmental record.

3.6.5 Barred inner shelf versus differential erosion lagoons

Pacific lagoons classified as the "barred inner shelf" type contain an array of sediment stratigraphies and environmental histories (Chapters 4-6), dependent upon coastal factors including geomorphology, tectonic activity, site characteristics (e.g., lagoon size, tidal exchange, salinity), human disturbance, and core proximity to the coast, streams, or inlets. Satellite image and topographical map analysis suggests close similarities between LBO and other barred inner shelf sites throughout Jalisco, particularly regarding lagoon size and beach

ridge dimensions. It is suggested that any future reconstructions would yield similar environmental histories to the LBO record, depicting basal sediments during a low relative sea level period, sea level rise (swamp/marsh development, beginning of beach ridge development), marine evidence via transgression ~5000 years BP, and sea level stabilization leading to backbarrier lagoon development. Additional sites should unequivocally be sought as they might offer improved resolution during the backbarrier phase.

LAD’s unsuitability for a long-term paleoenvironmental analysis stems from its sandy sediments deposited from the Rio Maria Garcia, flowing through the site during the mid-Holocene (Lankford, 1977). Its relict floodplain is carved along the lagoon’s southeastern edge and is currently occupied by farmland (Figure 3.1). While timing and cause for the river diversion are unknown, a significant earthquake during the mid-Holocene is a possibility. Unlike LBO, LAD is susceptible to overwash events from its position near sea level and its relatively narrow beach ridge system, as some nearshore ridges are drowned. Unsubmerged beach ridge sections along LAD’s southeastern edge possess a similar width to beach ridges at LBO, further suggesting that these two lagoons are similar in age. Unlike at LBO, an abundance of offshore marine sands and dense coastal vegetation are likely the responsible agents for LAD’s vertically accreting foredunes. Despite frequent barrier breaching, LAD’s drowned river formation and resuspended sediments make it suboptimal to determine a paleohurricane record. Probing nearshore mangrove peat and the lagoon center reveals sandy clay and medium- to coarse-grained sand similar to cores 1-7. It is suggested that “differential erosion” lagoons, as defined by Lankford (1977) along the Pacific coast, possess similar impenetrable sandy sediments and should be avoided for paleoenvironmental reconstruction.

3.7 Summary and conclusion

This study presents a paleoenvironmental reconstruction from Boquita and Agua Dulce on Jalisco's coast, two lagoons with contrasting formations and characteristics. Boquita, a "barred inner shelf" lagoon, reveals a ~6800 year history, containing terrestrial conditions during low sea level (~6800-6290 yr BP), swamp or marsh development and the beginning of beach ridge formation during a period of rising seas (6290-5170 yr BP), and a backbarrier lagoon phase when seas stabilized (5170 yr BP - current). Overwash sand layers suggestive of hurricane or tsunami events are non-existent throughout the backbarrier stage, due to an impenetrable beach ridge and narrow/deep continental shelf. Slightly dry and cakey to crumbly blue clay facies found in multiple cores with an inferred age of ~3150-1700 yr BP indicate a period of sub-aerial exposure and low water level, suggestive of a dry climatological period and low TC frequency from decreased ENSO activity. The overlying gray clay units with low LOI content and/or elevated Cl concentration suggests a lack of adjacent vegetation along with continued high salinity conditions and aridity lasting until ~1030 yr BP. Brown organic clay during the most recent millennium indicates denser vegetation around the site and wetter conditions. Additional coastal fieldwork from "barred inner shelf" lagoons is necessary to further verify evidence of this dry period, for instance, since factors such as river diversion could have influenced Boquita's water level.

Agua Dulce is a drowned river valley dominated by medium- to coarse-grained sands throughout its nearshore and center areas. Unlike LBO, Agua Dulce was sensitive to marine disturbances. A sandy shoal discovered meters from shore was likely deposited by an intense TC or multiple events during an active period. Other differential erosion lagoons along Mexico's

Pacific coast likely contain similar sandy stratigraphies, and should therefore be avoided if seeking a long-term paleoenvironmental record.

Additional Pacific coast research must be performed to produce paleoenvironmental records and evaluate their sensitivities to extreme event deposition. Records from other peat-bearing or lacustrine environments might be suitable to record slopewash events from individual TCs. Sediment cores extracted just tens of meters landward from the coastal beach ridge might prove worthwhile for storm deposit detection. Extreme event driven clastic layers were recently discovered in a similar nearshore wetland in Guerrero state (Ramirez-Herrera et al., 2012), 550 km southeast of these sites.

3.8 References

Abbott, M. B., M. W. Binford, M. Brenner, and K. R. Kelts. 1997. A 3500 ^{14}C high-resolution record of water-level changes in Lake Titicaca, Bolivia/Peru. Quaternary Research **47**: 169-180.

Appleton, T. C. and P. F. Newell. 1977. X-ray microanalysis of freeze-dried ultrathin frozen sections of a regulating epithelium from the snail *Otala*. Nature **266**:854-855.

Armenteros, M., M. Diaz-Asencio, R. Fernandez-Garces, M. Eriksson, C. Alonso-Hernandez, and J. A. Sanchez-Cabeza. 2012. Historical changes of sediments and mollusk assemblages in the Gulf of Bataban (Caribbean Sea) in the twentieth century. Environmental Monitoring and Assessment **184**:4709-4723.

Brunetti, A., M. Denefle, M. Fontugne, C. Hatte, and P. A. Pirazzoli. 1998. Sea-level and subsidence data from a late Holocene back-barrier lagoon (Valle Standiana, Ravenna, Italy). Marine Geology **150**:29-37.

Bullock, S. H. 1986. Climate of Chamela, Jalisco, and trends in the south coastal region of Mexico. Archives for Meteorology Geophysics and Bioclimatology Series B-Theoretical and Applied Climatology **36**:297-316.

Byrne, R., D. Allen, D. Edlund, and C. Polansky. 1996. Can lake sediments provide a record of tropical storms? The case of Laguna de Juanacatlan, Jalisco, Mexico. Page 159 *in* Proceedings of the Twelfth Annual Pacific Climate (PACLIM) Workshop. Interagency Ecological Program for the Sacramento - San Joaquin Estuary.

Chen, Z., Z. Chen, and W. Zhang. 1997. Quaternary stratigraphy and trace-element indices of the Yangtze Delta, eastern China, with special reference to marine transgressions. Quaternary Research **47**:181-191.

Contreras-Espinosa, F. and B. G. Warner. 2004. Ecosystem characteristics and management considerations for coastal wetlands in Mexico. Hydrobiologia **511**:233-245.

Crooks, R. C. 1960. Tropical cyclones in the Eastern North Pacific, 1959. Mariners Weather Log **4**:29-32.

Curray, F., J. Emmel, and P. J. Crampton. 1969. Holocene history of a strand plain lagoonal coast, Nayarit, Mexico. Pages 63-100 *in* A. Ayala-Castanares, editor. Coastal Lagoons: A Symposium. Universidad Nacional Autonoma de Mexico. Mexico City.

Davis, B. A. S. and A. C. Stevenson. 2007. The 8.2 ka event and Early-Mid Holocene forests, fires and flooding in the Central Ebo Desert, NE Spain. Quaternary Science Reviews **26**:1695-1712.

Dean, W. E. 1974. Determination of carbonate and organic matter in calcareous sediments and sedimentary rocks by loss on ignition: comparison with other methods. Journal of Sedimentary Petrology **44**:242-248.

Englehart, P. J. and A. V. Douglas. 2001. The role of eastern North Pacific tropical storms in the rainfall climatology of western Mexico. International Journal of Climatology **21**:1357-1370.

Figueroa-Rangel, B. L., K. J. Willis, and M. Olvera-Vargas. 2008. 4200 years of pine-dominated upland forest dynamics in west-central Mexico: Human or natural legacy? Ecology **89**:1893-1907.

Figueroa-Rangel, B. L., K. J. Willis, and M. Olvera-Vargas. 2010. Cloud forest dynamics in the Mexican neotropics during the last 1300 years. Global Change Biology **16**:1689-1704.

Garduno-Monroy, V. H., D. C. Soria-Caballero, I. Israde-Alcantara, V. M. H. Madrigal, A. Rodriguez-Ramirez, M. Ostroumov, M. A. Rodriguez-Pascua, A. Chacon-Torres, and J. C. Mora-Chaparro. 2011. Evidence of tsunami events in the paleolimnological record of Lake Patzcuaro, Michoacan, Mexico. Geofisica Internacional **50**:147-161.

Gonzalez, J. I., J. Ochoa, and P. Ripa. 1996. Promedio mensual del nivel del mar Pacifico Oriental. GEOS **16**:41-42.

Gonzalez-Quintero, L. 1980. Paleoecologia de un sector costero de Guerrero, Mexico (3000 anos). Memorias **86**:133-157.

Grove, A. T. and A. Warren. 1968. Quaternary landforms and climate on the south side of the Sahara. The Geographical Journal **134**:194-208.

Jauregui, E. 2003. Climatology of landfalling hurricanes and tropical storms in Mexico. Atmosfera **16**:193-204.

Kennedy, L. M., S. P. Horn, and K. H. Orvis. 2006. A 4000-year record of fire and forest history from Valle de Bao, Cordillera Central, Dominican Republic. Palaeogeography Palaeoclimatology Palaeoecology **231**:279-290.

Kirby, M. E., C. J. Poulsen, S. P. Lund, W. P. Patterson, L. Reidy, and D. E. Hammond. 2004. Late Holocene lake level dynamics inferred from magnetic susceptibility and stable oxygen isotope data: Lake Elsinore, southern California (USA). Journal of Paleolimnology **31**:275-293.

Koutavas, A., P. B. deMenocal, and J. Lynch-Stieglitz. 2006. Holocene trends in tropical Pacific sea surface temperatures and the El Nino-Southern Oscillation. PAGES news **13**:22-23.

Kurunczi, S., S. Torok, and P. Chevallier. 2001. A micro-XRF study of the element distribution on the growth front of mussel shell (Species of Unio crassus Retzius). Mikrochimica Acta **137**:41-48.

Landa-Jaime, V. 2003. Benthic mollusck assemblage of the Agua Dulce/El Ermitaño, Jalisco, Mexico. Ciencas Marinas **29**:169-184.

Lankford, R. R. 1977. Coastal lagoons of Mexico: Their origin and classification. Pages 182-215 *in* M. Wiley, editor. Estuarine Processes. Academic Press Inc.

Liu, K. B. 2007. Paleotempestology. Pages 1978-1986 *in* S. Elias, editor. Encyclopedia of Quaternary Science. Elsevier, Amsterdam.

Metcalfe, S. E., M. D. Jones, S. J. Davies, A. Noren, and A. MacKenzie. 2010. Climate variability over the last two millennia in the North American Monsoon region, recorded in laminated lake sediments from Laguna de Juanacatlan, Mexico. The Holocene **20**:1195-1206.

Minoura, K. and S. Nakaya. 1991. Traces of tsunami preserved in inter-tidal lacustrine and marsh deposits: Some examples from Northeast Japan. Journal of Geology **99**:265-287.

Molinari, J., D. Vollaro, S. Skubis, and M. Dickinson. 2000. Origins and mechanisms of eastern Pacific tropical cyclogenesis: A case study. Monthly Weather Review **128**:125-139.

Moll, W. F. 2001. Baseline studies of the clay minerals as society source clays: Geological origin. Clays and Clay Minerals **49**:374-380.

Moore, N. H. and D. J. Slinn. 1984. The physical hydrology of a lagoon system on the Pacific coast of Mexico. Estuarine Coastal and Shelf Science **19**:413-426.

Moy, C. M., G. O. Seltzer, D. T. Rodbell, and D. M. Anderson. 2002. Variability of El Niño/Southern Oscillation activity at millennial timescales during the Holocene epoch. Nature **420**:162-165.

National Geophysical Data Center. 2011. Global Historical Tsunami Database.

National Oceanic and Atmospheric Administration. 2011. Historical hurricane tracks. Retrieved 12-29-2011, from http://www.csc.noaa.gov/hurricanes/.

Neff, H., D. M. Pearsall, J. G. Jones, B. A. de Pieters, and D. E. Freidel. 2006. Climate change and population history in the Pacific Lowlands of Southern Mesoamerica. Quaternary Research **65**:390-400.

Nichol, S. L., J. R. Goff, R. J. N. Devoy, C. Chague-Goff, B. Hayward, and I. James. 2007. Lagoon subsidence and tsunami on the west coast of New Zealand. Sedimentary Geology **200**:248-262.

Noren, A. J., P. R. Bierman, E. J. Steig, A. Lini, and J. Southon. 2002. Millennial-scale storminess variability in the northeastern United States during the Holocene epoch. Nature **419**:821-824.

Ota, Y., K. R. Berryman, L. J. Brown, and K. Kashima. 1989. Holocene sediments and vertical tectonic downwarping near Wairoa, Northern Hawke's Bay, New Zealand. New Zealand Journal of Geology and Geophysics **32**:333-341.

Page, M. J., N. A. Trustrum, and R. C. DeRose. 1994. A high resolution record of storm-induced erosion from lake sediments, New Zealand. Journal of Paleolimnology **11**:333-348.

Park, J. 2005. Holocene environmental change and human impact in Hoya San Nicolas, Guanajuato, Mexico. Journal of the Korean Geographical Society **40**:571-583.

Perez-Cruz, L. 2013. Hydrological changes and paleoproductivity in the Gulf of California during middle and late Holocene and their relationship with ITCZ and North American Monsoon variability. Quaternary Research **79**:138-151.

Phleger, F. B. and G. C. Ewing. 1962. Sedimentology and oceanography of coastal lagoons in Baja California, Mexico. Geological Society of America Bulletin **73**:145-182.

Ramirez-Herrera, M. T., A. Cundy, V. Kostoglodov, A. Carranza-Edwards, E. Morales, and S. Metcalfe. 2007. Sedimentary record of late-Holocene relative sea-level change and tectonic deformation from the Guerrero Seismic Gap, Mexican Pacific Coast. The Holocene **17**:1211-1220.

Ramirez-Herrera, M. T., A. B. Cundy, V. Kostoglodov, and M. Ortiz. 2009. Late Holocene tectonic land-level changes and tsunamis at Mitla lagoon, Guerrero, Mexico. Geofisica Internacional **48**:195-209.

Ramirez-Herrera, M. T., V. Kostoglodov, and J. Urrutia-Fucugauchi. 2004. Holocene-emerged notches and tectonic uplift along the Jalisco coast, Southwest Mexico. Geomorphology **58**:291-304.

Ramirez-Herrera, M. T., M. Lagos, I. Hutchinson, V. Kostoglodov, M. L. Machain, M. Caballero, A. Goguitchaichvili, B. Aguilar, C. Chague-Goff, J. Goff, A.-C. Ruiz-Fernandez, M. Ortiz, H. Nava, F. Bautista, G. I. Lopez, and P. Quintana. 2012. Extreme wave deposits on the Pacific coast of Mexico: Tsunamis or storms? - A multi-proxy approach. Geomorphology **139**:360-371.

Ramirez-Herrera, M. T. and J. Urrutia-Fucugauchi. 1999. Morphotectonic zones along the coast of the Pacific continental margin, southern Mexico. Geomorphology **28**:237-250.

Reyes, S. and A. Mejia-Trejo. 1991. Tropical perturbations in the Eastern Pacific and the precipitation field over North-Western Mexico in relation to the ENSO phenomenon. International Journal of Climatology **11**:515-528.

Russell, J. M., D. Verschuren, and H. Eggermont. 2007. Spatial complexity of 'Little Ice Age' climate in East Africa: sedimentary records from two crater lake basins in western Uganda. The Holocene **17**:183-193.

Schofield, J. E., K. J. Edwards, T. M. Mighall, A. Martinez Cortizas, J. Rodriguez-Racedo, and G. Cook. 2010. An integrated geochemical and palynological study of human impacts, soil erosion and storminess from southern Greenland since c. AD 1000. Palaeogeography Palaeoclimatology Palaeoecology **295**:19-30.

Scholz, C. A., T. C. Johnson, A. S. Cohen, J. W. King, J. A. Peck, J. T. Overpeck, M. R. Talbot, E. T. Brown, L. Kalindekafe, P. Y. O. Amoako, R. P. Lyons, T. M. Shanahan, I. S. Castaneda, C. W. Heil, S. L. Forman, L. R. McHargue, K. R. Beuning, J. Gomez, and J. Pierson. 2007. East African megadroughts between 135 and 75 thousand years ago and bearing on early-modern human origins. Proceedings of the National Academy of Sciences **104**:16416-16421.

Sirkin, L. 1985. Late Quaternary stratigraphy and environments of the West Mexican Coastal Plain. Palynology **9**:3-25.

Stuiver, M., P. J. Reimer, and R. W. Reimer. 2005. CALIB 6.0 (program and documentation).

Wakefield, S. J. and H. Elderfield. 1985. Interstital water iodine enrichments from the eastern Pacific. Journal of Marine Research **43**:951-961.

Woodruff, J. D., J. P. Donnelly, and A. Okusu. 2009. Exploring typhoon variability over the mid-to-late Holocene: evidence of extreme coastal flooding from Kamikoshiki, Japan. Quaternary Science Reviews **28**:1774-1785.

CHAPTER 4. A 4000 YEAR PALEOENVIRONMENTAL RECONSTRUCTION FROM LAGUNA NUXCO ON MEXICO'S PACIFIC COAST

4.1 Introduction

Approximately 8,475 km of Mexico's Pacific coast are classified as wetland, covering 892,800 ha (Contreras-Espinosa and Warner, 2004). These wetland areas include over 79 water bodies, ranging from bays and sounds to estuaries and lagoons varying in characteristics including size, morphology, and salinity (Lankford, 1977). Their paleoenvironmental histories are mostly unknown as few paleo-records exist. With 485 km of coastal wetlands covering 22,700 ha (Contreras-Espinosa and Warner, 2004) including tens of water bodies, the coastal state Guerrero is no exception with regard to poor paleorecords. Research has concentrated in the interior highlands (e.g., Berrio et al., 2006). Coastal reconstructions have the potential to offer information on paleoclimate, wetland restoration, and disturbance ecology among other disciplines, providing scientific, economic, and social implications.

Guerrero's coast is seasonally battered by tropical cyclones (TCs), capable of catastrophic geophysical and societal destruction. The most significant damage during the historical period was from Hurricane Pauline (1997). Only of category 1 intensity (on the Saffir-Simpson scale) as it approached the popular resort town Acapulco, Pauline dumped 400 mm of precipitation (Lawrence, 1999) resulting in 120 deaths and 300 million pesos (>22 million USD) in damage (Matias-Ramirez, 1998). Mudslides carried earth materials, including large boulders, down inland hills toward the coast (Spang et al., 2003). Although significant storm surge has never been reported near Acapulco, a 9 m surge in Oaxaca, southeast of Guerrero, inundated the coastal beach, creating vast overwash fans (Goman et al., 2005).

The case of Pauline begs the question regarding coastal Guerrero's sensitivity toward recording geophysical TC evidence. Coastal scientists can tackle this issue by applying the

principles and methods of paleotempestology, involving sediment core extraction and the implementation of geological and biological proxies (Liu, 2007). Paleoenvironmental reconstructions from coastal lakes, lagoons, and marshes have proven ideal in determining evidence of paleohurricanes (e.g., Liu and Fearn, 1993, 2000; Donnelly et al., 2001; Kiage et al., 2011; McCloskey and Liu, 2012, 2013). Mexico's Pacific coast lends an important spatial hub to add to the growing global database, which is vital for inter-basin correlations and furthering paleoclimatological understanding.

Methodological advances coupled with the necessity for long-term TC records from different ocean basins have allowed recent work to commence in regions once avoided due to complications and uncertainties. This includes areas with active tectonism (e.g., Woodruff et al., 2009) potentially requiring differentiation between tsunami (Fujiwara et al., 2000; Chague-Goff et al., 2002) and TC deposits (McCloskey and Liu, 2012, 2013). The reliability of extreme-event driven overwash sand is uncertain as the Pacific coast contains very high beach ridges compared to Gulf and Atlantic coasts. With local mudslides common and slopewash deposits attributed to TCs in some geomorphological settings (e.g., Kennedy et al., 2006), it is yet to be determined if this is a reliable TC proxy along Mexico's Pacific coast.

A literature review and remote sensing investigation deem Laguna Nuxco in Guerrero, western Mexico, fitting for analysis. This chapter presents a multi-proxy paleoenvironmental reconstruction from three nearshore sediment cores. The objectives are threefold. First, Nuxco's Late Holocene history must be reconstructed so that the paleoenvironmental conditions favorable or unfavorable to TC activity can be inferred. Second, sensitivity of the site to recent TC deposition will be determined. Third, if a modern analog deposit is present it will be applied

toward interpreting older sediments to produce a multi-millennial record of TC activity for this region.

4.2 Study area

The Pacific coastal state Guerrero (17.6131º N, 99. 95º W) is located along mainland Mexico’s west coast, wedged between states Michoacan to the northwest and Oaxaca to the southeast. The climate is semi-arid and monsoonal with a wet season occurring annually from May to November. Precipitation is ~130 cm/year along the coast (Bullock, 1986), increasing inland. Coastal vegetation is classified as a tropical dry forest with xeric-type shrubs. Paralleling the coast along Guerrero’s interior lies the Sierra Madre del Sur Mountains, the source of rivers and ephemeral streams emptying into the Pacific Ocean or coastal waters. Tectonic collision caused by the oceanic Cocos plate subducting under the North American plate along the Middle America Trench (MAT) is responsible for triggering earthquakes and tsunami. A narrow shelf (~70 km) and a steep continental slope (~5000 m) separate the MAT from the coast. Rocky cliffs and marine terraces, suggesting paleo-uplift, line most of Guerrero’s coast (Ramirez-Herrera et al., 2011).

Laguna Nuxco (17.2012° N, 100.7951° W) is located on Guerrero’s central coast, 80 km west-northwest of Acapulco (Figure 4.1). Nuxco is circular-shaped and 4 x 2.5 km in size with a 1.9 m mean depth (Yanez-Arancibia, 1977). Salinity is ~18-22 ppt (Contreras-Espinosa and Warner, 2004) and seasonally variable. Brackish copepods, ostracods, barnacle larvae, nematodes, and shells (*Amnicola sp.*, *Nassarius bailyi*, *Cerithidea mazatlanica*, *Bittlum sp*., *Melongena sp*., *Neritina cassiculum*, *Felaniella sericata*, *Mytella strigata*) reside on Nuxco’s floor (Yanez-Arancibia, 1977). Mangroves flank Nuxco’s western, southern, and eastern edges.

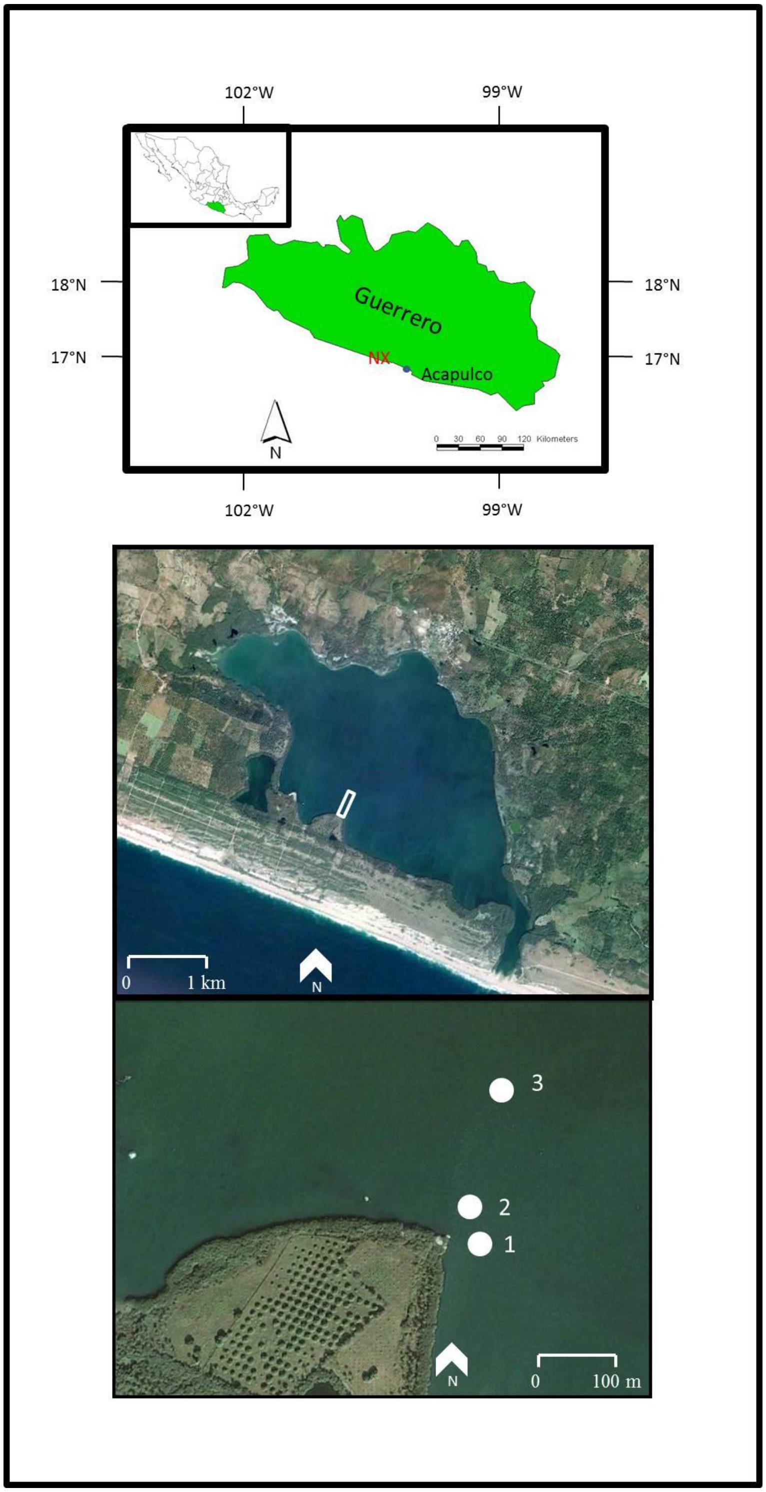

Figure 4.1 – Guerrero state, with subset of its location in Mexico (Top). Laguna Nuxco is shown, with red rectangle displaying coring locations (Middle). The three coring spots are pinpointed (Bottom). Images courtesy of Google Earth.

Landward topography is hilly with elevation surpassing 400 m about 10 km inland. The development of deltaic plains and a lack of paleo-uplift evidence in Nuxco's vicinity suggest relative tectonic stability (Ramirez-Herrera and Urrutia-Fucuguchi, 1999).

Nuxco is classified as a "barred inner shelf" lagoon, sharing a similar formation and characteristics to most Pacific coast lagoons. Formally a depression along the continental shelf, Nuxco was inundated by marine transgression 6000-5000 years BP, soon protected by beach ridges formed during stabilizing seas (Lankford, 1977). A 750 m wide relict beach ridge plain of ~10 m elevation exists behind a 50 m wide modern coastal beach with dunes, some ~20 m high. The geological setting is classified as a "rugged granitic terrain" (Lankford, 1977).

Nuxco's dynamism depends largely upon water level. Two km to the east of the lagoon lies Rio Nuxco which flows during the wet season and possesses a 100 km^2 drainage area. The mouth of the Rio Nuxco is cut off by the beach year-round, leading runoff from excessively wet periods into the lagoon (Lankford, 1977). Water level is similarly controlled by periods of intense and/or prolonged precipitation. Increased water input raises the lagoon level while stressing the margins. The hydrostatic pressure can erode the 180 m wide channel at Nuxco's southeastern corner, opening the inlet and partially draining the lagoon, subsequently allowing both marine water and species to intrude (Lankford, 1977). An example of such an event comes from Tropical Storm Odile (October 8-13, 2008) (Figure 4.2). Odile dumped 10 inches (>25 cm) of rainfall to the area over a two-day period (National Climatic Data Center, 2013), raising the water level and causing the blowout that released water into the Pacific. Stability is exhibited in an image taken in October 2010, as lack of TC activity (National Oceanic and Atmospheric Administration, 2011) and only trace precipitation (National Climatic Data Center, 2013) keeps lagoon water near sea level, preventing pressure against the inlet.

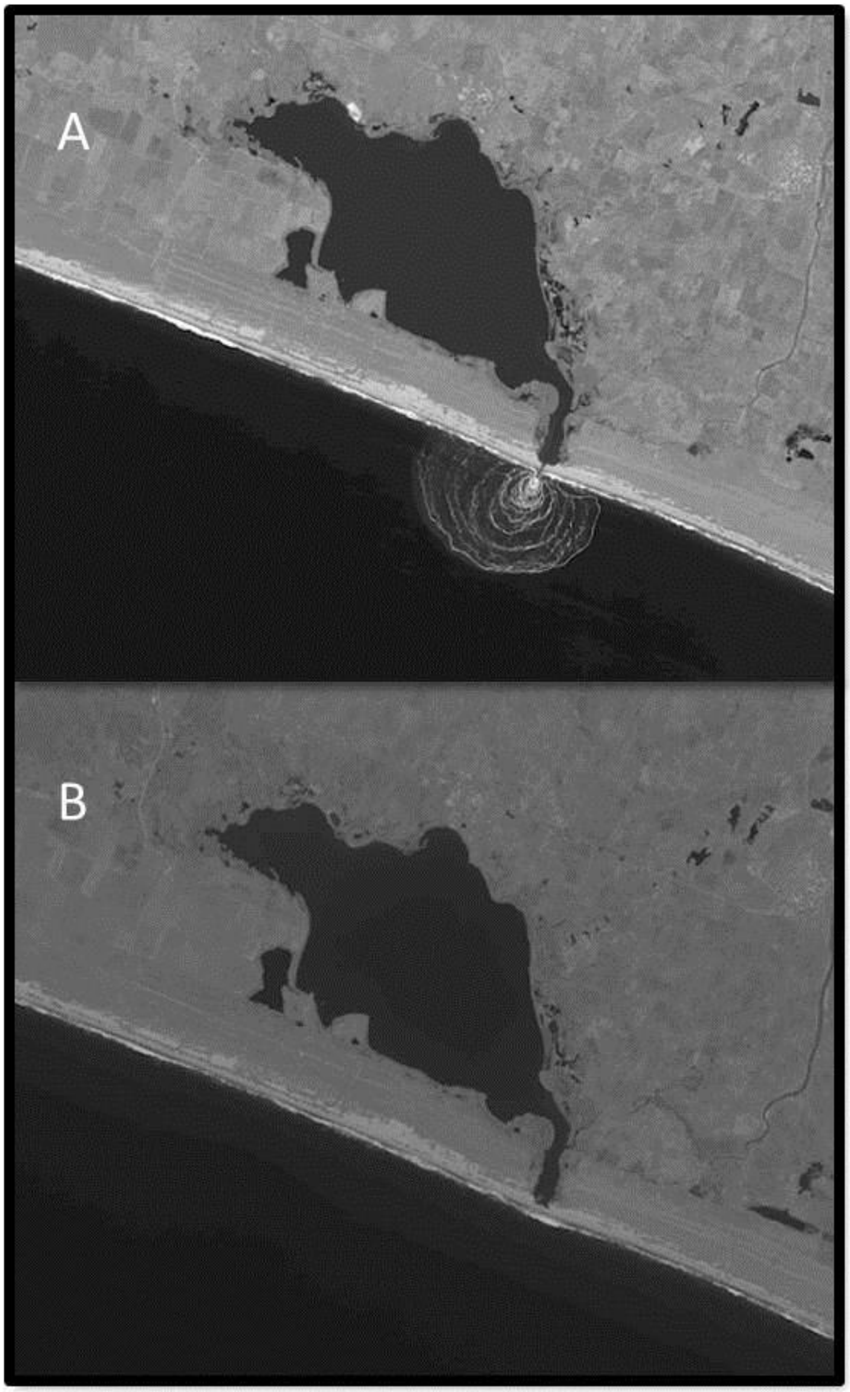

Figure 4.2 – Worldview 1 satellite images of Laguna Nuxco and surrounding area. Top (A) image (10-19-08) displays the blowout event caused by Tropical Storm Odile, common after heavy and prolonged precipitation. Bottom (B) image indicates stability during a period recording only trace rainfall (10-21-10). Images courtesy of Digital Globe (www.digitalglobe.com).

4.3 Extreme events

The Eastern North Pacific (ENP) active TC season occurs annually from May to November. TCs form west of Guatemala between 110º and 90º W and move in a west-northwest trajectory. Twenty hurricanes have passed within 200 km of Nuxco from 1949-2010 (Figure 4.3). The geophysical impacts of the hurricanes were unassessed in previous investigations (e.g., Lankford, 1977; Yanez-Arancibia, 1977), and they are only suggested cursorily from nearby Laguna Mitla (Paez-Osuna and Mandelli, 1985). Local residents claim that recent TC geophysical impacts such as storm surge inundation and mudslides have been negligible at and near Nuxco.

Tsunamis are less frequent than TCs with only nine events of maximum water height ≥2 m since 1732 (National Geophysical Data Center, 2011). Recent geomorphological effects from the area have been minimal (Jonathan et al., 2011), confirmed by local residents.

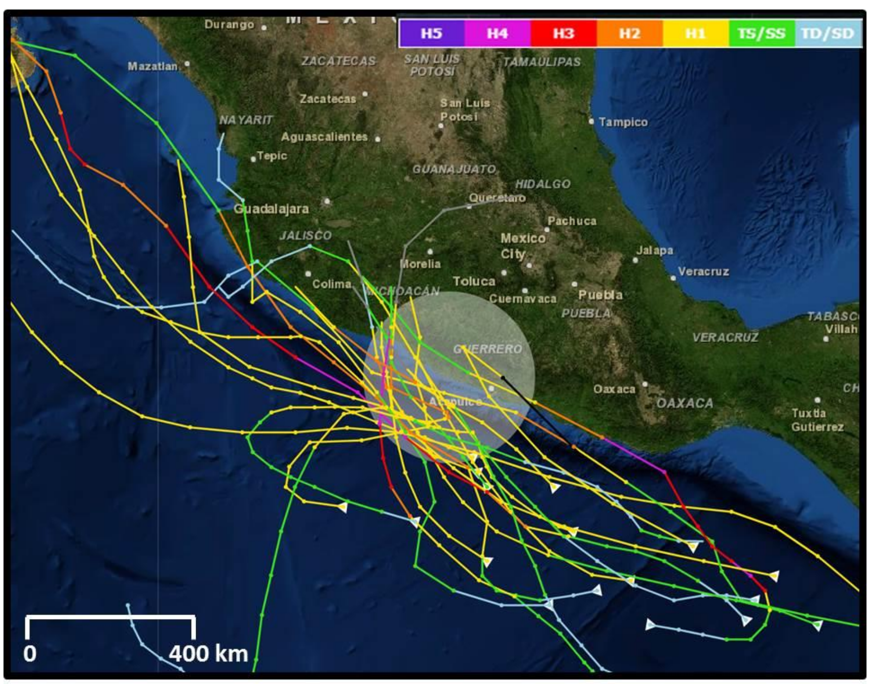

Figure 4.3 – Twenty hurricanes passed within 200 km of Nuxco (white circle) during the instrumental period. Most tracks are at tropical storm (green) or category 1 (yellow) intensity near Nuxco. Hurricane track data are from the National Oceanic and Atmospheric Administration (2011).

4.4 Methodology

Field expedition occurred during the dry season (December) in 2009. Three sediment cores were extracted near Nuxco's seaward edge in a shore-perpendicular transect. Core 1 was collected with a Russian peat borer, yielding ~50 cm segments transferred to pre-cut PVC tubes and secured with plastic wrap and duct tape to prevent moisture loss. Cores 2 and 3, taken in 130 cm core segments, were captured with a modified Livingstone corer with cylindrical, 2-inch diameter PVC tubes. At least 5 cm overlap was measured for each additional core segment to account for coretop disturbance. Surface samples were collected from the lagoon bottom and adjacent beach. All samples were stored in a 4ºC refrigerated room upon arrival at the Global Change and Coastal Paleoecology Laboratory, Department of Oceanography and Coastal Sciences, Louisiana State University.

Sediments were examined soon after arrival to ensure moisture and color preservation. Cores and select surface samples were lithologically described with the aid of a Munsell soil color chart and subjected to high-resolution loss-on ignition analysis (Dean, 1974) to determine water, organic, carbonate, and residual (siliciclastic) contents. Chemical composition of selected cores and surface samples was measured with a Delta Innov-X handheld X-ray fluorescence unit (XRF) with a tantalum X-ray tube and 2 cm resolution window. Three laser beams with 15 and 40 kilovolt excitation detected both light and heavy elements. The sediment surface was covered with plastic film to prevent disturbance and directly scanned for 90 seconds per sample. XRF analysis is useful for detecting relative elemental change (Jessen et al., 2008). Shell identification was aided with manuals and regional guides (Olsson, 1961; Melvin, 1966; Keen, 1971; Oliver, 1975) along with personal communications with Dr. Emilio Garcia of the Malacological Society of Baton Rouge, Louisiana (USA). Bulk sediment (1 cm^3) and organic

pieces (sieved and rinsed with deionized water) were sent to the National Ocean Sciences Accelerator Mass Spectrometry (NOSAMS) facility at Woods Hole Oceanographic Institution for radiocarbon dating. Calib 6.0 and the IntCal09 curve (Stuiver et al., 2005) aided in converting radiocarbon years to calibrated ranges and a median probability age, rounded to the nearest ten years. Sedimentation rates were calculated by linear interpolation between radiocarbon samples, and extrapolation to the core tops and bases.

4.5 Results

4.5.1 Sediment lithology, LOI, XRF

Core 1 (128 cm) was extracted 320 m north of shore in 1 m water depth. It is composed of scattered whole and broken shells (hash) embedded in gray clay (5Y 3/2) (Figure 4.4), exhibiting similarities to typical estuarine-type sedimentation (e.g., Goman et al., 2005). Hash is

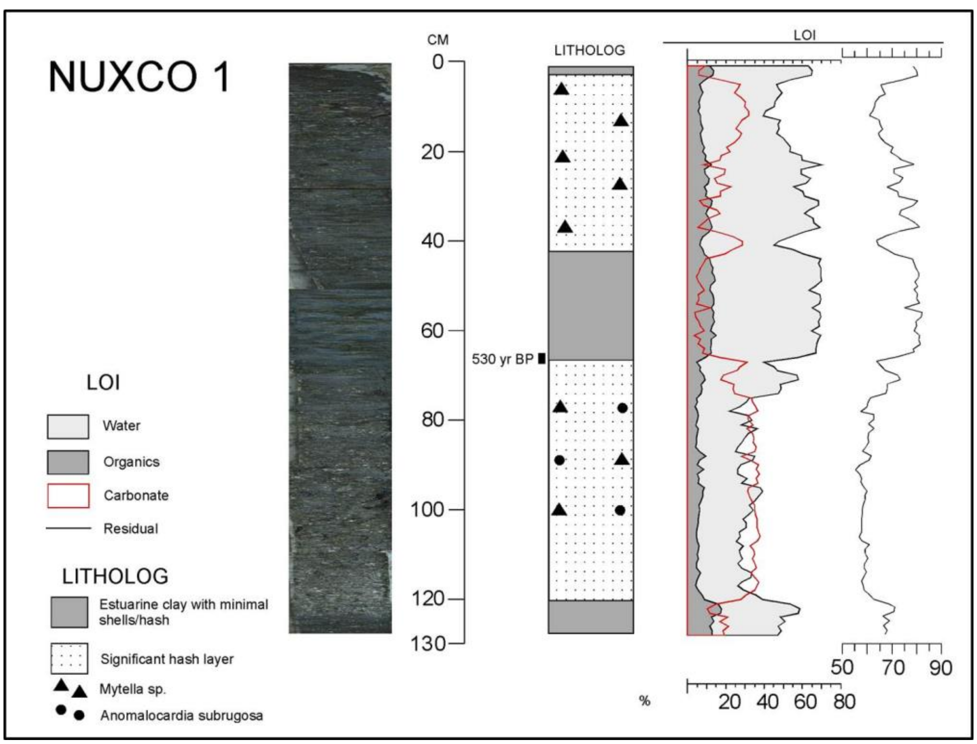

Figure 4.4 – Core 1 photos, lithology, and LOI results. Shelly sections contain low water and organic content with elevated carbonate percentages. The residual curve mirrors water content throughout core 1.

minimal at the core bottom from 128-120 cm. A slightly fining-upward hash sequence, noted visually, at 120-66 cm contains intact *Mytella sp.* and *Anomalocardia subrugosa* from 103-77 cm. Gray clay with few whole shells and minimal hash from 66-42 cm contains relatively high water (60%) and organics (15%) but low carbonate (10%). A *Mytella*-rich, slightly fining-upward hash layer from 42-4 cm exhibits a decrease in water (40%) and organics (~5%) with an increase in carbonate (30%). Clay from 4 cm to the coretop contains high water (60%) and low organic (10%) and carbonate (5%) contents. A plant/wood sample submitted for radiocarbon dating at 64 cm adjacent to the lowermost shell hash layer yields a 490±55 ^{14}C yr BP date (526 cal yr BP).

Core 2 (529 cm) was extracted 50 m north of core 1 from 2 m water depth. Due to its length and complex stratigraphy, core 2 was XRF-scanned and divided into two stratigraphic zones (Figure 4.5). Zone 2 (529-280 cm) consists of gray (Gley1 3/10Y), shelly clay (~60% water, ~15% organics) with *Anomalocardia subrugosa*. At least six carbonate-rich (>20%) and severely broken hash sections with low water (40-50%) and organic contents (5-10%) occur throughout the zone, some relatively thick (>10 cm). The shell hash layers do not possess fining or coarsening upward trends; nor do they contain sharp upper/lower boundaries. Core 2's residual content (mainly siliciclastics) is high toward the zone bottom and decreasing upcore, correlating negatively with water and organic contents. S and Cl concentrations are steady (Figure 4.6). I, Ca, and Sr concentrations are associated with carbonates and shell hash sections. Most lithogenic elements (e.g., Fe, Ti) correlate negatively with carbonates, I, Ca, and Sr. Zr concentrations display an irregular pattern while correlating positively with carbonates. Zone 1 (280-0 cm) contains gray estuarine clay (Gley1, 3/10Y) with *Mytella sp.* and less shell hash than

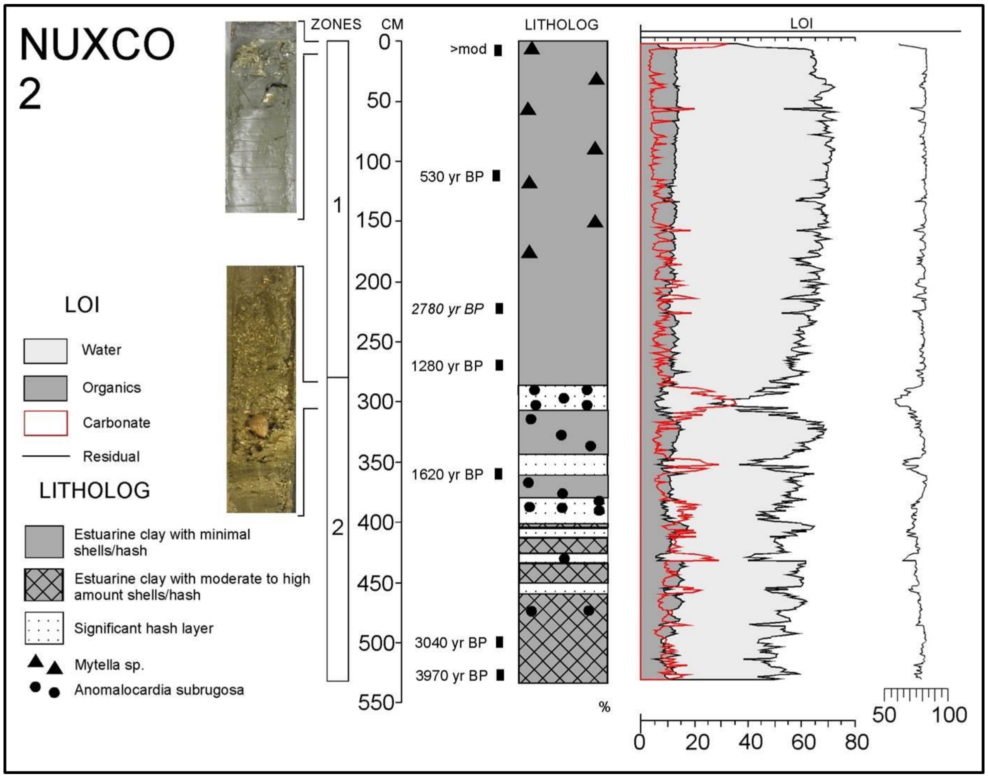

Figure 4.5 – Core 2 photos, zone delineation, lithology, and LOI results. The zone 1 core photo from the top ten cm displays clay with shells at the top. The bottom photo displays a zone 2 shell hash section from 305-280 cm, with brownish appearance likely from desiccation or lighting effects. Triangles represent *Mytella sp.* relative abundance from 180-0 cm. Circles indicate areas of high *Anomalocardia subrugosa* concentration. Calibrated radiocarbon dates are rounded to the nearest ten. The 2780 yr BP date at 229 cm is dismissed from further analysis, as the reversal indicates likely contamination.

zone 2. *Anomalocardia subrugosa* shells are absent from this zone. *Mytella sp.* are sparse from 280-180 cm, slightly increasing in the top 180 cm. Water (~70%) marginally increases along with organic contents (~15%). Carbonate spikes are thinner (5-1 cm) and more subdued (10-20%) than in zone 2. Residual content is fairly steady (~80%) throughout the zone. S and Cl concentrations are homogeneous, with I, Sr, and Ca relatively high in shell sections and low in clay. Remaining lithogenic elements are negatively correlated with I, Sr, and Ca. Zr concentrations are lower than in zone 2. Seven samples were submitted for radiocarbon dating including a bulk sediment sample from 9 cm yielding a post-modern date. The other

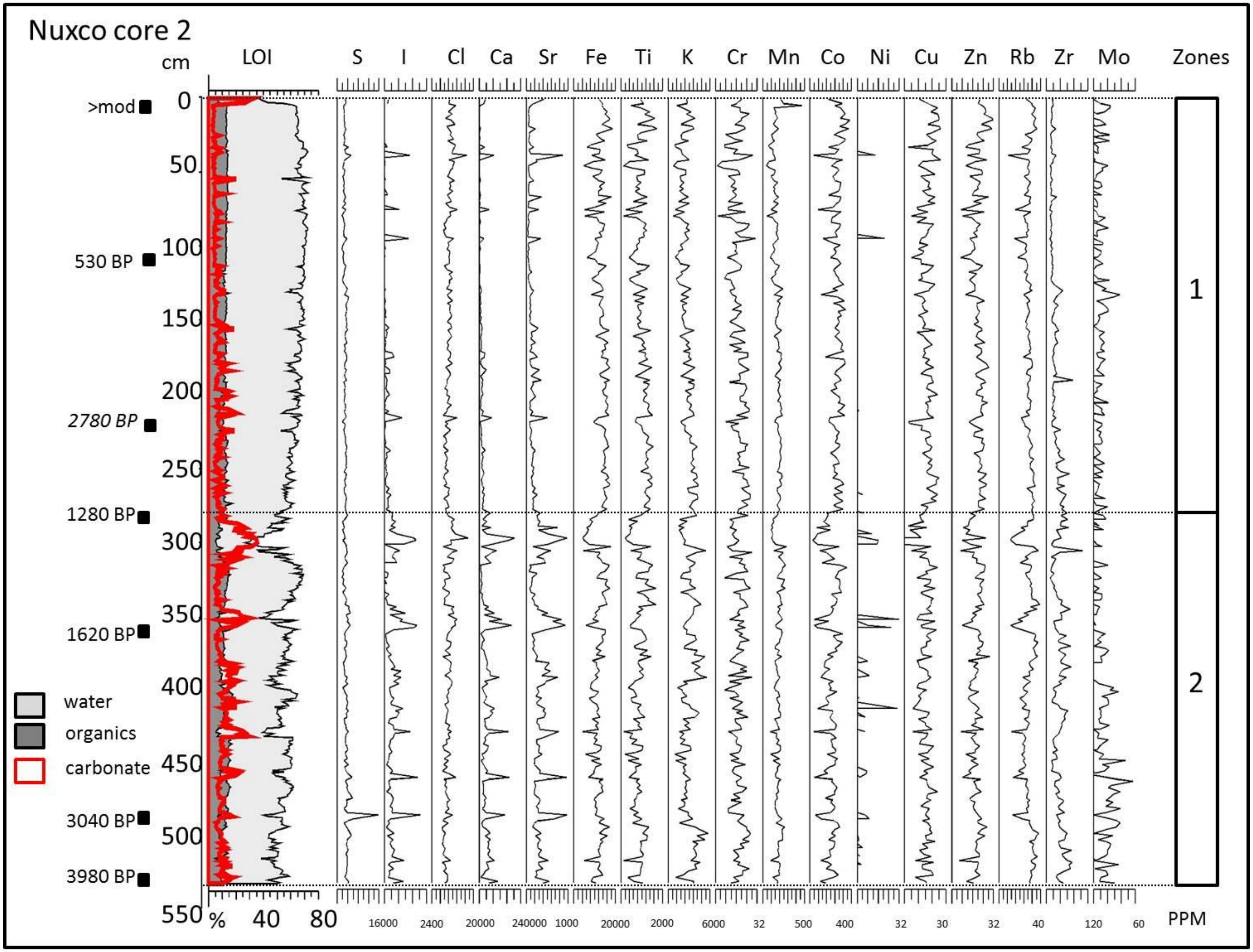

Figure 4.6 – Core 2 XRF results coupled with LOI curves. Zone 2 I, Ca, and Sr concentrations are positively correlated to carbonate and negatively correlated to most remaining elements (Fe, Ti, etc.). Zone 1 decreases in I, Ca, and Sr while increasing in most lithogenic elements.

samples were plant/wood from 105 cm (505±50 ^{14}C yr BP - 533 cal yr BP), 229 cm (2670±45 ^{14}C BP - 2784 cal yr BP), 273 cm (1330±25 ^{14}C yr BP - 1276 cal yr BP), 359 cm (1710±70 ^{14}C yr BP - 1623 cal yr BP), 488 cm (2900±30 ^{14}C yr BP - 3037 cal yr BP), and 524 cm (3630±220 ^{14}C yr BP - 3971 cal yr BP).

Core 3 (469 cm) was collected from ~2.5 m of water at a site 200 m north of core 2. Core 3 consists of gray estuarine clay (GLEY 1 3/10Y) with minimal shells and hash. It is divided into two stratigraphic zones (Figure 4.7). Zone 2 (469-240 cm) is fairly uniform in water (60-70%) and organic (15%) contents. Hash sections are thin (5-1 cm) with carbonate peaking at

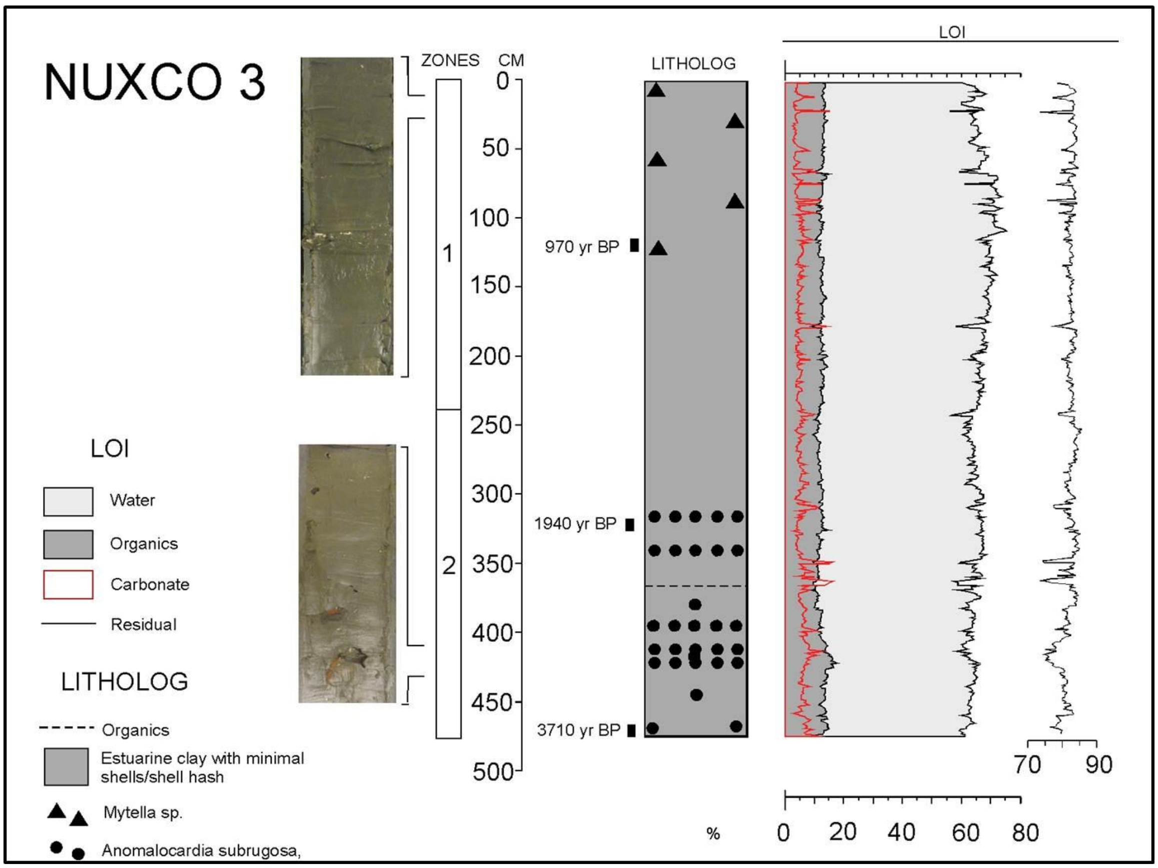

Figure 4.7- Core 3 photos, zone delineation, lithology, and LOI results. Horizontal rows of circles indicate *Anomalocardia subrugosa* beds. Water and organic contents are mostly steady, with thin carbonate peaks corresponding to shell layers.

~20%. Residual is ~80% at the bottom, increasing toward the zone top. *Anomalocardia subrugosa* layers occur at 324-319, 346-340, 400-396, 413-411, and 425-423 cm. Zone 1 (240-0 cm) contains few *Mytella sp*. from 240-130 cm, increasing from 130-0 cm. *Anomalocardia subrugosa* shells are absent in zone 1. Water (70-75%) is higher than zone 2, while organic content (15 %) is similar. Carbonate spikes are frequent and thin (3-1 cm), peaking at ~15%. Residual is consistently at ~85%, inversely related to water and organic contents. Three plant/wood radiocarbon samples from 121, 320, and 467 cm were dated 1050±60 ^{14}C yr BP (967 cal yr BP), 1980±120 ^{14}C yr BP (1941 cal yr BP), and 3440±130 ^{14}C yr BP (3709 cal yr BP), respectively (Table 4.1).

4.5.2 Sedimentation rate

Sedimentation rates show similar patterns for cores 2 and 3 (Figure 4.8). Core 2 contains slow sedimentation toward the bottom (0.0387 cm/yr), increasing (0.1981 to 0.0910 cm/yr) from ~359 cm to surface. Core 3 sedimentation rate is low (0.0831 cm/yr) from the bottom to 320 cm, increasing to 0.1247 cm/yr and 0.2052 cm/yr from 320 cm to the coretop (Figure 4.8).

4.6 Discussion

4.6.1 Stratigraphic correlation

The longest and oldest cores, 2 and 3, contain some stratigraphic similarities. Zone 2 for both cores is characterized by gray estuarine clay and the presence of *Anomalocardia subrugosa*. Water (60-70%), organics (10-15%) (Figure 4.9), and residual contents (80-85%) (Figures 4.5, 4.7) are similar across clay sections with minimal shells. Elevated carbonate content in core 2 stems from more frequent and distinct hash deposition than core 3, the latter containing only minimal shell hash of a scattered distribution. Clay throughout zone 1 is of similar color and texture for cores 2 and 3. *Mytella* abundance marginally increases upcore, with more shells in

Table 1 – Radiocarbon dating results for Nuxco cores 1-3.

Core/sample ID	Depth (cm)	Laboratory #	Material	Radiocarbon age BP	Cal BP (2δ)	Relative area under probability distribution	Med. Prob
Nuxco 1B 25	64	OS-92859	Plant/Wood	490±55	334-349	0.016	
					439-445	0.005	
					451-566	0.819	526
					586-645	0.16	
Nuxco 2A 9	9	OS-91677	Sediment	>mod			
Nuxco 2A 105	105	OS-92317	Plant/Wood	505±50	481-565	0.787	533
					587-643	0.213	
Nuxco 2C1 16	229	OS-92320	Plant/Wood	2670±45	2738-2860	1	2784
Nuxco 2 273	273	OS-83947	Plant/Wood	1330±25	1183-1205	0.147	
					1236-1300	0.853	1276
Nuxco 2D 28	359	OS-92321	Plant/Wood	1710±70	1418-1466	0.048	
					1490-1495	0.005	
					1509-1816	0.948	1623
Nuxco 2E 37	488	OS-91728	Plant/Wood	2900±30	2950-3160	1	3037
Nuxco 2 524	524	OS-84453	Plant/Wood	3630±220	3396-4529	0.999	3971
					4563-4565	0.001	
Nuxco 3A 121	121	OS-92318	Plant/Wood	1050±60	795-1081	0.998	967
					1114-1118	0.002	
Nuxco 3 320	320	OS-84454	Plant/Wood	1980±120	1626-1668	0.019	
					1690-2183	0.934	1941
					2197-2204	0.003	
					2234-2305	0.044	
Nuxco 3D 128	467	OS-92319	Plant/Wood	3440±130	3396-3993	0.984	3709
					4039-4075	0.016	

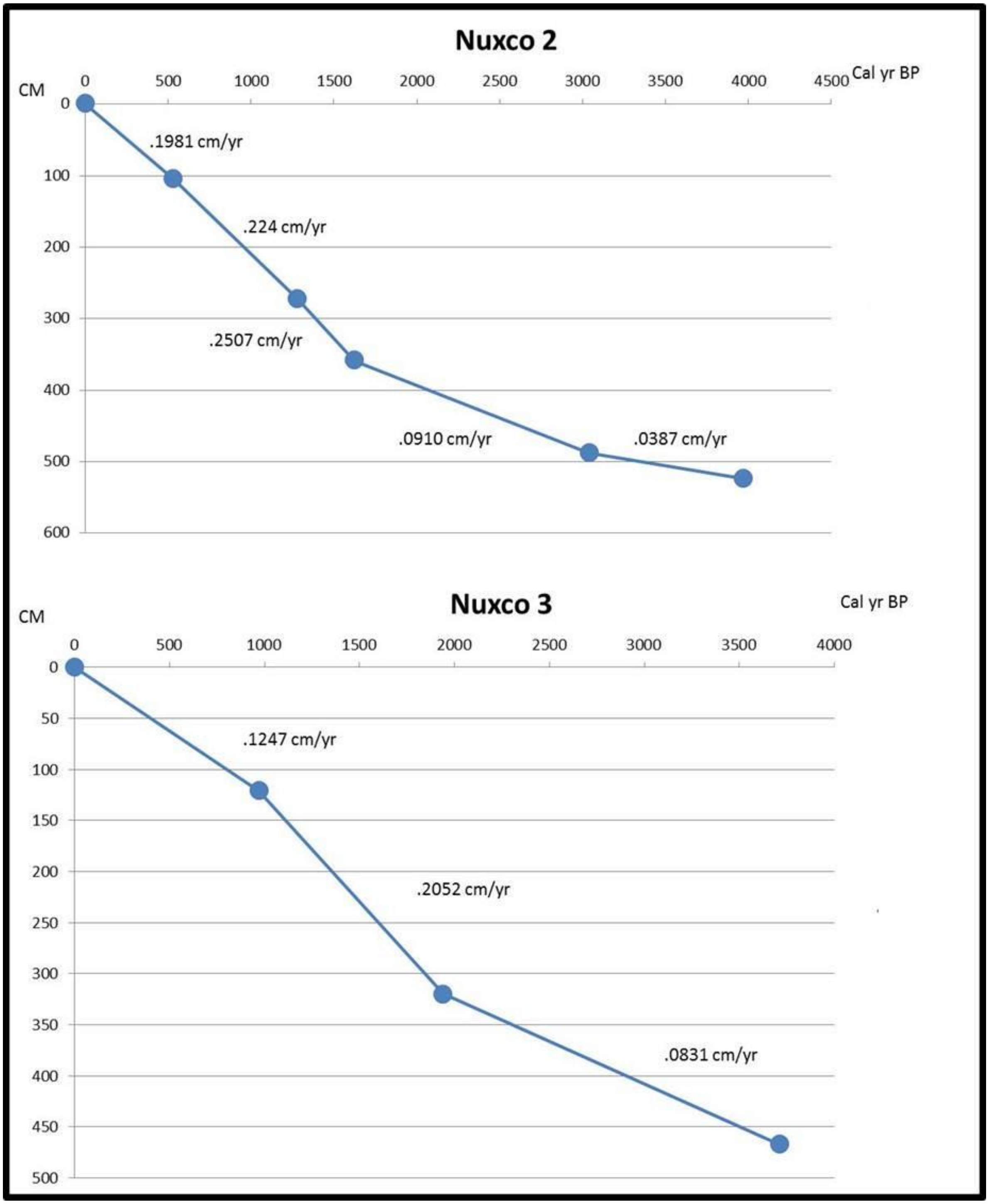

Figure 4.8 - Core 2 and 3 sedimentation rates. Sedimentation is assumed to start at modern.

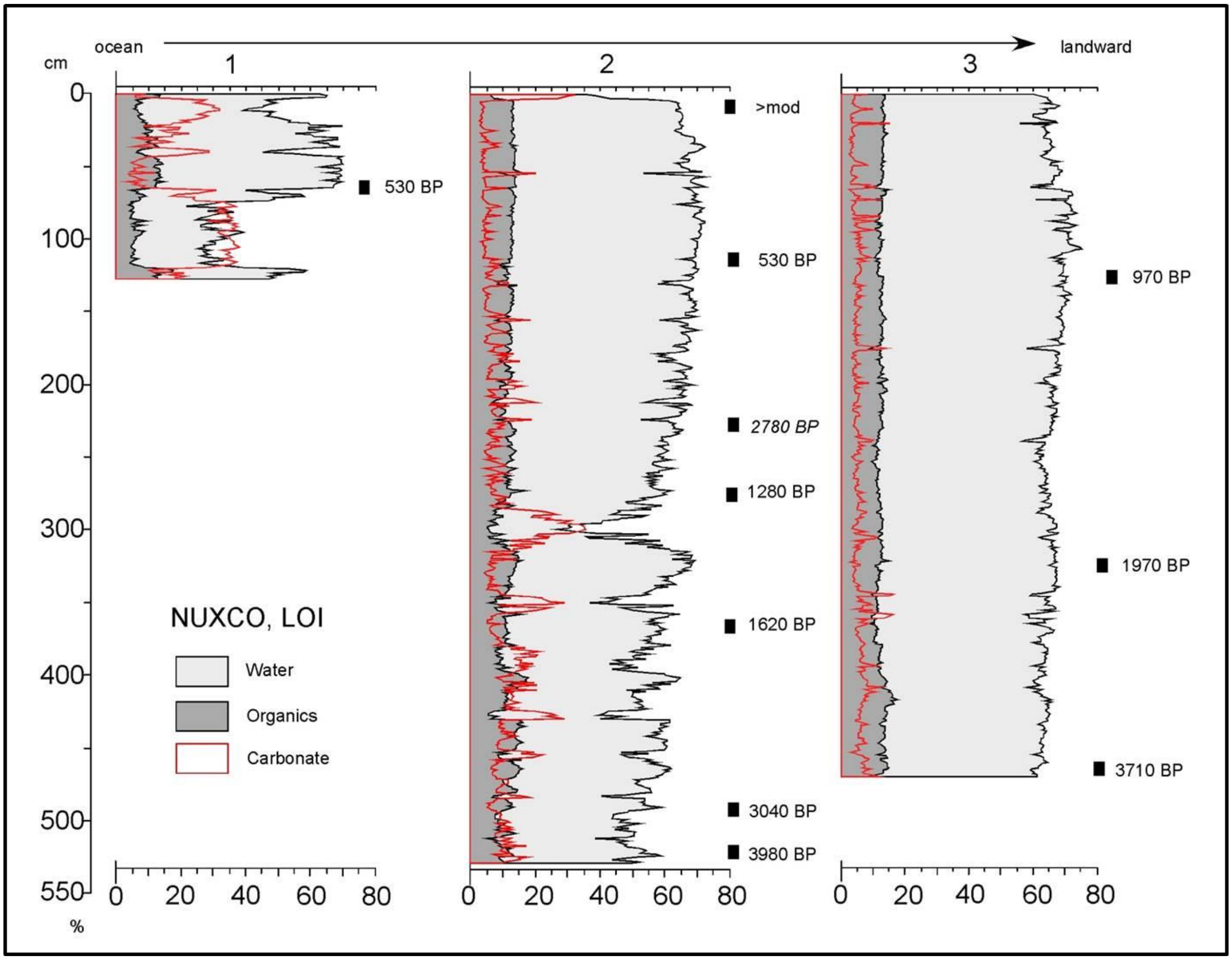

Figure 4.9 – LOI results for cores 1-3, ordered in its shore-perpendicular transect. Core 1 contains the most severe decreases in water and organics, and sharpest carbonate increases due to shell (hash) abundance. Core 2 displays a similar phenomenon for its bottom ~2.5 meters. Core 3 is devoid of significant hash layers.

core 2 than core 3. Their scattered arrangement in both cores 2 and 3 does not permit cross-core correlations. Water (70-75%), organics (15%), and residual (80-85%) are similar throughout zone 1. Carbonate content is lower in core 3 from decreased shell content. LOI results, visual inspection, and microscopic analyses from clay and hash facies suggest that sand is likely minimal to non-existent throughout Nuxco cores. A lack of sand in normally deposited estuarine/lagoonal sediment is similarly described by Goman et al. (2005) from a paleoenvironmental analysis from Laguna Pastoria in nearby Oaxaca.

Correlations between core 1 and the long cores 2 and 3 are limited due to the short length of core 1. Core 1 exhibits the thickest and most distinct shell hash sequences with the highest carbonate contents while correlations to cores 2 and 3 are limited from a lack of thick hash sequences in the top sediments.

4.6.2 Environmental reconstruction

4.6.2.1 Holocene sea level

The nearest Holocene sea level record was obtained from the coastal state Nayarit (Curray et al., 1969), located 800 km northwest of Nuxco. Approximately 10,000 years ago, sea level was over 30 m below present and rising rapidly, resulting in the transport of offshore sediments toward the coast. This rapid rise began to slow slightly around 7000 years BP when sea level was ~10 m below present. Marine transgression inundated coastal depressions around ~5000 years BP, followed immediately by a period of stabilizing seas, with levels near present throughout the last ~3000 years. Longshore drift and shelf sand deposition during stabilizing seas facilitated beach ridge development and its eventual progradation and vertical growth. These processes resulted in the formation of backbarrier lagoons throughout Mexico's Pacific coast (Curray et al., 1969). Throughout the Late Holocene, upland erosion increased the sediment supply for the nearby Rio Balsas (Kennett et al., 2008), accelerating beach ridge progradation (e.g., Watts and Bradbury, 1982; Goman et al., 2005) as these riverine clastics deposited offshore.

4.6.2.2 Geochemical proxies

X-ray fluorescence can aid in determining sedimentary provenance and paleoenvironmental conditions. Some elements possess high concentrations in saltwater compared to freshwater, and can therefore help determine marine influence or periods of high

salinity (Chague-Goff et al., 2002). Oceanic components (e.g., algae) generally contain high concentrations of Sr (Bowen, 1956), for instance, as relatively high levels in sediments can indicate marine disturbance (Ramirez-Herrera et al., 2007; Woodruff et al., 2009). High concentrations of S, I, Ca, and Cl are often suggestive of marine influence or elevated salinity (Wakefield and Elderfield, 1985; Chen et al., 1997; Ramirez-Herrera et al., 2007; Tjallingii et al., 2007; Nichol et al., 2007; Schofield et al., 2010). Alternatively, elevated lithogenic element concentrations (e.g., Ti, Fe, Zn) usually indicate a terrigenous sediment source (e.g., Bradbury, 2000; Woodruff et al., 2008; Metcalfe et al., 2010; Schofield et al., 2010; Unkel et al., 2010).

4.6.2.3 Shells as a paleoenvironmental proxy

Mutual exclusivity exists between *Anomalocardia subrugosa* (zone 2) and *Mytella sp.* (zone 1) sections in cores 2 and 3 (Figure 4.10). *Anomalocardia subrugosa* (Wood, 1828) are subtidal species preferring shallow water and sometimes sandy substrates for habitation (Dr. Emilio Garcia, personal communication; Ramirez-Herrera et al., 2011). Two *Cerithium (Tericium) stercusmuscarum* (Figure 4.10) shells in core 2 (458, 488 cm) lie adjacent to *Anomalocardia subrugosa. Cerithium* is an estuarine and sand flat specie (Keen, 1971) commonly occurring *in situ* in 'old' sediments (e.g., Parker, 1964). *Mytella* is an intertidal specie common in marine, brackish, or freshwater environments in tidal flats, mud flats, and shallow lagoons, often clinging to rocks and vegetation (Olsson, 1961; Keen, 1971) while common on the floor near mangroves (Parker, 1964; Abbott and Dance, 1982). *Mytella sp.* is difficult to identify to the specie level, as most contain a flaky skin (periostracum) and are of similar dimensions. The individuals found in the cores are likely *strigata*, previously identified from Nuxco and nearby Pacific coast environments (e.g., Yanez-Arancibia, 1977). A similar

Figure 4.10 –*Mytella sp.* (top) and *Anomalocardia subrugosa* (middle) are common in cores 1-3. Two *Cerithium stercusmuscarum* (bottom) are discovered at 458 and 488 cm in core 2.

assemblage change from *Anomalocardia subrugosa* to *Mytella* from Pastoria in Oaxaca was attributed to evolution from bay to lagoon (Goman et al., 2005).

4.6.3 Paleoenvironmental history

4.6.3.1 Zone 2 – Estuarine lagoon (~4000-~1300 yr BP)

Sea level during zone 2 was 1-2 m below present and stable (Curray et al., 1969). Core 2 "shelly" clay dominated by *Anomalocardia subrugosa* along with thick hash units (Figure 4.11) indicates increased ocean interaction during an evolutionary phase sensitive to marine influence. Elevated and steady S and Cl concentrations suggest brackish conditions from the recent transgression along with constant tidal exchange. Marine indicators I, Ca, and Sr are in high concentration while correlating with carbonate content, further indicating shell presence (e.g., Koinig et al., 2003). Low lithogenic element concentrations suggest limited terrigenous input. One exception is Zr, which exhibits relatively high concentrations. Since Zr concentrations are often elevated in nearshore and beach sediments, high concentrations in Nuxco's sediments can suggest transport of nearshore material into the sites from high energy processes, including beach formation (van Soelen et al., 2012). High concentrations indicate clastic transportation into the nearshore from near the beach ridge, as reflected from the low water content in core 2. The provenance of these sediments is further confirmed as surface samples extracted from the beach and nearshore were both Zr-rich.

4.6.3.2 Zone 1 – Lagoon (~1300 yr BP-current)

Nuxco's evolution to a lagoon occurred approximately 1300 years BP, suggested from slightly increased water and organic contents, indicating finer-grained deposition and the absence of thick hash sections (Figure 4.11). Elevated S and Cl concentrations indicate continued brackish conditions from tidal influence. The increase in lithogenic element concentrations

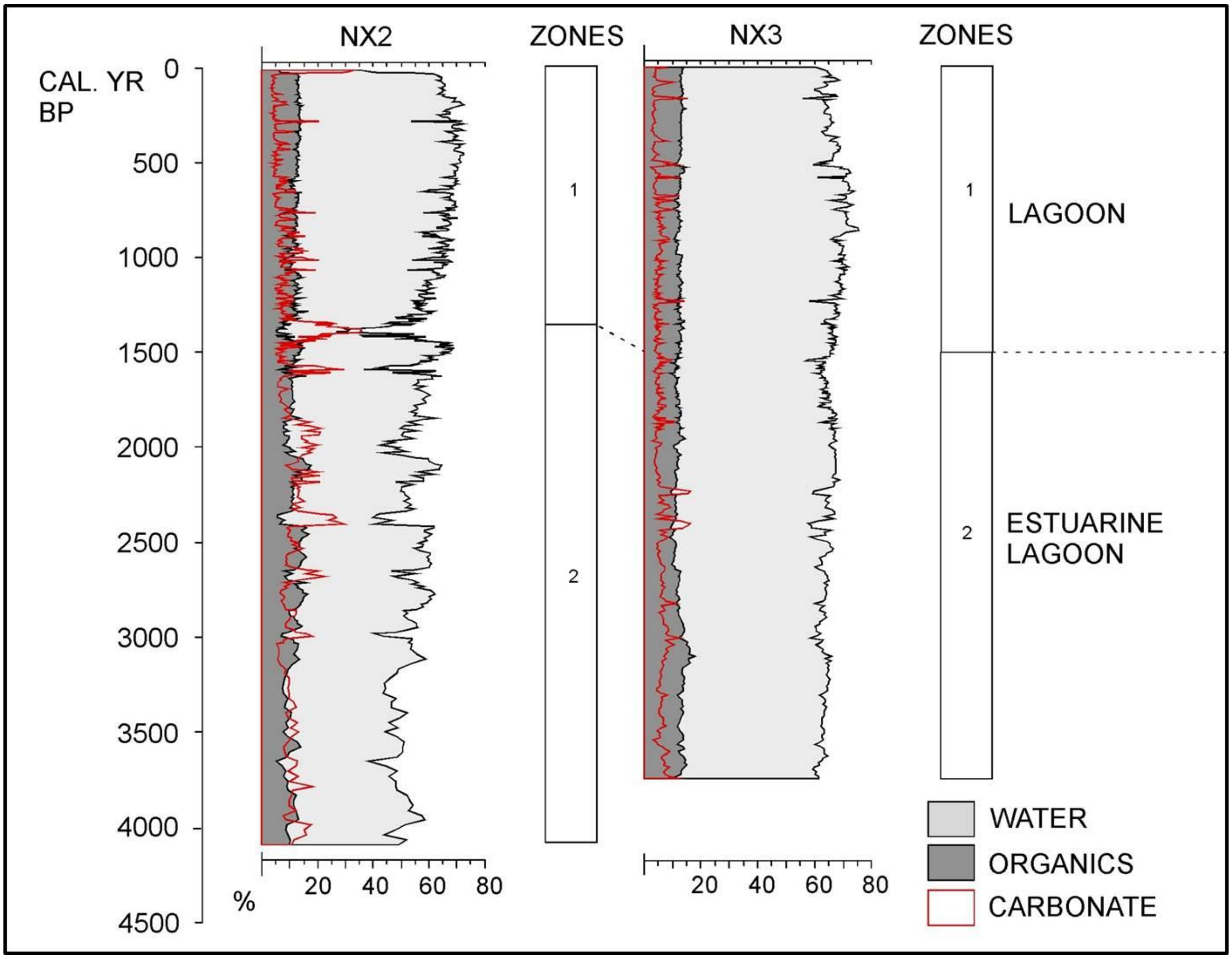

Figure 4.11 – Core 2 and 3 LOI plotted on an age scale, with environmental setting indicated.

indicates amplified terrestrial influence, while intensified erosion from land use documented throughout the neighboring uplands (Watts and Bradbury, 1982) explain the greater sedimentation rates. Calmer conditions led to lower Zr concentrations as the stabilized seas promoted beach ridge progradation and vertical development. The softer substrate and quieter conditions are unfavorable habitats for *Anomalocardia subrugosa* and *Cerithium stercusmuscarum.* The strengthened beach ridges and sheltered conditions likely facilitated vegetation (e.g., mangrove) development along Nuxco's southern edge, a common occurrence among tropical and subtropical areas (e.g., Chatenoux and Peduzzi, 2007; McCloskey and Liu, 2012). The stability fostered suitable habitats for *Mytella*, with increased quantity in core 2

indicating a nearshore source. Nuxco's "estuarine lagoon" and "lagoon" phases temporally correspond to a similar paleoenvironmental evolution documented from Laguna Tetitlan, located 20 km east-southeast (Gonzalez-Quintero, 1980).

4.6.4 Extreme event-induced overwash deposition

Generally, overwash sand deposition is a reliable coastal indicator of extreme events (Liu and Fearn, 1993, 2000; Nanayama et al., 2000). These overwash features have been attributed to both TCs (Goman et al., 2005) and tsunamis (Ramirez-Herrera et al., 2012) from sediments extracted from sites near Nuxco. Both LOI and XRF results coupled with visual inspection of sediment cores suggest a lack of sand along Nuxco's nearshore areas. Additionally, microscopic analysis of shell hash sections failed to reveal presence of sand grains. Nuxco's inlet areas were deemed disturbed and avoided during fieldwork since blowouts are capable of transporting sand into the area and resuspending surface sediments (Contreras-Espinosa, 1993). Since beach sand is carbonate-poor (0.32-0.59%), thin concentration spikes throughout zone 1 are unlikely to indicate indistinct overwash layers caused by minor events. The deep continental slope and narrow shelf adjacent to Nuxco were likely significant factors in inhibiting storm surge and tsunami run-up, as documented in other basins (e.g. Selvakumar and Ramasamy, 2012). Similarly, the wide and tall beach ridge system prevented typical overwash deposition.

4.6.5 Nearshore processes

4.6.5.1 Estuarine lagoon stage

Shell breakage in coastal environments generally occurs from the constant stress caused by processes ranging from diurnal waves and currents, to storms and TCs (e.g., Norris, 1986; Albertzart and Wilkinson, 1990). It is suggested that normal waves and currents transported hash into Nuxco via gaps that were likely common in the developing beach ridge system. Shell

fragments were deposited landward of the relatively heavy and coarser-grained clastics (e.g., sand). Hash that failed to reach the site collected on the higher elevation areas of the coastal shelf and underdeveloped beach ridge sections, where some was eventually deposited into the nearshore area by localized waves or aeolian transport. This typical deposition consisting of intact shells and hash is common in estuarine/lagoonal environments (e.g., Morton, 1978). Thorbjarnarson et al. (1985) discovered normally-deposited shells and shell hash in subtidal and intertidal locations from a coastal backbarrier lagoon in New Jersey.

The mechanism responsible for collecting and transporting distinct shell and shell hash facies into similar-type environments as Nuxco is best determined by analyzing the characteristics of the deposit (e.g., layer thickness, shell diversity and presence of offshore species, upper and lower contact description, degree of fragmentation and abrasion). In core 2, the six distinct shell hash facies exhibiting severely broken hash and gradational contacts share some resemblance to descriptions of "current/wave winnowed" units documented throughout the Gulf of California shorelines (Meldahl, 1993). Low sedimentation rates in zone 2 offer ideal conditions for this type of deposition (e.g., Meldahl, 1993). Significant hash deposition absent in core 3 further suggests that the transport mechanism might have been of relatively low energy. Spatial variation in the location and size of the tidal inlet(s) caused by alterations in coastal sediment supply might have led to temporal inconsistency of thick hash deposition along Nuxco's nearshore.

Both storms and TCs are capable of exhuming shells from the sea floor and depositing them landward. Generally, storm and TC-induced shell hash signatures fine upward and contain evidence of landward thinning (Davis et al., 1989), resembling the common structure of overwash sand layers (e.g., McCloskey and Keller, 2009; Hawkes and Horton, 2012). The

rapidity of such deposition might only slightly abrade shells and shell hash, while often leaving an erosional contact on the bottom of the unit (Meldahl, 1993). Deposition from high energy events, including tsunamis, usually contain distinct traits that are absent from hash units discovered from Nuxco (e.g., Bryant et al., 1992; Meldahl, 1993). From coastal Japan, Fujiwara et al. (2000) found thick, tsunami-induced sand sheets containing shells and shell hash. From sediments extracted from Pastoria, Goman et al. (2005) discovered hurricane-induced shell beds dominated by *Laevicardium elenense* shells, commonly found offshore. It has been noted, however, that it is difficult to identify deposits accurately as TC or tsunami-induced (Davies et al., 1989), especially since both are often bioturbated or resuspended in similar environmental settings (Thorbjarnarson et al., 1985; Nichols et al., 1991; Meldahl, 1993). Further complication stems from hash continuously winnowing into Nuxco's nearshore from the landward edge of the beach ridge throughout the last 4000 years (Dr. Emilio Garcia, personal communication). Due to the capability of high energy processes to break/concentrate shells and transport them landward, relatively weak storms, TCs, or tsunamis cannot be entirely ruled out as the cause of the six events found in core 2.

4.6.5.2 Lagoonal stage

During the time of zone 1, strengthened beach ridges prevented thick hash deposition to reach the core 2 and 3 sites. The rarity of *Mytella* at the bottom of zone 1 marks the gradual stabilization of the beach ridges as vegetation has yet to fully establish. Despite hash winnowing into the nearshore from the beach ridges, this disturbance is not triggered by typical waves and currents as discerned during the estuarine lagoon stage, but precipitation-induced blowouts. As precipitation and runoff raise water level within the site, hash likely collects from the landward edges of the beach ridge and is subsequently deposited into the nearshore as the site drains via

the tidal inlet. After drainage, additional hash is deposited into the site from marine intrusion, via the inlet. Frequent carbonate spikes at the bottom of zone 1 from core 2 (~1280-530 years BP) indicate an excess of shells deposited into the nearshore from a relatively turbulent period causing frequent blowouts, likely triggered by a wet climatic period. Amplified ENSO behavior from 1200-1000 years BP diminished only slightly after this period (Moy et al., 2002), a likely cause for turbulence at the site as warm ENP waters during El Niño periods increase regional precipitation, while the diminishing vertical shear facilitates elevated TC frequencies (Jauregui, 2003). Alternatively, a decrease in hash toward the tops of cores 2 and 3 is suggestive of a more stable environment from fewer blowouts. ENSO behavior declined slightly over the last 500 years (Moy et al., 2002), a main contributor toward lessened precipitation and TC frequency. A paleoenvironmental reconstruction from an upland lake in Guerrero similarly reveals a dry period throughout the last ~750 years (Berrio et al., 2006). Additionally, Nuxco's stability is generally coincident with the timing of the Little Ice Age. The Little Ice Age is deemed a significant cause of colder and drier conditions from the 14th to 19th century in both northern and southern hemispheres (Jones et al., 1998), with dry conditions documented from many other tropical to subtropical regions worldwide (e.g., Russell and Johnson, 2007). During the 15th century, the Yucatan Peninsula experienced a drier climate, determined from multiple proxies including the appearance of the benthic foraminifer *Ammonia beccarii parkinsoniana* in a sinkhole lake, suggesting increased salinity from colder sea surface temperatures prompted by the Little Ice Age (Hodell et al., 2005).

The nearshore position and shallow bathymetry of the core 1 site deem it most sensitive toward receiving recent hash deposition. Occurrence of both *Mytella* and *Anomalocardia subrugosa* in the same hash unit indicate conditions suitable for both bivalve species, namely a

"shelly," shallow bathymetry and nearby vegetation establishment (Figure 4.12). Relatively quiet conditions caused sharper contacts of the hash facies with the normal clay deposition. Core 1 contains evidence of one significant blowout occurring ~530 years BP and at least one other event during recent times.

Three *Mytella* layers (>25% carbonate) captured in nearshore sediment from Pastoria (Oaxaca) were attributed to TC storm surge, jarring individuals from mangrove roots (Goman et al., 2005). This core was extracted further from mangroves and the lagoon edge than cores 2 and 3, while sensitive to storm surge inundation from Pastoria's relatively narrow, 300 m wide

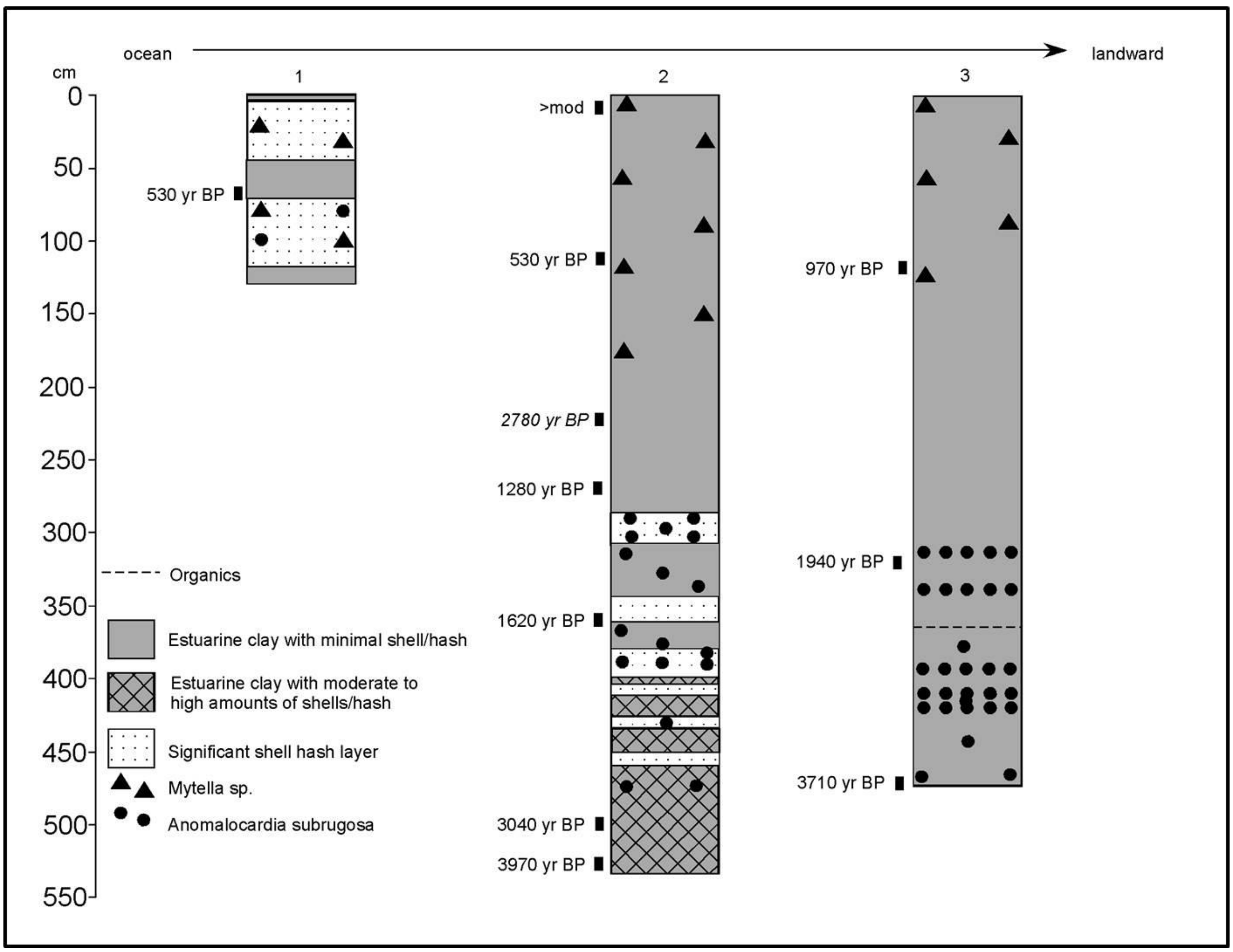

Figure 4.12 – Core 1-3 lithologs. Core 1 is the sole sample with a shell hash sequence featuring *Mytella* and *Anomalocardia subrugosa*. Shell hash common toward the bottom of core 2 is non-existent in core 3.

beach. As surge has not breached or entered Nuxco during the historical period, the disturbance model from Pastoria may not apply. Alternatively, the disturbance model at Nuxco indicates that *Mytella* shells were deposited along Nuxco's nearshore via lagoonal currents or precipitation-induced blowouts, responsible for dislodging shells from mangrove roots and sweeping individuals from the nearby floor and subsequently transporting them along the nearshore.

4.7 Summary and conclusion

This study presents a paleoenvironmental reconstruction from Laguna Nuxco, a barred inner shelf site on Mexico's Pacific coast. Three nearshore sediment cores were extracted, the longest providing a ~4000 year sedimentary record. Nuxco was an estuarine lagoon ~ 4000 yrs BP, containing clay dominated by *Anomalocardia subrugosa* along with six thick shell hash facies with >20% carbonate content, generally exhibiting severe breakage with gradational upper and lower contacts. Shells became damaged from the constant battering from waves (e.g., tidal activity, storms, TCs), and eventually transported into the nearshore during a period when the site was sensitive to such depositional processes. Hash sections resemble "current/wave winnowed" deposits discovered along the Gulf of California coast. While the processes responsible for depositing the six hash facies are suggested to be of relatively low energy, higher energy mechanisms including storms and distant TCs cannot be entirely ruled out. The lagoon phase began ~1300 yr BP as prograding and stabilizing beach ridges prevented significant hash deposition while facilitating vegetation growth (e.g., mangroves), indicated by *Mytella* shells discovered in nearshore sediments. Hash deposition into the nearshore occurs mostly from blowout events, triggered from periods of prolonged and intense precipitation often instigated by TCs. In core 2, frequent carbonate spikes indicate an influx of hash from ~1280-530 years BP suggesting heightened site dynamism from frequent blowouts, triggered by wetter conditions

from amplified ENSO behavior. Wet conditions have been documented from a nearby site in the highlands during this period. Alternatively, decreased shell hash toward the core top is attributed to a more stable environment, likely from less precipitation and runoff entering the lagoon from fewer blowouts. ENSO behavior slightly decreased during this timeframe, while dry conditions have been documented from the nearby highlands and the Yucatan Peninsula. Core 1, extracted nearest the beach ridge, contains thick shell hash sequences deposited from two significant blowouts, the oldest occurring ~ 530 years BP.

Nearshore cores are devoid of definitive TC-induced marine intrusion evidence. This includes overwash sand layers and molluscs favoring offshore habitats, introduced via storm surge intrusion. Storm surge is stymied from a steep continental slope and narrow shelf, while beach ridge progradation during a period of stable sea levels decreased sensitivity to marine inundation. A similar lack of overwash from nearby lagoons enables scientists a large-scale depiction of Pacific coast dynamics and sensitivities, essential for proper risk assessment. With extreme event evidence recently discovered only meters landward of the coastal beach ridge (Ramirez-Herrera et al., 2012), similar nearshore geomorphological settings might prove ideal in containing overwash and facilitating depositional differences between TC and tsunami deposits.

4.8 References

Abbott, R. T. and S. P. Dance. 1982. Compendium of seashells: A color guide to more than 4200 of the world's marine shells. E. P. Dutton, New York.

Albertzart, L. S. and B. H. Wilkinson. 1990. Barrier backbeach shell assemblages from the Central Texas Gulf Coast. PALAIOS **5**:346-355.

Berrio, J. C., H. Hooghiemstra, B. van Geel, and B. Ludlow-Wiechers. 2006. Environmental history of the dry forest biome of Guerrero, Mexico, and human impact during the last c. 2700 years. Holocene **16**:63-80.

Bowen, H. J. M. 1956. Strontium and barium in seawater and marine organisms. Journal of the Marine Biological Association of the United Kingdom **35**:451-460.

Bradbury, J. P. 2000. Limnologic history of Lago de Patzcuaro, Michoacan, Mexico for the past 48,000 years: impacts of climate and man. Palaeogeography Palaeoclimatology Palaeoecology **163**:69-95.

Bryant, E. A., R. W. Young, and D. M. Price. 1992. Evidence of tsunami sedimentation on the southeastern coast of Australia. Journal of Geology **100**:753-765.

Bullock, S. H. 1986. Climate of Chamela, Jalisco, and trends in the south coastal region of Mexico. Archives for Meteorology Geophysics and Bioclimatology Series B-Theoretical and Applied Climatology **36**:297-316.

Chague-Goff, C., S. Dawson, J. R. Goff, J. Zachariasen, K. R. Berryman, D. L. Garnett, H. M. Waldron, and D. C. Mildenhall. 2002. A tsunami (ca. 6300 years BP) and other Holocene environmental changes, northern Hawke's Bay, New Zealand. Sedimentary Geology **150**:89-102.

Chatenoux, B. and P. Peduzzi. 2007. Impacts from the 2004 Indian Ocean Tsunami: Analysing the potential protecting role of environmental features. Natural Hazards **40**:289-304.

Chen, Z., Z. Chen, and W. Zhang. 1997. Quaternary stratigraphy and trace-element indices of the Yangtze Delta, eastern China, with special reference to marine transgressions. Quaternary Research **47**:181-191.

Contreras-Espinosa, F. 1993. Ecosistemas costeros mexicanos. UNAM-CANABIO, Mexico, D.F.

Contreras-Espinosa, F. and B. G. Warner. 2004. Ecosystem characteristics and management considerations for coastal wetlands in Mexico. Hydrobiologia **511**:233-245.

Curray, F., J. Emmel, and P. J. Crampton. 1969. Holocene history of a strand plain lagoonal coast, Nayarit, Mexico. Pages 63-100 *in* A. Ayala-Castanares, editor. Coastal Lagoons: A Symposium. Universidad Nacional Autonoma de Mexico. Mexico City.

Davies, D. J., E. N. Powell, and R. J. Stanton. 1989. Taphonomic signature as a function of environmental process: Shells and shell beds in a hurricane-influenced inlet on the Texas coast. Palaeogeography Palaeoclimatology Palaeoecology **72**:317-356.

Davis, R. J., S. C. Knowles, and M. J. Bland. 1989. Role of hurricanes in the Holocene stratigraphy of estuaries: Examples from the Gulf Coast of Florida. Journal of Sedimentary Petrology **59**:1052-1061.

Dean, W. E. 1974. Determination of carbonate and organic matter in calcareous sediments and sedimentary rocks by loss on ignition: comparison with other methods. Journal of Sedimentary Petrology **44**:242-248.

Donnelly, J. P., S. S. Bryant, J. Butler, J. Dowling, L. Fan, N. Hausmann, P. Newby, B. Shuman, J. Stern, K. Westover, and T. Webb. 2001. 700 yr sedimentary record of intense hurricane landfalls in southern New England. Geological Society of America Bulletin **113**:714-727.

Fujiwara, O., F. Masuda, T. Sakai, T. Irizuki, and K. Fuse. 2000. Tsunami deposits in Holocene bay mud in southern Kanto region, Pacific coast of central Japan. Sedimentary Geology **135**:219-230.

Goman, M., A. Joyce, and R. Mueller. 2005. Stratigraphic evidence for anthropogenically induced coastal environmental change from Oaxaca, Mexico. Quaternary Research **63**:250-260.

Gonzalez-Quintero, L. 1980. Paleoecologia de un sector costero de Guerrero, Mexico (3000 anos). Memorias **86**:133-157.

Hawkes, A. D. and B. Horton, P. 2012. Sedimentary record of storm deposits from Hurricane Ike, Galveston and San Luis Islands, Texas. Geomorphology **171-172**:180-189.

Hodell, D. A., M. Brenner, J. H. Curtis, R. Medina-Gonzalez, E. I. C. Can, A. Albornaz-Pat, and T. P. Guilderson. 2005. Climate change on the Yucatan Peninsula during the Little Ice Age. Quaternary Research **63**:109-121.

Jessen, C. A., J. B. T. Pedersen, J. Bartholdy, M.-S. Seidenkrantz, and A. Kuijpers. 2008. A late Holocene palaeoenvironmental record from Altona Bay, St. Croix, US Virgin Islands. Danish Journal of Geography **108**:59-70.

Jauregui, E. 2003. Climatology of landfalling hurricanes and tropical storms in Mexico. Atmosfera **16**:193-204.

Jonathan, M. P., P. D. Roy, J. L. Sanchez-Zavala, S. Srinivasalu, M. C. Macias-Romo, and C. Lakshumanan. 2011. Field survey report on the 11th March 2011 tsunami in Pacific coast of Mexico. Natural Hazards **58**:859-864.

Jones, P. D., K. R. Briffa, T. P. Barnett, and S. F. B. Tett. 1998. High-resolution palaeoclimatic records for the millennium: interpretation, integration and comparison with General Circulation Model control-run temperatures. The Holocene **8**:455-471.

Keen, A. M. 1971. Sea shells of tropical West America. 2nd Edition. Stanford University Press, Stanford.

Kennedy, L. M., S. P. Horn, and K. H. Orvis. 2006. A 4000-year record of fire and forest history from Valle de Bao, Cordillera Central, Dominican Republic. Palaeogeography Palaeoclimatology Palaeoecology **231**:279-290.

Kennett, D. J., B. Voorheis, T. A. Wake, and N. Martinez. 2008. Human impacts on marine ecosystems in Guerrero, Mexico. Pages 103-124 *in* T. C. Rick and J. M. Erlandson, editors. Human Impacts on Ancient Marine Ecosystems: A Global Perspective. University of California Press, Berkeley.

Kiage, L. M., D. Deocampo, T. A. McCloskey, T. A. Bianchette, and M. Hursey. 2011. A 1900-year paleohurricane record from Wassaw Island, Georgia, USA. Journal of Quaternary Science **26**:714-722.

Koinig, K. A., W. Shotyk, A. F. Lotter, C. Ohlendorf, and M. Sturm. 2003. 9000 years of geochemical evolution of lithogenic major and trace elements in the sediment of an alpine lake - the role of climate, vegetation, and land-use history. Journal of Paleolimnology **30**:307-320.

Lankford, R. R. 1977. Coastal lagoons of Mexico: their origin and classification. Pages 182-215 *in* M. Wiley, editor. Estuarine Processes. Academic Press Inc.

Lawrence, M. B. 1999. Eastern North Pacific hurricane season of 1997. Monthly Weather Review **127**:2440-2454.

Liu, K. B. 2007. Paleotempestology. Pages 1978-1986 *in* S. Elias, editor. Encyclopedia of Quaternary Science. Elsevier, Amsterdam.

Liu, K. B. and M. L. Fearn. 1993. Lake-sediment record of Late Holocene hurricane activities from coastal Alabama. Geology **21**:793-796.

Liu, K. B. and M. L. Fearn. 2000. Reconstruction of prehistoric landfall frequencies of catastrophic hurricanes in northwestern Florida from lake sediment records. Quaternary Research **54**:238-245.

Matias-Ramirez, L. G. 1998. Algunos efectos de la precipitacion del Huracan Paulina en Acapulco, Guerrero. Investigaciones Geographicas **37**:7-19.

McCloskey, T. A. and G. Keller. 2009. 5000 year sedimentary record of hurricane strikes on the central coast of Belize. Quaternary International **195**:53-68.

McCloskey, T. A. and K. B. Liu. 2012. A sedimentary-based history of hurricane strikes on the southern Caribbean coast of Nicaragua. Quaternary Research **78**:454-464

McCloskey, T. A. and K. B. Liu. 2013. A 7000 year record of paleohurricane activity from a coastal wetland in Belize. The Holocene **23**:278-291.

Meldahl, K. H. 1993. Geographic gradients in the formation of shell concentrations: Plio-Pleistocene marine deposits, Gulf of California. Palaeogeography Palaeoclimatology Palaeoecology **101**:1-25.

Melvin, A. G. 1966. Sea shells of the world. Charles E. Tuttle Company, Rutland.

Metcalfe, S. E., M. D. Jones, S. J. Davies, A. Noren, and A. MacKenzie. 2010. Climate variability over the last two millennia in the North American Monsoon region, recorded in laminated lake sediments from Laguna de Juanacatlan, Mexico. The Holocene **20**:1195-1206.

Morton, R. A. 1978. Large-scale rhomboid bed forms and sedimentary structures associated with hurricane washover. Sedimentology **25**:183-204.

Moy, C. M., G. O. Seltzer, D. T. Rodbell, and D. M. Anderson. 2002. Variability of El Niño/Southern Oscillation activity at millennial timescales during the Holocene epoch. Nature **420**:162-165.

Nanayama, F., K. Shigeno, K. Satake, K. Shimokawa, S. Koitabashi, S. Miyasaka, and M. Ishii. 2000. Sedimentary differences between the 1993 Hokkaido-nansei-oki tsunami and the 1959 Miyakojima typhoon at Taisei, southwestern Hokkaido, northern Japan. Sedimentary Geology **135**:255-264.

National Climatic Data Center. 2013. NNDC Climate Data Online (Acapulco, MX).

National Geophysical Data Center. 2011. Global Historical Tsunami Database.

National Oceanic and Atmospheric Administration. 2011. Historical hurricane tracks. Retrieved 12-29-2011, from http://www.csc.noaa.gov/hurricanes/.

Nichol, S. L., J. R. Goff, R. J. N. Devoy, C. Chague-Goff, B. Hayward, and I. James. 2007. Lagoon subsidence and tsunami on the west coast of New Zealand. Sedimentary Geology **200**:248-262.

Nichols, M. M., G. H. Johnson, and P. C. Peebles. 1991. Modern sediments and facies model for a microtidal coastal plain estuary, the James Estuary, Virginia. Journal of Sedimentary Petrology **61**:883-899.

Norris, R. D. 1986. Taphonomic gradients in shelf fossil assemblages: Pliocene Purisima Formation, California. PALAIOS **1**:256-270.

Oliver, A. P. H. 1975. Guide to Shells. Quadrangle, New York.

Olsson, A. A. 1961. Mollusks of the Tropical Eastern Pacific. Paleontological Research Institution, Ithaca.

Paez-Osuna, F. and E. F. Mandelli. 1985. ^{210}Pb in a tropical coastal lagoon sediment core. Estuarine, Coastal, and Shelf Science **20**:367-374.

Parker, R. H. 1964. Zoogeography and ecology of some macro-invertebrates, particularly mollusks, in the Gulf of California and the continental slope of Mexico. Dansk Naturhistorisk Forening, Copenhagen.

Ramirez-Herrera, M. T., A. Cundy, V. Kostoglodov, A. Carranza-Edwards, E. Morales, and S. Metcalfe. 2007. Sedimentary record of late-Holocene relative sea-level change and tectonic deformation from the Guerrero Seismic Gap, Mexican Pacific Coast. The Holocene **17**:1211-1220.

Ramirez-Herrera, M. T., V. Kostoglodov, and J. Urrutia-Fucugauchi. 2011. Overview of recent coastal tectonic deformation in the Mexican subduction zone. Pure and Applied Geophysics **168**:1415-1433.

Ramirez-Herrera, M. T., M. Lagos, I. Hutchinson, V. Kostoglodov, M. L. Machain, M. Caballero, A. Goguitchaichvili, B. Aguilar, C. Chague-Goff, J. Goff, A.-C. Ruiz-Fernandez, M. Ortiz, H. Nava, F. Bautista, G. I. Lopez, and P. Quintana. 2012. Extreme wave deposits on the Pacific coast of Mexico: Tsunamis or storms? - A multi-proxy approach. Geomorphology **139**:360-371.

Ramirez-Herrera, M. T. and J. Urrutia-Fucugauchi. 1999. Morphotectonic zones along the coast of the Pacific continental margin, southern Mexico. Geomorphology **28**:237-250.

Russell, J. M. and T. C. Johnson. 2007. Little Ice Age drought in equatorial Africa: Intertropical Convergence Zone migrations and El Niño-Southern Oscillation variability. Geological Society of America. Geology **35**:21-24.

Schofield, J. E., K. J. Edwards, T. M. Mighall, A. Martinez Cortizas, J. Rodriguez-Racedo, and G. Cook. 2010. An integrated geochemical and palynological study of human impacts, soil erosion and storminess from southern Greenland since c. AD 1000. Palaeogeography Palaeoclimatology Palaeoecology **295**:19-30.

Selvakumar, R. and S. M. Ramasamy. 2012. Revealing effect of bathymetry over tsunami run-up through factor analysis. Arabian Journal of Geosciences **6**:4701-4708.

Spang, R. M., S. H. Castaneda, and E. M. Gomez. 2003. Hurricane Pauline - its impact on Acapulco and subsequent debris flow prevention measures. *in* Proc. 3rd Int. Conf. Debris Hazards Mitigation, Davos, Switzerland.

Stuiver, M., P. J. Reimer, and R. W. Reimer. 2005. CALIB 6.0 (program and documentation).

Thorbjarnarson, K. W., C. A. Nittrouer, D. J. DeMaster, and R. B. McKinney. 1985. Sediment accumulation in a back-barrier lagoon, Great Sound, New Jersey. Journal of Sedimentary Petrology **55**:856-863.

Tjallingii, R., U. Rohl, M. Kolling, and T. Bickert. 2007. Influence of the water content on X-ray fluorescence core-scanning measurements in soft marine sediments. Geochemistry Geophysics Geosystems **8**.10.1029/2006GC001393.

Unkel, I., M. Fernandez, S. Bjorck, K. Ljung, and B. Wohlfarth. 2010. Records of environmental changes during the Holocene from Isla de los Estados (54.4 degrees S), southeastern Tierra del Fuego. Global and Planetary Change **74**:99-113.

van Soelen, E. E., G. R. Brooks, R. A. Larson, J. S. S. Damste, and G. J. Reichart. 2012. Mid- to late-Holocene coastal environmental changes in southwest Florida, USA. Holocene **22**:929-938.

Wakefield, S. J. and H. Elderfield. 1985. Interstital water iodine enrichments from the eastern Pacific. Journal of Marine Research **43**:951-961.

Watts, W. A. and J. P. Bradbury. 1982. Paleoecological studies at Lake Patzcuaro on the west-central Mexican Plateau and at Chalco in the Basin of Mexico. Quaternary Research **17**:56-70.

Wood, W. 1828. Supplement to the Index testaceologicus, or, a catalogue of shells, British and foreign. London.

Woodruff, J. D., J. P. Donnelly, D. Mohrig, and W. R. Geyer. 2008. Reconstructing relative flooding intensities responsible for hurricane-induced deposits from Laguna Playa Grande, Vieques, Puerto Rico. Geology **36**:391-394.

Woodruff, J. D., J. P. Donnelly, and A. Okusu. 2009. Exploring typhoon variability over the mid-to-late Holocene: evidence of extreme coastal flooding from Kamikoshiki, Japan. Quaternary Science Reviews **28**:1774-1785.

Yanez-Arancibia, A. 1977. Taxonomia, ecologia Y estructura de las comunidades de peces en lagunas costeras con bocas efimeras del Pacifico de Mexico. Annual Meeting of the American Society of Limnology and Oceanography, Savannah, Georgia, USA.

CHAPTER 5. PALEOENVIRONMENTAL RECONSTRUCTION FROM MEXICO'S PACIFIC COAST – A MULTI-CORE SEDIMENTARY ANALYSIS FROM LAGUNA MITLA, GUERRERO

5.1 Introduction

Approximately 892,800 ha of wetlands occupy Mexico's Pacific coast, stretching 8,475 km from Chiapas state to Baja California Norte (Contreras-Espinosa and Warner, 2004). This includes a wide array of bays, inlets, sounds, estuaries, lagoons, and lakes of varying formations, sizes, depths, and salinities (Lankford, 1977). These pristine regions have been scientifically underutilized, as research regarding coastal dynamics and paleoenvironmental histories is limited. Guerrero state is no exception, as limited research has been conducted on its 485 km of coastal wetland, covering 22,700 ha (Contreras-Espinosa and Warner, 2004) and including tens of water bodies. Paleoenvironmental analyses can lend residents, policymakers, and scientists information regarding disturbance ecology, paleoclimate, wetland restoration, and coastal erosion among other avenues. Necessity for research is compounded as these regions contain significant economic value and vast wildlife habitats (Lankford, 1977).

Guerrero's coast is frequently affected by both tsunamis and tropical cyclones (TCs), capable of geophysical and societal destruction. Runup from Pacific coast tsunamis is capable of marine inundation many km inland (National Geophysical Data Center, 2011), often transporting terrigenous and marine sediments landward. Similarly, TC storm surge is capable of inundating coastal beaches in this region, as recently documented by Hurricane Pauline's 9 m surge documented in Oaxaca state (Goman et al., 2005). A sediment core extracted from a wetland located ~5 km from the coast and landward of Laguna Mitla contained a sand layer rich in marine elements, attributed to a significant tsunami event ~3400 years BP (Ramirez-Herrera et al., 2007). Seaward of this wetland area, Mitla is deemed fitting for uncovering sedimentary

evidence of additional marine events, whether from TCs or tsunamis. While TC deposition has not been discovered from Mitla, marine shells and sand layers recently discovered from lagoon sediments from Pastoria in Oaxaca state (Goman et al., 2005) are attributed to storm surge inundation, lending the possibility that similar deposits might occur in Mitla. Multi-centennial to -millennial records of tsunamis and/or TCs could improve risk assessment, crucial due to the regional economic importance of tourism and recent spikes in coastal populations (Brenner and Aguilar, 2002).

This chapter presents a multi-core paleoenvironmental reconstruction from Laguna Mitla. In this study, six cores are extracted from Mitla's "stable" area, far from potential disturbance from tidal inlet openings. The research objectives are twofold. Firstly, the paleoenvironment must be reconstructed, with the main goals of determining site dynamics, suitability to extreme event deposition, and changes in sensitivity to disturbance over time. Secondly, extreme event deposition is sought with the aim of determining long-term records. Findings would have implications toward risk assessment for Mexico's Pacific coast.

5.2 Physical environment and study site

Guerrero state is located along the western edge of mainland Mexico (Figure 5.1) bordered by the states of Michoacan to the northwest and Oaxaca to the southeast. The granite and basalt-rich Sierra Madre del Sur mountains (Spang et al., 2003) parallel the Pacific Ocean, forming western Mexico's 'spine.' Mountain-sourced rivers and ephemeral streams form an intricate matrix along the foothills, emptying into the ocean or coastal water bodies. The climate is semi-arid and monsoonal with a wet season from May-November, coinciding with the TC season. Annual coastal precipitation totals ~130 cm (Bullock, 1986), increasing inland. The oceanic Cocos plate subducts under the continental North American plate at the Middle America

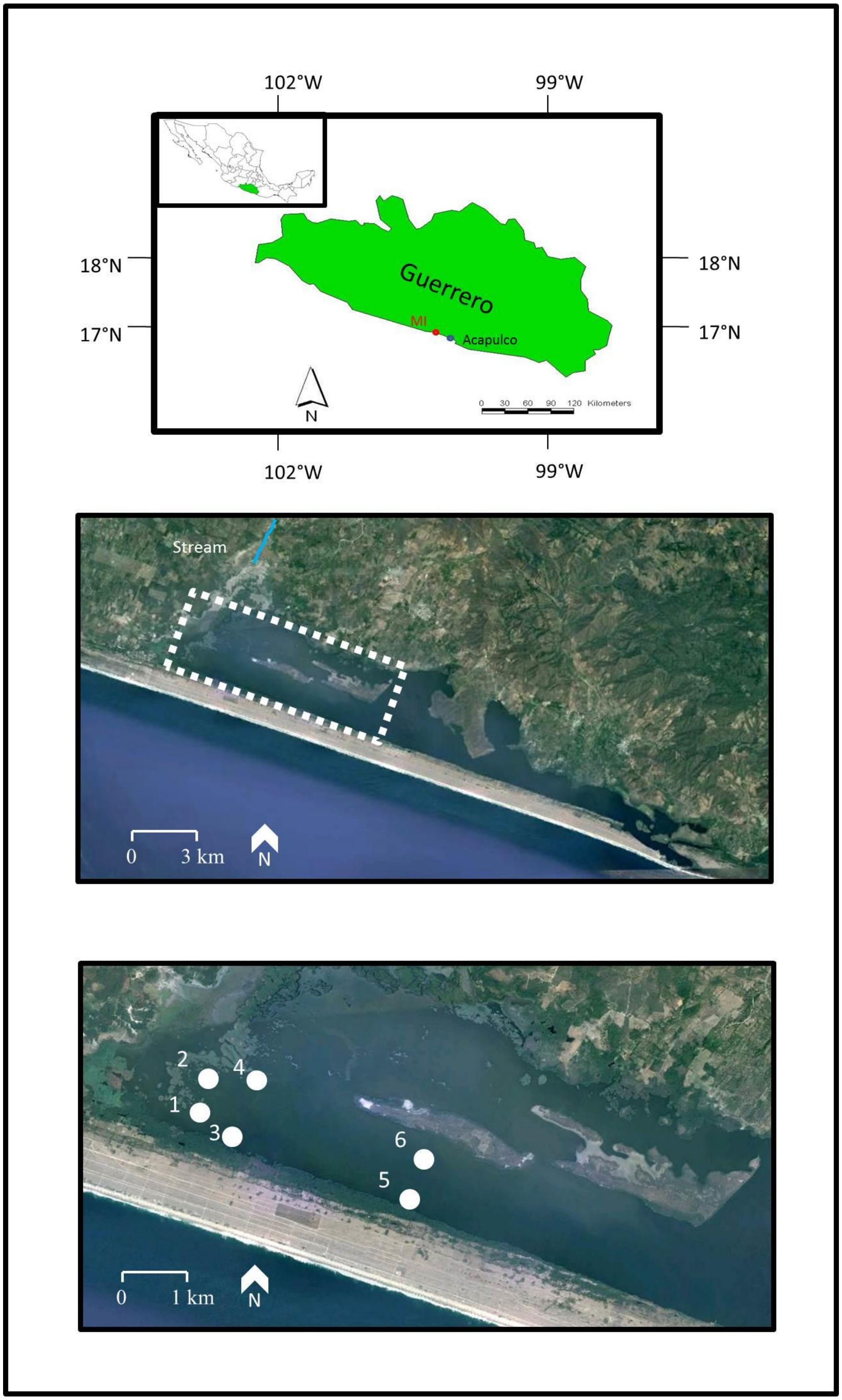

Figure 5.1 – Guerrero state, with Laguna Mitla's location labeled (MI) (top). Laguna Mitla and the surrounding environment are shown (middle). The western area captured in the white box is subset below, with core locations (1-6) depicted (bottom).

Trench 70 km west-southwest of Mitla. This collision is responsible for much of the earthquake and tsunami activity in this region. The continental shelf is narrow. Rocky cliffs and elevated terraces indicating paleo-uplift dot Guerrero in most areas, despite their absence in Mitla's vicinity (Ramirez-Herrera et al., 2011). The presence of alluvial and deltaic plains near Mitla indicates a tectonically stable environment (Ramirez-Herrera and Urrutia-Fucuguchi, 1999).

Laguna Mitla (17.0474º N, 100.3342º W) is located on Guerrero's central coast, 40 km west-northwest of Acapulco. It is 22 x 4 km in size with water depth mostly ~0.5-1 m. The current water level is close to sea level. Mitla contains a tidal inlet at its southeast corner that was artificially closed in 1968 (Yanez-Arancibia, 1977), limiting oceanic exchange. Current salinity is low at ~3.5 ppt (Contreras-Espinosa and Warner, 2004). Slope runoff is responsible for depositing inorganic sediments into the lagoon (Paez-Osuna and Mandelli, 1985). A small ephemeral stream enters into Mitla's western edge. The stream is generally 15 m wide, and can be followed uphill to the town of San Francisco, located 20 km inland of Mitla. Shells including *Bittium sp*., *Mytella strigata*, *Triphora sp*., and *Amnicola sp*. are common on Mitla's floor (Yanez-Arancibia, 1977; Contreras-Espinosa, 1993). Adjacent vegetation largely consists of mangroves and *Typha*. North of Mitla are vast wetland areas as well as abundant agricultural land.

Mitla is classified as a "barred inner shelf" lagoon, the most common Pacific coast classification (Lankford, 1977). A former depression along the continental shelf margin, the lagoon was formed during a mid-Holocene marine transgression, later protected by beach ridges formed from stabilizing seas (Lankford, 1977; Voorheis, 2004). The beach ridge plain is 900 m wide, with some ridges rising to ~8 m elevation. Some dirt roads, farms, and small cottages are present on the beach ridge plain. Seaward of the beach ridge system lies a narrow beach of low

relief. A chain of elongated islands occurring near Mitla's center are likely relict beach ridge formed from a Pleistocene highstand, as similar features are common throughout coastal Mexico (e.g., Thom, 1967; Lankford, 1977).

5.3 History of extreme events and their impacts

TCs originate south of Mexico and travel in a west to northwest pattern. TCs often parallel Mexico's west coast as the Sierra Madre mountains act as a barrier to inland encroachment (Sanson, 2004). Twenty-two hurricanes passed within 200 km of Mitla during the historical period, beginning 1949 (Jauregui, 2003) (Figure 5.2). The most devastating TC in recent memory is Hurricane Pauline (1997), despite only of category 1 intensity (on the Saffir-Simpson Scale) at landfall. In Acapulco, Pauline's destruction caused 300 million pesos (>22 million USD) in damage and 120 deaths (Matias-Ramirez, 1998). Its >400 mm of precipitation (Lawrence, 1999) sparked mass flooding and mudslides, washing gravel and boulders down inland hills toward the coast (Spang et al., 2003). Despite significant storm surge undocumented in Acapulco, Pauline's 9-m surge inundated coastal beaches causing impressive overwash fans in Oaxaca (Goman et al., 2005). Shell hash occurring near Mitla's center has been attributed to Hurricane Tara (1961) (Paez-Osuna and Mandelli, 1985), although the identification, source, and depositional process of these shells are poorly known. TC geophysical impacts are otherwise undocumented from Mitla and nearby areas. Local residents claim that recent storm surge inundation and/or tremendous mudslides have not occurred at Mitla.

Nine tsunamis with maximum water height ≥2 m have occurred in Guerrero since 1732 (National Geophysical Data Center, 2011). While local tsunamis are capable of inundation many km inland (Corona and Ramirez-Herrera, 2012), geomorphological effects of recent Pacific coast events have been minimal in this area (Jonathan et al., 2011).

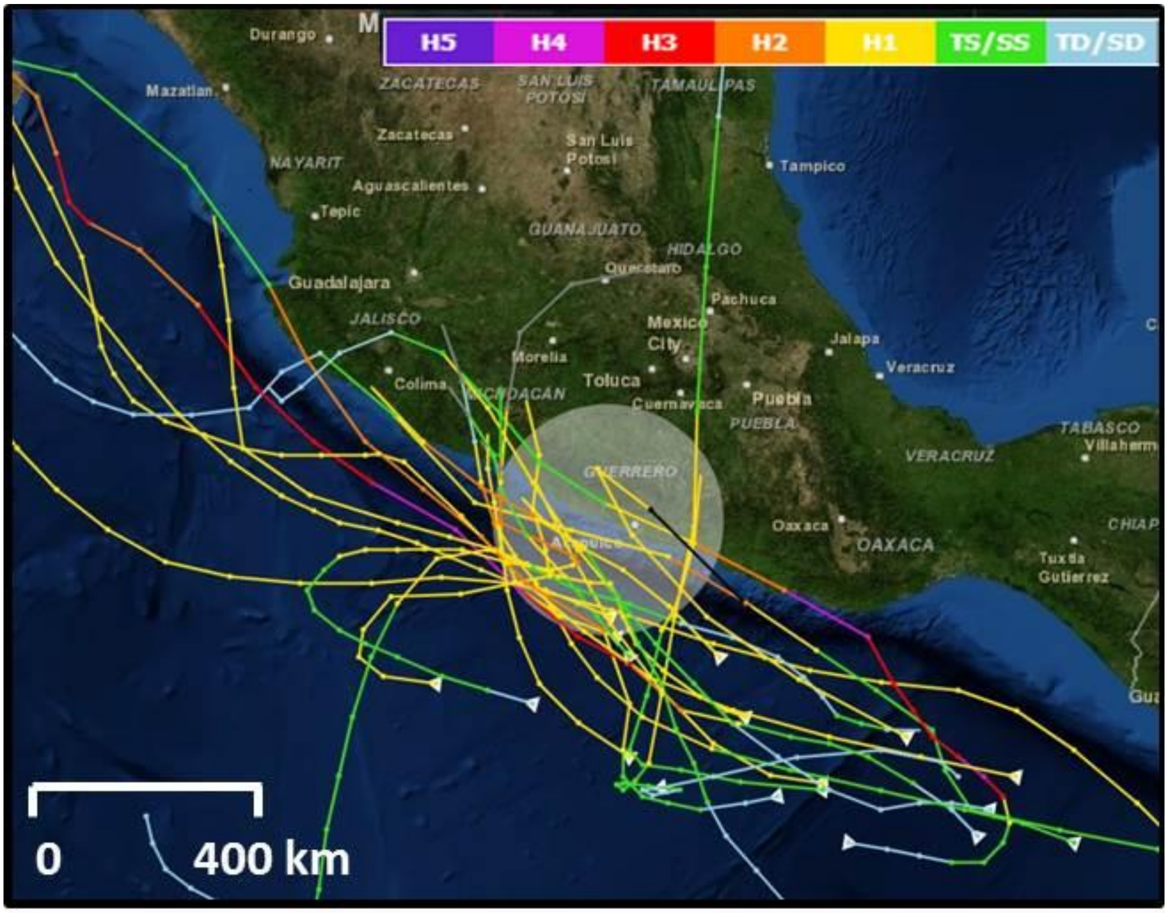

Figure 5.2 – From 1949-2010, 22 TCs of hurricane intensity from 1949-2010 have passed within 200 km of Laguna Mitla from 1949-2010 (National Oceanic and Atmospheric Administration, 2011). Most TCs parallel the coast and are low (tropical storm, category 1) intensity.

5.4 Methodology

During December 2009, six sediment cores were extracted in three shore-perpendicular transects from Mitla's western section. The cores were taken in ~ 50 cm core segments with a Russian peat borer. Sediments were transferred to pre-cut PVC tubes and secured with plastic wrap and duct tape to prevent moisture loss. In addition, 37 surface sediment samples were collected from Mitla's bottom and the adjacent beach to determine modern environmental conditions. All samples were transported to the Global Change and Coastal Paleoecology Laboratory at Louisiana State University, and stored in a 4ºC cold room.

Each core was lithologically described with the aid of a Munsell soil color chart. All cores were subjected to loss-on ignition (LOI) analysis (Dean, 1974) at 1 cm resolution to determine water, organic, and carbonate contents. Fragments of plant detritus were picked and sent to the National Ocean Sciences Accelerator Mass Spectometry (NOSAMS) laboratory at the Woods Hole Oceanographic Institution (WHOI) for AMS radiocarbon dating. The ^{14}C dating results were converted to calendar years using Calib 6.0 and the INTCAL 09 calibration curve (Stuiver et al., 2005). Calib 6.0 supplied the median value of the probability distribution on the calendar year axis for each date, rounded to the nearest decade by the author. When applicable, sedimentation rates were determined between each pair of calibrated radiocarbon dates by linear interpolation, and the core top and bottom by extrapolation.

Cores 2, 4, 5, and 6 were analyzed geochemically due to their spatial locations and stratigraphies. A Delta Innov-X handheld X-ray fluorescence (XRF) unit with a tantalum X-ray tube was used to measure chemical elemental composition. Sediments were covered with plastic film to prevent disturbance and scanned directly at 2-cm intervals. Three laser beams with 15 and 40 kilovolt excitation detected an array of light and heavy elements, with results reported in parts per million (ppm). Elements with low concentrations and/or exhibiting sporadic patterns were eliminated from output.

Ninety-seven clastic samples were processed with a Horiba Partica LA-950 laser diffraction particle size analyzer to determine grain-size. A hydrogen peroxide and hydrochloric acid pretreatment rid samples of organics and carbonates. Results were reported in microns (μ) for mean, median, and mode, with cumulative frequency distributions included and separated into size classes.

5.5 Results

Sediments are mostly dominated by inorganic (clay/silt) deposition. Sand is uncommon and restricted to a select few sediment cores. Organic-rich sediment sections consist of decomposed woody or muddy peat, or dark brown organic clay facies.

5.5.1 Stratigraphy, LOI, grain-size, sedimentation rate

5.5.1.1 Transect A

5.5.1.1.1 Core 1. Core 1 (190 cm) is extracted from the site's western, seaward edge in ~50 cm water depth. Its bottom contains two thin, dark brown (Munsell 2.5 YR, 3/1) organic-rich clastic layers (Figure 5.3) at 173-170 and 183-177 cm. Remaining sediment is mottled gray to brown clay/silt (7.5 YR, 4/1, 5/1; GLEY 2 3/2, 4/2) low in water (~35-40 %), organics (6-12 %), and carbonate (1-3%). A section of silty-clay at 64-55 cm exhibits markedly lower contents of water (24-29 %) and organics (~5%).

5.5.1.1.2 Core 2. Core 2, the second longest core (329 cm) (Figure 5.4), was retrieved from ~50 cm water depth at a location about 520 m landward of core 1. From 329-196 cm lies dark, very muddy peat (60-80 % water, 60-90 % organics, 3-5 % carbonate) that contains gray clay bands characterized by decreasing water and organics values, and fluctuating carbonate content. The top 196 cm is mottled brown and gray clay (2.5 Y, 4/1, 4/2, 5/1), with darker (2.5 Y, 3/1) organic-rich clay at 145-115 cm. Radiocarbon dates obtained from 114 cm (1990±30 ^{14}C yr BP), 197 cm (3850±55 ^{14}C yr BP), 242 cm (4080±40 ^{14}C yr BP), and 316 cm (4430±30 ^{14}C yr BP) yield calibrated ages of 1940, 4271, 4583, and 5017 cal yr BP, respectively. All dates are deemed acceptable. Sedimentation rate decreases from 0.1452 and 0.1682 cm/yr in the lower organic section to 0.0356 and 0.0588 cm/yr in the upper half of the core (Figure 5.4).

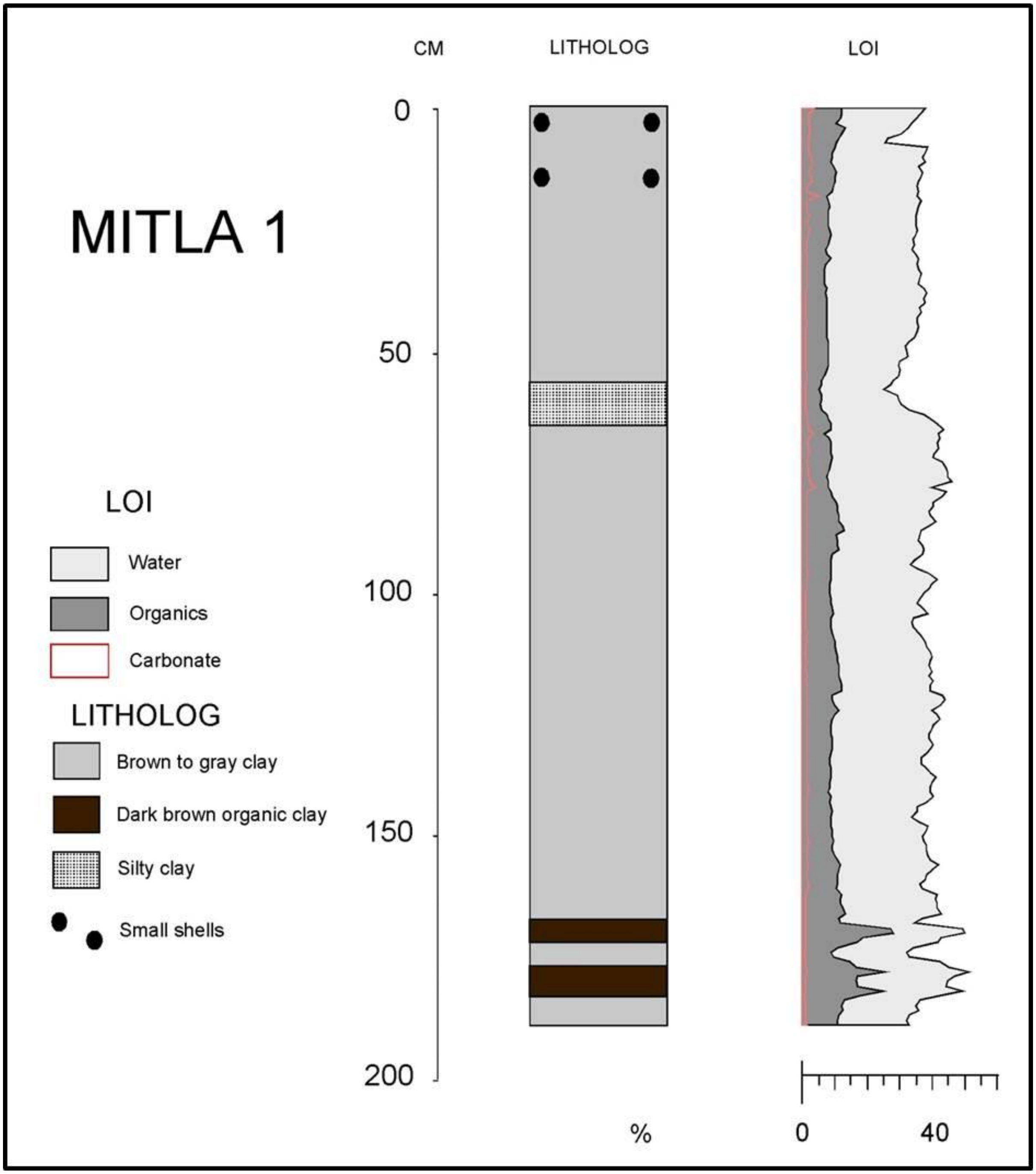

Figure 5.3 – Core 1 litholog and LOI results. Core 1 is primarily brown/gray clay relatively low in water, organics, and carbonate contents.

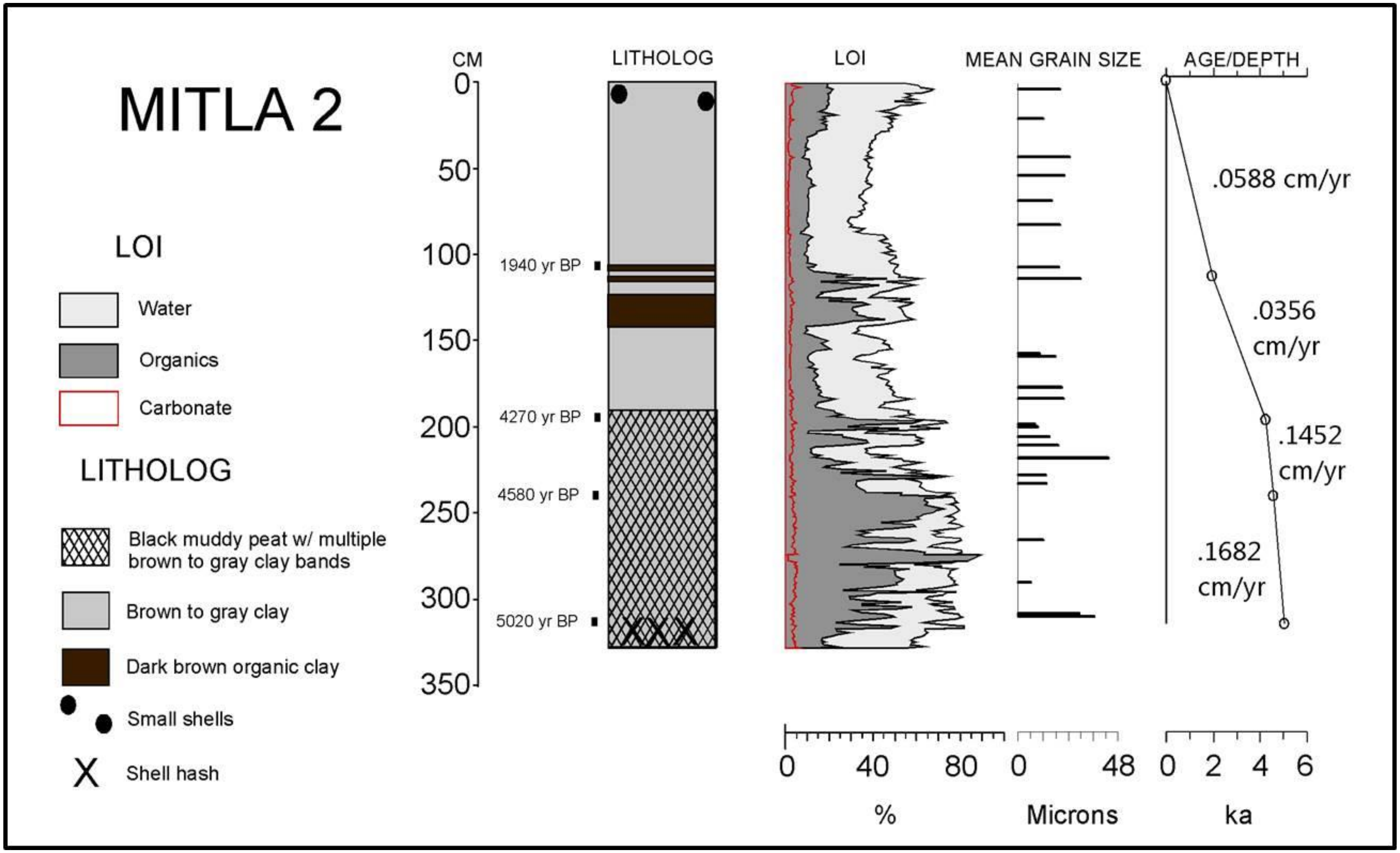

Figure 5.4 – Core 2 litholog and LOI results. Core 2 contains muddy peat throughout the bottom meter, and a peaty clay section at 145-115 cm. Remaining sediments are mottled brown/gray clay low in water, organic, and carbonate contents. Sedimentation is assumed to start at modern (e.g., Bradbury, 2000).

Twenty-five clastic samples were analyzed for grain-size at various intervals throughout the core. Mean grain size is relatively low (~12-20 μ) throughout the core. Thin clastic layers embedded in muddy peat from 329-196 cm and the dominant inorganic sequence from 196-0 cm does not exhibit fining or coarsening upward trends.

5.5.1.2 Transect B

5.5.1.2.1 Core 3. Core 3 (218 cm) is extracted 450 m ESE of core 1 near Mitla's southern shoreline in ~ 50 cm water depth. Peat exists from 218-164 cm (Figure 5.5). Dark brown clay (7.5 YR, 3/1) from 164-103 cm turns to a grayer shade (7.5 YR, 5/1) toward the coretop. These sections contain minor evidence of mottling and low LOI contents. One radiocarbon sample from 175 cm yields a date of 4110±30 ^{14}C yr BP (4632 cal yr BP).

5.5.1.2.2 Core 4. Extracted 900 m landward of core 3 in ~50 cm water depth, core 4 (216 cm) possesses dry and slightly mottled gray to brown clay (7.5 YR 2.5/1: 5 YR, 3/1) from 216-119 cm. Yellow sand (5Y, 8/4) deposition is sporadically intermixed and lacking sharp boundaries (Figure 5.6). Organic content is relatively low (peaking at 22%, 198 cm), decreasing in sandy sections (~1-2%). The top 119 cm contains mottled brown and gray (7.5 YR, 3/1: 4/1: 4/2: 10 YR, 5/4) clay consistent in water (30-40 %), organics (7-10 %), and carbonate (1-2 %). Small snail shells are scattered near the coretop. Samples were radiocarbon dated from 111 (3840±65 ^{14}C yr BP) and 198 cm (4110±30 ^{14}C yr BP), calibrated to 4254 cal yr BP and 4632 cal yr BP, respectively.

Thirty-nine samples were analyzed for grain-size throughout core 4, with high-resolution sampling in some sandy sections. Mean grain size decreases upcore as sandy sections lack structure, despite one sequence (205-200 cm) coarsening upward.

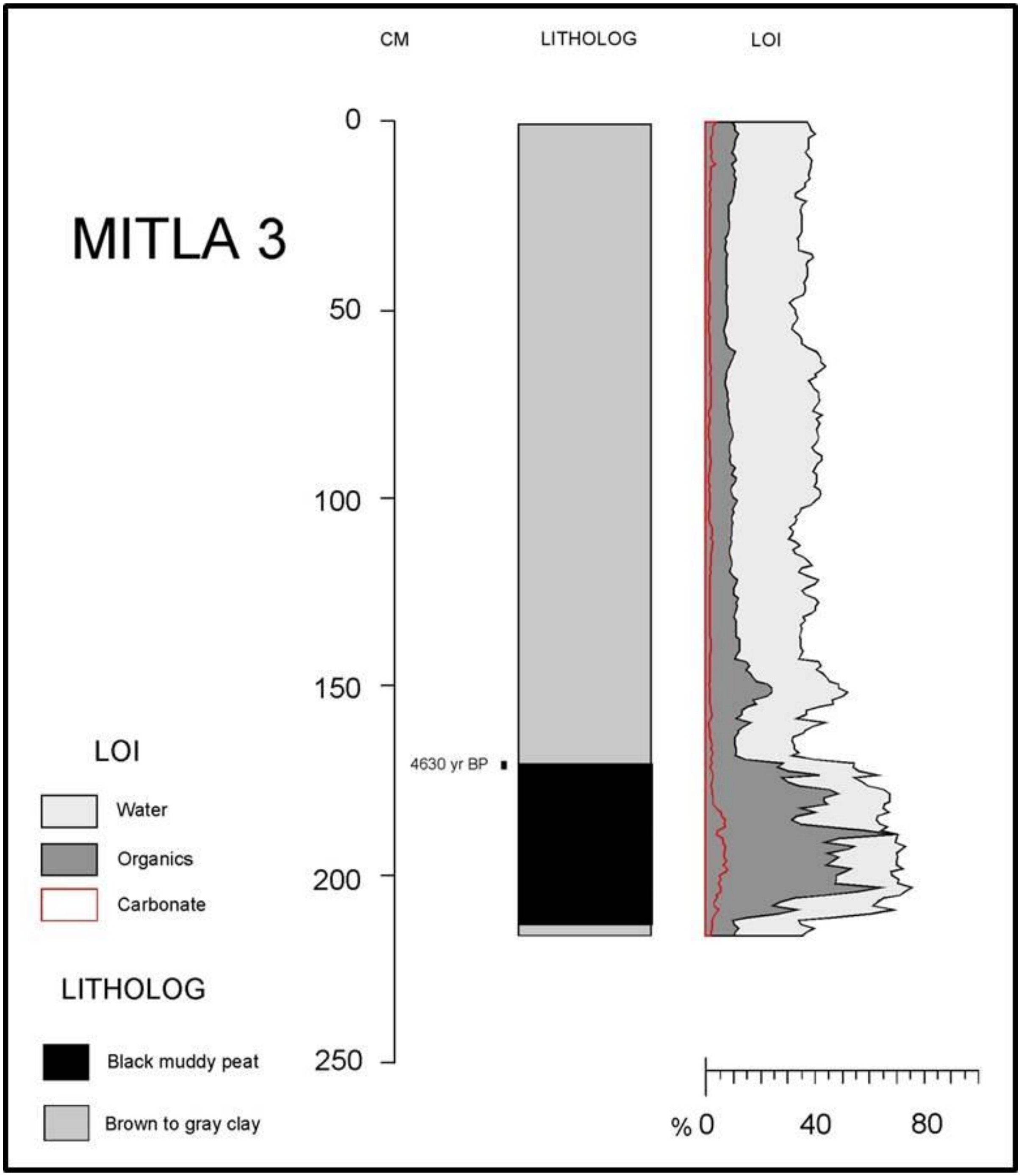

Figure 5.5 – Core 3 litholog and LOI results. Peat deposition ends around 4630 yr BP, with brown/gray clay with some mottling dominant until the current period.

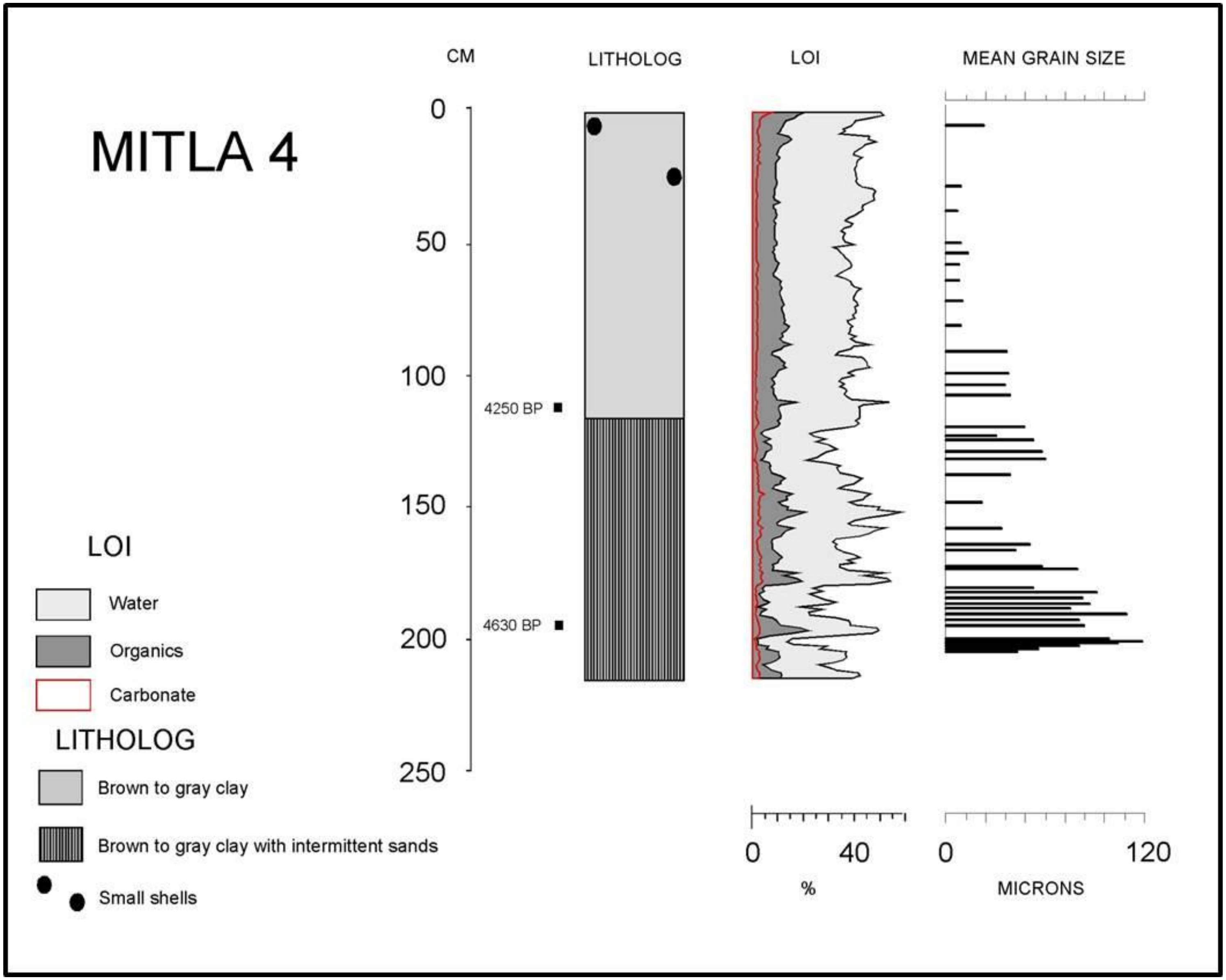

Figure 5.6 – Core 4 litholog and LOI results. Clay with sand from 216-119 cm is low in water and organic contents, ending 4250 yr BP. The remainder of core 4 is mottled brown/gray clay.

5.5.1.3 Transect C

5.5.1.3.1 Core 5. Extracted 2.9 km ESE of core 3 in ~ 1 m water depth, core 5 (479 cm) is mainly black peat (7.5 YR, 3/2) with high water (~85%) and organic (~80%) contents. Inorganic silt/clay bands of various thicknesses and structures occur throughout the core (Figure 5.7). Five stratigraphic zones are delineated. Zone 5 (479-400 cm) contains gray coarse sand (2.5 Y, 7/4) at the bottom, transitioning to muddy dark peat (7.5 YR, 2.5/1). Zone 4 (400-290 cm) consists of multiple thin gray clay bands (7.5 YR, 3/3, 4/2). Most clastic bands have low carbonate contents, except for four carbonate-rich layers at 294-292 (14% content), 309-308 (8%), 327-325 (13%), and 394-392 cm (6%). Zone 3 (290-210 cm) contains homogeneous peat with no visible clastics. A slight decrease in organics from 275-234 cm is not matched by a corresponding drop in water. Zone 2 (210-100 cm) contains four gray clay layers (7.5 YR, 4/2, 5/1) with significant decreases in organics (~35%) yet only slight drops in water (~70%) and negligible carbonate increases. Two layers (145-131, 198-183 cm) are faint gray clayey peat, while the remaining two (166-162, 174-172 cm) are distinct and structureless gray clay sections with sharp upper and lower boundaries. Zone 1 (100-0 cm) contains three thick tan to gray (7.5 YR 3/2, 4/1) structureless clay sections at 30-0, 79-65, and 99-89 cm marked by sharp decreases in water (50%), organics (10%), and carbonate (3%) contents.

Radiocarbon dates obtained from 2 cm (> modern), 34 cm (1840±45 ^{14}C) yr BP, 61 cm (2710±110 ^{14}C yr BP), 125 cm (3160±30 ^{14}C yr BP), 207 cm (4070±30 ^{14}C yr BP), 290 cm (4500±30 ^{14}C yr BP), 324 cm (4760±30 ^{14}C yr BP), 414 cm (6050±35 ^{14}C yr BP), and 475 cm (6000±60 ^{14}C yr BP) yield calibrated dates of post-modern age, 1777, 2836, 3388, 4558, 5167, 5520, 6903, and 6842 cal yr BP, respectively. The sample at 414 cm is rejected as it is older than

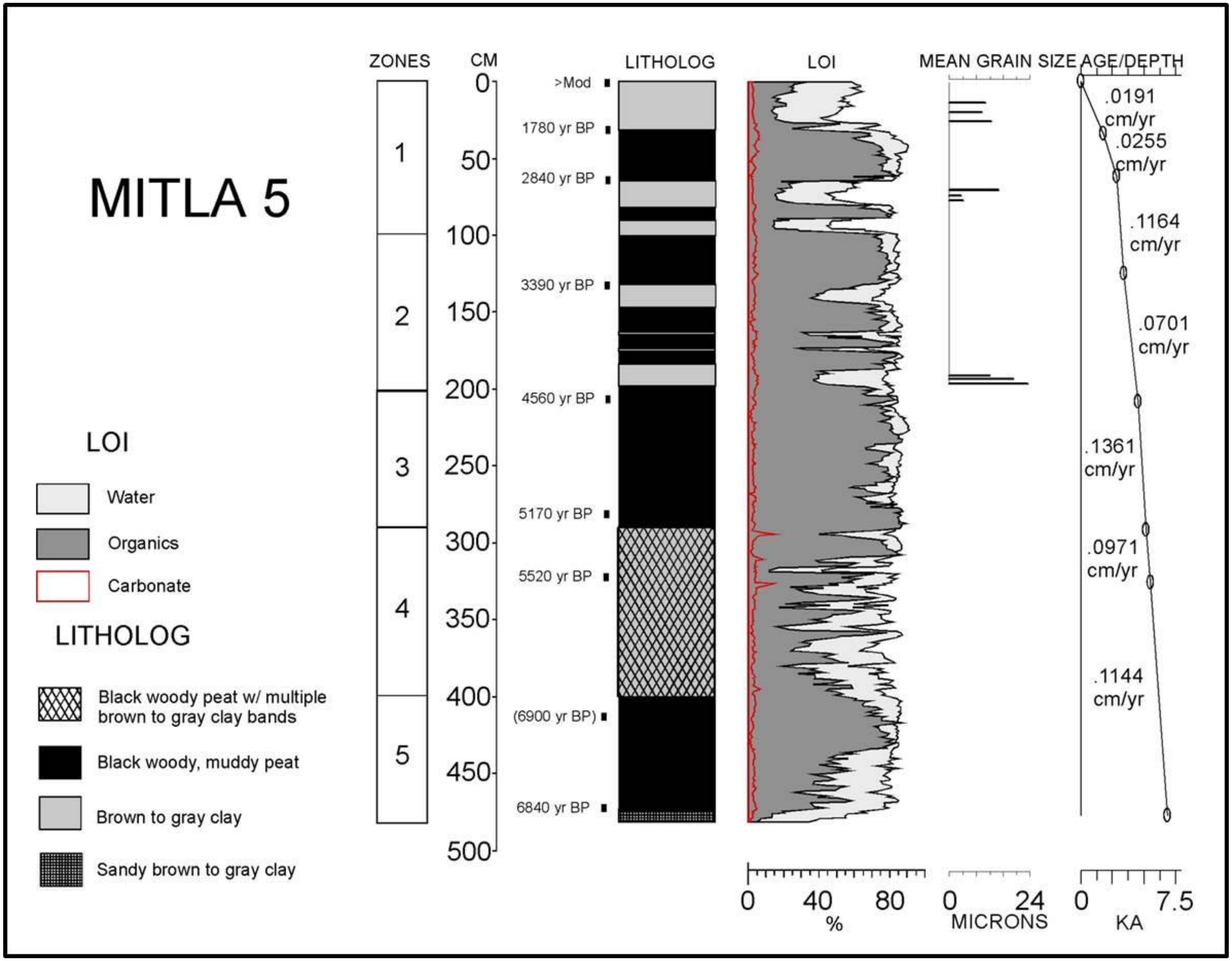

Figure 5.7 – Core 5 litholog, LOI results, and zone delineation. Core 5 is mostly peat high in water and organic content. Embedded clastic bands vary in structure, thickness, and LOI content.

the sample below it. Sedimentation rates are high in the peat sections from 488-61 cm (0.0701 - 0.1361 cm/yr), decreasing in the clayey top 61 cm (0.0191, 0.0255 cm/yr).

Nine samples were analyzed for grain-size, including six samples from two clay layers from zone 1 and three samples from a thick clay layer from zone 2. The clay layer from zone 2 clay exhibits a fining upward pattern, while three from zone 1 do not possess clear internal structures.

5.5.1.3.2 Core 6. Core 6 was taken from 550 m landward of core 5. Extracted from ~ 1 m water depth, it is the shortest core (129 cm - Figure 5.8) due to the presence of stiff bottom sediments. An alternating series of black to gray sandy peat (7.5 YR, 3/1) and coarse gray sand (7.5 YR, 6/1) occurs from 129-88 cm. Light and dark gray sand (7.5 YR, 4/1, 6/1) from 88-56 cm is marked by low water, organic, and carbonate contents. Sand sections do not exhibit sharp lower or upper boundaries. Black peat (7.5 YR, 3/1) occurs at 45-56 cm. The top 45 cm contains iterations of reddish, gray, and brown clay (2.5 YR, 4/3: 7.5 YR, 4/1). Shell hash at 45-33 cm is responsible for a carbonate spike (32%). One organic sample from 127 cm was radiocarbon dated to 2800±80 ^{14}C yr BP or 2919 cal yr BP (Table 5.1).

Twenty-four samples from core 6 were analyzed for grain-size. High-resolution sampling from two sand layers suggests that they are composed of fine sand without clear internal structure.

5.5.2 Geochemistry

Muddy peat at the bottom of core 2 contains low concentrations of most elements (Fe, Ti, K, Cr, Mn, Co, Ni, Cu, Zn, Tb, Zr, S, I, Ca, Sr) except Cl and Mo (Figure 5.9). The trends reverse upcore in the clay section above for most elements, but S, I, Ca, and Sr remain low throughout the core.

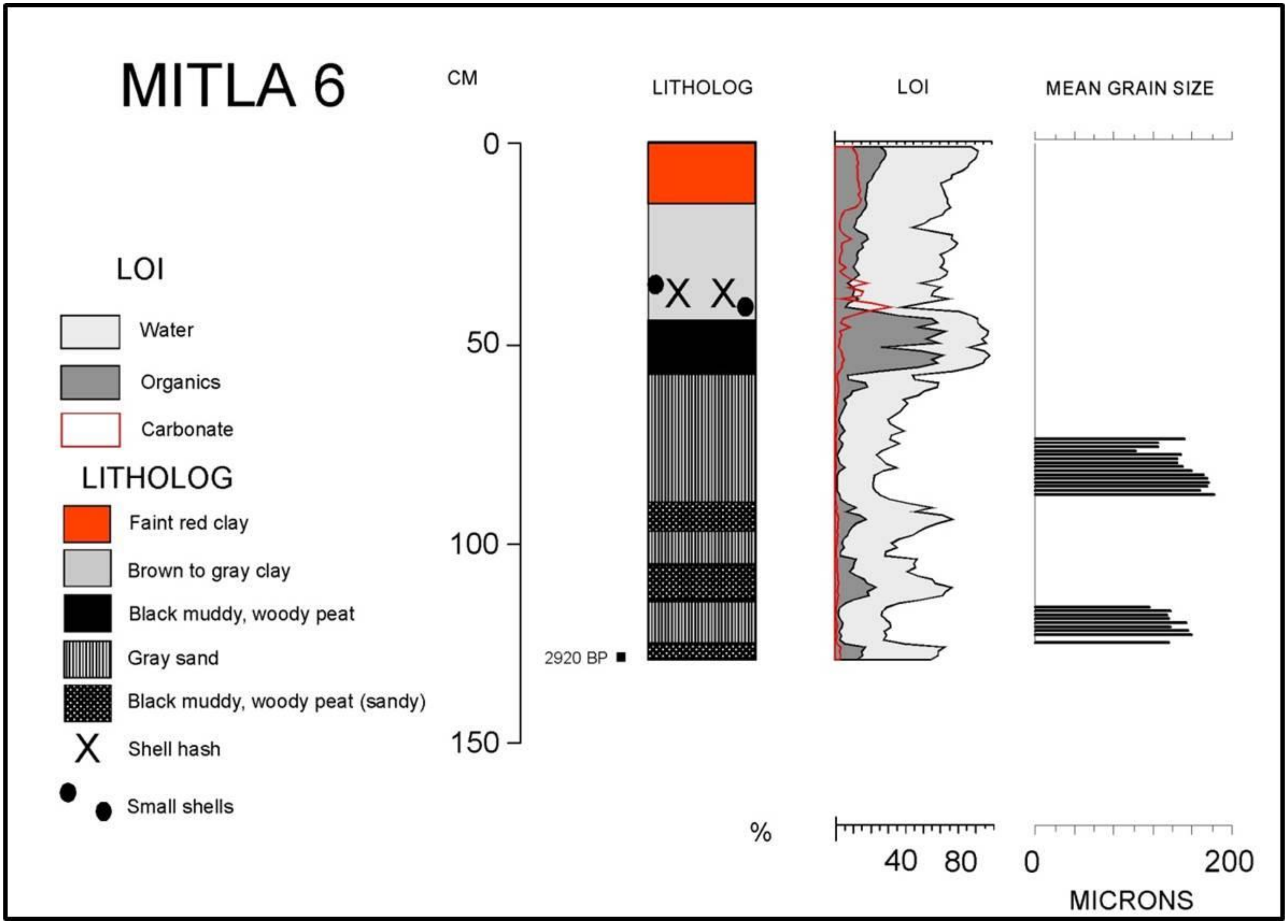

Figure 5.8 – Core 6 litholog and LOI results. Sand from 129-56 cm does not exhibit sharp upper or lower boundaries. The remainder of core 6 is peat and gray to red clay.

Table 5.1 – Laguna Mitla radiocarbon dating results.

Core/ sample ID	Depth (cm)	Lab #	Material	Radiocarbon age (BP)	Cal BP (2δ)	Rel. area under prob. distrib.	Med. prob
Mitla 2D 40	114	OS-90703	Plant/Wood	1990±30	1878-1997	1	1940
Mitla 2F 35	197	OS-93080	Plant/Wood	3850±55	4094-4123	0.04	
					4144-4418	0.96	4271
Mitla 2G 39	242	OS-90697	Plant/Wood	4080±40	4438-4488	0.12	
					4496-4655	0.631	4583
					4667-4707	0.076	
					4756-4811	0.174	
Mitla 2I 39	316	OS-93065	Plant/Wood	4430±30	4875-5068	0.762	5017
					5109-5123	0.019	
					5169-5172	0.003	
					5182-5275	0.216	
Mitla 3F 25	175	OS-91548	Plant/Wood	4110±30	4523-4710	0.746	4632
					4719-4722	0.002	
					4754-4814	0.252	
Mitla 4D 28	111	OS-92322	Plant/Wood	3840±65	4010-4029	0.012	
					4083-4422	0.988	4254
Mitla 4F 33	198	OS-93067	Plant/Wood	4110±30	4523-4710	0.746	4632
					4719-4722	0.002	
					4754-4814	0.252	
Mitla 5AAA 2	2	OS-90761	Plant/Wood	> mod			
Mitla 5AAA 34	34	OS-90770	Plant/Wood	1840±45	1630-1653	0.03	
					1692-1881	0.97	1777
Mitla 5 61	61	OS-84452	Plant/Wood	2710±110	2490-2643	0.087	
					2674-3084	0.886	2836
					3088-3157	0.027	
Mitla 5 125	125	OS-83891	Plant/Wood	3160±30	3341-3447	1	3388
Mitla 5 207	207	OS-83892	Plant/Wood	4070±30	4440-4486	0.159	
					4499-4503	0.004	
					4507-4645	0.69	4558
					4676-4693	0.02	
					4762-4801	0.126	
Mitla 5 290	290	OS-83942	Plant/Wood	4500±30	5046-5296	1	5167
Mitla 5H 45	324	OS-93066	Plant/Wood	4760±30	5333-5348	0.043	
					5353-5371	0.035	
					5464-5587	0.922	5520
Mitla 5 414	414	OS-83941	Plant/Wood	6050±35	6795-6991	1	6903
Mitla 5L 44	475	OS-90763	Plant/Wood	6000±60	6677-6707	0.03	
					6713-6987	0.97	6842
Mitla 6C 49	127	OS-92903	Plant/Wood	2800±80	2755-3082	0.956	2919
					3091-3143	0.044	

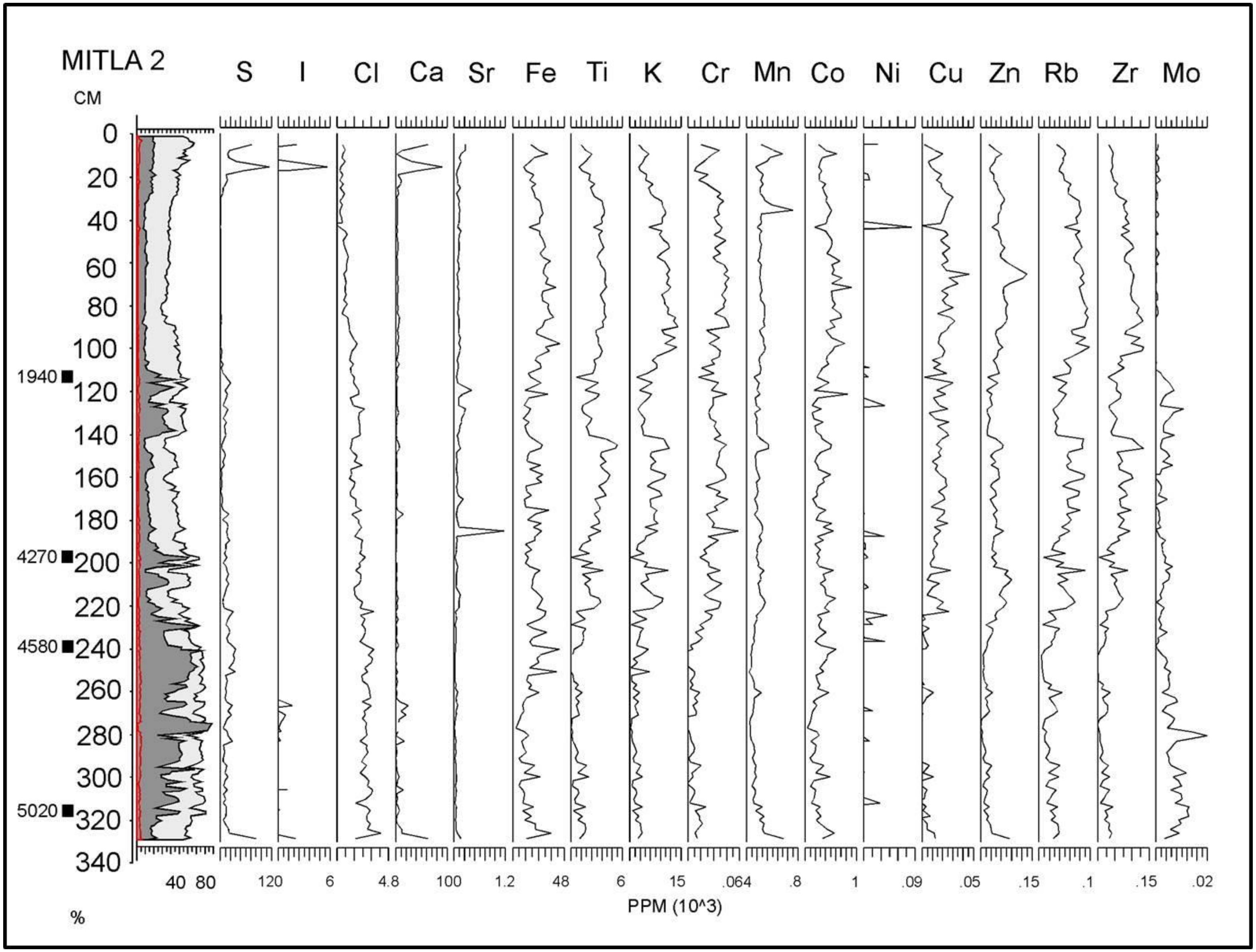

Figure 5.9 – Core 2 XRF results (ppm) paired next to LOI results. Most lithogenic elements are in low concentration in peat, increasing in clay sections. Sections of low LOI contents generally contain the most elevated concentrations of lithogenic elemental concentrations throughout core 2. Cl concentration steadily decreases upcore.

For core 4, the sandy clay near the bottom is relatively high in most elements. The mottled clay in the upper part is high in most elements but low in Ca, Sr, I, S, and Cl (Figure 5.10).

Core 5 results are grouped by zone (Figure 5.11). Zone 5 concentrations are relatively low. Most elements (e.g., Fe, Ti, K, Co, Zn, Rb, Zr) are in high concentration at the bottom of zone 4 with Sr, I, Ca, and S elevated toward the zone top. Concentrations are relatively low throughout zone 3. Zone 2 clay has increases in most elements (e.g., Sr, I, Ca, S, Fe, Ti, K, Cr, Zn, Rb). Zone 1 clay contains the highest concentrations of most elements (e.g, Fe, Ti, K, Cr, Zn, Rb, and Zr). Element I, Ca, and S concentrations are low in clay and with small concentration peaks in peat. Cl steadily decreases upcore.

Black/gray sand near the bottom of core 6 is high in Fe, Ti, Cr, Co, Zn, and Zr, while low in Sr, S, I, and Ca (Figure 5.12). Peat is low in most elements while I, Ca, and Sr spikes occur throughout the shell/shell hash layer at 56-45 cm. Reddish clay near the coretop is high in most elements. Cl concentration decreases upcore, similar to cores 2, 4, and 5.

5.6 Discussion

5.6.1 Stratigraphic correlation

5.6.1.1 Transect A

Cores 1 and 2 are dominated by brown or gray mottled clay with low LOI contents (Figure 5.13). Core 2 contains muddy peat at its bottom (~5020 – 4580 yr BP) with core 1 too short to contain a matching section. Core 1 organic clay stratigraphically matches a section from core 2 at ~120 cm (1940 yr BP). Core 1 silty clay (64-55 cm) correlates to an inorganic section with decreased LOI contents in core 2 (Figure 5.13).

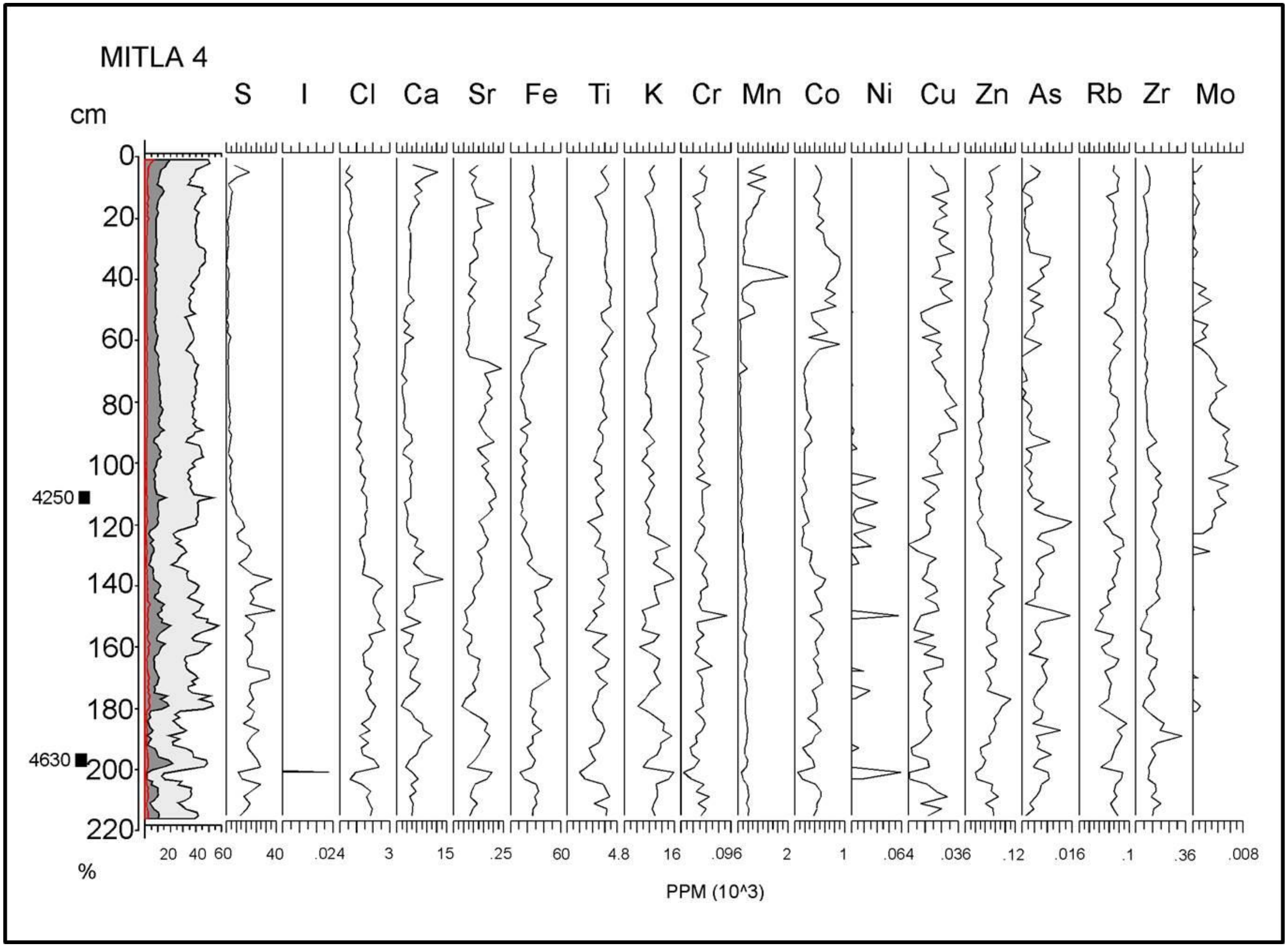

Figure 5.10 – Core 4 XRF results (ppm) paired with LOI results. Sandy clay from 216-119 cm is relatively high in many elements including S, Fe, K, Zn, and Zr. The top 119 cm is low in S, Ca, Sr, and I and relatively high in Ti, Fe, Co, and Cu. Cl steadily decreases upcore.

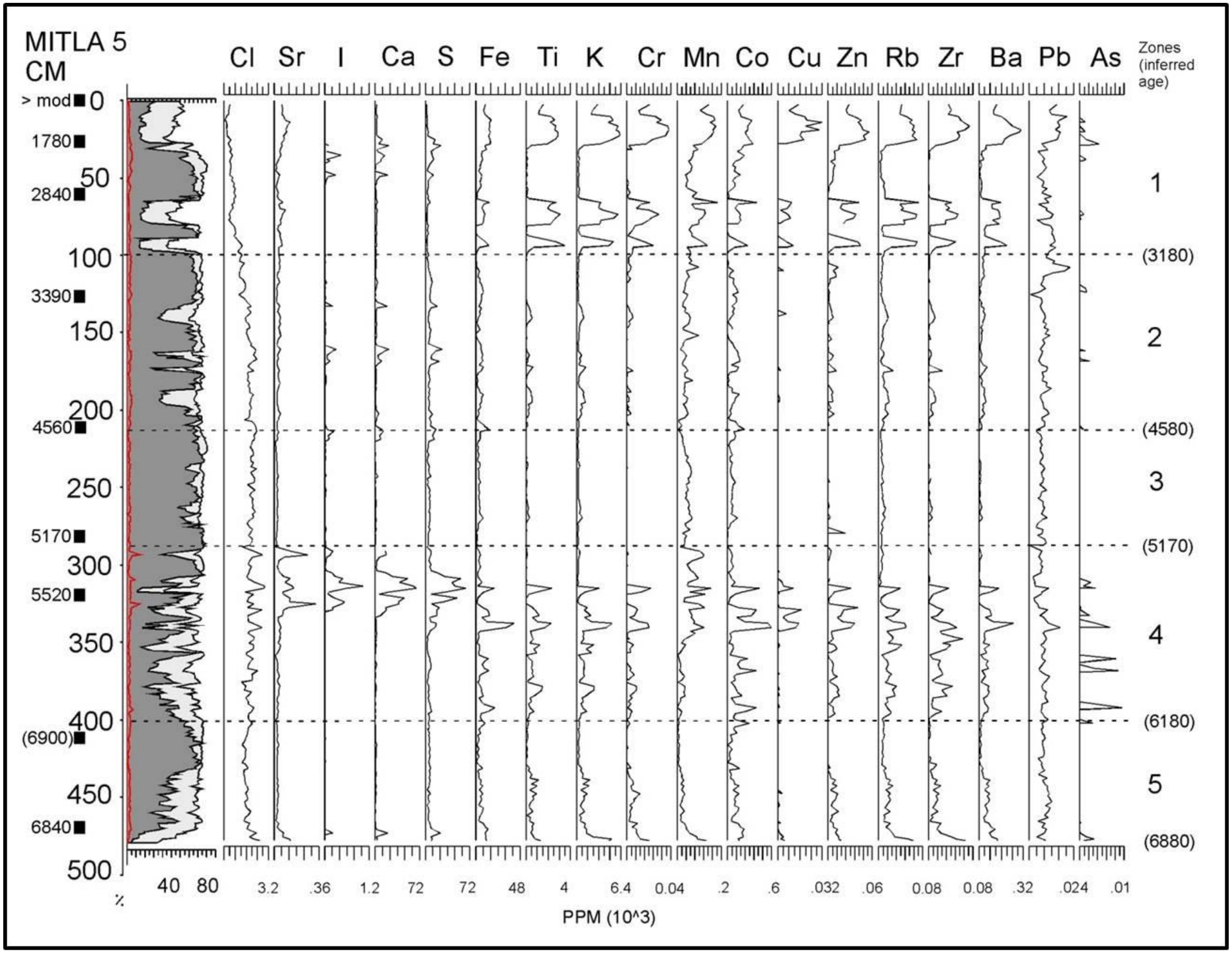

Figure 5.11 – Core 5 XRF results (ppm) paired with LOI results and zone delineation. Peat is low in elemental concentrations. Clay sections contain increases in lithogenic elements, with zone 1 clastics containing the highest concentrations.

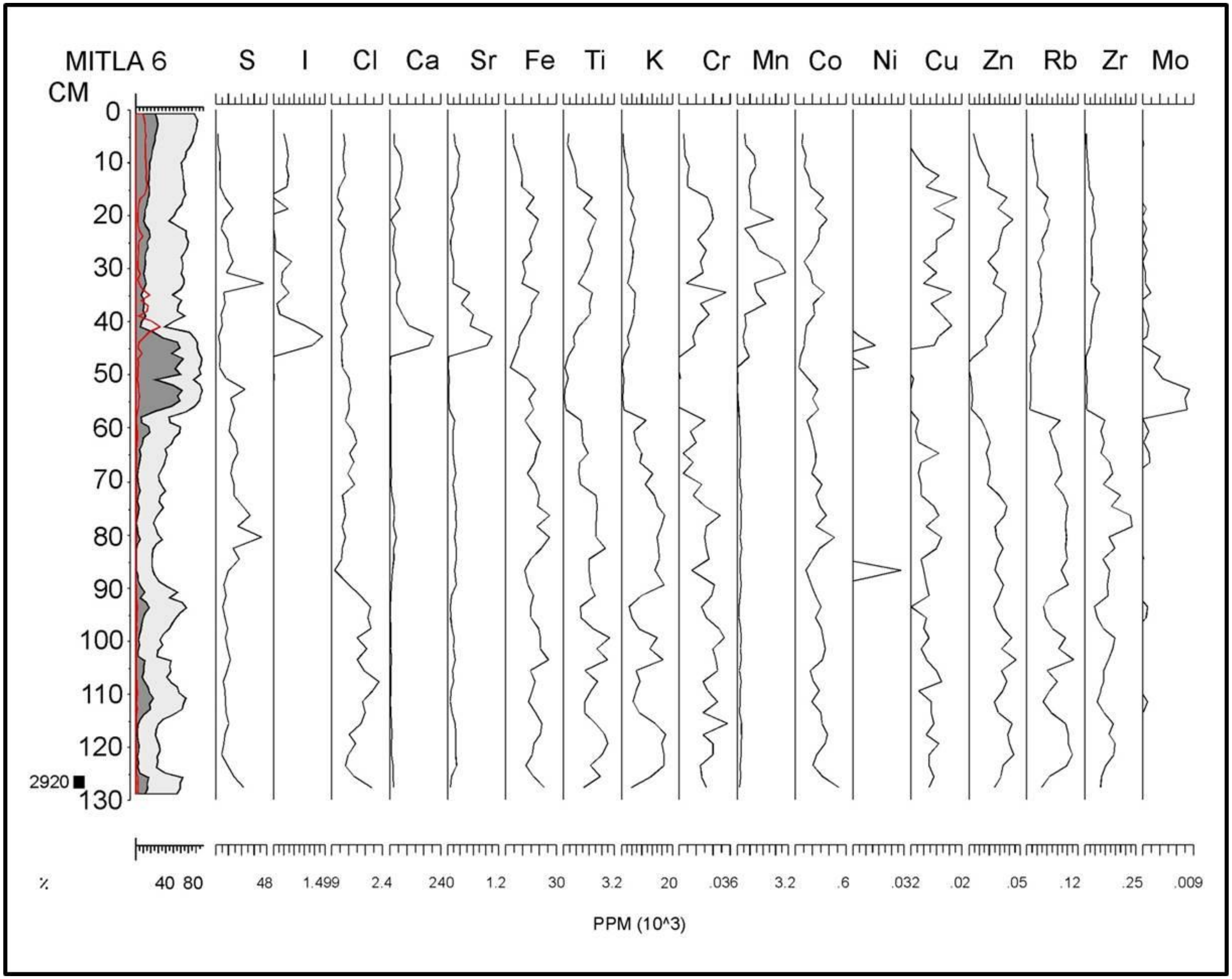

Figure 5.12 – Core 6 XRF results paired with LOI curves. Sand sections low in water and organics are high in most elements including Fe, Ti, Zr, and Zn. Peaks in S, I, Ca, and Sr correspond to a shell/shell hash layer at 45-33 cm.

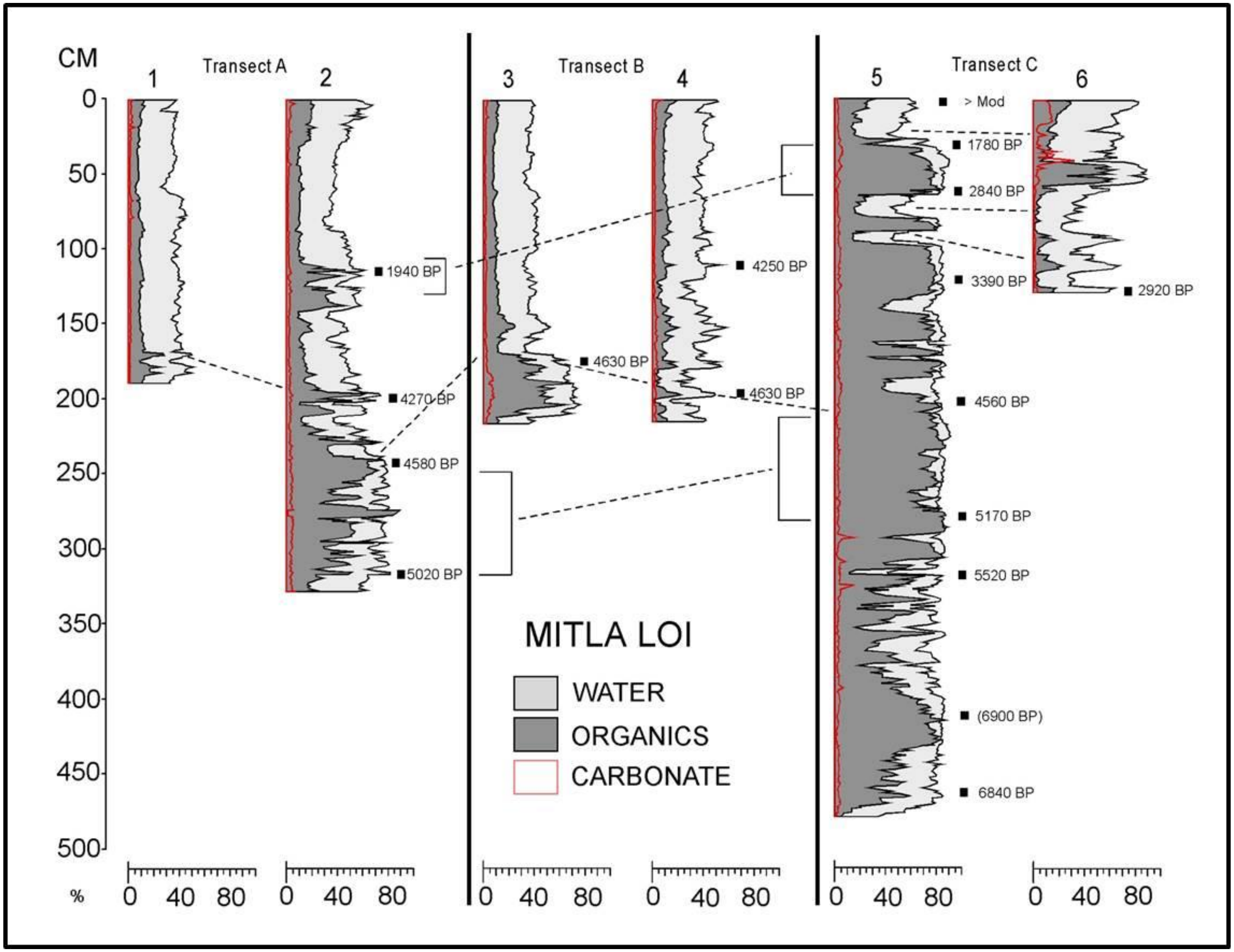

Figure 5.13 – Mitla LOI results for cores 1-6, separated by transect location (A – left, B – center, C – right). Stratigraphic correlations within and between transects are indicated with dotted lines.

5.6.1.2 Transect B

Cores 3 and 4 are dominated by brown and gray clay, with deposition beginning ~4630 and ~4250 yr BP, respectively. Minor variability in LOI contents limit cross-core correlations. The bottom of core 3 (>4630 yr BP) contains peat lacking sand, while the bottom of core 4 (>4630 - 4250 yr BP) consists of gray clay with intermittently deposited sand.

5.6.1.3 Transect C

Organic-rich peat with large macrofossils dominates core 5 and a small section near the top of core 6. Clastics correlate temporally (Figure 5.13) despite core 6 containing sand while core 5 possesses structureless gray clay. Cross-core correlations are limited from the short length of core 6.

5.6.1.4 Inter-transect stratigraphic comparisons

Stratigraphic consistencies are discernible when comparing transect A, B, and C sediments. Core 1-4 brown/gray clay (~4500 yr BP – present) does not resemble structureless gray clay in core 5, intermittently embedded since ~4550 yr BP, nor core 6 sand and reddish clay since 2920 yr BP. With the exception of basal sand in core 5, sand is present only in landward cores 4 and 6, yet cross-core correlations between cores 4 and 6 are difficult, as core 4 lacks sand since ~4500 yr BP.

Organic-rich deposition for cores 1 and 2 varies between dark brown clay and muddy peat. Core 4 lacks peat and organic-rich clays, while peat in core 3 contains higher LOI contents with larger macrofossils than cores 1 and 2. Further east in transect 3, cores 5 and 6 contain the “purest” peat, possessing elevated LOI content and the highest quantity and largest macrofossils. Stratigraphic correlations for all cores are presented in Figure 5.13. Close stratigraphic similarity exists between the long cores 2 and 5 despite their extraction 3 km apart (Figure 5.14).

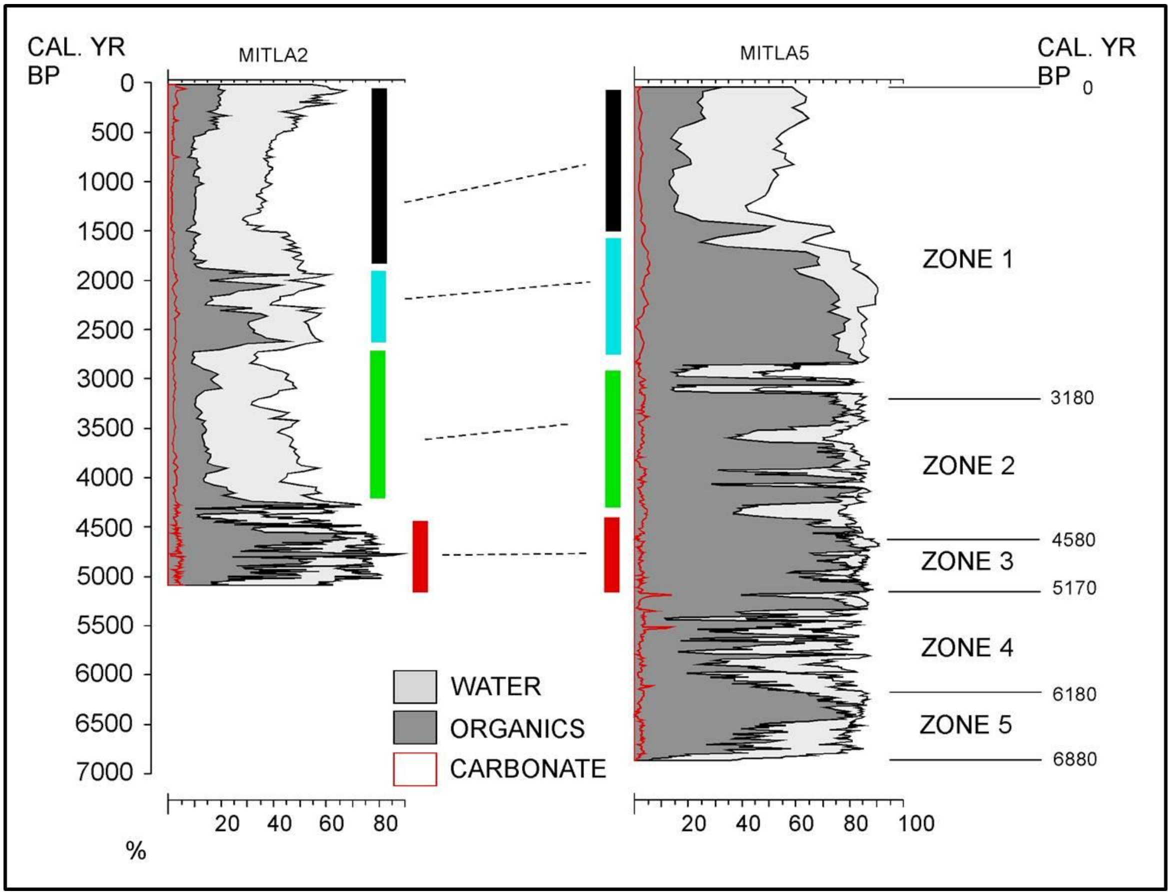

Figure 5.14 – A comparison of LOI contents between cores 2 and 5, with zone delineations listed. LOI contents are graphed on an age scale (y-axis). The multi-colored rectangles indicate similar stratigraphic sections for the cores. Throughout zone 3, both cores were dominated by peat sediments (red rectangle). Throughout zone 2, core 5 is dominated by peat, with four clay layers embedded (green rectangle). Alternatively, core 2 is dominated by clay deposition. At the bottom of zone 1, both cores contain peat sediments (blue rectangle). The tops of both cores are clay (black rectangle).

Both relatively stable throughout zone 3, core 2 contains distinct clay deposition absent in core 5. Peat/peaty clay sections also indicate good temporal connection. Clay in core 2 contains lower LOI contents and higher grain sizes than clay in core 5.

5.6.2 Environmental reconstruction

Clay sediments are interpreted to indicate lagoonal environments, similar to Mitla's current setting. As lagoonal clay is generally comprised of terrigenous material once subjected

to mechanical attrition, these sediments contain elevated lithogenic element concentrations (e.g., Fe, Ti) corresponding with the relatively small grain-sizes (Weltje and von Eynatten, 2004). Clay throughout cores 2, 4, 5, and 6 generally possess high lithogenic element concentrations.

Water depth is shallower at the core 2 site than at cores 5 and 6 by ~50 cm, mainly due to greater terrigenous deposition at the former site. As Mitla lies adjacent to a steep topographical gradient, rainstorms and TCs are largely responsible for transporting significant amounts of water and terrigenous sediments down the slopes and into the site. Terrigenous deposition is likely highly variable both spatially and temporally, while focused toward the landward edges of the site. Small dips in LOI contents in lagoonal clay sections occur mostly in transect A cores, indicating intermittent coarse-grained deposition via runoff and stream input. Core 2 dips in LOI contents generally contain increases in terrigenous elemental concentrations (Fig 5.9). Minor mottling in cores 1-4 might stem from bioturbation (e.g., Jakobsson et al., 2000) occasional subaerial weathering due to water level fluctuations (e.g., Berrio et al., 2006). Clastic components from transect A and B cores generally contain lower LOI content than the easternmost core 5 (Figure 5.13). Similarly, core 2 mean grain size is greater than cores 4 and 5 among matching stratigraphic sections. Lithogenic element concentrations are higher in landward cores than core 5 among corresponding stratigraphic sections.

Lagoonal clay dominates cores in transects A and B, pinpointing the centralized location of the limnic (lagoonal) environment for Mitla's western section. The drowned relict beach ridge remnant in this section permits runoff from the northwest corner to enter this area. As the relict ridge likely contains higher elevation toward the east, significant amounts of water are prevented from entering the eastern edge of the study site. Infrequent and structureless clastic

deposition in core 5 suggests lower energy conditions and decreased sensitivity to lagoonal phases nearer Mitla's middle section.

In seasonally wet/dry climates like coastal Guerrero, increases in water level are driven by alterations in precipitation regime. During wet periods, the site would experience more precipitation entering the site directly, along with increases in runoff and stream input. Regionally, water level fluctuations have been interpreted to indicate evidence of climate change at many sites, including a nearby highland lake (e.g., Berrio et al., 2006). Precipitation regimes throughout the eastern north Pacific (ENP) basin are largely driven by TC activity, with approximately 40% of warm season rainfall derived from TCs (Englehart and Douglas, 2001). These activity periods are largely associated with phases of El Niño-Southern Oscillation. In addition to El Niño phases leading to increases in non-TC rainfall regionally, the accompanying warm water and decreased vertical shear are responsible for more frequent and wetter TCs (Rodgers et al., 2000; Jauregui, 2003).

When water level at the site diminishes during dry climatic conditions, the site would be ideal for vegetation (e.g., mangroves, grasses) to develop and thrive. Peat sediments are suggestive of vegetation development and minimal water levels stemming from these dry climatic periods. Peat and peaty clay sections exhibit inter-core associations throughout the site (Figure 5.14), and are more frequent in cores 2 and 5, suggesting that these cores mark the periphery of the lagoonal environment throughout most of the backbarrier period. Peat intervals discovered during previous reconstructions at Mitla were interpreted as backbarrier mangrove swamps near sea level (Ramirez-Herrera et al., 2007). Lithogenic element concentrations are mostly low in peat sections from a lack of clastic input.

Certain elements are useful in determining marine influence or elevated salinity in sediments, mainly due to their relative abundance in seawater or marine components opposed to freshwater (Chague-Goff et al., 2002). Strontium (Sr), for example, is abundant in algae and sea shells (Bowen, 1956), and high concentrations in sediments are widely indicative of marine influence (Ramirez-Herrera et al., 2007; Woodruff et al., 2009). Other elements suggestive of marine conditions or high salinity include S, I, Ca, and Cl (Wakefield and Elderfield, 1985; Chen et al., 1997; Ramirez-Herrera et al., 2007; Nichol et al., 2007; Schofield et al., 2010). Chlorine (Cl) concentrations decrease upcore for cores 2, 4, 5, and 6, indicating an overall freshening of this site and decreased salinity over time.

5.6.3 Paleoenvironmental history

Regional Holocene sea level reconstructions are few in the literature. The nearest record comes from Nayarit state, 800 km from Mitla (Curray et al., 1969). Accordingly, seas might have been up to 10 m below present ~7000 years ago. Sea level rose rapidly during this time, transporting offshore clastics nearer the site. The rate of sea level rise decreased dramatically ~5000 years ago, with levels near present ~3000 years ago. The presence of mangrove peat throughout core 5, coupled with comparison of Nayarit's sea level record to depth of calibrated radiocarbon dates suggests that Mitla has been at or near sea level throughout the last 7000 years.

5.6.3.1 ~6900-6200 years BP

A palynological investigation of core 5 indicates that throughout zone 5, the site was a mangrove swamp dominated by *Rhizophora* and *Laguncularia* (Chapter 6). Due to the preferred environment of *Rhizophora*, Mitla was positioned near mean sea level and tidal range, which was likely 6-7 m below present (Curray et al., 1969). A lack of clastic deposition throughout the

zone indicates that the site was relatively undisturbed by marine and terrestrial processes (Figure 5.15).

5.6.3.2 ~6200-5200 years BP

Rising seas during zone 4 (Curray et al., 1969) are responsible for clay deposition in core 5, marking the beginning stage of beach ridge formation. The terrigenous elemental signal of these clays indicates that they were previously shelf sediments, accumulating on the continental shelf from erosional processes and fluvial deposition (Figure 5.16). Accelerated sea level rise

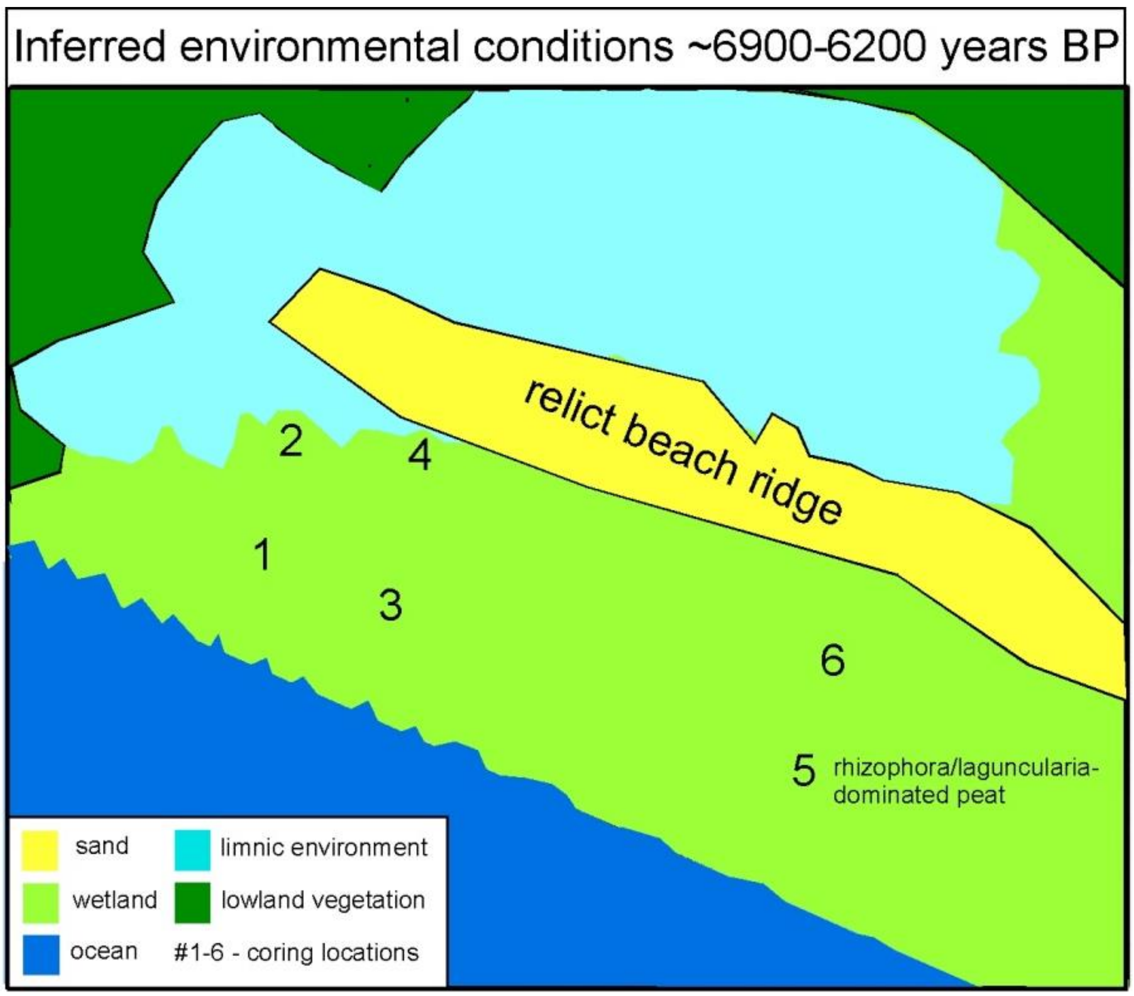

Figure 5.15 - Environmental conditions at Mitla from ~6900-6200 years BP, inferred from core 5 stratigraphy. Sea level was likely 6-7 m below present, and the site was a mangrove swamp (Chapter 6). Precipitation and runoff entering the site from the adjacent topography created a small limnic (lagoonal) environment, focused toward the landward edge of the site as water was likely trapped by the beach ridge remnant. Water level was relatively low in the limnic environment.

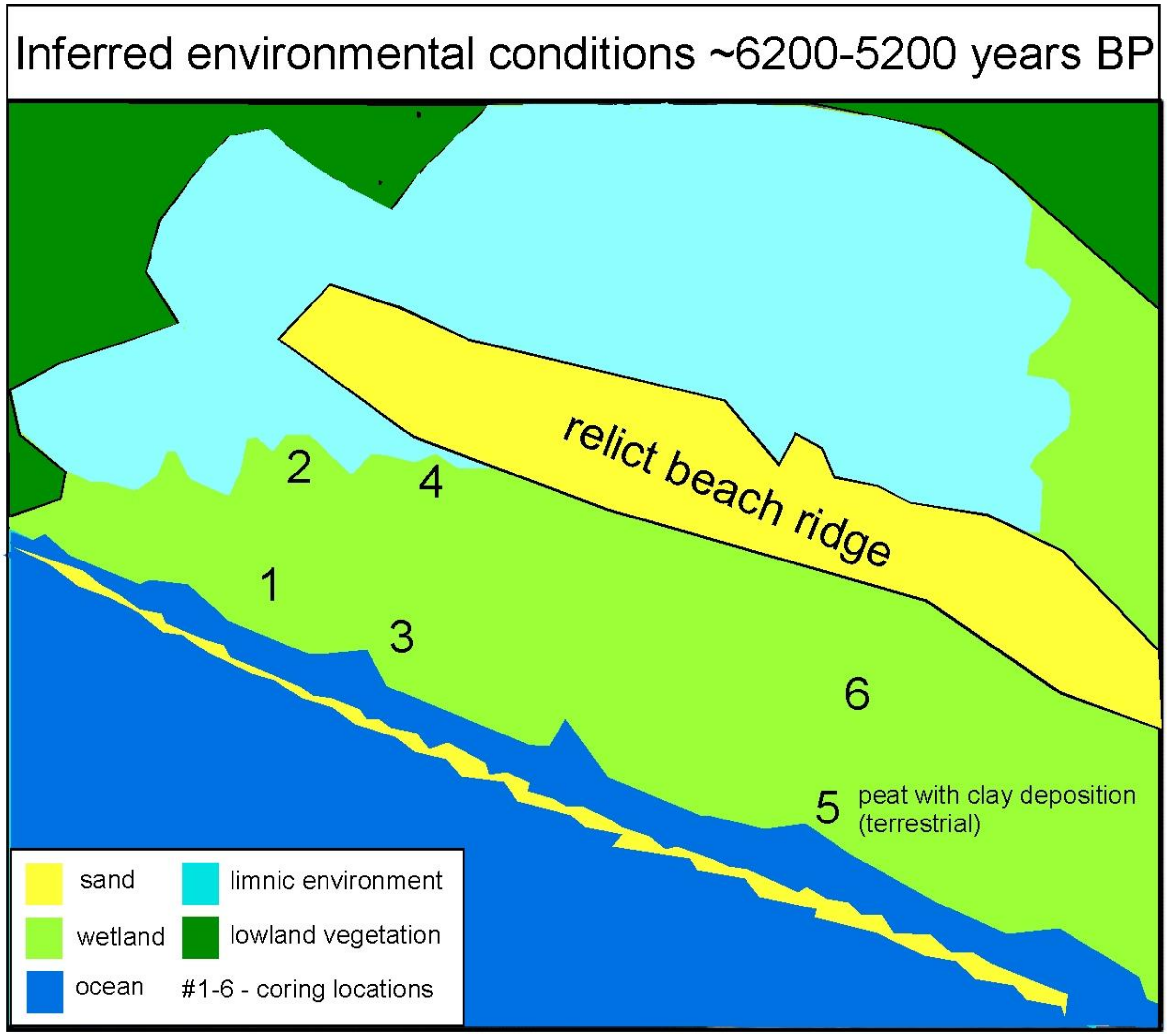

Figure 5.16 - Environmental conditions at Mitla from ~6200-5200 years BP, inferred from core 5 stratigraphy. Rapidly rising seas transport terrigenous clays into the site. Sea level rise continues to push sand from offshore closer to the site.

inundated Mitla's nearshore area ~5200 years ago, indicated from clay deposition rich in carbonate content and marine elements S, Sr, I, and Ca. After this inundation, sea level stabilized (Curray et al., 1969), signaling the beginning of beach ridge establishment and Mitla's backbarrier environment (Figure 5.17).

5.6.3.3 ~5200-4500 years BP

Peat sediments in cores 2, 3, and 5 indicate a backbarrier marsh or swamp dominating Mitla's western side (Figure 5.18). Only sporadic clay deposition in core 2 and a lack of clay in

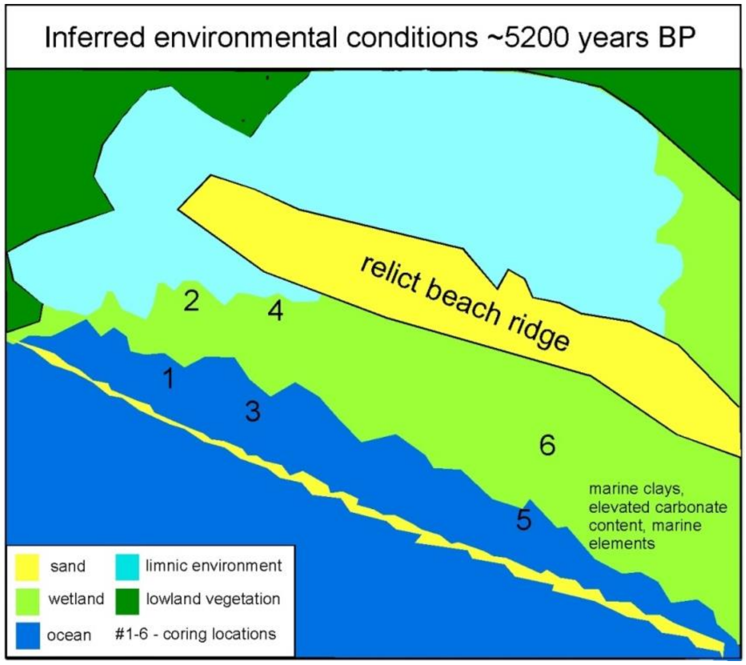

Figure 5.17 - Environmental conditions ~5200 years BP, inferred from core 5 stratigraphy. Rapidly rising seas inundate the site, transporting marine clays with elevated carbonate content into core 5.

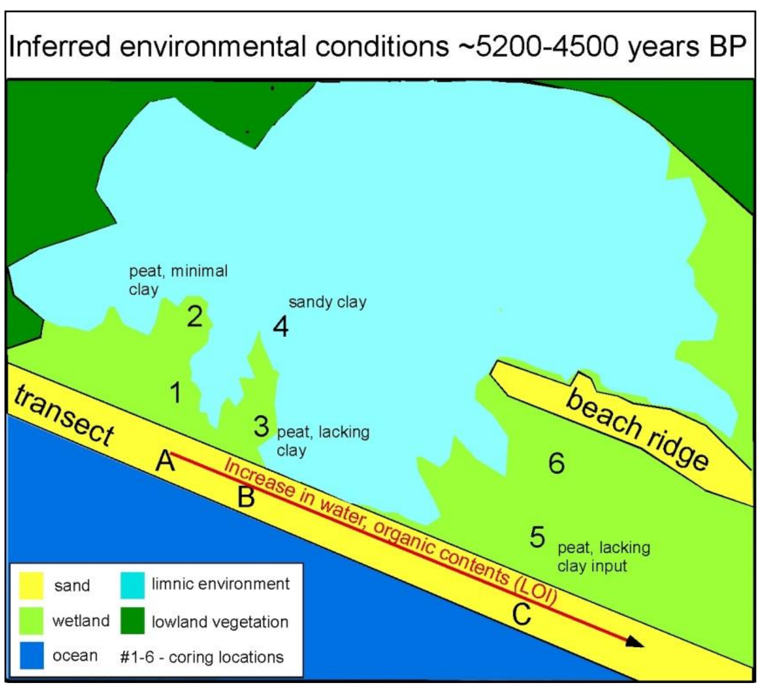

Figure 5.18 – Environmental conditions 5200-4500 years BP, inferred from stratigraphies of cores 2, 3, 4, and 5. The study sites were dominated by peat sediments, with limited clastic deposition in landward cores 2 and 4 suggesting low water level. The climate was likely dry, corresponding to paleoclimatic evidence from many upland sites during this time (e.g., Ohngemach, 1977; Arnauld et al., 1997). Beach ridge dimensions were relatively small at this time.

cores 3 and 5 suggest minimal fluvial input and low water levels, due to relatively dry conditions. Clay at the bottom of core 4 suggests that higher water levels were focused toward the northwestern end of Mitla. Localized currents aided in eroding sand from the relict beach ridge and redepositing it into the area of core 4. The elevated Cl concentrations in cores 2 and 5 suggest relatively high salinity, possibly brackish to saline conditions. Relatively arid conditions are similarly documented from paleoenvironmental reconstructions performed from highland lakes during this time period (e.g., Ohngemach, 1977). Notably, a paleoenvironmental reconstruction conducted from a highland lake in the neighboring state of Michoacan contained evidence of its lowest water level from 6000-4000 years BP (Arnauld et al., 1997).

5.6.3.4 ~4500-3200 years BP

Mitla's western side was generally a lagoonal environment throughout this time period (Figure 5.19). Cores 1, 2, 3, and 4 are dominated by lagoonal clay with elevated terrigenous

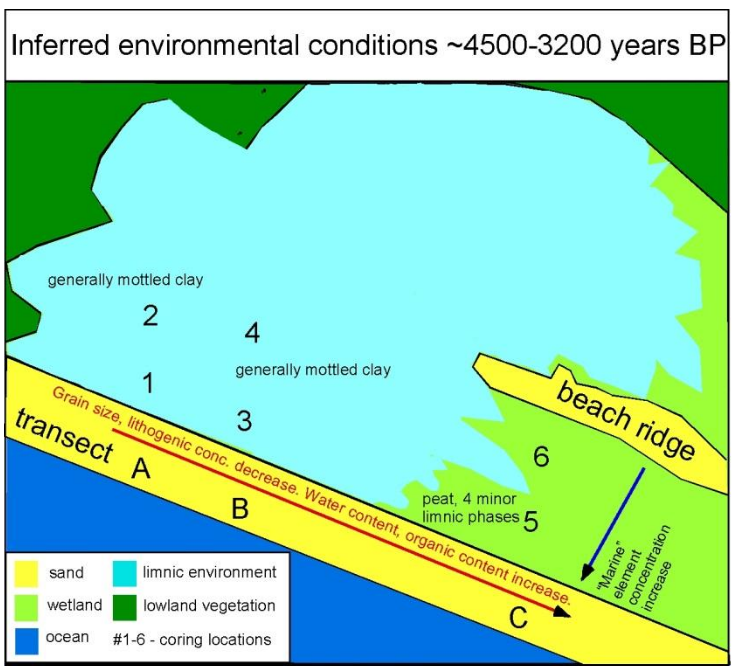

Figure 5.19– Environmental conditions from 4500-3200 years BP, inferred from stratigraphies of cores 2, 3, 4, and 5. Transect A and B cores indicate a limnic environment throughout much of Mitla's western side. Core 5 contains evidence of 4 limnic phases, suggestive of wet climatic conditions. Stable seas and sediment deposition from longshore transport cause the coastal beach ridge system to prograde.

element concentrations. Peat deposition dominates throughout zone 2 in core 5. Four clay layers (inferred 4430-4220, 4080, 3950, and 3680-3480 yr BP) with spikes in terrigenous element concentrations indicate an expansion of the spatial extent of the lagoon during a wet period. A peat section at 4270 yr BP in core 2 correlates to peat sediments in core 5, suggesting low water throughout Mitla's western side during an arid period.

Low concentrations of marine elements I, S, Ca, and Sr characterize the clay sediments from cores 2, 4, 5, and 6. However, concentration maxima exist in landward sediments, particularly sand layers in cores 4 and 6 (Figure 5.20). Similarly, surface samples collected near

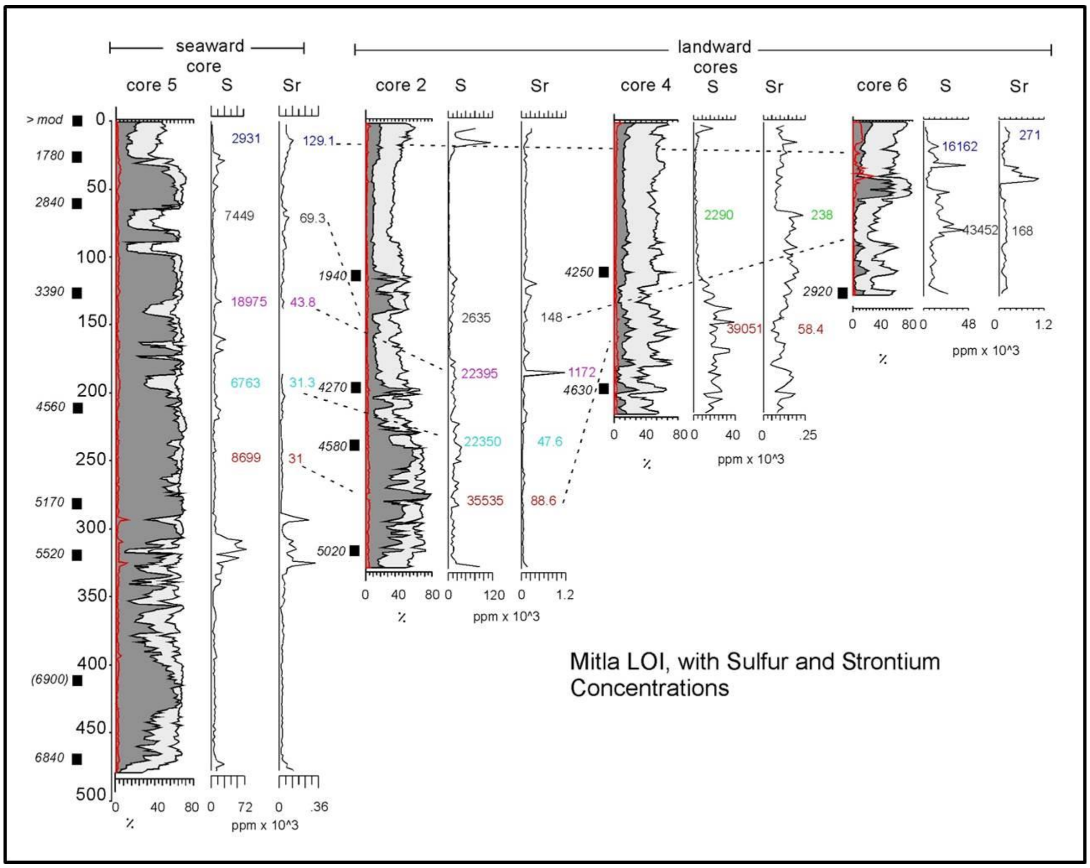

Figure 5.20 – Sulfur and strontium concentrations for cores 5, 2, 4, and 6. Numbers represent element concentrations (ppm) and are color coded to indicate possible stratigraphic correlations. Generally, landward cores 2, 4, and 6 contain higher concentrations of Sulfur and strontium than the seaward core 5. The stratigraphic section at ~60 cm (green font) for core 4 does not cross-correlate, yet indicates higher Sr concentrations in this landward core than backbarrier clay for the seaward core 5.

the relict beach ridge are higher in these elements than samples extracted near cores 1, 3, and 5. In addition, clay from the top of the landward core 6 contains higher concentrations in marine elements compared to clay near the top of the seaward core 5. The surplus in 'marine' elements from clastics in the landward cores opposed to the seaward cores suggests that material eroded from the relict beach ridge and transported toward the nearshore during low-water periods, instead of marine intrusions. A microfossil analysis of core 5 similarly indicates a lack of marine microrganisms (dinoflagellates) in this zone, suggesting a lack of marine influence (Chapter 6).

5.6.3.5 ~3200 years BP-present

Lagoonal clays dominate most of the site during the Late Holocene, suggesting wetter conditions than the previous periods (Figure 5.21). The presence of faint red clay and sand in core 6 suggests transport from the adjacent relict beach ridge during lagoonal periods. Decreasing Cl concentration upcore in cores 2, 4, 5, and 6 further indicates fresher conditions (Chague-Goff et al., 2000; Ramirez-Herrera et al., 2009).

Decreases in LOI contents are more distinct than >3200 yr BP in clay sections throughout cores 1, 2, and 5. Human activities led to land degradation in the region, well-documented during the Late Holocene throughout central and western Mexico (e.g., Heine, 1987; O'Hara et al., 1994; Berrio et al., 2006) and beginning around 3600 yr BP from nearby highland areas (e.g., Watts and Bradbury, 1982; O'Hara et al., 1993). It is suggested that land degradation increased erosion from the steep slopes adjacent to Mitla, increasing runoff and terrestrial sediment input. Land degradation throughout the Late Holocene triggered increased discharge and sediment load from a stream in nearby Oaxaca (Joyce and Mueller, 1992). Notably, sedimentation rates significantly increase during this period in cores 2 and 4.

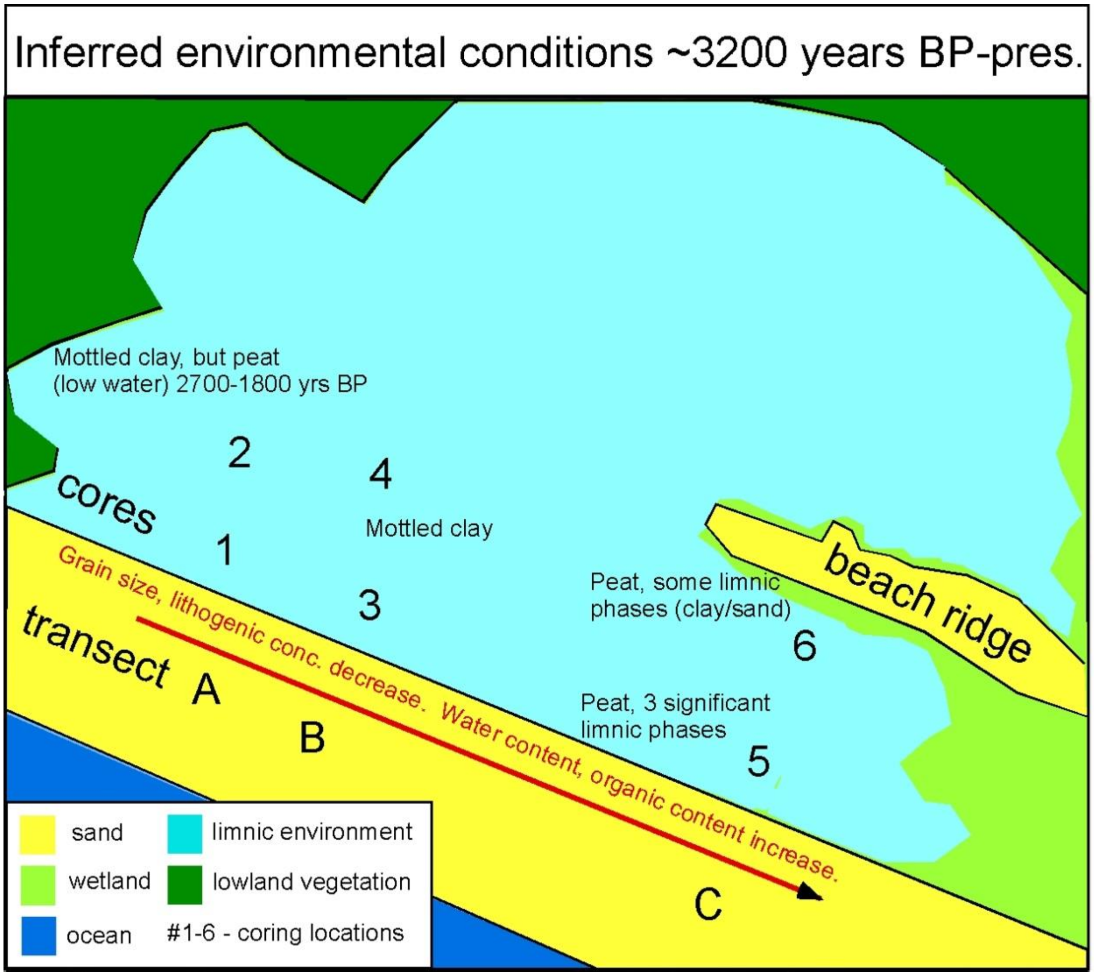

Figure 5.21 – Environmental conditions ~3200 years BP-present, inferred from cores 1-6. Transects A and B generally indicate evidence of a lagoonal environment, with the exception of organic sediments 2700-1800 years BP in core 2, indicating low water level and a dry climatic period. Core 5 contains peat with embedded clay layers, suggesting an increased extent of the lagoonal environment from wetter climatic conditions. Beach ridge progradation continues during this phase.

The predominance of clastics in the upper part of core 5 indicates increases in the extent of the lagoonal environment from wet periods during ~3170-3080, 2990-2870, and 1570 yr BP-present. Temporally, the wet periods determined from core 5 exhibit good correlation to a multi-centennial ENSO record determined from inorganic layers deposited via intensified stream discharge into Laguna Pallacacocha in Ecuador (Moy et al., 2002). The most frequent and intense El Niño periods were documented at ~1200 years BP in the Pallacacocha record, with

heightened activity also captured from ~3500-2500 years BP (Moy et al., 2002). During El Niño periods, warm ENP surface waters increase non-TC rainfall (Rodgers et al., 2000), while the low vertical shear is largely responsible for more frequent (Jauregui, 2003) and wetter (Rodgers et al., 2000) TCs. The wetter conditions coupled with the increase in TC frequency throughout these amplified El Niño periods significantly increased the precipitation and runoff entering Mitla. El Niño activity documented from Pallacacocha was amplified throughout the Late Holocene, explaining the relatively long-lasting lagoonal phases at Mitla. Alternatively, core 2 peaty clay at 2700-1800 yr BP correlates to the peat section in core 5 from 2800-1500 yr BP. This low water period suggests aridity and low TC activity. A relatively dry period from 2500-1500 years BP was determined from Laguna Tetitlan (Gonzalez-Quintero, 1980), 10 km west-northwest of Mitla.

5.6.4 Marine intrusion

Sand layers have been interpreted as indicators of TC overwash (Liu and Fearn, 1993, 2000; Kiage et al., 2011; Hawkes and Horton, 2012) and tsunami runup (Nanayama et al., 2000; Bondevik et al., 2003; Tuttle et al., 2004) in a wide variety of coastal environments. Sand layers are absent among nearshore cores 1, 3, and 5, covering a 3.5 km swath of Mitla. The absence of overwash sand can be explained by the high and wide beach ridge plain, which may have prevented barrier breaching and overwash transport, whereas the narrow (60 km) and steep (~5000 m along edge) continental shelf probably stymied significant runup and storm surge events. Pacific coast sites Laguna Boquita (Jalisco - Chapter 3), Laguna Nuxco (Guerrero – Chapter 4), and Manchon Swamp (Guatemala - Neff et al., 2006) are similarly devoid of overwash sand layers throughout their backbarrier stages. The absence of overwash sand at these sites is noteworthy, especially as extreme events, namely tsunamis, are capable of

inundation many km inland in this region of the Pacific coast (Corona and Ramirez-Herrera, 2012). In addition to overwash sand, geochemical proxies fail to reveal definitive evidence of marine intrusion throughout Mitla's backbarrier stage. Small spikes of marine element concentrations at the top of core 2 can be explained by the presence of shell fragments, eroding from the relict beach ridge at Mitla's center.

A sediment core extracted from a wetland area 5 km inland and behind Laguna Mitla contained a thick, ~100 cm sand layer rich in Sr and Ca concentrations (Ramirez-Herrera et al., 2007 - Figure 5.22). Due to the vast inundation distance required to transport these clastics noted in Ramirez-Herrera et al. (2007), this layer was attributed to a tsunami, with an inferred age of ~3400 years BP. This "marine" signature contains similarities to sand layers discovered from cores 4 and 6 in this study, notably their relatively landward location and elevated concentrations of marine elements, including Sr and Ca. The lack of sand layers in nearshore cores 1, 3, and 5, and the landward core 2 suggests that the thick layer discovered by Ramirez-Herrera et al. (2007) may be reworked material from the relict beach ridge. While the spatial extent and shape of the relict beach ridge is unknown and was not investigated during fieldwork, it is suggested that additional drowned remnants exist landward of the exposed remnants among Mitla's center. Since core 6 is located 750 m south of the relict beach ridge and contains sand layers transported into the site during periods of increased water level, it is suggested that similar processes (e.g., water level fluctuations, currents, etc) redistributed and transported this marine-rich sand into the landward locations analyzed by Ramirez-Herrera et al. (2007). It must be noted that a 3.8 m sediment core extracted just adjacent of these relict beach ridges was dominated by sand (Ramirez-Herrera et al., 2007). Thin sand layers rich in marine elements with inferred ages <2800 years BP were discovered in another wetland sediment core (Ramirez-Herrera et al.,

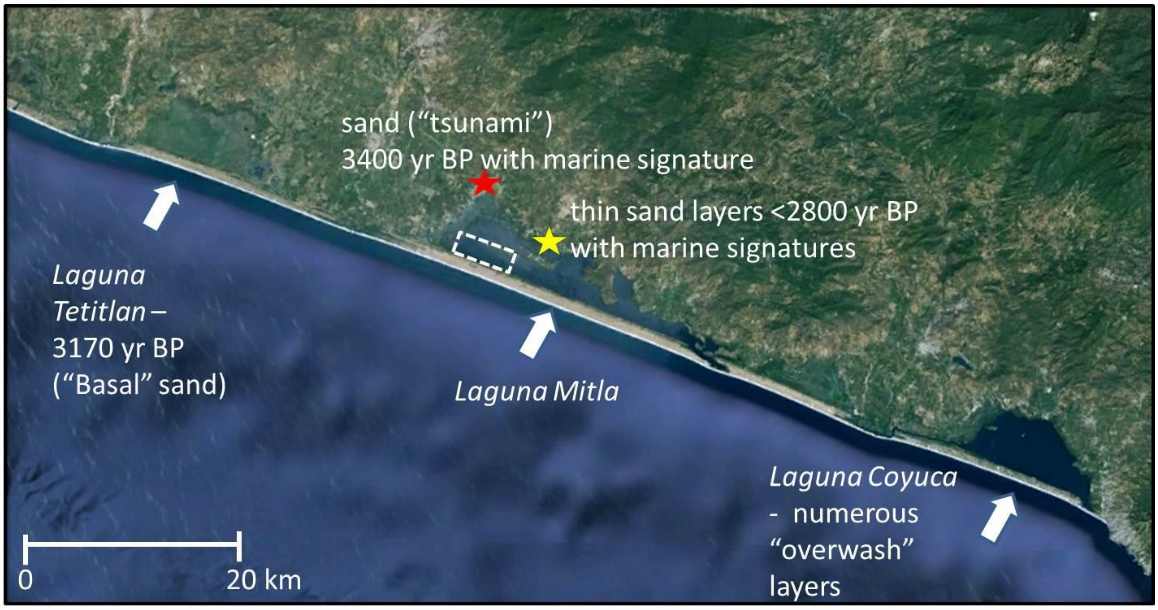

Figure 5.22 – Location of lagoons Tetitlan, Mitla, and Coyuca, all containing sand layers attributed to overwash events (Gonzalez-Quintero, 1980; Kennett et al., 2004 - cited in Ramirez-Herrera et al., 2007; Ramirez-Herrera et al., 2007, 2009). The white box located inside Laguna Mitla displays the coring area for this study. The red (Ramirez-Herrera et al., 2007) and white (Ramirez-Herrera et al., 2009) stars indicate coring locations from other studies. Thin sand layers in sediment extracted by Ramirez-Herrera et al. (2009) are not considered marine events by the authors, yet the coring location is included in this map as sand layers are coincident with peaks in marine chemical elements.

2009) extracted landward of Laguna Mitla and 3 km from the coast. Unlike the core containing sand attributed to the 3400 year BP tsunami, the core extracted 3 km from the coast did not contain a similar clastic deposit, indicating high spatial variability of sand deposition, and possibly location of remnant ridges.

Similarly, the absence of sand from the nearshore cores 1, 3, and 5 and landward core 2 pose questions regarding "marine" overwash events inferred from nearby lagoonal sediment records (Figure 5.23). These sedimentary evidences include basal sand dated to 3170 yr BP from Laguna Tetitlan (Gonzalez-Quintero, 1980), along with numerous sand layers and a buried shell midden, dated to ~3000 yr BP from Laguna Coyuca (Kennett et al., 2004 – cited in Ramirez-Herrera et al., 2007), both within 20 km of Mitla. Shell middens are generally viewed as waste

remnants resultant from meals eaten by nomadic groups (e.g., Kennett and Voorhies, 1996). The ~3000 year date roughly coincides with human migration into this region, documented from charcoal concentrations at Laguna Mitla (Chapter 6) and pollen evidence marking agricultural practices in the Michoacan highlands (Watts and Bradbury, 1982). The precise coring location at these sites and their proximity to relict beach ridge remnants could not be determined. It must be noted that these sites share many similarities to Mitla, most notably formation histories and beach ridge dimensions (Lankford, 1977). It is imperative that clastic source and depositional pattern in Pacific coast lagoons is investigated through multiple cores covering a vast area, not reliant on a single core. In addition to erosion and resuspension from relict beach remnants, additional mechanisms capable of sand deposition in Pacific coast lagoons can include tidal inlet dynamics (Lankford, 1977) and aeolian transport (e.g., Tamura, 2012). Sediment extracted from Mitla's nearshore mangrove swamp was comprised mostly of sand (Ramirez-Herrera et al., 2007), possibly from erosional processes.

Alternatively, extreme event deposition has been reported from sites along Mexico's Pacific coast, but their geomorphological settings are different from that of Mitla. Marine shells found in the sediment cores from Laguna Pastoria in Oaxaca have been interpreted to be deposited by TCs during its bay phase, prior to Late Holocene beach ridge formation (Goman et al., 2005). Sediment profiles extracted 120 km west-northwest of Mitla and only tens of meters landward of the coastal beach ridge were found to contain sand deposits attributed to the 1979 and 1985 tsunamis (Ramirez-Herrera et al., 2012). However, this study region is also prone to event deposition attributable to hurricanes paralleling the coast, including category 2 Hurricanes Andres (1979) and Odile (1984). Therefore, the sedimentary record must be carefully examined to avoid incorrect identification of the origin of the extreme event. Duplicating this methodology

throughout the coast could facilitate comparisons between tsunami and TC deposition, ideal for coastal risk assessment.

5.7 Summary and conclusion

This chapter presented a multi-core paleoenvironmental reconstruction from Laguna Mitla on Mexico's Pacific coast. The main objective was to reconstruct a multi-centennial paleoenvironmental history of coastal environmental changes, with the aim of finding paleoevidence of TCs to produce a long-term record of TC activity. Six sediment cores were extracted in three shore-perpendicular transects from the western part of the lagoon, the longest providing a ~6900 year record. At ~6900 years BP, Mitla was a marsh or swamp environment positioned near sea level. Rising seas aided clastic deposition into the site, initiating the construction of the coastal beach ridge system. Mitla's backbarrier environment was formed ~5200 years ago during a time of stable sea level. Cores from Mitla's western side were dominated by peat high in Cl, indicating a brackish or saline marsh/swamp and low water level until ~4500 years BP, a time when peat changed to lacustrine clay throughout much of the site, indicating a transition to a limnic environment. Four distinct lacustrine episodes during 4500-3200 yr BP exhibited by brown to gray layers and peaks in terrigenous elements captured in core 5 suggest increased water level, implying a wet climate. The increased precipitation may be attributed to an increase in ENSO frequency and TC activity. Amplified ENSO activity after 3200 yr BP resulted in a wetter climate, encouraging three periods of expanded lagoonal phases and high lake levels (3170-3080, 2990-2870, and 1570 yr BP-present). Human activities and earthquakes might have intensified soil erosion and land degradation upstream from Mitla (e.g., O'Hara et al., 1994; Carroll and Bohacs, 1999; Berrio et al., 2006), affecting the amounts of runoff and stream input entering the site.

Previous work at Laguna Mitla reported the discovery of sand layers rich in marine chemical elements at locations up to 5 km inland from the coast, with a thick sand deposit interpreted to indicate the occurrence of a tsunami 3400 years ago. However, sand was completely absent from our cores taken in nearshore locations, suggesting that the sand reported in previous studies was not brought by seawater invading from the ocean. Indeed, sand layers containing marine chemical signatures are only found from cores taken near the elongated island in the middle of the lagoon, suggesting that the sand was likely reworked material derived from wave erosion of the relict beach ridge. Results from this study therefore do not support the reconstruction of a tsunami event at this site 3400 years ago. Previously documented overwash signatures from nearby lagoons with similar dimensions and morphologies are similarly called into question. This research has significant implications for hazard assessment for the Pacific coastal regions of Mexico.

5.8 References

Arnauld, C., S. E. Metcalfe, and P. Petrequin. 1997. Holocene climatic change in the Zacapu lake basin, Michoacan: Synthesis of results. Quaternary International **43-4**:173-179.

Berrio, J. C., H. Hooghiemstra, B. van Geel, and B. Ludlow-Wiechers. 2006. Environmental history of the dry forest biome of Guerrero, Mexico, and human impact during the last c. 2700 years. Holocene **16**:63-80.

Bondevik, S., J. Mangerud, S. Dawson, A. Dawson, and O. Lohne. 2003. Record-breaking height for 8000-year-old tsunami in the North Atlantic. EOS, Transactions, American Geophysical Union **84**:289-300.

Bowen, H. J. M. 1956. Strontium and barium in seawater and marine organisms. Journal of the Marine Biological Association of the United Kingdom **35**:451-460.

Bradbury, J. P. 2000. Limnologic history of Lago de Patzcuaro, Michoacan, Mexico for the past 48,000 years: Impacts of climate and man. Palaeogeography Palaeoclimatology Palaeoecology **163**:69-95.

Brenner, L. and A. G. Aguilar. 2002. Luxury tourism and regional economic development in Mexico. The Professional Geographer **54**:500-520.

Bullock, S. H. 1986. Climate of Chamela, Jalisco, and trends in the South coastal region of Mexico. Archives for Meteorology Geophysics and Bioclimatology Series B-Theoretical and Applied Climatology **36**:297-316.

Carroll, A. R. and K. M. Bohacs. 1999. Stratigraphic classification of ancient takes: Balancing tectonic and climatic controls. Geology **27**:99-102.

Chague-Goff, C., S. L. Nichol, A. V. Jenkinson, and H. Heijnis. 2000. Signatures of natural catastrophic events and anthropogenic impact in an estuarine environment, New Zealand. Marine Geology **167**:285-301.

Chague-Goff, C., S. Dawson, J. R. Goff, J. Zachariasen, K. R. Berryman, D. L. Garnett, H. M. Waldron, and D. C. Mildenhall. 2002. A tsunami (ca. 6300 years BP) and other Holocene environmental changes, northern Hawke's Bay, New Zealand. Sedimentary Geology **150**:89-102.

Chen, Z., Z. Chen, and W. Zhang. 1997. Quaternary stratigraphy and trace-element indices of the Yangtze Delta, eastern China, with special reference to marine transgressions. Quaternary Research **47**:181-191.

Contreras-Espinosa, F. 1993. Ecosistemas costeros Mexicanos. UNAM-CANABIO, Mexico, D.F.

Contreras-Espinosa, F. and B. G. Warner. 2004. Ecosystem characteristics and management considerations for coastal wetlands in Mexico. Hydrobiologia **511**:233-245.

Corona, N. and M. T. Ramirez-Herrera. 2012. Mapping and historical reconstruction of the great Mexican 22 June 1932 tsunami. Natural Hazards and Earth System Sciences **12**:1337-1352.

Curray, F., J. Emmel, and P. J. Crampton. 1969. Holocene history of a strand plain lagoonal coast, Nayarit, Mexico. Pages 63-100 *in* A. Ayala-Castanares, editor. Coastal Lagoons: A Symposium. Universidad Nacional Autonoma de Mexico Mexico City.

Dean, W. E. 1974. Determination of carbonate and organic matter in calcareous sediments and sedimentary rocks by loss on ignition: comparison with other methods. Journal of Sedimentary Petrology **44**:242-248.

Englehart, P. J. and A. V. Douglas. 2001. The role of eastern North Pacific tropical storms in the rainfall climatology of western Mexico. International Journal of Climatology **21**:1357-1370.

Goman, M., A. Joyce, and R. Mueller. 2005. Stratigraphic evidence for anthropogenically induced coastal environmental change from Oaxaca, Mexico. Quaternary Research **63**:250-260.

Gonzalez-Quintero, L. 1980. Paleoecologia de un sector costero de Guerrero, Mexico (3000 anos). Memorias **86**:133-157.

Hawkes, A. D. and B. Horton, P. 2012. Sedimentary record of storm deposits from Hurricane Ike, Galveston and San Luis Islands, Texas. Geomorphology **171-172**:180-189.

Heine, K. 1987. Anthropogenic sedimentological changes during the Holocene in Mexico and Central America. Striae: A monograph series for Quaternary studies **26**:51-63.

Jakobsson, M., R. Løvlie, H. Al-Hanbali, E. Arnold, J. Backman, and M. Mörth. 2000. Manganese and color cycles in Arctic Ocean sediments constrain Pleistocene chronology. Geology **28**:23-26.

Jauregui, E. 2003. Climatology of landfalling hurricanes and tropical storms in Mexico. Atmosfera **16**:193-204.

Jonathan, M. P., P. D. Roy, J. L. Sanchez-Zavala, S. Srinivasalu, M. C. Macias-Romo, and C. Lakshumanan. 2011. Field survey report on the 11th March 2011 tsunami in Pacific coast of Mexico. Natural Hazards **58**:859-864.

Joyce, A. A. and R. G. Mueller. 1992. The social impact of anthropogenic landscape modification in the Rio Verde drainage basin, Oaxaca, Mexico. Geoarcheology **7**:503-526.

Kennett, D. J. and B. Voorheis. 1996. Oxygen isotopic analysis of archeological shells to detect seasonal use of wetlands on the Southern Pacific Coast of Mexico. Journal of Archaeological Science **23**:689-704.

Kennett, D. J., B. Voorheis, J. Iriarte, J. G. Jones, D. Piperno, M. T. Ramirez-Herrera, and T. A. Wake. 2004. Avances en el proyecto Arcaico-Formativo: Costa de Guerrero. Instituto Nacional de Antropologia e Historia, Mexico.

Kiage, L. M., D. Deocampo, T. A. McCloskey, T. A. Bianchette, and M. Hursey. 2011. A 1900-year paleohurricane record from Wassaw Island, Georgia, USA. Journal of Quaternary Science **26**:714-722.

Lankford, R. R. 1977. Coastal lagoons of Mexico: Their origin and classification. Pages 182-215 *in* M. Wiley, editor. Estuarine Processes. Academic Press Inc.

Lawrence, M. B. 1999. Eastern North Pacific hurricane season of 1997. Monthly Weather Review **127**:2440-2454.

Liu, K. B. and M. L. Fearn. 1993. Lake-sediment record of Late Holocene hurricane activities from coastal Alabama. Geology **21**:793-796.

Liu, K. B. and M. L. Fearn. 2000. Reconstruction of prehistoric landfall frequencies of catastrophic hurricanes in northwestern Florida from lake sediment records. Quaternary Research **54**:238-245.

Matias-Ramirez, L. G. 1998. Algunos efectos de la precipitacion del Huracan Paulina en Acapulco, Guerrero. Investigaciones Geographicas **37**:7-19.

Moy, C. M., G. O. Seltzer, D. T. Rodbell, and D. M. Anderson. 2002. Variability of El Niño/Southern Oscillation activity at millennial timescales during the Holocene epoch. Nature **420**:162-165.

Nanayama, F., K. Shigeno, K. Satake, K. Shimokawa, S. Koitabashi, S. Miyasaka, and M. Ishii. 2000. Sedimentary differences between the 1993 Hokkaido-nansei-oki tsunami and the 1959 Miyakojima typhoon at Taisei, southwestern Hokkaido, northern Japan. Sedimentary Geology **135**:255-264.

National Geophysical Data Center. 2011. Global Historical Tsunami Database.

National Oceanic and Atmospheric Administration. 2011. Historical hurricane tracks. Retrieved 12-29-2011, from http://www.csc.noaa.gov/hurricanes/.

Neff, H., D. M. Pearsall, J. G. Jones, B. A. de Pieters, and D. E. Freidel. 2006. Climate change and population history in the Pacific Lowlands of Southern Mesoamerica. Quaternary Research **65**:390-400.

Nichol, S. L., C. Chague-Goff, J. R. Goff, M. Horrocks, B. G. McFadgen, and L. C. Strotz. 2007. Geomorphology and accommodation factors on tsunami deposition: Chatham Island, Southwest Pacific Ocean. Sedimentary Geology **229**:41-52.

O'Hara, S. L., S. E. Metcalfe, and F. A. Streetperrott. 1994. On the arid margin - The relationship between climate, humans and the environment - A review of evidence from the highlands of Central Mexico. Chemosphere **29**:965-981.

O'Hara, S. L., F. A. Street-Perrott, and T. P. Burt. 1993. Accelerated soil erosion around a Mexican highland lake caused by prehispanic agriculture. Nature **362**:48-51.

Ohngemach, D. 1977. Pollen sequence of the Tlaqua crater (La Malinche Volcano, Tlaxcala, Mexico). Boletin de la Sociedad Botanica de Mexico **36**:33-44.

Paez-Osuna, F. and E. F. Mandelli. 1985. ^{210}Pb in a tropical coastal lagoon sediment core. Estuarine, Coastal, and Shelf Science **20**:367-374.

Ramirez-Herrera, M. T., A. Cundy, V. Kostoglodov, A. Carranza-Edwards, E. Morales, and S. Metcalfe. 2007. Sedimentary record of late-Holocene relative sea-level change and tectonic deformation from the Guerrero Seismic Gap, Mexican Pacific Coast. Holocene **17**:1211-1220.

Ramirez-Herrera, M. T., A. B. Cundy, V. Kostoglodov, and M. Ortiz. 2009. Late Holocene tectonic land-level changes and tsunamis at Mitla lagoon, Guerrero, Mexico. Geofisica Internacional **48**:195-209.

Ramirez-Herrera, M. T., V. Kostoglodov, and J. Urrutia-Fucugauchi. 2011. Overview of recent coastal tectonic deformation in the Mexican subduction zone. Pure and Applied Geophysics **168**:1415-1433.

Ramirez-Herrera, M. T., M. Lagos, I. Hutchinson, V. Kostoglodov, M. L. Machain, M. Caballero, A. Goguitchaichvili, B. Aguilar, C. Chague-Goff, J. Goff, A.-C. Ruiz-Fernandez, M. Ortiz, H. Nava, F. Bautista, G. I. Lopez, and P. Quintana. 2012. Extreme wave deposits on the Pacific coast of Mexico: Tsunamis or storms? - A multi-proxy approach. Geomorphology **139**:360-371.

Ramirez-Herrera, M. T. and J. Urrutia-Fucugauchi. 1999. Morphotectonic zones along the coast of the Pacific continental margin, southern Mexico. Geomorphology **28**:237-250.

Rodgers, E. B., R. F. Adler, and H. F. Pierce. 2000. Contribution of tropical cyclones to the North Pacific climatological rainfall as observed from satellites. Journal of Applied Meteorology **39**:1658-1678.

Sanson, L. Z. 2004. The mechanical influence of continental topography on the trajectories of tropical cyclones near the west coast of Mexico. Atmosfera **17**:151-170.

Schofield, J. E., K. J. Edwards, T. M. Mighall, A. Martinez Cortizas, J. Rodriguez-Racedo, and G. Cook. 2010. An integrated geochemical and palynological study of human impacts, soil erosion and storminess from southern Greenland since c. AD 1000. Palaeogeography Palaeoclimatology Palaeoecology **295**:19-30.

Spang, R. M., S. H. Castaneda, and E. M. Gomez. 2003. Hurricane Pauline - its impact on Acapulco and subsequent debris flow prevention measures. *in* Proc. 3rd Int. Conf. Debris Hazards Mitigation, Davos, Switzerland.

Stuiver, M., P. J. Reimer, and R. W. Reimer. 2005. CALIB 6.0 (program and documentation).

Tamura, T. 2012. Beach ridges and prograded beach deposits as palaeoenvironment records. Earth-Science Reviews **114**:279-297.

Thom, B. G. 1967. Mangrove ecology and deltaic geomorphology: Tabasco, Mexico. Journal of Ecology **55**:301-343.

Tuttle, M. P., A. Ruffman, T. Anderson, and H. Jeter. 2004. Distinguishing tsunami from storm deposits in eastern North America: The 1929 grand banks tsunami versus the 1991 Halloween storm. Seismological Research Letters **75**:117-131.

Voorheis, B. 2004. Coastal Collectors in the Holocene: The Chantuto People of Southwest Mexico. University Press of Florida.

Wakefield, S. J. and H. Elderfield. 1985. Interstital water iodine enrichments from the eastern Pacific. Journal of Marine Research **43**:951-961.

Watts, W. A. and J. P. Bradbury. 1982. Paleoecological studies at Lake Patzcuaro on the west-central Mexican Plateau and at Chalco in the Basin of Mexico. Quaternary Research **17**:56-70.

Weltje, G. J. and H. von Eynatten. 2004. Quantitative provenance analysis of sediments: review and outlook. Sedimentary Geology **171**:1-11.

Woodruff, J. D., J. P. Donnelly, and A. Okusu. 2009. Exploring typhoon variability over the mid-to-late Holocene: evidence of extreme coastal flooding from Kamikoshiki, Japan. Quaternary Science Reviews **28**:1774-1785.

Yanez-Arancibia, A. 1977. Taxonomia, ecologia y estructura de las comunidades de peces en lagunas costeras con bocas efimeras del Pacifico de Mexico. Annual Meeting of the American Society of Limnology and Oceanography, Savannah, Georgia, USA.

CHAPTER 6. A 6900 YEAR MULTI-PROXY PALEOENVIRONMENTAL RECONSTRUCTION FROM LAGUNA MITLA ON MEXICO'S PACIFIC COAST

6.1 Introduction

Mexico's Pacific coast is vulnerable to both human-induced and natural environmental stresses. These pressures are exacerbated by land degradation stemming from increased urbanization around the many resort centers. As the regional economy is largely tourism-based, vulnerability and response to stressors including extreme climate change, drought, and coastal erosion are pertinent topics that must be addressed in the future. Notably, this region is battered annually by an assortment of extreme events, including tropical cyclones (TCs) and tsunamis, both capable of catastrophic geophysical and societal damage. This was recently evidenced by Hurricane Pauline (1997), for example. Only a category 1 hurricane approaching the resort town Acapulco, Pauline dumped over 400 mm of precipitation (Lawrence, 1999), resulting in 300 million pesos (>22 million USD) in damage and over 200 deaths (Matias-Ramirez, 1998). Strong winds and heavy rains engulfed Acapulco as mudslides washed gravel and boulders down inland hills toward the coast (Spang et al., 2003). Meanwhile, Pauline's 9-m storm surge inundated beaches, creating impressive overwash fans in the coastal state of Oaxaca (Goman et al., 2005).

Ultimately, a paleoenvironmental reconstruction of this region must be conducted to determine any long-term vulnerability to environmental stresses. Coastal lakes, lagoons, and marshes have proven ideal for such reconstructions. With 485 km of coastal wetland covering 22,700 ha (Contreras-Espinosa and Warner, 2004) including tens of water bodies, the Pacific coastal state of Guerrero contains a plethora of areas to determine for paleoenvironmental reconstruction. Necessity for coastal research is heightened due to the dearth of paleoenvironmental reconstructions in Guerrero and its neighboring states.

Six cores had been collected from an inactive portion of Laguna Mitla, a large coastal water body near Acapulco, to determine site dynamics and uncover evidence of extreme event-induced marine intrusion. Unlike cores extracted from the western section of Mitla, a nearshore core (5) closer to the lagoon's middle section is mostly peat with numerous clay layers embedded, deemed ideal for a more detailed, multi-proxy (sedimentological, geochemical, microfossil) examination. Analysis can examine the paleoenvironment further by providing additional information on paleoclimate, human disturbance, and extreme event-induced marine intrusion.

This chapter presents a multi-proxy paleoenvironmental reconstruction for core 5 from Laguna Mitla. The objectives are threefold. Firstly, the paleoenvironmental history is reconstructed to assess whether factors including climate change, extreme events, or human disturbance play a major role in Mitla's geological development and sedimentary record. Ecological and geomorphological changes are also noted. Secondly, the lagoon's sensitivity to extreme event deposition is further assessed, especially with regard to the presence of any marine intrusion. Finally, as TCs remain a central focus of this research, a major aim is to determine activity periods through analyzing the site's paleoclimatic and paleoenvironmental histories.

6.2 Study area

Coastal Guerrero is wedged between the Sierra Madre del Sur mountains and Pacific Ocean. Rivers and ephemeral streams flow from the hills toward the ocean. The climate is semi-arid and monsoonal with a rainy season from May to November, which coincides with the TC activity regimes. Coastal precipitation is ~1300 mm/yr (Bullock, 1986), increasing inland. The oceanic Cocos plate subducts under the North American plate along the Middle America Trench on the outskirts of the narrow continental shelf, 70 km west-southwest of Mitla. Rocky

cliffs and elevated terraces indicating paleo-uplift line the majority of Guerrero's coast (Ramirez-Herrera et al., 2011).

Laguna Mitla (17.0474º N, 100.3342º W) is located 40 km west-northwest of Acapulco on Guerrero's central coast (Figure 6.1). It is 22 x 4 km in size with water depth 0.5-1.0 m in its western part. A small, ephemeral stream enters Mitla from the northwest corner. This stream is approximately 15 m wide at its widest point, and can be traced uphill to the small town of San Francisco, 20 km inland of Mitla. Mitla contains a tidal inlet at its eastern end but it was artificially closed in 1968 (Yanez-Arancibia, 1977). Salinity is low, at ~3.5 ppt (Contreras-Espinosa and Warner, 2004). Shells *Bittium sp*., *Mytella strigata*, *Triphora sp*., and *Amnicola sp*. (Yanez-Arancibia, 1977; Contreras-Espinosa, 1993) are common on Mitla's floor. Mangroves (*Rhizophora mangle, Avicennia nitida*, *Laguncularia racemosa*) surround the lagoon with *Typha* patches along the edges. Rocky cliffs and elevated terraces are non-existent near Mitla. The presence of alluvial and deltaic plains near Mitla suggests a tectonically stable environment (Ramirez-Herrera and Urrutia-Fucugauchi, 1999). Minimal subsidence has been documented throughout the last few decades at the site (Ramirez-Herrera et al., 2007). This area experiences a semi-diurnal tide, and is considered micro-tidal (<1.0 m range) (Lankford, 1977).

Mitla is formally classified as a "barred inner shelf" lagoon (Lankford, 1977). Formerly a depression along the edge of the continental shelf, Mitla became inundated during a mid-Holocene marine transgression, later protected by beach ridges developing when seas stabilized (Lankford, 1977). Beach ridges are 900 m wide, with recent developments including dirt roads, farms, and small cottages. Seaward of the beach ridges is a narrow beach of low relief. A relict beach ridge near Mitla's center was likely deposited from a Pleistocene sea level highstand, with similar features discovered throughout coastal Mexico (e.g., Thom, 1967; Lankford, 1977).

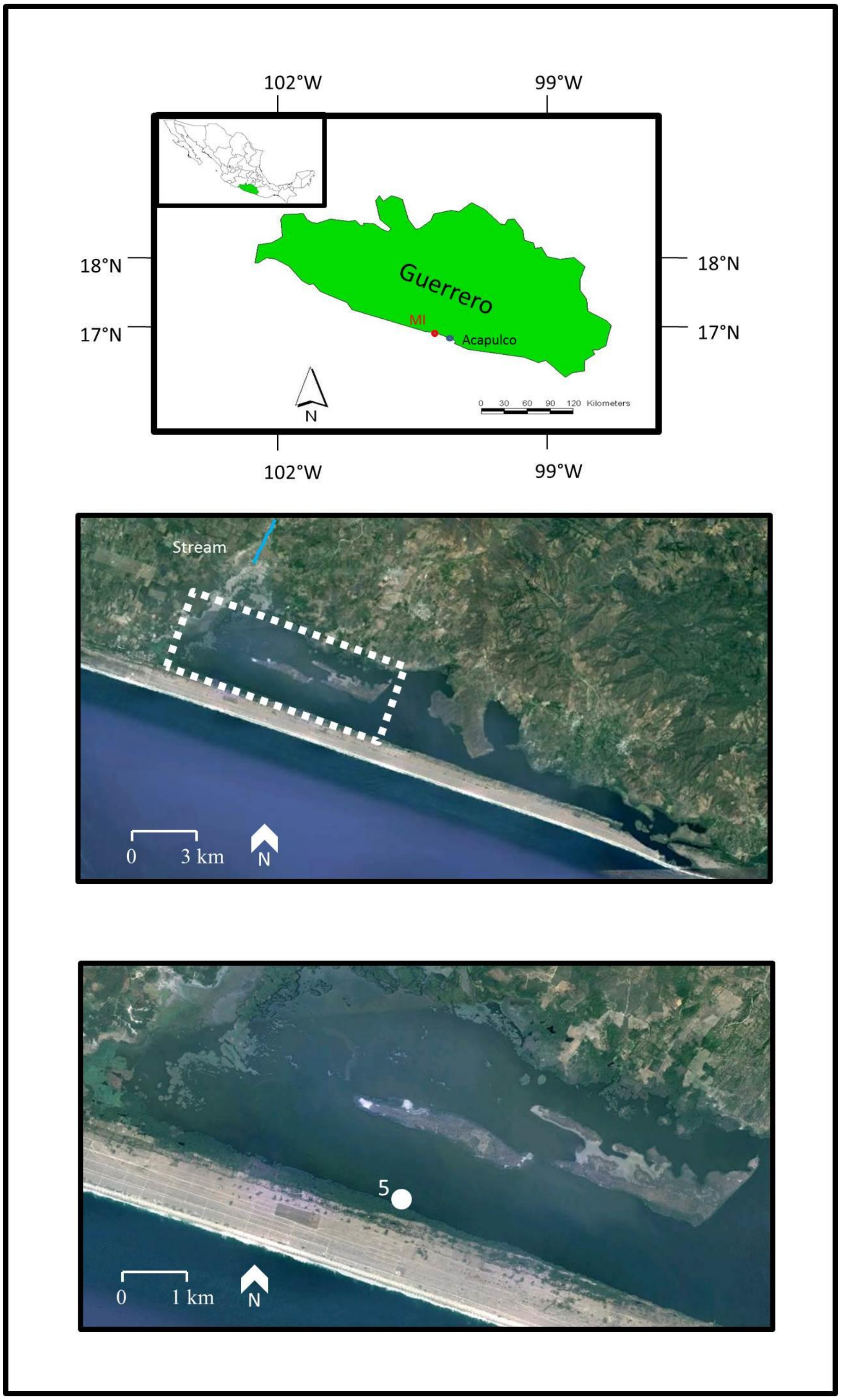

Figure 6.1 – Guerrero state, with Laguna Mitla (MI) location labeled (top). Laguna Mitla is shown in its entirety (middle) with the western area subset and core 5 location displayed (bottom). The ephemeral stream along Mitla's northwestern corner is highlighted in blue.

6.3 History and geophysical impacts of extreme events

TC cyclogenesis generally originate southeast of Guerrero, and just west of Guatemala. TCs travel west to northwest, often paralleling the coast as the Sierra Madre mountains create a barrier preventing most direct landfalls (Sanson, 2004). Twenty-two hurricanes have traveled within 200 km of Mitla since 1949 (Figure 6.2). Shell hash found toward Mitla's center was attributed to Hurricane Tara's (1961) impact (Paez-Osuna and Mandelli, 1985) although its origin has not been confirmed. Geophysical impacts from other TCs are undocumented at Mitla and vicinity. Residents assert that TC storm surge has not breached the beach ridges or

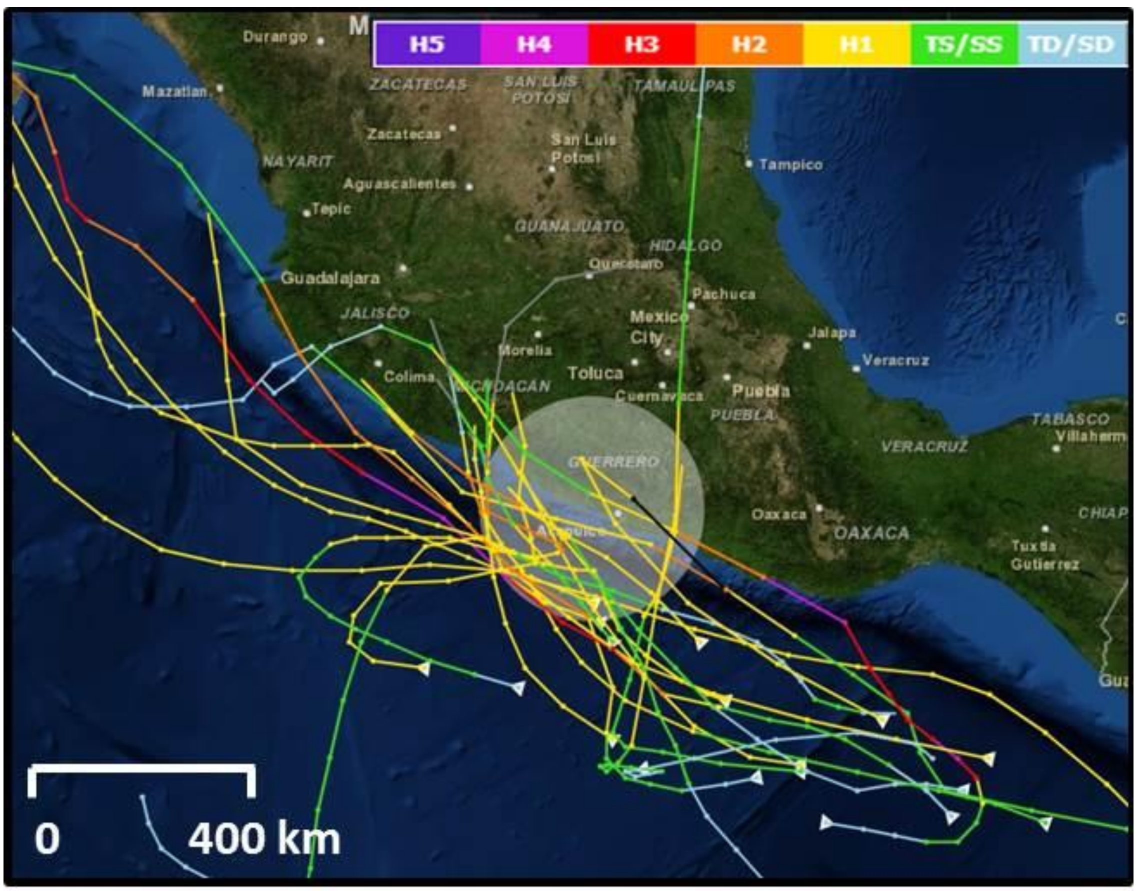

Figure 6.2 – Twenty-two hurricanes passed within 200 km (gray circle) of Laguna Mitla from 1949-2010. Most tracks parallel the coast at tropical storm (green) or category 1 (yellow) intensity (National Oceanic and Atmospheric Administration, 2011).

inundated Mitla during the historical period. Significant mudslides from heavy or lingering precipitation have not occurred during recent times.

Nine tsunamis with maximum water height ≥2 m have occurred in Guerrero since 1732 (National Geophysical Data Center). Often inundating many km inland (Corona and Ramirez-Herrera, 2012), geomorphological effects of recent tsunamis are minimal (Jonathan et al., 2011), according to local residents.

6.4 Methodology

Field expedition occurred during the dry season (December) of 2009. Core 5 was extracted from the western, seaward edge with a Russian peat borer, yielding twelve ~50 cm core segments. A ~10 cm overlap was measured for each subsequent core segment to account for coretop disturbance. Sediments were transferred to pre-cut PVC tubes and wrapped with plastic film and duct tape to prevent moisture loss. Core 5 was transported to the Global Change and Coastal Paleoecology Laboratory at Louisiana State University, later stored in a 4ºC refrigerated room.

Core 5 was analyzed soon after arrival to ensure preservation. A litholog was sketched with the aid of a Munsell soil color chart. Loss-on ignition (LOI) (Dean, 1974) was administered at 1 cm resolution to determine water, organic, and carbonate contents. Nine macrofossil samples were sieved and rinsed in de-ionized water, later sent to the National Ocean Sciences Accelerator Mass Spectometry (NOSAMS) laboratory at Woods Hole Oceanographic Institution for radiocarbon dating. Output was converted to median probability calendar years using Calib 6.0 and the INTCAL 09 curve (Stuiver et al., 2005), rounded to the nearest decade. Sedimentation rates were calculated between each pair of calibrated radiocarbon dates using linear interpolation, with rates estimated to the core top and bottom by extrapolation.

Core 5 was covered with plastic film and scanned directly with a Delta Innov-X handheld X-ray fluorescence (XRF) unit with a tantalum X-ray tube and two-cm resolution window to determine chemical composition. Light and heavy elements were detected with three laser beams using 15 and 40 kilovolt excitation. Core 5 was scanned "wet" to limit sediment extraction or other disturbance to the core. A XRF analysis of both wet and dry samples reveals similar elemental output (Stallard et al., 1995). Elements with low concentrations and/or sporadic patterns were eliminated from output.

Forty-eight samples at ~10 cm intervals were processed for pollen and microfossils following guidelines of Faegri and Iversen (1989). Up to two lycopodium spores were added to each sample to determine pollen concentration. Processed samples were mounted on microscopic slides and examined for pollen at 40X magnification with a Moticam digital biological microscope. At least 300 pollen grains were counted for each sample. Reference slides were provided by the Global Change and Coastal Paleoecology Laboratory at Louisiana State University. Pollen reference books and databases from Mexico and other regions were consulted to aid identification (Gonzalez-Quintero, 1969; Huang, 1972; Bartlett and Barghoorn, 1973; McAndrews et al., 1973; Markgraf and D'Antoni, 1978; Villanueva-G., 1984; Lozano-Garcia and Hernandez, 1990; Palacios-Chavez et al., 1991; Roubik and Moreno, 1991; Herrera and Urrego, 1996; Colinvaux et al., 1999; Willard et al., 2004; Bush and Weng, 2006). Fungal spores were identified using many guides (Jarzen and Elsik, 1986; van Geel, 1986, 2001; Ellis and Ellis, 1988; van Geel et al., 2003, 2011; Chmura et al., 2006; McAndrews and Turton, 2010) and grouped using terminology in Gelorini et al. (2011). Charcoal fragments > 10 µm were counted following methodology from Liu et al. (2008).

6.5 Results

6.5.1 Lithology, LOI, XRF

Core 5 (479 cm) mostly consists of dark muddy peat (7.5 YR, 3/2) high in water (~85%) and organics (~80%), and low in carbonate (~2-3%) (Figure 6.3). Clastic (clay/silt) facies of varying thickness and structure are embedded throughout. Core stratigraphy with LOI, geochemical, and microfossil data helped delineate five zones.

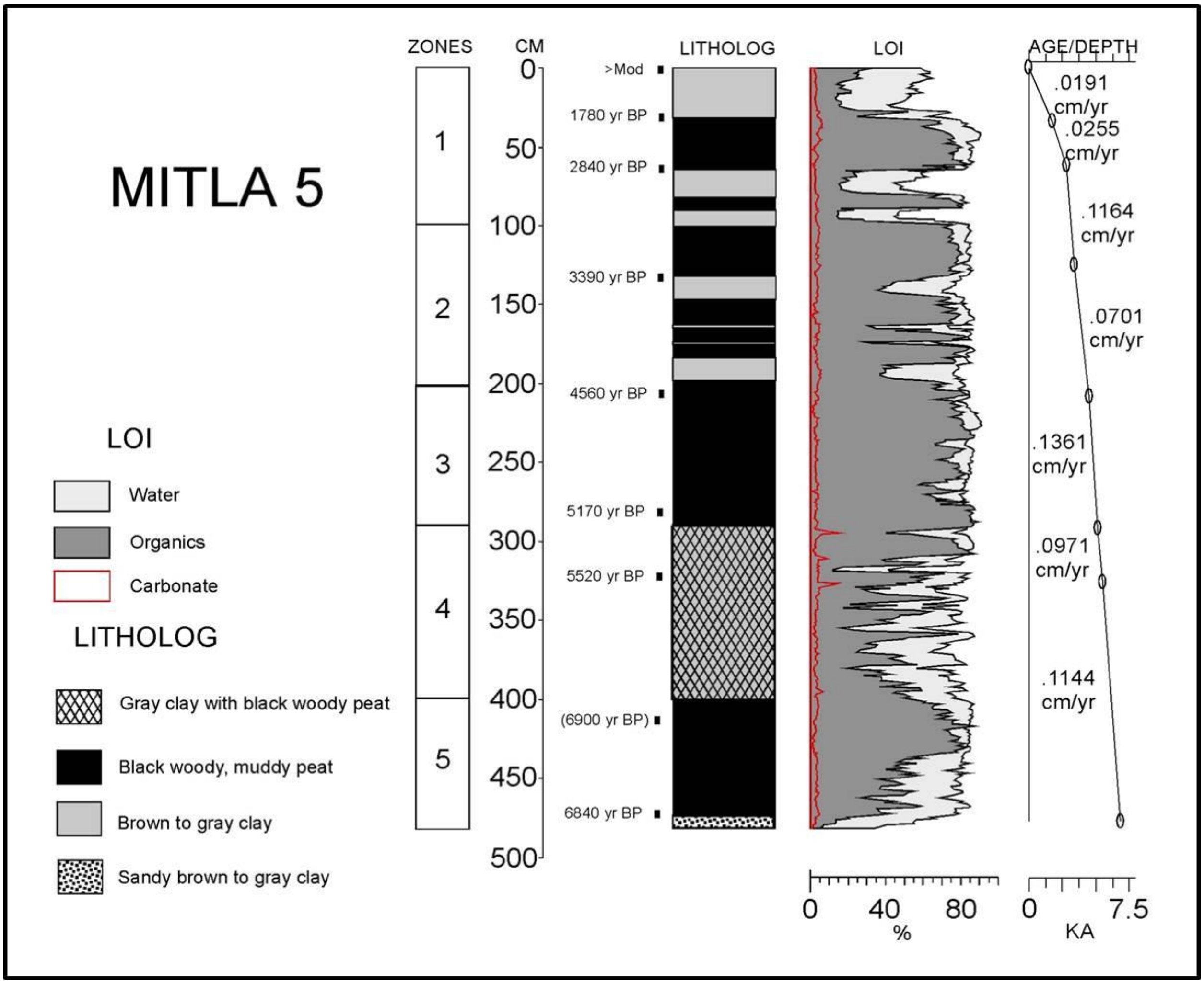

Figure 6.3 – Litholog, LOI results, zone delineation, and age-depth curve for core 5.

Zone 5 (479-400 cm) contains gray (2.5 Y, 7/4) sand at the bottom transitioning to dark peat at the top. Within the peat section water and organic content increase from bottom to top while most elemental concentrations decrease upward (Figure 6.4).

Zone 4 (400-290 cm) contains multiple thin gray clay layers (7.5 YR, 3/3, 4/2) with sharp decreases in water and organics. Several clay layers contain carbonate spikes at 294-292 (14% carbonate), 309-308 (8%), 327-325 (13%), and 394-392 cm (6%). Lithogenic elements (e.g., Fe, Ti, K, Co, Zn, Rb, Zr) are high in the lower part of the zone but become depleted near the zone top. However, Sr, I, Ca, and S concentrations are elevated toward the zone top in conjunction with the carbonate spikes.

Zone 3 (290-210 cm) is homogeneous peat with little clay content. Water, organic, and carbonate contents are uniform. Slight decreases in organics at 275-234 cm do not contain corresponding drops in water despite a ~1-2% carbonate increase compared to adjacent peat. Elemental concentrations are mostly low.

Zone 2 (210-100 cm) contains four clastic sections (7.5 YR, 4/2, 5/1) with significant decreases in organics (~35% content) yet slight drops in water (~70%) and negligible carbonate increases. Two thick sections (145-131, 198-183 cm) are faint peaty gray clay, lacking clear upper and lower boundaries. The remaining two (166-162, 174-172 cm) are thin, distinct structureless clastic layers with sharp contacts. Slight increases in most elements (Sr, I, Ca, S, Fe, Ti, K, Cr, Zn, Rb, etc.) occur in or adjacent to the inorganic layers.

Zone 1 (100-0 cm) contains three thick tan-gray (7.5 YR 3/2, 4/1) clay sections at 30-0, 79-65, and 99-89 cm with large drops in water (50%), organic (10%), and carbonate (3%) content. Most elements including Fe, Ti, K, Cr, Zn, Rb, and Zr occur in high concentrations in clay. Minor peaks in I, Ca, and S occur in some peat sections.

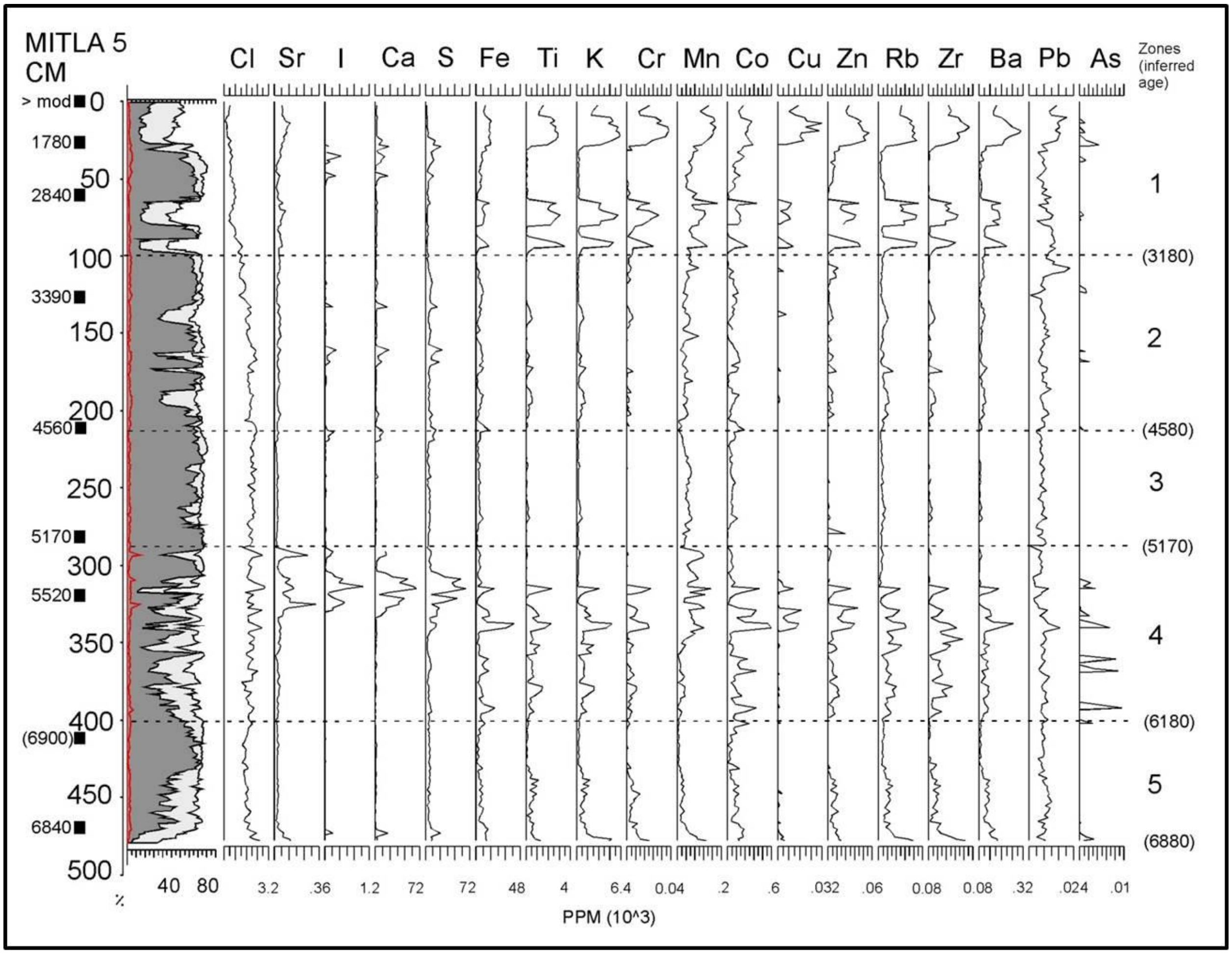

Figure 6.4 – XRF results divided by zone and paired with LOI results (far left).

Plant/wood samples were submitted for radiocarbon dating from 2 cm (> modern), 34 cm (1840±45 ^{14}C yr BP - 1777 cal yr BP), 61 cm (2710±110 ^{14}C yr BP - 2836 cal yr BP), 125 cm (3160±30 ^{14}C yr BP - 3388 cal yr BP), 207 cm (4070±30 ^{14}C yr BP - 4558 cal yr BP), 290 cm (4500±30 ^{14}C yr BP - 5167 cal yr BP), 324 cm (4760±30 ^{14}C yr BP - 5520 cal yr BP), 414 cm (6050±35 ^{14}C yr BP - 6903 cal yr BP), and 475 cm (6000±60 ^{14}C yr BP - 6842 cal yr BP) (Table 6.1). Sedimentation rates are relatively high from 488-61 cm (0.0701 - 0.1361 cm/yr) but decrease (0.091, 0.0255 cm/yr) in the top 61 cm (Figure 6.3).

Table 6.1 – Radiocarbon dating results for core 5.

Core/ sample ID	Depth (cm)	Lab #	Material	Radiocarbon age (BP)	Cal BP (2δ)	Rel. area under prob. distrib.	Med. prob
Mitla 5AAA 2	2	OS-90761	Plant/Wood	> mod			
Mitla 5AAA 34	34	OS-90770	Plant/Wood	1840±45	1630-1653	0.03	
					1692-1881	0.97	1777
Mitla 5 61	61	OS-84452	Plant/Wood	2710±110	2490-2643	0.087	
					2674-3084	0.886	2836
					3088-3157	0.027	
Mitla 5 125	125	OS-83891	Plant/Wood	3160±30	3341-3447	1	3388
Mitla 5 207	207	OS-83892	Plant/Wood	4070±30	4440-4486	0.159	
					4499-4503	0.004	
					4507-4645	0.69	4558
					4676-4693	0.02	
					4762-4801	0.126	
Mitla 5 290	290	OS-83942	Plant/Wood	4500±30	5046-5296	1	5167
Mitla 5H 45	324	OS-93066	Plant/Wood	4760±30	5333-5348	0.043	
					5353-5371	0.035	
					5464-5587	0.922	5520
Mitla 5 414	414	OS-83941	Plant/Wood	6050±35	6795-6991	1	6903
Mitla 5L 44	475	OS-90763	Plant/Wood	6000±60	6677-6707	0.03	
					6713-6987	0.97	6842

6.5.2 Pollen

Pollen was well-preserved, rarely showing signs of corrosion or degradation. Twenty-eight (28) taxa were identified and grouped by vegetation type. At least thirty-two (32) taxa were classified as 'unknown' or 'indeterminable.' Unknown taxa generally had minimal counts, most <1% of the pollen sum. The only exception is a *granulate-tricolporate* (GTC) pollen type that occurs at up to 27% at 24 cm. Indeterminable taxa percentages range from 1-18%.

Mangrove pollen (*Rhizophora*, *Laguncularia*) dominate throughout the core (Figure 6.5). Temperate taxa *Pinus* (mostly 5-30%) and *Quercus* (2-15%) also occur in elevated percentages. Other trees, shrubs, forbs, grasses, sedges, and ferns generally have low percentages. Charcoal concentration is low throughout the core. Fungal spore concentrations are mostly elevated in the lower part of the core while decreasing in the top meter (Figure 6.6).

Zone 5 – 479-400 cm (9 samples). The bottom of zone 5 (479-442 cm) contains high *Rhizophora* (32-88%) with low *Laguncularia, Conocarpus,* GTC, *Batis, Cheno-Am,* and *Typha* percentages. *Pinus* and *Quercus* percentages are elevated. The top of zone 5 (432-400 cm) is peat with low *Rhizophora* (19-48%) and relatively high *Laguncularia* percentages (9-40%). Fungal spore concentrations are high, particularly *Cercophora-type*, *Tetraploa-type*, uni-septate, and tetrad classifications.

Zone 4 – 400-290 cm (9 samples). Zone 4 contains both minimum and maximum *Rhizophora* percentages (0-90%). Sections low in *Rhizophora* are high in *Laguncularia* (50% - 303 cm) and/or *Conocarpus* (60% - 353 cm). GTC, *Batis*, and *Typha* spikes exist, mostly from 391-340 cm. *Pinus* and *Quercus* percentages are stable. Total pollen concentration fluctuates widely, spiking at 381 cm. Fungal spore concentrations are elevated, namely uni- and multi-septate groups.

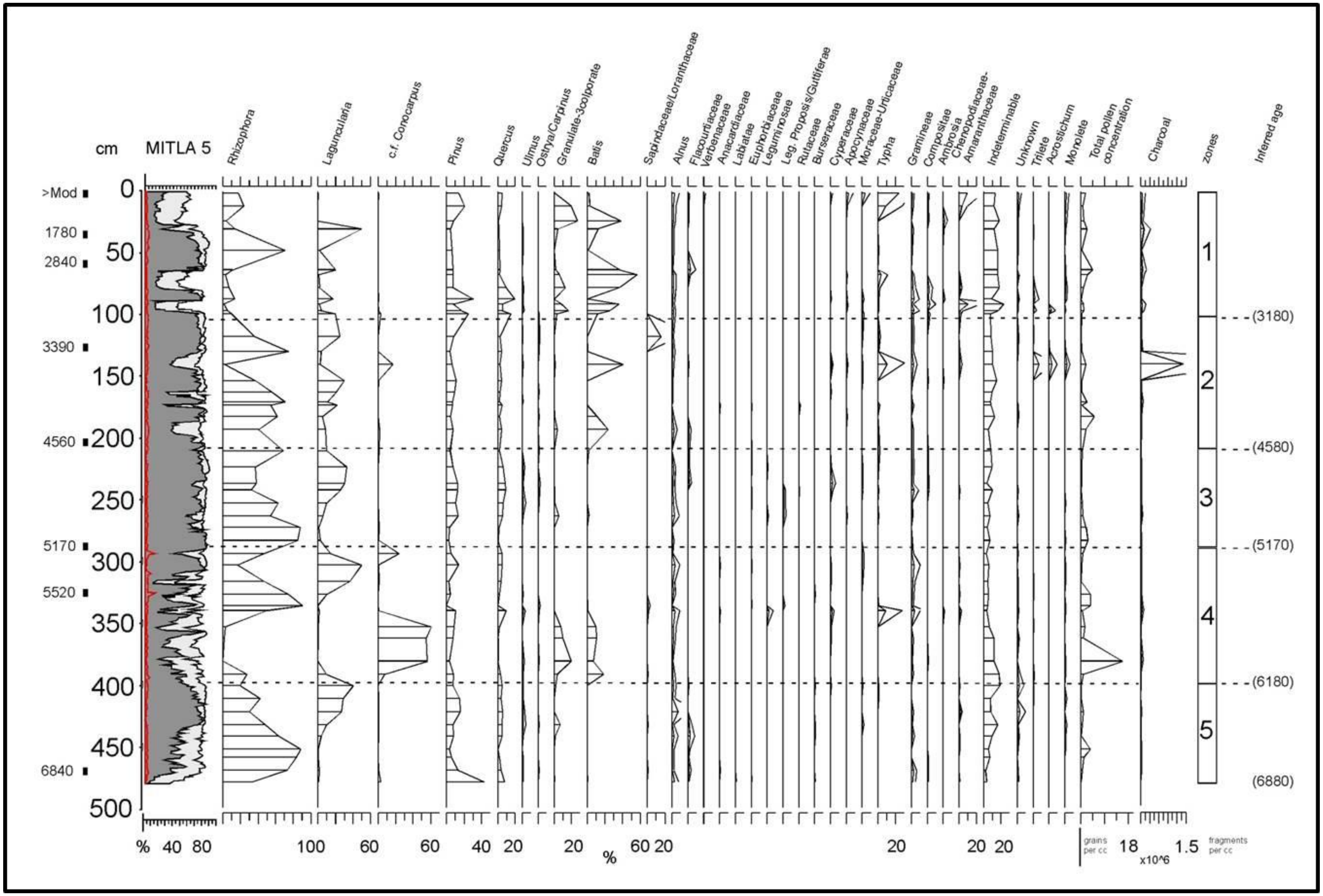

Figure 6.5 – Core 5 pollen percentage diagram, with LOI curves. A 3X exaggeration line is added to taxa with low percentages. Percentages of mangrove taxa are generally high in peat, decreasing in clay layers.

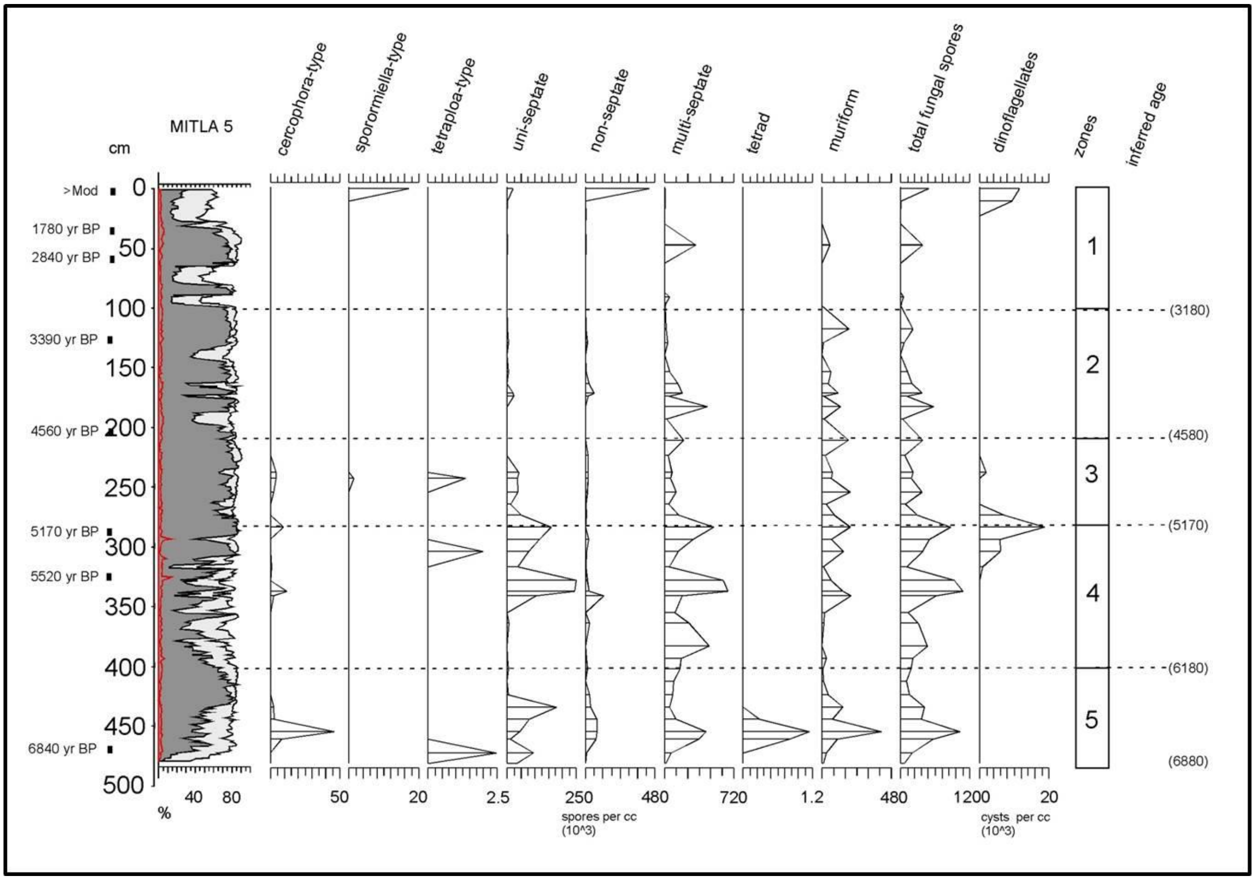

Figure 6.6 – Core 5 fungal spore and dinoflagellate concentrations, with LOI curves.

Zone 3 – 290-210 cm (8 samples). *Rhizophora* (37-85%) and *Laguncularia* (~1-33%) percentages widely vary throughout zone 3. *Pinus* and *Quercus* are stable with relatively high percentages. GTC, *Batis*, and *Cheno-Ams* percentages are low. Total pollen concentrations are very low. Fungal spore concentrations are high, including *Cercophora-type, Tetraploa-type,* uni-septate, multi-septate, and muriform classes.

Zone 2 – 210-100 cm (10 samples). Peat contains medium to high *Rhizophora* percentages and relatively high *Laguncularia*. *Cheno-Ams, Typha*, and GTC percentages are low. *Pinus* and *Quercus* percentages are relatively high. Fungal spore concentrations are low. Clayey peat at 198-183 cm exhibits a slight decrease in *Rhizophora* with increases in GTC, *Batis*, and total pollen concentration. Inorganic layers at 166-162 and 174-172 cm exhibit only a

slight decrease in *Rhizophora* and negligible increases in *Laguncularia*, while the abundance of most remaining taxa is stable. The clayey peat at 166-162 cm unit contains a peak in multi-septate fungal spores, while the 174-172 cm layer contains peaks in uni-septate fungal spores and charcoal. Clayey peat at 145-131 cm near the zone top contains a significant decrease in *Rhizophora* with small spikes in GTC, *Batis*, *Typha*, ferns, and total pollen concentration, along with a sharp increase in charcoal.

Zone 1 – 100-0 cm (12 samples). The sole peat sample (48 cm) is high in *Rhizophora* (70%), low in *Pinus* and *Quercus*, and high in fungal spores, mostly multi-septate. One clay/peat transitional sample at 31 cm contains a *Laguncularia* spike at 49% with decreases in GTC, *Cheno-Ams*, and *Typha* while fungal spores are absent. Other transitional samples at 63 and 87 cm also contain a *Laguncularia* spike. The clay layers are characterized by low percentages of low in *Rhizophora* and *Laguncularia*, and higher percentages of GTC, *Pinus*, and *Quercus*. They also contain small peaks in Compositae, Gramineae, Moraceae-Urticaceae, *Ambrosia*, *Cheno-Ams*, *Typha*, and fern spores. Fungal spore concentrations are low in clay except for a notable spike in *Sporormiella-type*. Dinoflagellate cysts occur in the top two samples and are absent elsewhere in the zone.

6.6 Discussion

6.6.1 Environmental reconstruction

6.6.1.1 Holocene sea level history

Only a few regional Holocene sea level records are documented in the literature. The nearest record was derived from Nayarit state (Curray et al., 1969), located 800 km northwest of Mitla. The Nayarit record provides the best estimate for regional sea levels throughout the Holocene. Sea level might have been up to 9 m below present 7000 years ago, a period when

marine transgression was relatively fast and capable of transporting a mixture of terrigenous and deep sea sediments toward the coast. Rapidly rising seas soon inundated coastal depressions throughout the region around 5000 years BP, followed by stabilizing seas resulting in backbarrier lake and lagoon formation along Mexico's Pacific coast (Curray et al., 1969; Lankford, 1977). After backbarrier formation, the rate of sea level rise continued to decrease, with levels approaching present levels about 3000 years BP. Beach ridge progradation accelerated from longshore drift and shelf sand deposition via stable seas. At present, the direction of littoral drift changes seasonally, with sediments transported from the north during the fall and winter, and from the south during the spring and summer (Lankford, 1977).

The presence of mangrove peat throughout the core, coupled with comparison of Nayarit's sea level record to depth of calibrated radiocarbon dates, suggests that Mitla has been at or near sea level throughout the last ~6900 years. Slight inconsistencies between core 5 stratigraphy and the Nayarit sea level record can stem from the distance separating these two sites, peat compaction, and minor land-level changes from tectonic activity. This is discussed in more detail in section 6.6.2.

6.6.1.2 Peat vs. clay stratigraphy

Backbarrier mangrove peat sections indicate swamp environments and relatively low water level, due to their susceptibility to drown from prolonged and/or rapid freshwater or saltwater inundation (Blasco et al., 1996). In Cuba, Peros et al. (2007) found that *Rhizophora* generally lives in areas with ~30 cm of water inundation. Urrego et al. (2010) discovered relatively low percentages of *Rhizophora* pollen in scattered patches of mangroves with high inundation levels (~80 cm). Peat sediments discovered from a previous paleoenvironmental reconstruction at Mitla was similarly interpreted to indicate backbarrier mangrove swamps

positioned close to sea level (Ramirez-Herrera et al., 2007). Pollen signatures of peat environments mostly contain grains of local vegetation, with the exception of some wind-driven grains entering the site primarily from temperate tree taxa (e.g., *Pinus*, *Quercus*) located landward of the lagoon. Lithogenic element concentrations are low in peat from a lack of terrigenous sediment input.

Unlike peat sections, backbarrier clay sediments are interpreted to indicate limnic (lagoonal) environments, similar to Mitla's current environmental setting. Mechanical attrition and sedimentation processes cause these inorganic sediments to contain elevated concentrations of terrigenous elements (e.g., Fe, Ti, Zr), corresponding with relatively small grain-sizes (Weltje and von Eynatten, 2004). With the exception of two thin inorganic layers with small lithogenic element concentrations in zone 2, all backbarrier clay layers are relatively thick and encompass periods ranging from many hundreds of years to over a thousand years, therefore representative of relatively long-term environmental change as opposed to instantaneous events. A multi-core paleoenvironmental reconstruction spanning 3.5 km from Mitla's western edge indicates that this entire area has been a limnic environment throughout much of the last 5200 years (Chapter 5). Backbarrier lagoonal clay in core 5 indicates periods of increased size of the limnic environment from periods of excessive precipitation and runoff entering the site, triggered by wet climatic conditions. Previous paleoenvironmental reconstructions from Mitla dismiss lithologic change as climatically driven (e.g., Ramirez-Herrera et al., 2007), despite water level variations documented throughout western Mexico attributed to climate change (e.g., Berrio et al., 2006). Unlike peat sediment containing pollen signals dominated by localized vegetation, lagoon sediment contains pollen grains derived from regional sources (e.g., Peros et al., 2007), as individual grains are capable of transport spanning many kilometers (Melia, 1984).

Geochemical proxies can aid in detecting elevated salinity and marine influence in sediments, as certain elements contain higher concentrations in seawater compared to freshwater (Chague-Goff et al., 2002). Marine components including algae and sea shells, for instance, contain high concentrations of Sr (Bowen, 1956), with elevated levels in sediments suggesting marine influence (Ramirez-Herrera et al., 2007; Woodruff et al., 2009). Other elements indicative of marine disturbance or high salinity include S, I, Ca, and Cl (Wakefield and Elderfield, 1985; Chen et al., 1997; Ramirez-Herrera et al., 2007; Nichol et al., 2010; Schofield et al., 2010). Throughout core 5, clay layers rich in these elements are suggestive of marine intrusions. Small spikes in marine elemental concentrations occur in some peat sections throughout the core. As these core sections are absent of inorganic sediment deposition, the spikes in marine elements likely do not indicate intrusion events. Alternatively, these core sections suggest periods of elevated salinity.

6.6.2 Paleoenvironmental history

6.6.2.1 Zone 5 (6880 - 6180 yr BP)

High *Rhizophora* pollen percentages at the zone bottom indicate a mangrove swamp at or near mean sea level and tidal range. Regional records suggest that sea level might have been 9 m below present at this time (Curray et al., 1969). While a comparison of the calibrated radiocarbon dates and their site depth (4.79 m core plus ~1 m water depth) to the regional sea level record suggests that this site was up to 3 m above sea level throughout this zone, this is likely not the case, due to the preferred environments of *Rhizophora*. While it is therefore suggested that sea level near the site is approximately 6 m below present at the bottom of the zone, slight uplift of the site throughout the last 6880 years cannot be ruled out as a factor explaining the discrepancies in these records. The elevated Cl concentrations at the zone bottom

indicate high salinity from its position near the ocean. An emergence of *Laguncularia* pollen at the zone top signals a gradual drop in relative sea level, possibly from tectonic uplift. Favoring lower salinities or higher elevations than *Rhizophora*, increases in *Laguncularia* pollen at the expense of *Rhizophora* are largely attributed to tectonic-induced land-level changes from the Pacific coastal state of Baja California Sur (Sirkin et al., 1994). As the top section of the zone possesses increases in water and organic contents, it is suggested that the vegetation during this period was lusher, or that the mangrove area expanded spatially. Throughout the entire zone, peat lacking clastic input and containing low elemental concentrations indicate a relatively stable wetland environment, unaltered by riverine sediments or extreme event deposition.

6.6.2.2 Zone 4 (6180 - 5170 yr BP)

Comparison of radiocarbon dates and site depth to the regional record suggests that sea level is near site level. The rising seas transported clastics into the site, explaining the jagged LOI output. This process marks the beginning stages of beach ridge formation, previously documented during this time for the site (Ramirez-Herrera et al., 2009). The terrigenous origin of this sediment indicates that they were shelf muds, previously deposited to the upper edges of the continental shelf by fluvial and erosional processes before their transport into the site from the rising seas. Rapid and inconsistent clastic deposition at the bottom of the zone suggests that this site was irregularly sealed from the ocean, exhibiting similarities to a sheltered bay morphology. The susceptibility of *Rhizophora* to withstand these high-energy conditions lead to significant decreases in pollen percentage, while spikes in *Batis* and *Conocarpus* pollen indicate colonization in the disturbed vegetation stands. Despite *Conocarpus* favoring relatively fresh conditions and high elevations, they are capable of growing in saline environments (Urrego et al., 2010). A halt in relative sea level momentarily minimized clastic deposition, as *Rhizophora*

quickly recolonized at this time. Clay deposition at the zone top accompanied by a decrease in *Rhizophora*, presence of dinoflagellate cysts, and increases in *Laguncularia*, carbonate content, and S, I, Ca, and Sr concentrations suggest an influx of marine sediments from another sea level resurgence, responsible for inundating the site. Similar marine environments during this timeframe have been documented from Pacific coastal states of Nayarit (Curray et al., 1969; Sirkin, 1985) and Jalisco (Chapter 4), and Guatemala (Neff et al., 2006).

6.6.2.3 Zone 3 (5170-4580 yr BP)

Stabilizing seas after the marine inundation sealed Mitla from the ocean, as the site became a backbarrier mangrove swamp dominated by *Rhizophora* and *Laguncularia*. Low energy conditions, a lack of clastic deposition, low concentrations of marine and lithogenic elements, and minor variation of *Rhizophora* and *Laguncularia* populations indicate a stable wetland environment and minimal water-level changes throughout zone 3. As fungal spores decompose organics and are often associated with low inundation levels, high concentrations can further indicate low water level (e.g., Berrio et al., 2006, Chmura et al., 2006). The low marine element concentrations and absence of clastic deposition suggest that the elevated dinoflagellate concentrations might indicate cyst reproduction (Kremp and Heiskanen, 1999) from the recent transgression instead of a separate marine intrusion. Dinoflagellates can flourish in environments with relatively high salinities (Paerl et al., 2006), and elevated cyst concentrations are often documented in sediments recent of marine intrusion deposits (e.g., Liu et al., 2008).

While Holocene paleoclimate records are scarce for the Pacific coasts of Mexico and Central America, dry conditions throughout zone 3 are consistent with reconstructions from the highlands from similar time periods. A summary of paleoclimatic reconstructions from Mexico's highlands compiled Metcalfe et al. (2000) indicates that most sites experienced dry

conditions around 5000 years BP. Additionally, a dry period from ~6500-5000 years BP was determined for Lake Texcoco in the Mexico City Basin (Gonzalez-Quintero and Fuentes-Mata, 1980). Similarly, low water level and poor pollen preservation was detected from a maar lake from the upland state of Guanajuato (Park, 2005). Perhaps most notably, a paleoenvironmental reconstruction from a mountain lake in the neighboring state Michoacan revealed evidence of its lowest water levels from 6000-4000 years BP (Arnauld et al., 1997). Bark remnants scattered throughout zone 3 and relatively high *Pinus* and *Quercus* percentages might indicate an increase in these temperate tree populations and a cooler climate, possibly triggered by relatively cool mid-Holocene sea surface temperatures (Clement et al., 2000).

6.6.2.4 Zone 2 (4580-3180 yr BP)

Similarly to zone 3, sea level is likely near site level throughout zone 2. Four distinct clay layers occurring in the predominantly peaty sediments indicate four episodes of higher water levels and lagoon expansion during 4600-3200 years BP. Overall, zone 2 is a fresher environment than zone 3, suggested by decreasing Cl concentrations. Evidence of increased water level is further suggested from small concentrations of *Conocarpus*, favoring fresher environments (Urrego et al., 2010). Minor peaks in *Batis*, *Cheno-Ams*, *Gramineae*, and ferns from the clay layers can indicate small localized populations establishing, or pollen grains entering into the nearshore from the lagoon fringes. For example, the pollen from *Batis*, a salt-tolerant plant, was likely transported into the core 5 site from the many hectares of both salt marsh and pans positioned adjacent to relict beach ridge remnants and Mitla's western edge. Detailed paleoclimatic reconstructions covering this time period are rare from Mitla's vicinity, but it is suggested that climatic variability increased during this period (see Brown, 1985 and Metcalfe et al., 2000 for summary). From the Middle America Trench, wet conditions were

determined from an increase in oak pollen from 6500 to 3000 years BP (Habib et al., 1970). Alternatively, a reconstruction from Lake Patzcuaro reveals mainly dry conditions during this period (Watts and Bradbury, 1982).

High charcoal concentration and small *Cheno-am* and *Gramineae* percentages at the top clastic layer (3680-3480 yr BP) indicate localized fire burning and the beginning of local land disturbance from human migration into the area. This time period is similar to other evidences of human migration into the area. One example comes from Lake Patzcuaro, containing evidence of Zea (corn) pollen along with other disturbance indicators *Cheno-ams* and *Gramineae* around 3500 years BP (Watts and Bradbury, 1982).

Associated with clay layers, slight increases in concentrations of marine elements associated with a lack of dinoflagellates likely do not indicate marine intrusions, but likely material transport from the relict beach ridge area at Mitla's center during periods of high water level. Surface samples and sand layers discovered in cores extracted landward of core 5 suggest that this relict beach ridge material is rich in marine elements (Chapter 5).

6.6.2.5 Zone 1 (3180 yr BP – current)

Distinct episodes of clay deposition with elevated concentrations of lithogenic elements suggest high water levels and wet conditions around 3100, 2900, and 1570 yr BP-present. These phases are generally longer-lasting than during zone 2, possibly stemming from strengthened beach ridges. Elevated *Pinus* and *Quercus* pollen percentages indicate a regional signal, while a lack of *Conocarpus* pollen, an absence of fungal spores and extremely limited "marine" element concentrations from the relict ridge indicate higher water levels than zone 2. Decreasing Cl and small *Typha* populations suggest fresher conditions throughout this time period. A spike in *Laguncularia* from the limnic/peat transitional section around 1800 yr BP indicates brief

colonization during the beginning years of the lagoon phase as *Rhizophora* drowned from increasing water level. High *Batis* pollen percentages are probably derived from mud flat communities occurring locally around the edges of the expanding lagoon. Unknown GTC pollen display a similar abundance pattern to *Batis* (Figure 6.5), suggesting a similar environmental setting.

Regional paleoenvironmental records indicate high levels of human activity in the adjacent uplands in western Mexico during the Late Holocene (e.g., Ohngemach, 1977). Land degradation likely accelerated terrestrial sediment input into Mitla, a possible reason for high lithogenic element concentrations in zone 1. Similarly, small peaks in pollen percentage of taxa attributed to land degradation due to their rapid colonization in disturbed and cleared plots (e.g., Gramineae, Compositae, *Ambrosia*, Cheno-Am) (Goman et al., 2010) occur throughout zone 1. *Sporormiella* fungal spores at the core top are similarly attributed to human disturbance, since it is commonly associated with livestock dung (e.g., van Geel et al., 2003). High concentrations of unidentified plankton are similarly discovered from recent sediments from nearby Tetitlan, also suggested from human activity (Gonzalez-Quintero, 1980). Their concentrations in Mitla might represent algal blooms and eutrophication from increased heavy metal input (e.g., Watts and Bradbury, 1982; Gilbert and Terlizzi, 1999; Pospelova et al., 2002). Slight increases in charcoal concentrations are also consistent with increased human activities and anthropogenic burning.

Similar to zones 3 and 2, wet periods detected throughout zone 1 exhibit temporal similarities to regional paleoclimatic records. Increased Late Holocene climatic variability has been documented throughout Central America (Horn, 2007). The western Mexico highlands have experienced generally wet conditions (Heine, 1987; Park, 2005; Borejsza and Frederick, 2010), with only a few regions showing evidence of prolonged dry periods (e.g., Almeida-

Lenero et al., 2005). A paleoenvironmental reconstruction from coastal Nayarit uncovered relatively dry conditions from 3300-1700 years BP, with wetter conditions dominating from 1700 years BP to recent times (Sirkin, 1985). Similar wet periods at 3000-2500 yr BP and 1500-present were discovered from Laguna Tetitlan, 10 km west-northwest of Mitla (Gonzalez-Quintero, 1980). Core 5 peat containing a carbonate peak (~6%) and I, S, and Ca spikes might designate extreme aridity and increased evaporation (e.g., Neff et al., 2006) during the low water period of ~2800-1800 yr BP. Amplified aridity during this time period was similarly documented from Tetitlan (Gonzalez-Quintero, 1980) and Laguna Boquita in Jalisco (Chapter 3). Similarly, a marine core extracted from the Middle America Trench contained decreased *Quercus* pollen from ~3000-1750 years BP, suggestive of dry conditions (Habib et al., 1970).

6.6.3 Climate change and TC activity in the eastern north Pacific basin

Coastal precipitation totals along western Mexico are largely influenced by TC activity. Individual events are capable of upwards of 300 mm of rainfall in this region (Englehart and Douglas, 2001). TCs account for 40% of the warm season precipitation in the Acapulco area, and are capable of exceeding 60% (Englehart and Douglas, 2001). Similar to landfalling TCs, nonlandfalling TCs paralleling the study site are similarly capable of substantial precipitation, many dropping over >100 mm near Acapulco (Englehart and Douglas, 2001). El Niño-Southern Oscillation (ENSO) is a major control of TC activity in the eastern north Pacific (ENP) basin. In addition to El Niños bringing more non-TC precipitation to this coast (Rodgers et al., 2000), the accompanying warm surface waters and decreased vertical shear are largely responsible for the more frequent (Landsea and Gray, 1989; Goldenberg and Shapiro, 1996; Jauregui, 2003; Chu, 2004), more intense (Gray and Sheaffer, 1991), and wetter (Rodgers et al., 2000) TCs than during neutral and La Niña phases along Mexico's Pacific coast. During the historical period,

more TCs have affected the Mitla region during strong El Niño than strong La Niña phases (Figure 6.7). Records of multi-centennial ENSO activity detected from inorganic laminae deposition into Ecuador's Laguna Pallacacocha from heightened stream discharge exhibit good temporal agreement with lagoonal phases determined from Mitla's sedimentary record (Moy et

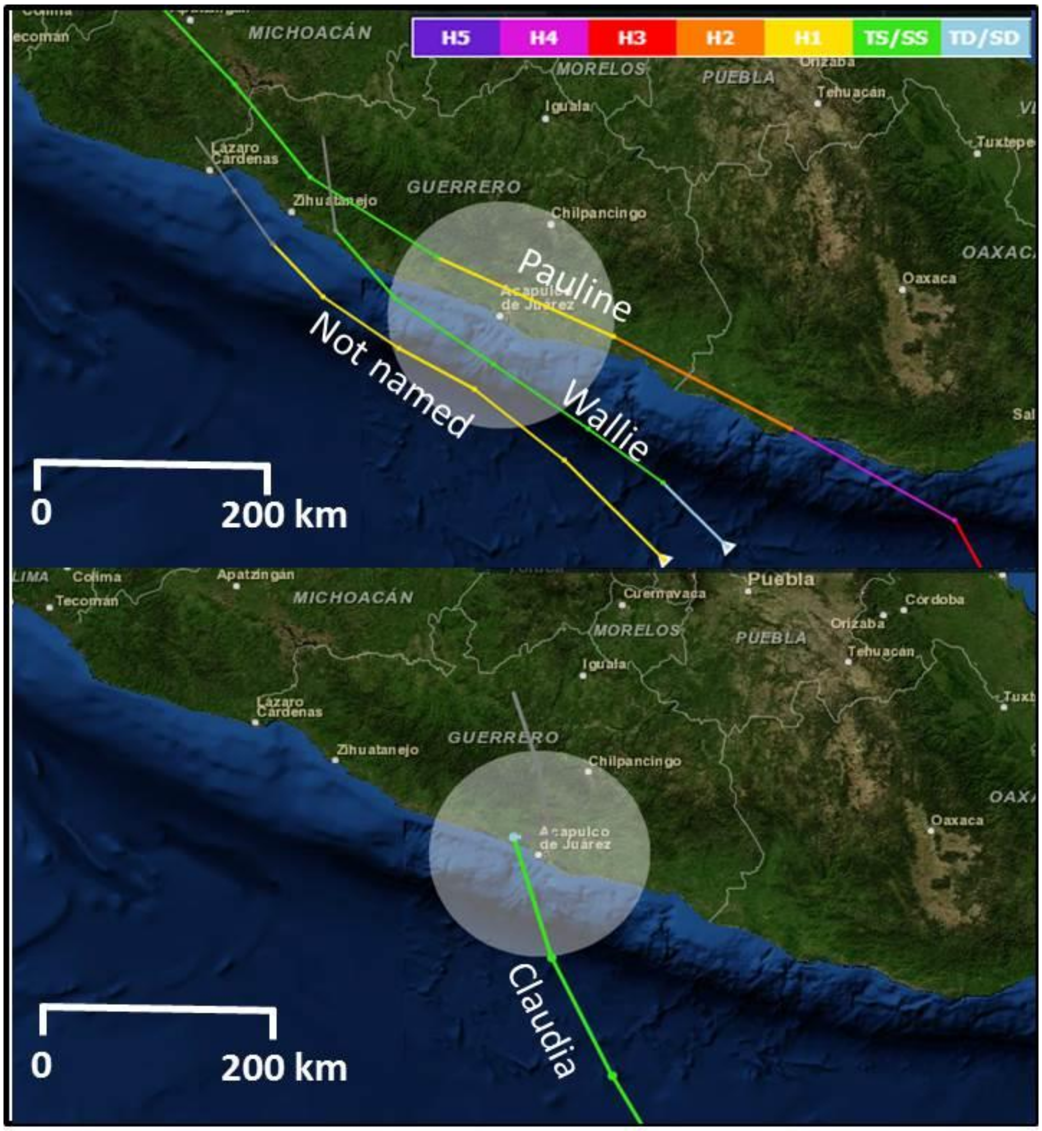

Figure 6.7– TC tracks 100 km from Acapulco during strong El Niño ('97, '91, '82, '72, '65, '57 - top) and La Niña (2010, 1999, '88, '75, '73, '55 – bottom) years, based on ≥1.5 C° anomaly for five consecutive months from Niño 3.4 region. Strong El Niño tracks have affected the Acapulco area more so than during La Niña years. Pauline dropped over 16 inches (40 cm) of rainfall in the Acapulco area. Rainfall from TS Claudia was negligible. Precipitation data from the National Climatic Data Center (2013).

al., 2002 - Figure 6.8). Generally, many coastal regions contain evidence of El Niño phases that were more intense and frequent during the Late Holocene than the mid-Holocene (Clement et al., 2000; Markgraf et al., 1992; Sandweiss et al., 1996; Moy et al., 2002; Riedinger et al., 2002). This is similarly suggested for Mitla, as distinct clay deposition in zone 1 suggests higher water levels and longer-lasting limnic environments than during zone 2. The temporally short limnic phases containing low water throughout zone 2 are in good temporal agreement with diminished ENSO activity (e.g., fewer and less intense extreme phases) detected from Ecuador (Moy et al., 2002) and the Galapagos Islands (Conroy et al., 2008). Elevated ENSO activity detected during zone 3 did not register lagoon phases in Mitla, as signals were far less pronounced. Climatological boundary conditions (e.g., Inter-tropical Convergence Zone - ITCZ) were likely different during this period. With the ITCZ in a more northerly position during zone 3, increased precipitation might have been focused toward northwestern Mexico, while causing cold water upwelling nearer Mitla (Perez-Cruz, 2013). ITCZ migration southward throughout much of the past 5000 years is likely a significant factor in increasing ENSO frequency and intensity due to diminishing easterly flow (Clement et al., 2000; Haug et al., 2001). Koutavas et al. (2006) admits that the relationship between ENSO and the ITCZ is still poorly understood and requires additional attention.

Due to the relationship between ENSO and TC activity, it is suggested that wet periods characterized by lagoonal clay indicate periods of increased TC activity. While ENP activity periods are suggested to be temporally antiphased with the Atlantic basin (Elsner and Kara, 1999), inter-basin correlations can be troublesome as some studies suggest that TC activity does not occur simultaneously throughout the basin (McCloskey and Liu, 2013). Some temporal association stems between Mitla's paleoclimatic record and a multi-centennial record of TC-

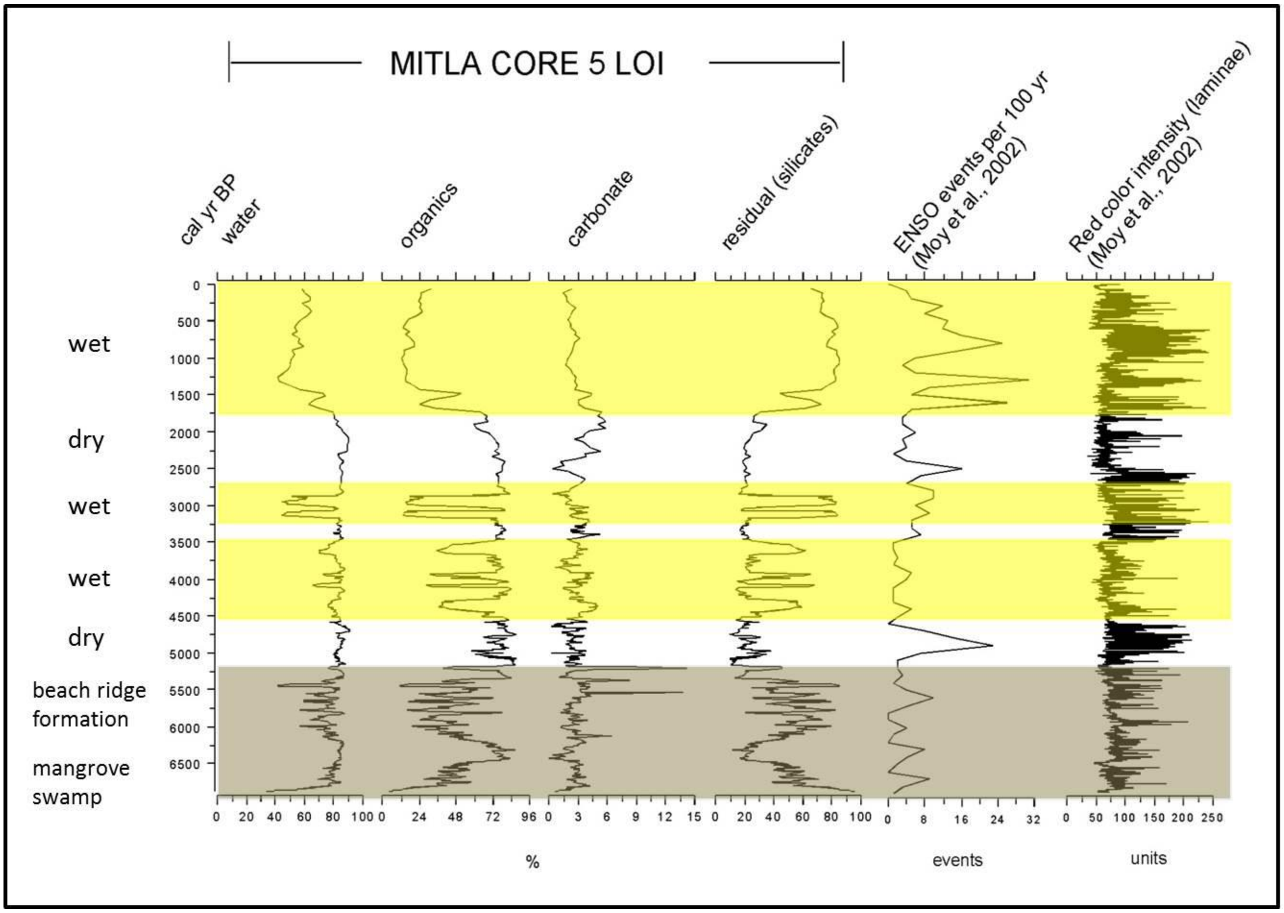

Figure 6.8 – Core 5 LOI graph next to ENSO events per 100 years and red color intensity depicting slopewash laminae (Moy et al., 2002). Wet periods depicted by decreasing water and organics (and increasing residual) show association with increased ENSO events and red color intensity.

induced overwash events from the U.S. Gulf and Atlantic coasts (Liu and Fearn, 2000; Scileppi and Donnelly, 2007). Temporal association also exists to paleorecords from Nicaragua's Caribbean coast, where high TC activity is associated with a southward migrating ITCZ (McCloskey and Liu, 2012). Most significantly, Mitla's wet periods exhibit some antiphased relationship with hurricane records retrieved from Vieques, Puerto Rico, which are correlated with periods of diminished El Niño activity (Donnelly and Woodruff, 2007). The low water period at Laguna Mitla from 2800-1800 compares to the active hurricane period at Vieques, corresponding with numerous overwash sand layers from ~2500-1000 yr BP. While the ~4500-

3500 year record contains evidence of four limnic phases, their short temporal nature suggests that this period as a whole is relatively dry. Fittingly, this associates to an active period at Vieques, from 4900-3600 years BP. Inconsistencies when comparing long-term sedimentary records can stem from differences in age models, resolutions, proxies, and regional climatic conditions. Inter-basin correlations would benefit from additional multi-centennial ENP climate records.

6.6.4 Sensitivity to marine intrusion events

Throughout Mitla's 5200 year backbarrier history, the absence of clastic deposition accompanied by both elevated marine elemental concentrations and dinoflagellates indicate insensitivity to marine extreme-event sedimentary deposition. Despite the utility of marine element concentrations in extreme event detection when clastics are absent in coastal sites from Japan (Minoura and Nakaya, 1991), small spikes in marine elements at Mitla do not accompany spikes in dinoflagellates, and are generally interpreted to indicate increased salinity during periods of low water level. A multi-core investigation from the western side of the lagoon covering a 3.5 km transect similarly yielded a lack of overwash deposition and marine inundation (Chapter 5). Recent overwash is likely limited by the wide and prograding beach ridge system. The narrow (60 km wide) continental shelf with its steep slope (5 km near edge) is a likely contributing factor in minimizing storm surge. Five cores extracted from Laguna Boquita, located 600 km northwest of Mitla, is similarly absent of extreme event deposition and evidence of marine overwash throughout its 5200 year backbarrier record (Chapter 3). Three cores extracted from Laguna Nuxco, located 40 km northwest of Mitla (Chapter 4) similarly fail to possess extreme event driven sand or other definitive evidence of extreme events (e.g., shells of marine origin). While a lack of sedimentary research along the Pacific coast hampers the

implementation of many additional examples, sediment extracted from Manchon Swamp on the Pacific coast of Guatemala similarly lacks overwash evidence (Neff et al., 2006).

Evidence of marine intrusion has previously been suggested from Mitla in the form of a ~100 cm thick sand layer, retrieved from a sediment core extracted 5 km landward of the coast and positioned behind the lagoon in a wetland area (Ramirez-Herrera et al., 2007). This deposit was attributed to a powerful tsunami, given the inundation distance noted by the authors required to transport this coastal sand. Lack of backbarrer marine overwash detected from the seaward core 5 poses questions regarding the origin and transport mechanism of this sand. It is suggested that the sand source is the relict beach ridge in Mitla's center. Cores extracted south of the beach ridge contained sand deposits rich in marine elements, transported into the site from increasing water level (Chapter 5). Similarly, a 3.8 m sediment core extracted adjacent of these relict beach ridges was dominated by sand (Ramirez-Herrera et al., 2007). The size and extent of these relict ridges is unknown, but it is suggested that they cover a relatively large extent since sand deposition was discovered in a core extracted over 1 km from the visible ridge segment (Chapter 5).

Other evidences attributed to marine incursions at nearby sites include basal sand ~3170 yr BP from Tetitlan (Gonzalez-Quintero, 1980), as well as a shell midden with a date of ~3000 yr BP and numerous sand layers from Laguna Coyuca (Kennett et al., 2004, cited in Ramirez-Herrera et al., 2007), 40 km east of Mitla. It must be noted that Coyuca and Tetitlan are both "barred inner shelf" lagoons, sharing similar evolutions and beach ridge dimensions as Mitla. Precise coring locations, as well as presence and location of relict ridge segments are unknown for both of these sites. Findings from Mitla indicate that care should be administered before attributing sand layers to extreme events at Pacific coast environments. It is suggested that

numerous cores be extracted to determine sand source, which could additionally include eroded material from the coastal beach ridge system (Ramirez-Herrera et al., 2007) along with shelf sand introduced by tidal inlets (Lankford, 1977).

Sand layers discovered from pits dug in swampland just adjacent to the Ixtapa Estuary, 150 km west-northwest of Mitla and only hundreds of meters landward of the coastal beach ridge have recently been attributed to tsunami in 1979 and 1985 (Ramirez-Herrera et al., 2012). However, this coastal region was directly hit by the category 2 hurricanes Andres (1979) and Odile (1984), both paralleling the coast. It is questionable whether sand layers previously attributed to be tsunami deposits were actually storm surge deposits, or neither (formed by alternative processes). Attention must be devoted to TC sensitivity in these nearshore areas. Extracting additional sediment cores to uncover older deposits and their landward extent is crucial toward assessing coastal sensitivity toward marine intrusion.

6.7 Summary and conclusion

This study presents a multi-proxy paleoenvironmental reconstruction from a 478 cm sediment core from Laguna Mitla on Mexico's Pacific coast, providing a ~6900 year record. Main objectives include determining a paleoclimatic record, along with any evidence of human disturbance or marine intrusion from extreme events, particularly TCs. At ~6880 years BP, the site was a mangrove swamp during a period of low sea level. Rising seas began beach ridge formation ~6180 yr BP, transporting clastics into the nearshore. Sea levels stabilized after ~5200 yrs BP, forming Mitla's backbarrier environment. Clay sediments containing terrigenous geochemical signatures, low *Rhizophora* pollen, and high pollen percentages of regional vegetation are indicative of limnic phases at the core 5 site. Seven limnic phases are inferred (~4430-4220 yrs BP, 4080, 3950, 3680-3480, 3170-3080, 2990-2870, and 1570-present)

indicating wetter climatic conditions. These intervals generally correspond with wet periods determined from regional upland and coastal paleoclimatic records. Limnic phases correlate to periods of increased El Niño frequency and intensity, a major force controlling ENP precipitation trends, including TC activity. Thick and distinct lagoonal clay deposition throughout the Late Holocene represents a wetter climate and intensified human activity in the Mexican highlands. Peros et al. (2007) acknowledges the difficulty in paleoenvironmental reconstructions from sites with constantly fluctuating water levels, especially as factors including human disturbance and tectonic activity capable of disrupting stream dynamics, for instance. Additional coastal reconstructions can verify this record. The abundance of Pacific coast lagoons and marshland makes such analysis possible.

Additionally, core 5 lacks marine intrusion evidence consistent with extreme event deposition. Beach ridge progradation and a narrow continental shelf are inimical to the occurrence of overwash processes depositing sand into the nearshore by TC or tsunami events. This finding challenges the occurrence of tsunamis and other marine intrusion events previously reported in the literature.

6.8 References

Almeida-Lenero, L., H. Hooghiemstra, A. M. Cleef, and B. van Geel. 2005. Holocene climatic and environmental change from pollen records of lakes Zempoala and Quila, central Mexican highlands. Review of Palaeobotany and Palynology **136**:63-92.

Arnauld, C., S. E. Metcalfe, and P. Petrequin. 1997. Holocene climatic change in the Zacapu lake basin, Michoacan: Synthesis of results. Quaternary International **43-4**:173-179.

Bartlett, A. S. and E. S. Barghoorn. 1973. Phytogeographic history of the Isthmus of Panama during the past 12,000 years (A history of vegetation, climate, and sea-level change). Pages 203-299 *in* A. Graham, editor. Vegetation and Vegetational History of Northern Latin America. Elsevier Scientific Publishing Company, Amsterdam.

Berrio, J. C., H. Hooghiemstra, B. van Geel, and B. Ludlow-Wiechers. 2006. Environmental history of the dry forest biome of Guerrero, Mexico, and human impact during the last c. 2700 years. The Holocene **16**:63-80.

Blasco, F., P. Saenger, and E. Janodet. 1996. Mangroves as indicators of coastal change. Catena **27**:167-178.

Borejsza, A. and C. D. Frederick. 2010. Fluvial response to Holocene climate change in low-order streams of central Mexico. Journal of Quaternary Science **25**:762-781.

Bowen, H. J. M. 1956. Strontium and barium in seawater and marine organisms. Journal of the Marine Biological Association of the United Kingdom **35**:451-460.

Brown, R. B. 1985. A summary of late-Quaternary pollen records from Mexico west of the Isthmus of Tehuantepec Pages 71-94 *in* V. M. Bryant and R. G. Holloway, editors. Pollen records of late-Quaternary North American sediments. AASP Foundation.

Bullock, S. H. 1986. Climate of Chamela, Jalisco, and trends in the South coastal region of Mexico. Archives for Meteorology Geophysics and Bioclimatology Series B-Theoretical and Applied Climatology **36**:297-316.

Bush, M. B. and M. B. Weng. 2006. Introducing a new (freeware) tool for palynology. Journal of Biogeography **34**:377-380.

Chague-Goff, C., S. Dawson, J. R. Goff, J. Zachariasen, K. R. Berryman, D. L. Garnett, H. M. Waldron, and D. C. Mildenhall. 2002. A tsunami (ca. 6300 years BP) and other Holocene environmental changes, northern Hawke's Bay, New Zealand. Sedimentary Geology **150**:89-102.

Chen, Z., Z. Chen, and W. Zhang. 1997. Quaternary stratigraphy and trace-element indices of the Yangtze Delta, eastern China, with special reference to marine transgressions. Quaternary Research **47**:181-191.

Chmura, G. L., P. A. Stone, and M. S. Ross. 2006. Non-pollen microfossils in Everglades sediments. Review of Palaeobotany and Palynology **141**:103-119.

Chu, P. S. 2004. ENSO and tropical cyclone activity. Pages 297-332 *in* R. J. Murnane and K. B. Liu, editors. Hurricanes and Typhoons: Past, Present, and Future. Columbia University Press, New York.

Clement, A. C., R. Seager, and M. A. Cane. 2000. Suppression of El Niño during the mid-Holocene by changes in the Earth's orbit. Paleoceanography **15**:731-737.

Colinvaux, P., P. De Oliveira, and J. E. M. Patino. 1999. Amazon Pollen Manual and Atlas. Harwood Academic Publishers, Amsterdam.

Conroy, J. L., J. T. Overpeck, J. E. Cole, T. M. Shanahan, and M. Steinitz-Kannan. 2008. Holocene changes in eastern tropical Pacific climate inferred from a Galapagos lake sediment record. Quaternary Science Reviews **27**:1166-1180.

Contreras-Espinosa, F. 1993. Ecosistemas Costeros Mexicanos. UNAM-CANABIO, Mexico, D.F.

Contreras-Espinosa, F. and B. G. Warner. 2004. Ecosystem characteristics and management considerations for coastal wetlands in Mexico. Hydrobiologia **511**:233-245.

Corona, N. and M. T. Ramirez-Herrera. 2012. Mapping and historical reconstruction of the great Mexican 22 June 1932 tsunami. Natural Hazards and Earth System Sciences **12**:1337-1352.

Curray, F., J. Emmel, and P. J. Crampton. 1969. Holocene history of a strand plain lagoonal coast, Nayarit, Mexico. Pages 63-100 *in* A. Ayala-Castanares, editor. Coastal Lagoons: A Symposium. Universidad Nacional Autonoma de Mexico. Mexico City.

Dean, W. E. 1974. Determination of carbonate and organic matter in calcareous sediments and sedimentary rocks by loss on ignition: comparison with other methods. Journal of Sedimentary Petrology **44**:242-248.

Donnelly, J. P. and J. D. Woodruff. 2007. Intense hurricane activity over the past 5,000 years controlled by El Nino and the West African monsoon. Nature **447**:465-468.

Ellis, M. B. and J. P. Ellis. 1988. Microfungi on miscellaneous substrates: An identification handbook. Timber Press, Portland.

Elsner, J. B. and A. B. Kara. 1999. Hurricanes of the North Atlantic: Climate and Society. Oxford University Press, New York.

Englehart, P. J. and A. V. Douglas. 2001. The role of eastern North Pacific tropical storms in the rainfall climatology of western Mexico. International Journal of Climatology **21**:1357-1370.

Faegri, K. and J. Iversen. 1989. Textbook of Pollen Analysis. 4th Edition. John Wiley & Sons, New York.

Gelorini, V., A. Verbeken, B. van Geel, C. Cocquyt, and D. Verschuren. 2011. Modern non-pollen palynomorphs from East African lake sediments. Review of Palaeobotany and Palynology **164**:143-173.

Gilbert, P. M. and D. E. Terlizzi. 1999. Cooccurence of elevated urea levels and dinoflagellate blooms in temperate estuarine aquaculture ponds. Applied and Environmental Microbiology **65**:5594-5596.

Goldenberg, S. B. and L. J. Shapiro. 1996. Physical mechanisms for the association of El Niño and west African rainfall with Atlantic major hurricane activity. Journal of Climate **9**:1169-1187.

Goman, M., A. Joyce, and R. Mueller. 2005. Stratigraphic evidence for anthropogenically induced coastal environmental change from Oaxaca, Mexico. Quaternary Research **63**:250-260.

Goman, M., A. Joyce, R. Mueller, and L. Paschyn. 2010. Multiproxy paleoecological reconstruction of prehistoric land-use history in the western region of the lower Rio Verde Valley, Oaxaca, Mexico. Holocene **20**:761-772.

Gonzalez-Quintero, L. 1969. Morfologia polinica: la flora del Valle del Mezquital, Hidalgo. Paleoecologia:1-185.

Gonzalez-Quintero, L. 1980. Paleoecologia de un sector costero de Guerrero, Mexico (3000 anos). Memorias **86**:133-157.

Gonzalez-Quintero, L. and M. Fuentes-Mata. 1980. El Holoceno de la porcon central de la Cuenca del Valle de Mexico. Pages 133-158 Memorias III Coloquio sobre Paleobotanica y Palinologia (Coordinacion, Fernando Sanchez). Instituto Nacional de Antropologia e Historia, Mexico.

Gray, W. M. and J. D. Sheaffer. 1991. El Niño and QBO influences on tropical cyclone activity. Pages 257-284 *in* M. H. Glantz, R. W. Katz, and N. Nicholls, editors. Teleconnections linking worldwide climate anomalies. Cambridge University Press, New York.

Habib, D., D. Thurber, D. Ross, and J. Donahue. 1970. Holocene palynology of the Middle American Trench near Tehuantepec, Mexico. Memoirs of the Geological Society of America **126**:233-261.

Haug, G. H., K. A. Hughen, D. M. Sigman, L. C. Peterson, and U. Rohl. 2001. Southward migration of the intertropical convergence zone through the Holocene. Science **293**:1304-1308.

Heine, K. 1987. Anthropogenic sedimentological changes during the Holocene in Mexico and Central America. Striae: a monograph series for Quaternary studies **26**:51-63.

Herrera, L. F. and L. E. Urrego. 1996. Atlas de polen de plantas utiles y cultivadas de la Amazonia colombiana. Tropenbos Colombia.

Horn, S. P. 2007. Lake Quaternary lake and swamp sediments: Recorders of climate and environment. Pages 427-445 *in* J. Bundschuh and G. E. Alvarado, editors. Central America: Geology, Resources, and Hazards. Taylor and Francis, London.

Huang, T.-C. 1972. Pollen Flora of Taiwan. National Taiwan University - Botany Department Press.

Jarzen, D. M. and W. C. Elsik. 1986. Fungal palynomorphs recovered from recent river deposits, Luangwa Valley, Zambia. Palynology **10**:35-60.

Jauregui, E. 2003. Climatology of landfalling hurricanes and tropical storms in Mexico. Atmosfera **16**:193-204.

Jonathan, M. P., P. D. Roy, J. L. Sanchez-Zavala, S. Srinivasalu, M. C. Macias-Romo, and C. Lakshumanan. 2011. Field survey report on the 11th March 2011 tsunami in Pacific coast of Mexico. Natural Hazards **58**:859-864.

Kennett, D. J., B. Voorheis, J. Iriarte, J. G. Jones, D. Piperno, M. T. Ramirez-Herrera, and T. A. Wake. 2004. Avances en el proyecto Arcaico-Formativo: Costa de Guerrero. Instituto Nacional de Antroplogia e Historia.

Koutavas, A., P. B. deMenocal, and J. Lynch-Stieglitz. 2006. Holocene trends in tropical Pacific sea surface temperatures and the El Nino-Southern Oscillation. PAGES news **13**:22-23.

Kremp, A. and A.-S. Heiskanen. 1999. Sexuality and cyst formation of the spring-bloom dinoflagellate *Scrippsiella hangoei* in the coastal northern Baltic Sea. Marine Biology **134**:771-777.

Landsea, C. W. and W. M. Gray. 1989. Eastern North Pacific tropical cyclone climatology - low frequency variations. Geneva.

Lankford, R. R. 1977. Coastal lagoons of Mexico: their origin and classification. Pages 182-215 *in* M. Wiley, editor. Estuarine Processes. Academic Press Inc.

Lawrence, M. B. 1999. Eastern North Pacific hurricane season of 1997. Monthly Weather Review **127**:2440-2454.

Liu, K. B. and M. L. Fearn. 2000. Reconstruction of prehistoric landfall frequencies of catastrophic hurricanes in northwestern Florida from lake sediment records. Quaternary Research **54**:238-245.

Liu, K. B., H. Lu, and C. Shen. 2008. A 1200-year proxy record of hurricanes and fires from the Gulf of Mexico coast: Testing the hypothesis of hurricane-fire interactions. Quaternary Research **69**:29-41.

Lozano-Garcia, M. D. S. and E. M. Hernandez. 1990. Palinologia de la Estacion de Biologia Tropical Los Tuxtlas. Universidad Nacional Autonoma de Mexico.

Markgraf, V. and H. L. D'Antoni. 1978. Pollen Flora of Argentina. The University of Arizona Press, Tucson.

Markgraf, V., J. R. Dodson, A. P. Kershaw, M. S. McGlone, and N. Nicholls. 1992. Evolution of late Pleistocene and Holocene climates in the circum-South Pacific land areas. Climate Dynamics **6**:193-211.

Matias-Ramirez, L. G. 1998. Algunos efectos de la precipitacion del Huracan Paulina en Acapulco, Guerrero. Investigaciones Geographicas **37**:7-19.

McAndrews, J. H., A. A. Berti, and G. Norris. 1973. Key to the Quaternary pollen and spores of the Great Lakes Region. Royal Ontario Museum Life Sciences Miscellaneous Publication.

McAndrews, J. H. and C. L. Turton. 2010. Fungal spores record Iroquoian and Canadian agriculture in 2nd millennium A.D. sediment of Crawford Lake, Ontario, Canada. Vegetation History and Archaeobotany **19**:495-501.

McCloskey, T. A. and K. B. Liu. 2012. A sedimentary-based history of hurricane strikes on the southern Caribbean coast of Nicaragua. Quaternary Research **78**:454-464.

McCloskey, T. A. and K. B. Liu. 2013. A 7000 year record of paleohurricane activity from a coastal wetland in Belize. The Holocene **23**:278-291.

Melia, M. B. 1984. The distribution and relationship between palynomorphs in aerosols and deep-sea sediments off the coast of Northwest Africa. Marine Geology **58**:345-371.

Metcalfe, S.E., S. L. O'Hara, M. Caballero, and S. J. Davies. 2000. Records of Late Pleistocene-Holocene climatic change in Mexico - A review. Quaternary Science Reviews **19**:699-721.

Minoura, K. and S. Nakaya. 1991. Traces of tsunami preserved in inter-tidal lacustrine and marsh deposits: Some examples from Northeast Japan. Journal of Geology **99**:265-287.

Moy, C. M., G. O. Seltzer, D. T. Rodbell, and D. M. Anderson. 2002. Variability of El Niño/Southern Oscillation activity at millennial timescales during the Holocene epoch. Nature **420**:162-165.

National Climatic Data Center. 2013. NNDC Climate Data Online (Acapulco, MX).

National Geophysical Data Center. 2011. Global Historical Tsunami Database.

National Oceanic and Atmospheric Administration. 2011. Historical hurricane tracks. Retrieved 12-29-2011, from http://www.csc.noaa.gov/hurricanes/.

Neff, H., D. M. Pearsall, J. G. Jones, B. A. de Pieters, and D. E. Freidel. 2006. Climate change and population history in the Pacific Lowlands of Southern Mesoamerica. Quaternary Research **65**:390-400.

Nichol, S. L., C. Chague-Goff, J. R. Goff, M. Horrocks, B. G. McFadgen, and L. C. Strotz. 2010. Geomorphology and accommodation factors on tsunami deposition: Chatham Island, Southwest Pacific Ocean. Sedimentary Geology **229**:41-52.

Ohngemach, D. 1977. Pollen sequence of the Tlaqua crater (La Malinche Volcano, Tlaxcala, Mexico). Boletin de la Sociedad Botanica de Mexico **36**:33-44.

Paerl, H. W., L. M. Valdes, A. R. Joyner, B. L. Peierls, M. F. Piehler, S. R. Riggs, R. R. Christian, L. A. Eby, L. B. Crowder, J. S. Ramus, E. J. Clesceri, C. P. Buzzelli, and R. A. Luettich, Jr. 2006. Ecological response to hurricane events in the Pamlico Sound system, Carolina, and implications for assessment and management in a regime of increased frequency. Estuaries and Coasts **29**:1033-1045.

Paez-Osuna, F. and E. F. Mandelli. 1985. ^{210}Pb in a tropical coastal lagoon sediment core. Estuarine, Coastal, and Shelf Science **20**:367-374.

Park, J. 2005. Holocene environmental change and human impact in Hoya San Nicolas, Guanajuato, Mexico. Journal of the Korean Geographical Society **40**:571-583.

Palacios-Chavez, R., B. Ludlow-Wiechers, and G. Villanueva. 1991. Flora palinologica de la Reserva de la Biosfera de Sian Ka-an, Quintana Roo, Mexico. Centro de Investigaciones de Quintana Roo.

Perez-Cruz, L. 2013. Hydrological changes and paleoproductivity in the Gulf of California during middle and late Holocene and their relationship with ITCZ and North American Monsoon variability. Quaternary Research **79**:138-151.

Peros, M. C., E. G. Reinhardt, and A. M. Davis. 2007. A 6000-year record of ecological and hydrological changes from Laguna de la Leche, north coastal Cuba. Quaternary Research **67**:69-82.

Pospelova, P., G. L. Chmura, W. S. Boothman, and J. S. Latimer. 2002. Dinoflagellate cyst records and human disturbance in two neighboring estuaries, New Bedford Harbor and Apponagansett Bay, Massachusetts (USA). The Science of the Total Environment **298**:81-102.

Ramirez-Herrera, M. T., A. Cundy, V. Kostoglodov, A. Carranza-Edwards, E. Morales, and S. Metcalfe. 2007. Sedimentary record of late-Holocene relative sea-level change and tectonic deformation from the Guerrero Seismic Gap, Mexican Pacific Coast. Holocene **17**:1211-1220.

Ramirez-Herrera, M. T., A. B. Cundy, V. Kostoglodov, and M. Ortiz. 2009. Late Holocene tectonic land-level changes and tsunamis at Mitla lagoon, Guerrero, Mexico. Geofisica Internacional **48**:195-209.

Ramirez-Herrera, M.T., V. Kostoglodov, and J. Urrutia-Fucugauchi. 2011. Overview of Recent Coastal Tectonic Deformation in the Mexican Subduction Zone. Pure and Applied Geophysics **168**:1415-1433.

Ramirez-Herrera, M. T., M. Lagos, I. Hutchinson, V. Kostoglodov, M. L. Machain, M. Caballero, A. Goguitchaichvili, B. Aguilar, C. Chague-Goff, J. Goff, A.-C. Ruiz-Fernandez, M. Ortiz, H. Nava, F. Bautista, G. I. Lopez, and P. Quintana. 2012. Extreme wave deposits on the Pacific coast of Mexico: Tsunamis or storms? - A multi-proxy approach. Geomorphology **139**:360-371.

Ramirez-Herrera, M. T. and J. Urrutia-Fucugauchi. 1999. Morphotectonic zones along the coast of the Pacific continental margin, southern Mexico. Geomorphology **28**:237-250.

Riedinger, M. A., M. Steinitz-Kannan, W. M. Last, and M. Brenner. 2002. A ~6100 C-14 yr record of El Niño activity from the Galapagos Islands. Journal of Paleolimnology **27**:1-7.

Rodgers, E. B., R. F. Adler, and H. F. Pierce. 2000. Contribution of tropical cyclones to the North Pacific climatological rainfall as observed from satellites. Journal of Applied Meteorology **39**:1658-1678.

Roubik, D. W. and J. E. Moreno. 1991. Pollen and Spores of Barro Colorado Island. Missouri Botanical Garden.

Sandweiss, D. H., J. B. Richardson, E. J. Reitz, H. B. Rollins, and K. A. Maasch. 1996. Geoarchaeological evidence from Peru for a 5000 years BP onset of El Niño. Science **273**:1531-1533.

Sanson, L. Z. 2004. The mechanical influence of continental topography on the trajectories of tropical cyclones near the west coast of Mexico. Atmosfera **17**:151-170.

Schofield, J. E., K. J. Edwards, T. M. Mighall, A. Martinez Cortizas, J. Rodriguez-Racedo, and G. Cook. 2010. An integrated geochemical and palynological study of human impacts, soil erosion and storminess from southern Greenland since c. AD 1000. Palaeogeography Palaeoclimatology Palaeoecology **295**:19-30.

Scileppi, E. and J. P. Donnelly. 2007. Sedimentary evidence of hurricane strikes in western Long Island, New York. Geochemistry Geophysics Geosystems **8**:10.1029/2006GC001463.

Sirkin, L. 1985. Late Quaternary stratigraphy and environments of the West Mexican Coastal Plain. Palynology **9**:3-25.

Sirkin, L., S. Pedrin-Aviles, G. Padilla-Arredondo, and E. Diaz-Rivera. 1994. Holocene vegetation and climate of Baja California Sur, Mexico. Revista Mexicana de Ciencas Geologicas **11**:79-86.

Spang, R. M., S. H. Castaneda, and E. M. Gomez. 2003. Hurricane Pauline - its impact on Acapulco and subsequent debris flow prevention measures. *in* Proc. 3rd Int. Conf. Debris Hazards Mitigation, Davos, Switzerland.

Stallard, M. O., S. E. Apitz, and C. A. Dooley. 1995. X-ray fluorescence spectrometry for field analysis of metals in marine sediments. Marine Pollution Bulletin **31**:297-305.

Stuiver, M., P. J. Reimer, and R. W. Reimer. 2005. CALIB 6.0 (program and documentation).

Thom, B. G. 1967. Mangrove ecology and deltaic geomorphology: Tabasco, Mexico. Journal of Ecology **55**:301-343.

Urrego, L. E., C. Gonzalez, G. Uran, and J. Polania. 2010. Modern pollen rain in mangroves from San Andres Island, Colombian Caribbean. Review of Palaeobotany and Palynology **162**:168-182.

van Geel, B. 1986. Application of fungal and algal remains and other microfossils in palynological analyses. Pages 497-505 *in* B. E. Berglund, editor. Handbook of Holocene Palaeoecology and Palaeohydrology. John Wiley & Sons, New York.

van Geel, B. 2001. Non-pollen palynomorphs. Pages 99-119 *in* J. P. Smol, H. J. B. Birks, and W. M. Last, editors. Tracking Environmental Change using Lake Sediments. Volume 3: Terrestrial, Algal, and Siliceous Indicators. Kluwer Academic Publishers, Dordrecht.

van Geel, B., J. Buurman, O. Brinkkemper, J. Schelvis, A. Aptroot, G. van Reenen, and T. Hakbijl. 2003. Environmental reconstruction of a Roman Period settlement site in Uitgeest (The Netherlands), with special reference to coprophilous fungi. Journal of Archaeological Science **30**:873-883.

van Geel, B., V. Gelorini, A. Lyaruu, A. Aptroot, S. Rucina, R. Marchant, J. S. S. Damste, and D. Verschuren. 2011. Diversity and ecology of tropical African fungal spores from a 25,000-year palaeoenvironmental record in southeastern Kenya. Review of Palaeobotany and Palynology **164**:174-190.

Villanueva-G., R. 1984. Plantas de importancia apicola en el ejido de plan del rio, Veracruz, Mexico. Biotica **9**:279-340.

Wakefield, S. J. and H. Elderfield. 1985. Interstital water iodine enrichments from the eastern Pacific. Journal of Marine Research **43**:951-961.

Watts, W. A. and J. P. Bradbury. 1982. Paleoecological studies at Lake Patzcuaro on the west-central Mexican Plateau and at Chalco in the Basin of Mexico. Quaternary Research **17**:56-70.

Weltje, G. J. and H. von Eynatten. 2004. Quantitative provenance analysis of sediments: review and outlook. Sedimentary Geology **171**:1-11.

Willard, D. A., S. R. Cooper, D. Gamez, and J. Jensen. 2004. Atlas of pollen and spores of the Florida Everglades. Palynology **28**:175-227.

Woodruff, J. D., J. P. Donnelly, and A. Okusu. 2009. Exploring typhoon variability over the mid-to-late Holocene: evidence of extreme coastal flooding from Kamikoshiki, Japan. Quaternary Science Reviews **28**:1774-1785.

Yanez-Arancibia, A. 1977. Taxonomia, ecologia Y estructura de las comunidades de peces en lagunas costeras con bocas efimeras del Pacifico de Mexico. Annual Meeting of the American Society of Limnology and Oceanography, Savannah, Georgia, USA.

CHAPTER 7. SUMMARY AND CONCLUSIONS

7.1 Restatement of purpose

This research examined the paleoenvironments of four coastal lagoons (Mitla, Nuxco, Boquita, and Agua Dulce) on Mexico's Pacific coast, through the extraction and analysis of ~70 m of sediment cores. Using a multi-proxy approach, the main objective of this study was to establish a multi-millennial record of coastal environmental changes with the aim of uncovering geological, biological, and/or geochemical evidence of tropical cyclones (TCs) to determine long-term activity periods. Some examples of evidence sought included storm surge-induced sand layers and terrigenous slopewash deposition from intense TC precipitation. These four lagoons offered unique sediment stratigraphies as a function of their evolutionary histories, morphologies, sizes, salinities, tectonic settings, position of nearby streams, and coring locations.

7.2 Laguna Mitla

Laguna Mitla is a barred inner shelf site, the most common Pacific coast classification (Lankford, 1977). Six cores were extracted from Mitla in three shore-perpendicular transects, with the longest core (core 5) offering a ~6880 year record. From 6880-6180 yrs BP, Mitla was a *Rhizophora* and *Laguncularia*-dominated mangrove swamp positioned near sea level. Sea level rise deposited clastics into the site from 6180-5170 yrs BP, sparking the beginning stages of beach ridge formation. After rising seas inundated the site ~5170 yr BP, seas stabilized and the backbarrier environment formed.

Core 5 was the longest core extracted from Mitla and the most ideal for paleoenvironmental reconstruction, containing seven distinct clay layers with terrigenous geochemical signatures embedded in mangrove peat throughout the backbarrier phase. While the mangrove peat sections indicate periods of low water level from dry climatic conditions, the

clay layers with inferred ages ~4430-4220, 4080, 3950, 3680-3480, 3170-3080, 2990-2870, and 1570 yrs BP-present indicate rising water level in the lagoon from wet climatic periods. Clay layers show good agreement with periods of frequent and intense El Niño phases (e.g., Moy et al., 2002), which tend to increase precipitation for the eastern north Pacific. Furthermore, these water level variations in Mitla sediments could be linked to ENP TC activity. This relationship is predicated from the warm surface waters and decreased vertical shear during El Niño phases leading to increased TC frequency (Landsea and Gray, 1989) and wetter events (Rodgers et al., 2000). Additionally, significant proportions of annual precipitation totals stem from TC activity along Mexico's arid and semi-arid Pacific coastal areas (Englehart and Douglas, 2001). Clay intervals in Mitla's sediments also show agreement with periods of a southerly migrating Inter Tropical Convergence Zone (Haug et al., 2001), possibly contributing to wetter conditions for the Mitla region by lessening easterly flow, thereby strengthening ENSO periods.

Wet periods determined from Mitla generally exhibit an anti-phase relationship with a 5000 year paleohurricane record from Puerto Rico, where high activity was attributed to reduced El Niño frequency and intensity (Donnelly and Woodruff, 2007). This anti-phase relationship between ENP and Caribbean hurricane activity is consistent with that suggested by Lander and Guard (1998).

Overwash or slopewash deposition from individual TCs was absent in Mitla's sediments. Alternative proxies of seawater intrusion, including dinoflagellates and high concentrations of chemical elements abundant in ocean water (e.g., S, Sr), were non-existent in Mitla's sediments, despite both exhibiting high concentrations from the marine transgression at ~5170 years BP. The absence of marine evidence is attributed to the well-developed prograding beach ridge

system, which spans one km in width at this site. Similarly, the narrow continental shelf and its steep slope are not conducive to overwash events.

The lack of both overwash deposition and alternative evidence of seawater intrusion events in the nearshore areas raises questions regarding documented marine evidence retrieved at Mitla from sites up to 5 km inland, attributed to a tsunami that occurred 3400 years ago. The lack of marine deposits retrieved from nearshore cores in Mitla, in conjunction with the presence of sand layers high in marine elements discovered in landward sediment cores nearest the relict ridge, suggests that this aforementioned 'marine' evidence is material possibly redeposited from this beach ridge by lacustrine processes during periods of high water level. It is therefore suggested that deposits previously attributed to tsunamis from Mitla and adjacent sites should be reexamined to confirm their source and mechanism of deposition.

7.3 Laguna Nuxco

Similar to Mitla, Laguna Nuxco is a barred inner shelf site, formed from rising mid-Holocene seas aiding in the construction of the coastal beach ridge system. Three sediment cores were extracted in a shore-perpendicular transect from Nuxco's nearshore near its inlet, with the longest core providing a ~4000 year backbarrier paleoenvironmental record. From ~4000-~1300 yrs BP, Nuxco was an estuarine lagoon possessing shelly clay in nearshore sediments along with *Cerithium stercusmuscarum* and *Anomalocardia subrugosa* bivalves living in local habitats. Six distinct shell hash layers with >20% carbonate were discovered. Their severe breakage indicates susceptibility to constant stress from tidal and wave activity. Waves eventually concentrated these hash layers and later deposited them into the nearshore during a time period when Nuxco was sensitive to these processes. The progradational contacts, severe breakage, and lack of offshore shells and/or sand in the hash layers reveal some similarities to "current/wave

winnowed" deposits discovered along the Gulf of California margins (Meldahl, 1993). The limited inland extent of hash deposition at Nuxco further suggests that shell layers were driven by localized processes, not extreme events. As storms and TCs are capable of concentrating and transporting shell hash into coastal environments, these mechanisms cannot be overlooked as potential causes of deposition.

Nuxco's current lagoon phase began approximately 1300 years BP, and was probably initiated from the prograding of the coastal beach ridge, thereby diminishing oceanic influence. Sediments during this phase are characterized by decreased shell hash, heightened terrestrial elemental concentrations, and the presence of *Mytella* shells, indicating nearshore (vegetation) mangrove development and more sheltered, calmer conditions. During this stage, the main mode of shell hash entry into the site likely occurred during precipitation-induced blowout events. Rising water levels collected shells from the nearshore, and they were later deposited after the site filled to capacity and caused the 'blowout,' releasing lagoon water into the ocean and depositing the shells into the nearshore. Core 2 contained an increase in frequency and intensity of carbonate spikes at the bottom of the zone (~1280-~530 years BP), indicating excessive shell hash deposition. This is attributed to a more turbulent environment causing more blowouts, likely stemming from increased ENSO behavior. Alternatively, hash deposition frequency and intensity lessens at the zone top (~530-current). This indicates a relatively stable environment and less precipitation-induced blowouts, stemming mostly from a dryer climate and decreased ENSO behavior. Similar to findings from Mitla, the lack of definitive marine evidence (e.g., overwash sand, shells of offshore origin) in the sedimentary record suggests that extreme event processes were stymied by the vast beach ridge system and narrow/deep continental shelf.

7.4 Laguna Boquita

While Laguna Boquita is too small for formal classification, its formation, morphology, and beach ridge dimensions exhibit similarities to regional barred inner shelf lagoons, including Nuxco and Mitla. Five cores were extracted from Boquita, the oldest core containing a ~6900 year paleoenvironmental history. Beach ridge formation began during a period of rising seas during ~6290-5170 yrs BP. After marine water inundated the site around ~5170 years BP, Boquita became a backbarrier 'lagunilla' as seas stabilized.

During Boquita's backbarrier environment, bluish-gray inorganic facies, severely desiccated in some cores, suggests a period of low water level and brackish conditions triggered by a lack of precipitation entering via the watershed from approximately ~3150-1700 yrs BP. This dry climatic period may also imply a decrease in TC activity, showing temporal similarities to relatively arid conditions documented from Laguna Mitla. An adjacent gray clay section with low LOI contents and high Cl concentration suggests increased salinity, a lack of nearby vegetation, and low water level, likely indicating dry conditions persisting until ~1030 yrs BP. An increase in wetness is documented from ~1030 yrs BP to present, which may be due to increased TC activity. Overall, Boquita's paleoclimatic history is in good agreement with the record from Laguna Mitla and could be similarly driven by ENSO activity (Moy et al., 2002).

Similar to lagoons Nuxco and Mitla, overwash clastic deposition was absent throughout the backbarrier phase of Laguna Boquita. This was due to the wide and tall beach ridge system, while the narrow and steep continental shelf was not conducive to high storm surges. Unequivocal slopewash deposition was also absent in Boquita's sedimentary record, probably because the coring sites were too far from the steep slopes on the backsides of the lagoon, therefore insensitive to recording such events.

7.5 Laguna Agua Dulce

Unlike lagoons Mitla, Nuxco, and Boquita, Agua Dulce is categorized as a differential erosion lagoon, possessing a drowned river valley morphology (Lankford, 1977). Similar to the other lagoons analyzed in this dissertation, Agua Dulce filled during a marine transgression ~5000 yrs BP (Lankford, 1977). Seven cores were extracted from the western side of Agua Dulce in an area most sensitive to storm surge inundation. Cores were generally dominated by medium- to coarse-grained sand, preventing accurate dating of sediments by means of radiocarbon techniques. Recent TCs likely transported sand into the northwestern side of Agua Dulce. This is suggested by a low water depth in this area and a submerged sandy shoal. Eyewitness accounts indicate that Hurricane Rick (2009) was responsible for the formation of vast overwash lobes adjacent to Agua Dulce, deposited weeks before our fieldwork. Constant resuspension disturbed these overwash deposits in the lagoon sediments, making it difficult for identifying storm signatures and undertaking a reliable paleoenvironmental reconstruction.

7.6 Overall synthesis

While the methodological approach taken for this study (e.g., site selection, multiple proxy analyses) was ineffective in discovering sediment deposits from individual TCs, it was largely successful in determining paleoenvironmental conditions for the four study sites. While Laguna Agua Dulce did not yield suitable sediments for a long-term reconstruction, field observations did help determine the site's susceptibility to overwash processes. While sediments extracted from Laguna Boquita did not allow a high resolution survey of the backbarrier paleoenvironment and failed to contain evidence of overwash processes, an examination of sediment lithology, loss-on ignition, and XRF results helped determine a period of limited water level and high salinity, likely from dry conditions and TC inactivity. At Laguna Mitla, the

multi-proxy approach helped suggest that the site lacked marine intrusion throughout its ~5200 year backbarrier history, since relatively small spikes in marine element concentrations were not coincident with the presence of dinoflagellates. Similarly, the terrigenous element concentrations in clay layers throughout Mitla's backbarrier period aided in determining a terrestrial source, likely entering the site during limnic environments caused by wet climatic periods. Finally, for Laguna Nuxco, shell identification helped determine stability of the coastal beach ridge, since, for instance, *Mytella sp.* generally live in protected areas attached to hard substrates. Shell identification also determined that species are not of marine origin and therefore can not be directly tied to overwash processes. Geochemical analysis indicated that salinity has been relatively throughout the last 4000 years, suggesting that Nuxco has always been influenced by marine water entering through the tidal inlet. This finding is different than results from Mitla, for instance, as decreasing Cl concentrations indicate diminishing marine influence and salinity, most pronounced during the Late Holocene.

A comparison of findings from the four coastal lagoons offers similarities and differences. In Jalisco, Agua Dulce is unique due to its drowned river valley morphology and relatively narrow beach, both responsible for the sandy sediments that dominate the northwestern edge of the site. Nearby Boquita contains a 'barred inner shelf' morphology, consisting of a wider beach and beach ridge system than Agua Dulce which is largely responsible for the lack of marine inundation documented throughout its ~5200 year backbarrier stage. Climatically-driven water level fluctuations have been suggested by alterations in clastic texture and changes in marine element concentrations. In Guerrero, sites Nuxco and Mitla are both 'barred inner shelf' lagoons with wider beach and beach ridge systems than Boquita. Similar to Boquita, Mitla's backbarrier environment began around 5200 years BP. Mitla's backbarrier record consists of

alterations of mangrove peat and lagoonal clay, indicating limnic environments occurring during wet climatic periods. Sediment lithology is largely dependent on coring location, as easternmost sites are dominated by peat while cores extracted on the far western side of the site nearer stream input are dominated by clay with terrigenous geochemical signatures. Unlike sediments extracted from Mitla, Nuxco's ~4000 year paleorecord contains an abundance of shells, likely due to the coring proximity to the tidal inlet. The nearshore locations of the sediment cores were unideal to determine definitive evidence of water level changes. However, the identification of shells discovered in the sediments proved useful in determining geomorphological change to the beach ridge (alteration from *Anomalocardia subrugosa* to *Mytella* suggests vegetation growth and increased beach ridge stability).

Overall, similarities exist when comparing the paleoclimatic histories of lagoons Boquita, Nuxco, and Mitla. The dry period detected for Boquita from ~3150 to ~1030 years BP is temporally similar to a peat section found from Mitla, indicating dry conditions from ~2870 - ~1570 years BP. Similarly, a wet period suggested for Boquita from ~1030 years BP to present temporally correlates with a limnic phase for Mitla, from ~1570 years BP to present. Broad similarities exist between these records and paleo-ENSO records, particularly the sedimentary record retrieved Laguna Pallacacocha in Ecuador (Moy et al., 2002). Older records from Mitla's core 5 show solid temporal association with marine, coastal, and upland paleoclimatic records (Chapter 6). Despite Laguna Nuxco failing to contain definitive evidence of water level variations, an influx of shell hash entering the nearshore from ~1280 to ~530 years BP temporally correlates to a wet period detected from Mitla, along with increased ENSO activity from Pallacacocha (Moy et al., 2002).

7.7 Future research

As indicated in Chapter 2, paleoenvironmental reconstructions in Mexico, particularly on the Pacific coast, are uncommon. Despite the findings presented in this dissertation, much regional paleoenvironmental work must be performed to further verify these results and conclusions, for instance. Sedimentological data should be retrieved from other coastal areas to determine their overall value in improving regional paleoenvironmental, paleoclimatological, and/or paleotempestological records. For example, future research on Mexico's Pacific coast could include sediment coring in areas of differing morphology and physical setting, opposed to the barred inner shelf lagoons focused on in this study. By doing this, the sensitivity of these areas to marine intrusion can be determined, along with their susceptibility to climatically-induced water level fluctuations. Additionally, to receive overwash deposition, studies mimicking the methodology of Ramirez-Herrera et al. (2012) may be duplicated, involving sediment core extraction adjacent to the wide coastal beach ridge that covers much of Mexico's Pacific coast. These studies would have the potential of not only comparing TC and tsunami deposition, but also obtaining a multi-decadal or -centennial record of either TC or tsunami risk, or possibly both. Also, an in-depth investigation of TC-rainfall would further explain its dominance in this region. This can be challenging, since precipitation data along the Pacific coast can be largely unreliable. A remote sensing investigation can possibly aid in determining change in water level and/or lagoon size before and after hyperactive TC periods. Finally, water bodies located along western Mexico's interior can be probed, as they may contain definitive evidence of slopewash deposition and/or water level changes. This might be best accomplished in areas northwest of Jalisco and Guerrero (e.g., states Baja Calfiornia Sur), since this region is

drier and therefore likely more prone to geophysical impacts of TCs (water level changes, increased runoff) than wetter areas to the south.

7.8 References

Donnelly, J. P. and J. D. Woodruff. 2007. Intense hurricane activity over the past 5,000 years controlled by El Niño and the West African monsoon. Nature **447**:465-468.

Englehart, P. J. and A. V. Douglas. 2001. The role of eastern North Pacific tropical storms in the rainfall climatology of western Mexico. International Journal of Climatology **21**:1357-1370.

Haug, G. H., K. A. Hughen, D. M. Sigman, L. C. Peterson, and U. Rohl. 2001. Southward migration of the intertropical convergence zone through the Holocene. Science **293**:1304-1308.

Lander, M. A. and C. P. Guard. 1998. A look at global tropical cyclone activity during 1995: Contrasting high Atlantic activity with low activity in other basins. Monthly Weather Review **126**:1163-1173.

Landsea, C. W. and W. M. Gray. 1989. Eastern North Pacific tropical cyclone climatology - low frequency variations. Geneva.

Lankford, R. R. 1977. Coastal lagoons of Mexico: Their origin and classification. Pages 182-215 *in* M. Wiley, editor. Estuarine Processes. Academic Press Inc.

Meldahl, K. H. 1993. Geographic gradients in the formation of shell concentrations: Plio-Pleistocene marine deposits, Gulf of California. Palaeogeography Palaeoclimatology, Palaeoecology **101**:1-25.

Moy, C. M., G. O. Seltzer, D. T. Rodbell, and D. M. Anderson. 2002. Variability of El Niño/Southern Oscillation activity at millennial timescales during the Holocene epoch. Nature **420**:162-165.

Rodgers, E. B., R. F. Adler, and H. F. Pierce. 2000. Contribution of tropical cyclones to the North Pacific climatological rainfall as observed from satellites. Journal of Applied Meteorology **39**:1658-1678.

VITA

Thomas Anthony Bianchette was born in 1983 in Warren, Michigan, a suburb of Detroit. After high school graduation in 2001, Thomas attended Mott Community College in Flint, where he majored in Geography and earned his Associate of Art degree in 2003. Thomas soon received his Bachelor of Science degree from Western Michigan University, majoring in Geography with a minor in Environmental Studies. Thomas then moved to Baton Rouge to attend Louisiana State University for the Fall 2005 semester. Working under Dr. Kam-biu Liu in the Department of Geography and Anthropology, Thomas successfully defended his thesis *Using Hurricane Ivan as a Modern Analog in Paleotempestology: Lake Sediment Studies and Environmental Analysis in Gulf Shores, Alabama* and earned his Master of Science degree in August, 2007. Thomas enrolled in the doctoral program in Oceanography and Coastal Studies, also under the direction of Dr. Kam-biu Liu. Thomas plans to receive his doctorate in May, 2014. Throughout his tenure at LSU, Thomas has worked as a research assistant and a laboratory manager. He has performed fieldwork in Texas, Louisiana, Alabama, Florida, Mexico, Dominican Republic, and The Bahamas. He has authored or co-authored papers in the Journal of Coastal Research, Journal of Quaternary Science, and American Journal of Climate Change. After graduation, Thomas is looking forward to spending time with his wife of 2 ½ years, Erin Vicknair, and his son, Gus, born September 3, 2013.